



pennsylvania

DEPARTMENT OF TRANSPORTATION

Bridge Deck Cracking: Effects on In-Service Performance, Prevention, and Remediation

FINAL REPORT

August 5, 2015

By: Travis Hopper, Amir Manafpour,
Aleksandra Radlińska, Gordon Warn,
Farshad Rajabipour, Dennis Morian,
and Shervin Jahangirnejad

Pennsylvania State University
The Thomas D. Larson Pennsylvania
Transportation Institute

COMMONWEALTH OF PENNSYLVANIA
DEPARTMENT OF TRANSPORTATION

CONTRACT # 355I01
PROJECT # 120103



Technical Report Documentation Page

1. Report No. FHWA-PA-2015-006-120103		2. Government Accession No.		3. Recipient's Catalog No.	
4. Title and Subtitle Bridge Deck Cracking: Effects on In-Service Performance, Prevention, and Remediation				5. Report Date 8/05/2015	
7. Author(s) Hopper, T., Manafpour, A., Radlinska, A., Warn, G., Rajabipour, F., Morian, D., Jahangirnejad, S.				6. Performing Organization Code LTI 2016-03	
9. Performing Organization Name and Address Thomas D. Larson Pennsylvania Transportation Institute Transportation Research Building The Pennsylvania State University University Park, PA 16802-4710				8. Performing Organization Report No.	
12. Sponsoring Agency Name and Address The Pennsylvania Department of Transportation Bureau of Planning and Research Commonwealth Keystone Building 400 North Street, 6 th Floor Harrisburg, PA 17120-0064				10. Work Unit No. (TR AIS)	
15. Supplementary Notes PennDOT Technical Advisor: Robert S. Watral, P.E. rwatral@pa.gov (717) 346-5974				11. Contract or Grant No. 355101-120103	
16. Abstract The main objectives of this project were: (a) to identify the causes of early-age cracking in concrete bridge decks, (b) to provide recommendations for effective mitigation of early-age cracking, (c) to assess the effect of cracks on the long-term durability and performance of concrete bridge decks, and (d) to identify the best and most cost-effective (on a life-cycle cost basis) remediation practices and optimum time to remediate to extend the life of bridge decks. The project was completed in 6 tasks and this document reports details of the methods of data collection, analysis, and conclusions for each task.				13. Type of Report and Period Covered Final Report 8/6/2013 – 8/05/2015	
17. Key Words Bridge deck, concrete cracking, field inspections, long-term performance, bridge deck deterioration modeling, deck performance database				14. Sponsoring Agency Code	
19. Security Classif. (of this report) Unclassified		20. Security Classif. (of this page) Unclassified		21. No. of Pages 266	22. Price N/A

Disclaimer

The contents of this report reflect the views of the author(s) who is(are) responsible for the facts and the accuracy of the data presented herein. The contents do not necessarily reflect the official views or policies of the US Department of Transportation, Federal Highway Administration, or the Commonwealth of Pennsylvania at the time of publication. This report does not constitute a standard, specification or regulation.

Credit

This work was sponsored by the Pennsylvania Department of Transportation and the U.S. Department of Transportation, Federal Highway Administration.

Executive Summary

The main objectives of this project were: **(a)** to identify the causes of early-age cracking in concrete bridge decks, **(b)** to provide recommendations for effective mitigation of early-age cracking, **(c)** to assess the effect of cracks on the long-term durability and performance of concrete bridge decks, and **(d)** to identify the best and most cost-effective (on a life-cycle cost basis) remediation practices and optimum time to remediate to extend the life of bridge decks. The project was completed in 6 tasks and this document reports details of the methods of data collection, analysis, and conclusions for each task.

Chapter 1 (Task 1) provides a comprehensive literature review on the research and best practices related to the (1) causes and mitigation of early-age bridge deck cracking, (2) effects of cracking on durability and long-term performance, (3) bridge deck inspection and crack evaluation methods, and (4) best practices to remediate cracks. The key information gained from the literature review are highlighted and summarized in the following bulleted lists.

Concrete materials related aspects that likely reduce the risk of bridge deck cracking include:

- Reducing the total cementitious materials (i.e., portland cement + SCM¹) content in order to reduce the cement paste/binder content to less than 27% vol (excluding air).
- Preventing excessive compressive strength (e.g., >5000psi at 28 days). Excessively strong mixtures have high elastic modulus and low creep, and result in higher restrain shrinkage stresses and higher risk of cracking.
- Limiting slump (e.g., to 4.0") to minimize the risk of settlement cracking.
- Avoiding too low or too high w/cm. Too low w/cm is prone to high autogenous shrinkage, high heat of hydration and high stiffness. Too high w/cm can result in high drying shrinkage and high risk of plastic shrinkage cracking.
- Using proper cement types. Type III and other cements with high heat of hydration, fine particle size, and rapid hardening/stiffening result in higher risk of cracking. Several transportation agencies reported successful use of type II cements.

In addition to the factors above, the following material technologies are recommended to reduce bridge deck cracking:

- Use of SCMs such as fly ash and slag (but not silica fume) reduces cracking by reducing the heat of hydration and reducing concrete stiffness. In addition, SCMs increase the electrical resistivity of concrete, which is very beneficial in lowering the rate of rebar corrosion.
- Optimizing and blending aggregate gradations to minimize the cement paste content. Several aggregate optimization methods are available, including those of Shiltstone and

¹ Supplementary cementitious materials such as fly ash or blast furnace slag

methods developed by and available through PACA, TXDOT, MnDOT, and optimizedgraded.com, to name a few.

- Aggregate mineral (such as dolomite or limestone) specified to have optimized coefficient of thermal expansion (CTE) to match the girders for the deck in question
- Air content maintained per ASTM C94 in the range (6% - 8%)

Construction practices that likely reduce the risk of early age deck cracking include:

- Proper and timely wet curing (i.e., starting no later than 15 minutes after finishing and lasting for 14 days²)
- Misting hoses are to be used to keep mats wet, and soaker hoses are to be placed as soon as concrete can support foot traffic.
- Preventing excessive water evaporation from the surface of fresh concrete by using foggers. Water evaporation from fresh concrete should be measured or estimated using ACI 308 method and should not exceed 0.1 lbs/ft²hr.
- Avoiding extreme ambient temperatures; concrete should not be placed at air temperatures below 45F (high risk of thermal cracking) or above 90F (high risk of plastic shrinkage cracking).
- Concrete temperature and girder temperature at deck placement should be maintained between 55 to 75F. Enforcing strict ambient temperature and thermal design restrictions, heat girders within 20F of deck and/or chill concrete to manage differential between deck and girders.
- Obtaining proper consolidation by using gang-mounted vibrators at 12” center-to-center.
- Using 56-day acceptance tests to encourage slow deck concrete strength gain.
- Proper sequence of pour is important in continuous span bridges. Cast positive moment regions ahead of the negative moment regions.

Structural design factors that likely reduce the risk of early age deck cracking include:

- Increased cover thickness to 2.5 or 3”.
- Prohibit the use of bar sizes greater than #5; increase deck thickness if required.
- Ensure the top main bar spacing is 6” or less.
- Place longitudinal bars outside (on top) of the transverse bars
- Stagger shear studs and deck slab bars to prevent weak plane.
- Use prestressed (P/S) girders for integral abutments.
- Decks on steel girders (due to higher stiffness, higher thermal conductivity) have shown more cracking than decks constructed on concrete girders.
- Simply supported decks crack least and integral abutment crack most.

² Seven days is widely recognized as the minimum (with additional time providing a benefit)

Other important findings from the literature are provided below:

- Cracking shortens corrosion initiation period. However, chloride build up off crack is more important than on crack.
- Corrosion propagation rate may or may not be affected by cracking.
- Effect of crack density and crack width on both corrosion initiation and propagation needs further study.
- Recommendations to reduce corrosion (applicable to cracked concrete):
 - Cover depth (2" min) reduces chlorides and oxygen availability that are required for rebar corrosion.
 - Increase concrete resistivity (low coulombs) by using SCMs to reduce corrosion propagation rate and to prolong corrosion initiation period.
 - Reduce crack density and crack width (<0.5mm or 0.02")
 - Prevent parallel to rebar cracks.
- The primary goal of bridge deck remediation (coatings, overlays) is to make cover concrete thicker and less permeable to moisture and salt.
- As such, remediation methods are primarily used to prolong corrosion initiation and must be applied before the active corrosion of rebar has started.
- Factors that should be considered in selection optimum bridge deck remediation strategy:
 - How effective the coating/overlay is in reducing water and chloride permeability?
 - How long will this effectiveness last?
 - How much does it cost?
- Among overlays, latex modified concrete (LMC) provides the best performance
- Corrosion resistant rebar:
 - Epoxy coated: reduces corrosion propagation rate
 - Stainless steel: prolongs corrosion initiation (increases critical chloride content threshold by 10x)
 - Galvanized: increases critical chloride content threshold by 2x and reduced corrosion propagation rate
- Corrosion inhibitors prolong corrosion initiation period (increase critical chloride content threshold by up to 8x)
- The performance of protective systems in cracked concrete is not known with certainty

Chapter 2 (Task 2) describes the efforts to design, launch, collect, and analyze a web-based survey to elicit the experience of PennDOT personnel with regard to early-age bridge deck cracking. The targeted participants included PennDOT Central Office and District personnel representing the design, construction, bridge inspection, and materials units. The survey was designed to collect information on early-age cracking experience, preferred crack prevention methods, and cracking remediation methods/strategies. A total of sixty two responses were received, including responses from each of the 12 Districts spanning a wide range of personnel roles. The following are

conclusions based on the analysis of the responses and PennDOT's comments/objectives (presented in italicized font):

- 84% of the responses indicated typical initial observation of early-age deck cracks within 3 months after concrete placement.
 - *PennDOT comments/objectives: Drying shrinkage, autogenous shrinkage, and thermal cracking can occur rapidly or slowly, depending upon conditions during placement. Typical shrinkage rates (drying, autogenous, etc.) over time will be investigated and reduced if possible.*

- Eighty two percent (82%) of the respondents indicated observing more early-age cracking during summer months versus fall/spring months.
 - *PennDOT comments/objectives: Possibly due to steel girders expanding due to high summer temperatures and coefficient of thermal expansion (CTE) differences between the deck and girders.*

- A majority of the respondents (67%) agreed it is beneficial to start summer placement around 7:00 PM in order to induce slight compression in deck (due to superstructure contraction during curing). However, the remaining one-third of the respondents (33%) preferred a different time frame starting at night or earlier in the morning.
 - *PennDOT comments/objectives: A timeline will be developed to derive the optimum concrete pour time to leverage the high girder temperatures while avoiding the sunlight's radiant heat during the period of maximum heat of hydration. Preferred deck placement times are between 4 AM and 10 AM such that the girders are warm and the peak solar radiation is avoided. 7 PM placement times are also preferred to minimize evaporation rates.*

- Curing techniques were indicated as “very effective” in crack prevention, followed by other construction practices, concrete mixture design, and structural details in this respective order. Most frequent recommendation was to apply curing as soon as possible, and to maintain the moisture level for at least 14 days.
 - *PennDOT comments/objectives: Internal curing options will be evaluated to optimize curing and reduce deck cracking.*

- Numerous recommendations were received with respect to construction practices. Following the placement sequence (e.g. with regards to negative and positive moments) was one of the most recommended crack prevention methods. Limiting the movement of freshly-placed concrete due to adjacent traffic was another recommendation, in addition to restricting the temperature difference between the concrete deck and beam to less than 22 °F.

- *PennDOT comments/objectives: A “thermal design” spreadsheet will be developed to quantify and optimize the temperature difference that should be maintained to minimize deck cracking.*
- With regards to structural details, limiting the concrete deck restraints was the main recommendation.
 - *PennDOT comments/objectives: The bridge standards will be evaluated to see where improvements could be made.*
- There were several recommendations concerning the concrete mix design, and the most frequent called for limiting the maximum 28-day compressive strength of the concrete (to varying magnitudes such as 4000 psi, 4500 psi or 5500 psi) through reduced cement content, among others. Another recurring recommendation was limiting the maximum concrete slump (to varying magnitudes such as 3.5” or 4”). Reducing the concrete strength gain was another recommendation.
 - *PennDOT comments/objectives: Restrained ring tests will be added during the mix design process to limit shrinkage to 450 microstrains, as well as using “optimized aggregate” gradation and Type II cement. A new Special Provision will be developed to pilot these recommendations.*
- The majority of responses indicated prior experience as the basis for selecting a particular remediation technique, followed by the cost, then other criteria (Section 4.7), and manufacturer. Other selection criteria included performance over time, scientific studies, and deck life per unit cost.
- For longer lasting remediation (5 to 10 years), latex modified concrete (LMC) overlay was indicated by the majority of the respondents as their districts’ remediation method followed by bituminous overlay with waterproof membrane. For methods with shorter life (1 to 5 years), the use of sealant was indicated as the prevalent method followed by epoxy injection/resin. The use of linseed oil was indicated as the predominant method for remediation lasting less than 1 year.
 - *PennDOT comments/objectives: DM-4, Part-A, Section 5.5.4 will be reviewed and upgraded based on current practice as to “Targeted Service Life” of preferred remediation methods.*
- Epoxy surface treatments (epoxy overlays, epoxy aggregate overlays, and epoxy/resin injection) and latex modified surface treatments were ranked first by the majority of respondents as the most successful remediation methods based on cost and effectiveness. The use of sealants was ranked second, and bituminous overlay with waterproof membrane, was ranked third.

- *PennDOT comments/objectives: DM-4 Figure 5.5.2.3-3 – “Bridge Deck Rehabilitation Guide” will be reviewed and upgraded based on current remediation “best practices”.*

Chapter 3 presents the findings and deliverables for Task 3 which include: (1) summary of inspection of 40 older bridge decks to obtain cracking data and concrete core samples, (2) analysis of deck inspection data for over 200 bridges, and (3) development of a Deck Performance Database (DPD) and (4) development of a concrete bridge deck deterioration models. The bridge deck selection process, visual inspection protocols, and materials testing procedures are summarized. Penn State and QES performed deck inspections on 40 older bridge decks, while deck surveys for an additional 163 new decks were performed by PennDOT. These bridges were geographically distributed across Pennsylvania. The main objective was to collect data on the extent of cracking for decks with different concrete types (i.e., AA, AAA, AAAP, and HPC concrete) and protective systems (i.e., epoxy-coated rebar, galvanized rebar, black rebar, and decks with various coatings and overlays). The set of 40 bridges was chosen to produce a broad range of design parameters. The metric chosen for the study to reflect the extent of cracking was crack density (yd of crack length/square yd of deck area), which allowed for straightforward comparison of the extent of cracking from one deck to another. Two cores (on and off crack) were extracted from 19 of the 40 inspected decks. Cores were evaluated at Penn State to determine the chloride content at the rebar level and the extent of rebar corrosion. Cracking data for 163 newly constructed bridge decks was provided by PennDOT, which included an initial deck inspection prior to opening the bridge to traffic, and a follow-up inspection occurring approximately 6 months to 1 year after the initial inspection. The gathered crack density data was correlated with the PennDOT deck condition ratings (0 to 9 scale) for concrete bridge decks. [Table 1](#) summarizes the factors that were found to have the greatest influence on deck performance from the analysis of the cracking data from the 40+163 inspected bridge decks, analysis of the chloride content and rebar corrosion from the core samples, and results of the deterioration modeling.

The development and initial deployment of the Deck Performance Database (DPD) to store and analyze cracking metric data, and development of the PSU Bridge Deck Life deterioration model to predict the longevity and performance of Pennsylvania bridge decks is also described in Chapter 3. The DPD uses the crack lengths gathered from each inspection and associated deck area to calculate the crack density for each inspection. Suitable models for bridge deck deterioration are described. A new semi-Markovian model was developed to estimate the Sojourn times (i.e., the average time a deck lasts in a particular condition rate (e.g., 6 years at CR8)) as a function of rebar type, single vs multiple span, bridge length, interstate vs non-interstate bridge, and District#. The following conclusions were made:

- Coated rebar results in longer Sojourn times
- Shorter, simply-span and non-interstate bridges have longer Sojourn times

- At present, it is not possible to determine effect of deck cracking on Sojourn times; however this will be possible in future with the aid of DPD developed in this project
- Deterioration model can be used to assess the effect of remediation on deck service life

Table 1. Summary of the variables that influenced deck performance

Parameters	Summary
Concrete Type	Early-age cracking performance of AAAP and HPC concrete decks was better than AAA concrete decks.
Concrete Mixture	Higher compressive strength correlated with higher crack density. It is advisable to place a limit on maximum compressive strength at 7days (4000psi) or 28 days (5000psi) Lower total cementitious materials content (cement+SCM) and higher portland cement replacement with SCM resulted in less cracking. It is suggested to limit the maximum cementitious materials content to 620 lbs/cy and use SCM to reduce heat, increase resistivity, and prevent alkali-silica reaction (ASR).
Protective System	Epoxy-coated rebar and galvanized rebar were more effective than black rebar in resisting corrosion. Black rebar corroded at lower chloride content levels and at earlier ages.
Half width construction	Decks constructed using half width construction, on average, cracked approximately 4 times more than decks using detours.
Girder Type	Decks supported by prestressed concrete girders, on average, cracked approximately 3 times less at early ages than decks supported by steel girders.

Chapter 4 (Task 4) describes best practice guidelines for deck remediation. In very general terms, a bridge has a general sequence of construction, remediation and replacement activities. The following table provides a general scenario of these activities over the anticipated one hundred year life of a PennDOT bridge.

Year Applied	Rehabilitation
1	Initial Construction
20	Minor Bridge & Deck Rehabilitation
40	Deck Replacement
60	Major Superstructure Replacement
80	Minor Bridge & Deck Rehabilitation
100	Bridge Replacement

In order to determine which sequence and timing of remediation will result in the optimum useful life of a deck based on cost-effectiveness, guidelines have been developed using Life-Cycle Cost

Analysis (LCCA). These guidelines for remediation are based on two general options: (1) a new deck with a targeted useful life of (~50-years), and (2) an existing deck of a certain age, a current deck rating, and a targeted useful life based on the expected useful lives of the superstructure and substructure. Chapter 4 explains the development of the spreadsheet that will be used to actually allow the asset managers to generate the optimum remediation sequences that provide the least-cost to attain the target useful life. The following lists the key information from this chapter:

- LCCA can be effective in evaluating bridge deck performance:
 - Useful for comparing alternative remediation strategies
 - Comparison of remediation sequences
 - Process is flexible, can vary analysis period, adjust to changing economics, etc.
 - Can consider user cost impacts
 - RealCost software can provide deterministic or probabilistic analysis results
- In general, fewer remediation treatments applied during the performance period results in lower LCC
- This can be achieved by:
 - Extending the time before remediation is needed (e.g., through routine preventative maintenance)
 - Use of longer performing remediation treatments
- Latex overlay and combination of latex and bituminous with waterproof membrane appear most cost effective for most circumstances

Chapter 5 (Task 5) provides a summary of the project findings as well as draft recommendations to PennDOT printed resources. The three major products of this project include (1) a final project report (this document), (2) a Deck Performance Database, and (3) the PSU Bridge Deck Life deterioration model. The following lists the most important recommendations from this project:

- Total cementitious materials (CM) content should be limited to max 620 lbs/cy.
- Use SCM to reduce concrete resistivity and heat of hydration. The min SCM dosage must be determined based on PennDOT specifications for AAAP concrete (Publication 408, Section 704) and AASHTO PP-65 document for ASR mitigation, whichever is greater.
- Do not use silica fume in bridge decks.
- A max compressive strength limit is advised: 4000psi at 7 days or 5000psi at 28 days.
- Limit max target slump to 4" (actual measured QC slump should not exceed 5.5").
- Blending of two or more aggregate sizes should be permitted and use of aggregate optimization methods should be encouraged to reduce binder content of concrete.
- Proper and timely water curing is very important. Curing must start no later than 15 minutes after texturing and should continue for 14 days.
- Do not exceed an evaporation rate of 0.10 lbs/ft².hr from freshly placed concrete.
- Discourage half-width construction of bridge decks, where possible.
- Use of prestressed concrete girders over steel girders may be advisable.

- Limit max rebar size to #5 and max rebar spacing of 6”.
- Consider internal curing technology.
- Consider use of shrinkage reducing admixtures (SRA) or fibers to reduce cracking and crack widths.
- Deck remediation (sealing, overlay, ...) must be employed before significant salt penetration and start of active corrosion.
- Monitor the performance of coating regularly (bi-annual). Consider using non-destructive testing (NDT) such as electrical resistivity to evaluate coating performance by qualitative measurement of the moisture content of the underlying concrete deck.
- Strict criterion should be taken to maintain inspection consistency for crack density measurements.
- Centralized method for proper maintenance/remediation tracking protocols should be developed and adopted.
- Determine the differences in standards/procedures for deck construction for each District causing variability in deterioration rates of decks in different Districts.
- Revise DM-4 to reduce the allowable tension stress in deck slabs, increase deck thickness if needed
- Improve deck joint performance (see D-3 report recommendations)
- Require that a thermal design be performed to keep the CTE of the deck-girder system and installation temperatures within 10% of initial value. Temperature range for thermal design of steel girders should be maintained between -20°F to 140°F. Typical range for concrete deck range is smaller due to its lesser thermal conductivity, greater thickness and insulating properties – unlike steel, surface temperature of concrete does not reflect the average temperature.
- Use BrM and BMS2 to study deck deterioration rates and perform “root cause analyses” for poor deck performance to continue to identify best practices to obtain the desired durability and longer life span of bridge decks.
- Contract specifications can be used to reduce the risk of early age cracking and are defined as prescriptive or performance-based. Criteria for the water-cement ratio, concrete placement temperature, and minimum time to initiate wet curing are examples of prescriptive specifications, while minimum compressive strength, adequate freeze-thaw resistance, and maximum allowable cracking criteria relate to performance-based specifications that have been used to reduce early age cracking.

Chapter 6 (Task 6) provides cost analysis for each approved design and construction recommendation. Based on observations from the LCCA work presented in Task 4, overall approach for improving the life cycle cost of bridge decks is to minimize the number of deck remediation treatments applied during the analysis period.

TABLE OF CONTENTS

Disclaimer	ii
Credit.....	ii
Executive Summary	iii
LIST OF FIGURES	xv
LIST OF TABLES	xx
CHAPTER 1 (TASK 1) Literature Review	1
1.1 Causes of Early Age Cracking in Deck Concrete	1
1.1.1 Types of shrinkage.....	2
1.1.2 Effect of concrete material properties on early age cracking	6
1.1.2.1 Effect of concrete ingredients	6
1.1.2.2 Effect of concrete mixture proportions	8
1.1.2.3 Effect of concrete’s fresh and hardened properties	9
1.1.3 Effect of construction methods on early age cracking of concrete.....	10
1.1.4 Effect of structural design factors on early-age cracking	12
1.1.5 Specifications to reduce early-age cracking	13
1.2 Effect of Cracks on Durability and Long-Term Performance of Concrete Bridge Decks. 19	19
1.2.1 Deterioration mechanisms in reinforced concrete structures	19
1.2.2 Effect of cracking on corrosion of reinforcing steel.....	23
1.2.3 Effect of cracking on other deterioration mechanisms in concrete	31
1.2.4 Effect of cracking on mass transport in concrete	33
1.2.5 Modeling tools for prediction of long-term performance of concrete decks.....	37
1.2.5.1 Service life modeling	37
1.2.5.2 Performance prediction models for bridge decks.....	39
1.3 Bridge Inspection and Cracking Metrics	42
1.3.1 Bridge deck inspection	42
1.3.1.1 Nondestructive evaluation.....	44
1.3.1.2 Destructive evaluation.....	48
1.3.2 Cracking metrics and condition ratings	48
1.3.2.1 Types of cracking	48
1.3.2.2 Cracking metrics	50
1.3.2.3 Condition rating.....	51
1.4 Management Practices for Remediation	52
1.4.1 Remediation method cost-effectiveness	52
1.4.1.1 Coatings.....	56
1.4.1.2 Overlays	56
1.4.1.3 Sealers	57
1.4.1.4 Epoxy injections.....	58
1.4.2 Maintenance.....	58
1.4.3 Optimization of rehabilitation methods and times to provide cost-effective outcomes	59
1.4.3.1 Models.....	60
1.4.3.2 Bridge management systems.....	60

1.4.3.3	Rating systems.....	61
1.4.4	Life cycle cost analysis of bridge decks	61
CHAPTER 2 (TASK 2)	Interview PennDOT Personnel and Document Interview Data.....	64
2.1	Introduction.....	64
2.2	Survey Design.....	64
2.3	Survey Distribution.....	68
2.4	Survey Response Data	68
2.4.1	Respondents' Information	68
2.4.2	Experience with Crack Detection.....	70
2.4.3	Experience with Summer Construction.....	70
2.4.4	Crack Prevention Methods	72
2.4.5	Short-Term Bridge Deck Performance Evaluation	76
2.4.6	Effect of Early-Age Cracking on Long-Term Bridge Deck Performance.....	77
2.4.7	Crack Remediation Methods and Strategies.....	78
2.5	Summary	82
CHAPTER 3 (TASK 3)	Review and Analysis of Bridge Condition Data	85
3.1	Introduction.....	85
3.2	Bridge Deck Selection Process and Field Inspections.....	85
3.2.1	Bridge Deck Inspections.....	88
3.2.2	Concrete Core Evaluation and Chloride Content Testing	88
3.3	Results and Discussion	90
3.3.1	Crack density results for 40 inspected bridge decks.....	90
3.3.2	Concrete core data and chloride content results	92
3.3.3	Analysis of Protective Systems	96
3.3.4	Analysis of Concrete Classes	98
3.3.5	Analysis of Other Variables	104
3.3.6	Comparison of 85-17 Study and Current Study	109
3.3.7	Correlation of Condition Rating to Crack Density.....	111
3.4	Deck Performance Database (DPD) and PSU Bridge Deck Life software	114
3.4.1	DPD Description and User Manual	114
3.4.2	Service Life Prediction and Deterioration Modeling	117
3.4.2.1	Data Collection.....	118
3.4.2.2	Data Preprocessing.....	118
3.4.3	Estimation algorithm for placement date of most recent deck	119
3.4.3.1	Sojourn time extraction and Weibull Fitting.....	120
3.4.3.2	AFT Weibull Distribution and Semi-Markov process	122
Semi-Markov Model Development	124	
3.4.3.3	Deterioration Modeling Results	127
3.4.3.4	Interpretation of AFT Weibull Parameter Estimations	127
3.4.3.5	Deterioration Curve Development: Example Case Analysis	131
3.4.3.6	Effect of Remediation	137
3.4.3.7	PSU Bridge Deck Life software (Deterioration Modeling Software).....	140
CHAPTER 4 (TASK 4)	Best Practice Decision Methodology, Matrix, and Guideline.....	141
4.1	Introduction.....	141
4.2	Remediation Treatments (2013 Baseline Costs per ECMS).....	141
4.3	Software	142

4.4	Treatment Matrix	142
4.4.1	The Selected Scenario Based on the Bridge Deck Deterioration Model.....	146
4.4.2	Treatments for New Bridge Decks	149
4.4.2.1	Cells with N/A in the “Present Value” Column.....	152
4.4.3	Treatments for Bridge Decks with Varying Ages and Deck Condition Ratings.....	152
4.4.3.1	An example:	154
4.4.4	Example of a 100-Year Analysis.....	155
4.4.5	Benefit of Starting Remediation Later in the Deck’s Life.....	156
4.5	A brief Overview of the LCCA Method and FHWA’s RealCost.....	157
CHAPTER 5 (TASK 5) Draft Changes to PennDOT Printed Resources.....		160
5.1	Factors Relevant to Bridge Deck Cracking and Deterioration Rates Considered/Addressed by the Project	160
5.2	Findings from Tasks 1 thru 4	162
5.3	Draft Recommendations to PennDOT Printed Material.....	164
CHAPTER 6 (TASK 6.3) Cost Analysis for each Approved Design and Construction Recommendation		169
6.1	Introduction.....	169
6.2	Basis for the Analyses.....	169
6.3	Scenarios	169
6.3.1	Base Scenario	170
6.3.2	Sealed versus Unsealed Scenario	171
6.3.3	AAA versus AAAP Mixture Design.....	171
6.3.4	Increased Cost Case of Two-inch Concrete Cover versus Three-inch Concrete Cover 171	
6.4	LCCA Results for the Examples.....	172
6.5	Conclusions.....	172
References.....		173
Appendix A: 40 Inspected Bridges		197
Appendix B: Bridge Deck Inspection Protocols.....		201
Appendix C: Core Sample Testing Procedure		210
Appendix D: Crack Density Results for 40 Inspected Bridge Decks		215
Appendix E: Bridge Decks Included in the #85-17 Study and the Current Study		237
* The condition rating for bridge 4908 reflects the rating in 2011 prior to rebuilding. The total crack density in 2011 was recorded as 0.4300 yd/sy.....		237
Appendix F: Data used for cracking data-condition rating correlation		238
Appendix G: Deterioration Modeling Results		242
Acknowledgements.....		244

LIST OF FIGURES

Figure 1. Early-age shrinkage cracking of a bridge deck (Kosmatka and Wilson 2011)	1
Figure 2. (a) Schematic illustration of shrinkage-induced cracking in concrete bridge decks; (b) Time-dependent stress and strength development in concrete, leading to early-age cracking	2
Figure 3. (a) Plastic shrinkage cracking in concrete (Kosmatka and Wilson 2011).....	3
Figure 4. Assigning performance grades in performance related specifications (Radlinska and Weiss 2012)	17
Figure 5. Allocating performance grades in shrinkage-based design approach (Radlinska and Weiss 2012)	17
Figure 6. Reactions involved in the corrosion process of steel reinforcement (PCA 2011).....	20
Figure 7. Initiation and propagation phases for corrosion in reinforced-concrete structure (Tuutti 1982)	21
Figure 8. Schematic diagram of the relationship between corrosion rate, oxygen availability and resistivity (PC: ordinary Portland cement, SCM: supplementary cementitious materials) (Scott and Alexander 2007)	22
Figure 9. Schematic modeling of the corrosion process for cracked (loaded) and un-cracked (unloaded) concrete, (Francois and Arliguie 1994, Tuutti 1982)	23
Figure 10. Chloride content at the rebar level (3.0in = 76.2mm) taken from uncracked regions of bridge decks versus age, $1\text{kg/m}^3=1.69\text{lbs/yd}^3$. (Lindquist et al. 2005).....	25
Figure 11. Chloride content at the rebar level (3.0in = 76.2mm) taken from cracked regions of bridge decks versus age, $1\text{kg/m}^3=1.69\text{lbs/yd}^3$ (Lindquist et al. 2005).....	26
Figure 12. Initiation times (time to start of propagation phase) for cracked NC (normal cement) and FA (fly-ash blended) concrete beams, 0.1 mm = 0.00394 in. (Li 2001).....	26
Figure 13. Effect of concrete quality and crack width on steel corrosion rate for PC (portland cement) and GGCS (ground granulated Corex slag) concrete specimens (Otieno et al. 2010a,b)	28
Figure 14. Effect of cover thickness (20 or 40 mm, 0.7874 to 1.5748 in.) on corrosion rates for PC (Portland cement), SM (50% slag replacement), FA (30% fly ash replacement), SF (7% condensed silica fume replacement) concrete specimens. (Values above the bars are averages for the two crack widths for the relevant cover depths) (0.2 or 0.7mm in the legend indicate crack widths; equivalent to 0.0079 to 0.0276 in.) (Scott and Alexander 2007)..	29
Figure 15. Effect of crack frequency on the cumulative weight loss due to corrosion based on linear polarization resistance (LRP) test (Arya and Ofori-Darko 1996).....	30
Figure 16. Schematic diagram of the relationship between corrosion rate, oxygen availability and resistivity, to account for crack width (PC: ordinary Portland cement, SCM: supplementary cementitious materials) (Otieno et al. 2010a)	31
Figure 17. Degradation of dynamic modulus of elasticity of concrete with different load induced damage undergoing freezing and thawing test (Yang et al. 2004)	32

Figure 18. Effect of crack width under loading, which is represented as COD (crack opening displacement), on the water permeability of normal strength concrete, 100 microns=0.004in., 1 cm/s = 0.394 in./s (Aldea et al. 1999a, Wang et al. 1997).....	33
Figure 19. Theoretical and experimental values of crack permeability as a function of effective crack width, (Akhavan et al. 2012).....	34
Figure 20. The effect of crack width on the ratio of diffusion coefficient of cracked concrete to uncracked concrete (D/D ₀). The results are shown for OC (ordinary concrete), HPC (high performance concrete) and HPCSF (high performance concrete containing silica fume) (Djerbi et al. 2008).....	35
Figure 21. Estimated diffusion coefficient of cracked samples (D _{composite}) as a function of crack volume fraction, 1 m ² /s = 10.764 ft ² /s (Akhavan and Rajabipour 2013).....	36
Figure 22. Effect of crack density on the diffusivity of water soluble chloride (WSC) and acid soluble chloride (ASC), 1 mm ⁻¹ = 304.8 ft ⁻¹ , 1 m ² /s = 10.764 ft ² /s (Mu et al. 2013).....	36
Figure 23. Predicted reductions in the corrosion initiation period for cracked concrete bridge decks (simulated using COMSOL by incorporating diffusion and binding) (Bentz et al. 2013)	39
Figure 24. The role of deterioration models in bridge management systems.....	40
Figure 25. Recommended Global Coordinate System as denoted by x and y axis for (a) two-way traffic, (b) one-way traffic variations, and (c) two-way traffic with median (FHWA 2013).	43
Figure 26. Data Collection Grid (FHWA 2013).....	44
Figure 27. Robotic Assisted Bridge Inspection Tool equipped with NDT technology (FHWA 2013)	46
Figure 28. Types of bridge deck cracking: (a) transverse, (b) longitudinal, (c) diagonal, (d) map (TRB 2004).....	49
Figure 29. PennDOT Drawing BC-783M Type I & Type II Patching.....	53
Figure 30. Pre 2015 Bridge Deck Rehabilitation Guide (PennDOT Design Manual, Part 4, 2012).	55
Figure 31. Epoxy Injection Procedure (VirginiaDOT 2009).....	58
Figure 32. Systematic Preventative Maintenance (FHWA 2011).....	59
Figure 33. Integrated LCA-LCCA model flow diagram (Kendall et al. 2008).....	63
Figure 34. Number of Respondents from Each District (CO=Central Office).....	68
Figure 35. Number of Respondents from each PennDOT Unit.....	69
Figure 36. Respondents Level of Experience with Respect to Various Aspects of Bridge Deck Construction.....	69
Figure 37. Respondents Observations of Initial Cracking.....	70
Figure 38. Respondents Past Experiences with Deck Placement Times.....	71
Figure 39. Respondents Opinion of Various Crack Prevention Methods.....	72
Figure 40. Evaluation Methods for Short-Term Bridge Deck Performance.....	77
Figure 41. Effect of Early-Age Cracking on Bridge Deck Long-Term Performance.....	78
Figure 42. Selection Basis for Remediation Method.....	79

Figure 43. Remediation Methods and their Longevity	80
Figure 44. Ranking of the Remediation Methods	81
Figure 45. Locations of bridges (indicated by red circles) inspected in Summer 2014.....	87
Figure 46. An example of a core with drill holes at the rebar level.....	89
Figure 47. Raw crack density versus age (40 inspected bridge decks without overlays)	92
Figure 48. Examples of (a) a completely intact epoxy-coated rebar (Core C2_4908_NC); (b) a rebar with minor corrosion; (c) an extremely corroded black rebar (Core C1_20506_C); (d) a corroded epoxy coated rebar (Core C2_36084_C, 37 year old deck); (e) rebar sample No. 1 for which percent effectiveness was approximated(Core C1_652_NC); (f) rebar sample No. 2 for which percent effectiveness was approximated (Core C1_12905_C).....	93
Figure 49. The black material within the crack seems to be a sealer such as linseed oil (Core C1_8407_C).....	95
Figure 50. Comparison of off-crack and on-crack (a) chloride content (b) diffusion coefficient	95
Figure 51. Ratio of diffusion coefficient of LMC overlay to the diffusion coefficient attributed to underlying concrete for the same core	96
Figure 52. Chloride content results for (a) black rebar; (b) epoxy-coated rebar; (c) galvanized rebar; (d) polymer impregnated concrete	97
Figure 53. (a) Percent effectiveness versus chloride content for the various rebar types; (b) Crack density vs age for different protective systems (40 inspected bridge decks).....	98
Figure 54. Average (data points) and range (error bars) of crack density for each concrete type at initial inspection (163 new bridge decks)	102
Figure 55. Average (data points) and range (error bars) of compressive strength for each concrete type at 28 and 7 days (163 new bridge decks)	102
Figure 56. Crack density at initial inspection (163 new bridge decks) versus cement content ..	102
Figure 57. Average (data points) and range (error bars) of cementitious materials content for each concrete type (163 new bridge decks)	102
Figure 58. Crack density at initial inspection (163 new bridge decks) versus w/cm ratio	102
Figure 59. Ratio of diffusion coefficient for on-crack to off-crack cores.....	102
Figure 60. Comparison of chloride content based on concrete type for off-crack locations	103
Figure 61. Crack depth over time for AA and AAA decks	103
Figure 62. Crack density versus age for different concrete classes (40 inspected bridge decks)	103
Figure 63. Crack density in terms of girder type (40 inspected bridge decks)	105
Figure 64. Comparison of crack density (40 inspected bridge decks) for positive and negative moment regions.....	105
Figure 65. Comparison of average (data points) and range (error bars) of crack density at initial inspection (163 new bridge decks) between single and multi-span bridges.....	105
Figure 66. Average (data points) and range (error bars) of crack density at initial inspection (163 new bridge decks) in terms of girder material	105
Figure 67. Average (data points) and range (error bars) of crack density at initial inspection (163 new bridge decks) in terms of structure type	106

Figure 68. Crack density at initial inspection (163 new bridge decks) versus beam spacing.....	106
Figure 69. Crack density at initial inspection (163 new bridge decks) versus deck thickness ...	106
Figure 70. Crack density at initial inspection (163 new bridge decks) versus bridge length	106
Figure 71. Crack density at initial inspection (163 new bridge decks) versus curing duration ..	107
Figure 72. Average (data points) and range (error bars) of crack density at initial inspection (163 new bridge decks) in terms of construction procedure	107
Figure 73. Crack density at initial inspection (163 new bridge decks) in terms of (a) low ambient temperature (b) high ambient temperature (c) moderate ambient temperature.	108
Figure 74. Average (data points) and range (error bars) of crack density at initial inspection (163 new bridge decks) in terms of placement month	109
Figure 75. Effect of traffic on early-age cracking (40 inspected bridge decks) in terms of (a) ADT; (b) ADTT	109
Figure 76. Comparison of 1988 Deterioration Factor to (a) current crack density; (b) current condition rating (for decks that were not replaced since #85-17 study)	110
Figure 77. Ranges of crack density values for each condition rating based on (a) 40 deck data (non-overlaid); (b) 163 deck data.	112
Figure 78. Main Menu page of Deck Performance Database	114
Figure 79. New Deck Entry page.....	115
Figure 80. Deck Specifications page	116
Figure 81. Inspection Form page	117
Figure 82. Algorithm used to improve placement date data accuracy. “con” is BMS2 construction date, “Recon” is BMS2 reconstruction date, “place” is the placement date which is the output for this algorithm, “CR” is condition rating, “inspstart” is the date of first inspection	120
Figure 83. Difference between Type I and Type II sojourn times observed from PennDOT bridge deck data	122
Figure 84. Ratio of average expected sojourn time to the baseline average expected sojourn time based on (a) Whether the rebar is protected or not; (b) Whether the deck is located on an Interstate or Non-interstate; (c) The type of span interaction; (d) Type of sojourn time. Dashed lines on figures represent baseline	129
Figure 85. Probability functions for example case define in Table 20 and using Type I sojourn times: a) PDF for CR 8 to CR5; b) PDF for CR9 and CR4; c) CDF for CR9 to CR3; d) survival functions for CR9 to CR3	133
Figure 86. Hazard rate functions for example case as defined in Table 20 and using Type I sojourn times.....	134
Figure 87. CR probabilities for deck entering (a) CR9, (b)CR8, (c)CR7 at time $t = 0$ for example case as defined in Table 20 and using Type I sojourn times	135
Figure 88. CR probabilities assuming deck entered CR6 at time $t = 0$ for example case as defined in Table 20 and using Type I sojourn times.....	136

Figure 89. Semi-Markov process deterioration curves for various initial CRs for example case. Dashed horizontal line at CR4 represents minimum acceptable performance	137
Figure 90. Deterioration curve for example deck with case 1 and 2 remediation	139
Figure 91. Extending the Useful Life of Pavement (Optimizing Highway Performance: Pavement Preservation, Federal Highway Administration, http://www.fhwa.dot.gov/construction/fs00013.pdf) Note that the effect of preservation illustrated delays, but does not replace rehabilitation.	149
Figure 92. Treatment Sequences and Life Cycle Costs for a BPN 1&2 Bridge with Deck Age of 5 Years	150
Figure 93. Expenditure Stream for the Three Alternatives.....	153
Figure 94. Inspectors conducting chain drag on deck. (FHWA 2013)	205
Figure 95. Example of crack inspection data for 1-direction 2-lane bridge deck.....	206
Figure 96. Example grid to be used for chain drag testing (sounding).....	208
Figure 97. Bridge 251 crack map.....	215
Figure 98. Bridge 252 crack map.....	215
Figure 99. Bridge 644 crack map.....	216
Figure 100. Bridge 645 crack map.....	216
Figure 101. Bridge 4908 crack map.....	217
Figure 102. Bridge 5081 crack map.....	218
Figure 103. Bridge 6457 crack map.....	218
Figure 104. Bridge 11525 crack map.....	219
Figure 105. Bridge 12517 crack map.....	219
Figure 106. Bridge 12518 crack map.....	220
Figure 107. Bridge 12524 crack map.....	220
Figure 108. Bridge 19168 crack map.....	221
Figure 109. Bridge 19170 crack map.....	221
Figure 110. Bridge 20506 crack map.....	222
Figure 111. Bridge 20507 crack map.....	222
Figure 112. Bridge 20588 crack map.....	223
Figure 113. Bridge 20589 crack map.....	223
Figure 114. Bridge 20613 crack map.....	224
Figure 115. Bridge 21651 crack map.....	224
Figure 116. Bridge 26993 crack map.....	225
Figure 117. Bridge 30643 crack map.....	226
Figure 118. Bridge 30700 crack map.....	226
Figure 119. Bridge 30752 crack map.....	227
Figure 120. Bridge 34391 crack map.....	227

LIST OF TABLES

Table 1. Summary of the variables that influenced deck performance.....	ix
Table 2. Grades of performance characteristics for high performance structural concrete (Goodspeed et al. 1996)	15
Table 3. Revised grades of performance characteristics for high performance structural concrete (Russell et al. 2006)	16
Table 4. Contractual specifications based on bridge deck performance (Welter 2009)	18
Table 5. Comparison of NDE methods (McCann and Forde 1997)	45
Table 6. Deterioration grades for NDE methods based on validation testing (Gucunski et al. 2013)	47
Table 7. Overall ranking of NDE methods based on validation testing (Gucunski et al. 2013)...	48
Table 8. Crack width definitions.....	50
Table 9. Condition State Definitions (AASHTO 2010).....	52
Table 10 Recommendations for Crack Prevention	73
Table 11- Additional PennDOT Experts’ Recommendations for Crack Prevention.....	75
Table 12. Summary of the variables that influenced deck performance (ordered from most influential to least influential).....	90
Table 13. ANOVA results for significance of all concrete types in relation to crack density (163 new bridge decks)	99
Table 14. Regression coefficients for each concrete type from a multivariate regression analysis (163 new bridge decks).....	100
Table 15 List of bridge decks included in both the #85-17 Study and the Current Study.....	111
Table 16. PennDOT (2009) condition rating system for concrete bridge decks	112
Table 17. Correlation of bridge deck condition rating to crack density (Poisson distribution assumed for confidence intervals)	113
Table 18. Transformed BMS2 variables used in analysis and their definitions (PennDOT 2009)	118
Table 19. Number of Type I and Type II sojourn times	122
Table 20. Variable values for example case	131
Table 21. Average expected sojourn times calculated using Eq. (5) for example case shown in Table 20	132
Table 22. The sojourn time distribution types (I or II) used to develop each curve shown in Figure 90.....	138
Table 23. Recommended treatments based on deck age and deck rating for BPN 1 and 2.....	144
Table 24. Recommended treatments based on deck age and deck rating for BPN 3 and 4.....	145
Table 25. Average time at specific deck condition ratings for remediated and unremediated decks	146
Table 26. Changes in deck ratings	148
Table 27. Remediation Guideline at deck age of 5 years (BPN 1&2).....	151
Table 28. Example of a 100-Year Analysis	156

Table 29. Benefit of Starting Remediation Later in the Deck’s Life.....	157
Table 30. Project summary of factors relevant to bridge deck cracking and deterioration.	160
Table 31. Summary of LIFE-365 Corrosion Initiation Results	169
Table 32. LCCA Results for the Examples.....	172
Table 33. Detailed information for 40 inspected bridges	197
Table 34. Example of crack inspection form for Figure 44.....	207
Table 35. Bridge Deck Cracking Inspection Form	209
Table 36. Crack density, delamination and patching/spalling results for 40 inspected bridge decks with original deck wearing surface (used in analysis).....	228
Table 37. Crack density, delamination and patching/spalling results for 40 inspected bridge decks with overlays (not used in analysis).....	231
Table 38. Chloride content results for original concrete decks	233
Table 39. Chloride content results for LMC overlay layers	236
Table 40. Bridge decks included in both the #85-17 Study and the Current Study.....	237
Table 41. Crack density and ratings data for 40 inspected bridge decks (all overlaid decks eliminated)	238
Table 42. Crack density and ratings data for 163 new bridge decks	238
Table 43. AFT Weibull parameter estimations for CR4 to CR9 (only significant variables are shown).....	242
Table 44. Ratio of average expected sojourn time to baseline average. All empty cells represent a value of 1.00.....	243

CHAPTER 1 (TASK 1)

Literature Review

1.1 Causes of Early Age Cracking in Deck Concrete

Early-age cracking in newly constructed concrete bridge decks has been a common problem reported by many state departments of transportation (DOTs) as well as several cities. Deck cracking (an example is shown in [Figure 1](#)) can be the primary cause of early deterioration of bridge decks, and it has been known to significantly decrease the durability and service-life of bridges. It is the nature of these cracks to facilitate penetration of chlorides and moisture and therefore, accelerate corrosion of the reinforcing steel. Aside from structural damage, cracking is also unsightly and the resulting distresses decrease the ride quality of the bridge.



Figure 1. Early-age shrinkage cracking of a bridge deck (Kosmatka and Wilson 2011)

This section describes the causes of early-age cracking and methods for the mitigation of cracking. Specifically, the effects of material properties, construction practices, structural design factors, and contractual specifications on the risk of early-age cracking of concrete bridge decks are described.

Cracking in concrete bridge decks results when the net internal tensile stresses are greater than the tensile strength of concrete. Often, tensile stresses are caused as a result of the restrained shrinkage or differential thermal cracking over the design temperature range (-20°F to 140°F) between steel girders and the expansion/contraction of concrete deck, although cracking may also occur due to mechanical loading (e.g., in areas of negative moment, overloading, and fatigue at a later age). [Figure 2](#) shows how tensile stresses develop as a result of restrained shrinkage and differential thermal expansion/contraction of a newly constructed concrete bridge deck. The tensile stresses increase with time as concrete experiences more shrinkage until these stresses exceed the tensile

strength of concrete, at which time the concrete cracks (Radlinska et al. 2007). In addition to stresses developed as a result of an external restraint, moisture and temperature gradients in concrete (due to preferential drying or cooling at surfaces) can cause a non-uniform shrinkage strain profile, which results in self-restraint and stress formation within concrete.

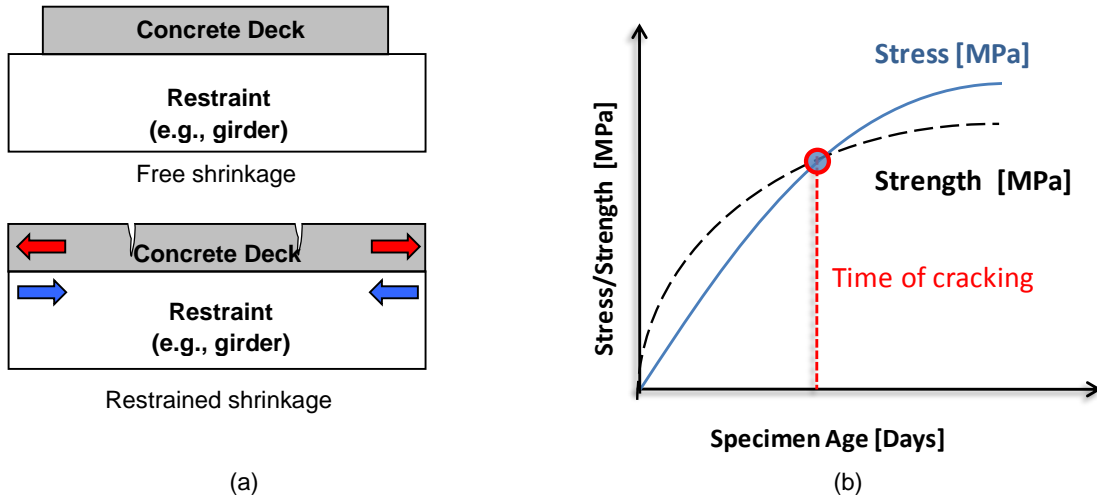
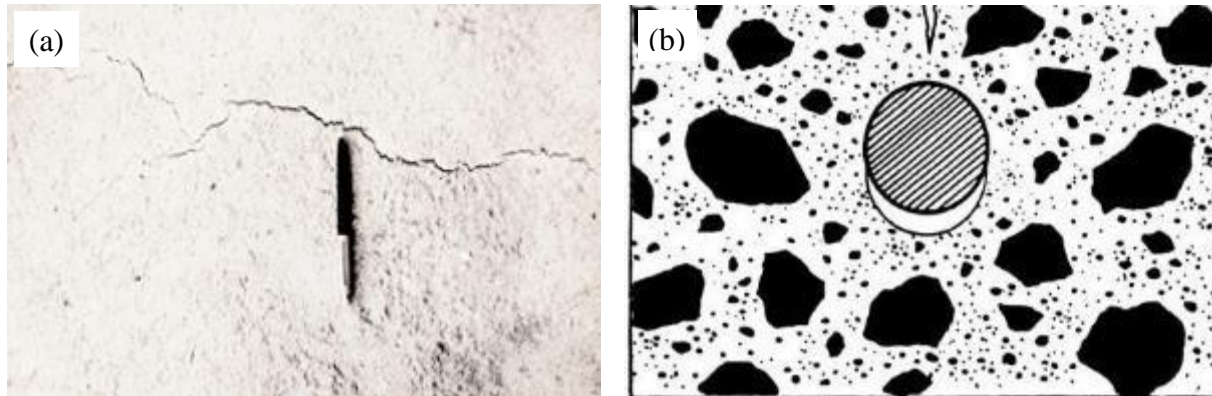


Figure 2. (a) Schematic illustration of shrinkage-induced cracking in concrete bridge decks; (b) Time-dependent stress and strength development in concrete, leading to early-age cracking

The following section describes several causes of early-age cracking in concrete decks, including plastic shrinkage, chemical and autogenous shrinkage, drying and carbonation shrinkage, thermal expansion/contraction, and mechanical loading. The subsequent sections describe how concrete material properties, construction methods, and structural design factors influence the risk of early-age cracking of concrete. The recommended mitigation methods for each of these factors are also mentioned, as well as contractual specifications that have been effective in reducing cracking in bridge decks.

1.1.1 Types of shrinkage

Plastic shrinkage: Plastic shrinkage cracking (two examples are shown in Figure 3) occurs when the evaporation of water from the surface of fresh concrete, exceeds the rate at which the bleed water reaches the surface. As a result, tensile stresses develop at the concrete surface and cause plastic cracking (Cohen et al. 1990, Mindess et al. 2003, Radlinska et al. 2007). In addition, differential settlement over a rebar can cause plastic shrinkage cracks. Factors affecting differential settlement over reinforcement include excessive slump, large rebar size and small cover depth.



**Figure 3. (a) Plastic shrinkage cracking in concrete (Kosmatka and Wilson 2011)
 (b) Settlement cracking due to flow of plastic concrete around rebar**

Plastic shrinkage can be reduced with proper curing, reducing evaporation rates, installing wind breaks, and early application of wet cure (Darwin et al. 2010), so the surface of fresh concrete never dries. The risk of plastic shrinkage cracking depends directly on the evaporation rate of bleed water from the surface of fresh concrete (Wittman 1976, Cohen et al. 1990, Radocea 1994). ACI 308R (2001) nomograph must be used to estimate the on-site evaporation rate as a function of the air and concrete temperature, relative humidity and wind speed. Special procedures, such as installing wind breaks and fogging, should be employed if the evaporation rate exceeds 0.2 lb/ft²hr for normal concrete and 0.1 lb/ft²hr for concrete with low w/cm (Krauss and Rogalla 1996). Studies also show that for high-performance bridge decks containing silica fume, the evaporation rates should not exceed 0.05 lb/ft²hr (Virginia DOT 1997).

Chemical and autogenous shrinkage: As cement hydrates, the total volume of hydration products (e.g., C-S-H gel, portlandite, and other products) is less than the volume of the reactants (i.e., cement and water). The reduction in volume, known as chemical shrinkage, is approximately equal to 1.77 in³ per 1 lb of Portland cement for neat cement paste (Jensen and Hansen 2001). As water is consumed by hydration reactions, the concrete self-desiccates, which results in a uniform desiccation of the entire cross section of the concrete member (Mindess et al. 2003). This volume reduction is known as autogenous shrinkage and is fundamentally different than drying shrinkage, as it occurs even in sealed concrete and in the absence of water evaporation to the ambient. Autogenous shrinkage is of particular concern for concretes with w/c (water to cement) ratios less than 0.36, high fineness cements, high cement paste volumes, and concrete containing silica fume (Jensen and Hansen 1996). Once concrete has set, further chemical shrinkage increases the risk of cracking of restrained concrete members. It is worth noting that chemical shrinkage does not cause cracking unless it leads to large autogenous shrinkage. Autogenous shrinkage, on the other hand, can result in substantially increased cracking risk (Bentz and Jensen 2004).

One method to mitigate autogenous shrinkage is through internal curing (Bentz and Weiss 2011). This method utilizes well-distributed internal water reservoirs to gradually release water to the interior of concrete, prevent self-desiccation, gain strength, and become less permeable (Bentz and

Jensen 2004, ACI-224R 2001, Mindess et al. 2003, Bentz et al. 2006). Internal curing can be divided into two categories: presaturated high absorption aggregates, and super absorbent polymers (SAPs). Light-weight fine aggregates are pre-wetted during the batching process, so as to typically absorb between 10% to 20% water (depending on the type of aggregate), which is released into the cement paste as required throughout the curing process. Equation (1) (Bentz and Snyder 1999) can be used to calculate the required lightweight aggregate to supply water for internal curing. Bentz et al. recommended adjusting the CS and α_{max} parameters of this equation based on the curing temperature and absorption capacity of the LWA (for further details please refer to literature).

$$M_{LWA} = \frac{C_f \cdot CS \cdot \alpha_{max}}{S \cdot \phi_{LWA}} \quad (1)$$

where M_{LWA} = mass of (dry) fine LWA needed per unit volume of concrete (kg/m³ or lb/yd³);
 C_f =cement factor (content) for concrete mixture (kg/m³ or lb/yd³)
 CS = chemical shrinkage of cement (g of water/g of cement or lb/lb);
 α_{max} =maximum expected degree of hydration of cement;
 S = degree of saturation of aggregate (0 to 1); and
 ϕ_{LWA} = absorption of lightweight aggregate (kg water/kg dry LWA or lb/lb).

Alternatively, SAPs can be used to soak up water during the mixing process or are prehydrated and release the absorbed water back into the concrete at a slow rate (Jensen and Hansen 2001, Geiker et al. 2004). Studies found that the use of SAPs (e.g., Hydromax 2012) produced stronger, more workable, and more durable concrete with lower shrinkage and delayed time to cracking, compared to conventional concrete (Kevern and Farney 2012, Jensen and Hansen 2001).

There has been rapidly developing interest in internal curing procedures for bridge decks and some states, including Indiana, are pursuing internal curing strategies in their newly placed bridge decks (Schlitter et al. 2010). The use of LWA in bridge decks results in a typical 10% to 12% increase in costs compared to conventional concrete, however it seems to be a more sustainable option with lower life cycle costs (Bentz and Weiss 2010). Internal curing has been reported to extend the service life of concrete bridges by more than 20 years (Cusson et al. 2010) and significantly reduce early-age cracking compared to conventional bridge decks (Guthrie and Yaede 2013).

Drying shrinkage: This type of shrinkage is due to the loss of moisture from the surface of hardened concrete, resulting in capillary stress development and shrinkage (similar mechanism as desiccation cracking of clays). Drying shrinkage depends greatly on the aggregate content or cement paste content of concrete, but to a lesser extent on the w/cm (water to cementitious materials ratio). Aggregates with low absorption and high modulus of elasticity are the most effective at reducing free shrinkage. Higher w/cm causes concrete to dry faster and decreases

stiffness, both of which result in larger drying shrinkage. However, a lower stiffness and higher creep can help in better relaxation of stresses caused by restraint shrinkage.

One method to mitigate drying shrinkage would be to use a shrinkage reducing admixture (SRA) such as Eclipse 4500 (2011). This product acts by chemically reducing the surface tension of water inside concrete pores during curing, which reduces the forces exerted by the water on the pore walls (Radlinska 2008, Eclipse 4500 2011). This reduction in strain leads to reduced drying shrinkage. Several studies found that this product significantly reduces the early-age crack development for bridge decks (Battaglia et al. 2008). However, in some cases this product destabilized the air void contents of the concrete mixes (Battaglia et al. 2008) and large amounts of air-entraining admixtures had to be added to achieve the proper air content.

Carbonation shrinkage: The ambient carbon dioxide can dissolve in concrete's pore water and produce carbonic acid. This acid chemically attacks the hardened cement paste and result in irreversible carbonation shrinkage. The magnitude of carbonation shrinkage is a function of relative humidity and temperature (Mindess et al. 2003). Since atmospheric CO₂ is always present in the field, carbonation shrinkage always occurs simultaneously with drying shrinkage. The majority of drying shrinkage measurements performed in laboratories and all field measurements result in reporting shrinkage values that are a combination of autogenous, drying and carbonation shrinkage.

Thermal expansion/contraction: Another source of volume instability and potential for cracking of concrete is thermal expansion/contraction between the deck and girders. The heat of hydration causes an increase in the temperature of fresh concrete. Often concrete sets near its peak temperature, and afterwards, as concrete cools, it contracts (ACI-231 2010), the girders can remain at ambient. Thermal cracking can occur due to both externally and internally applied temperature gradients between steel girders and concrete decks experiencing a temperature range of -20F to 140F, especially if the coefficients of thermal expansion are very different. The temperature difference between the concrete and that of the supports (e.g., steel forms or girders) provides a source of external temperature gradient (TRB Circular E-C107: 2006). Internal temperature gradients form when concrete does not cool at the same rate throughout. This occurs typically when a concrete surface cools or heats quickly (e.g., due to rain) while the interior of the concrete remains at a different temperature. Concretes with high cement content and low w/cm produce a considerable heat of hydration, and are especially prone to thermal cracking. As such, to reduce the risk of cracking, optimizing blended aggregate gradation to lower the cement paste content, and use of supplementary cementitious materials (especially during warm months) is advisable (ACI-231 2010). Additionally, concrete ingredients can be cooled down before mixing as part of a comprehensive thermal design concept.

Mechanical loading: Previous studies (Schmitt and Darwin 1995, Krauss and Rogalla 1996, Frosch et al. 2003, Hadidi and Saadeghvaziri 2005) have shown that tensile stresses due to mechanical loading of bridge decks are far smaller than the stresses due to restrained shrinkage. This remains true as long as DOT construction specifications are followed, such as preventing the opening of the bridge to traffic or heavy construction equipment before allowing the concrete to reach a minimum strength. Issa (1999) showed that vibrations due to adjacent traffic lanes will only contribute to plastic cracking when concrete is under-vibrated or has too high of slump. To reduce the moments causing tensile stress in bridge decks, it is recommended that concrete be first placed at the positive moment regions (center of a continuous bridge deck span) before the casting of negative moment regions (Babaei and Hawkins 1987, Issa 1999).

1.1.2 Effect of concrete material properties on early age cracking

Concrete material properties have been the subject of most past research for the mitigation of early-age cracking on concrete bridge decks. The following discussion on the role of material properties is divided into (A) the effect of concrete ingredients, (B) the effect of concrete mixture proportions, and (C) the effect of concrete's fresh and hardened properties.

1.1.2.1 *Effect of concrete ingredients*

Cement type: The type of cement can have an effect on the cracking risk of concrete. Type II cement, for example, has a lower heat of hydration and result in lower modulus of elasticity of concrete at early ages, which result in reduced risk of cracking (Krauss and Rogalla 1996, Brown et al. 2001). Whereas Type III cement has a rapid hardening and considerable heat of hydration, as a result, it is much more prone to cracking. Higher early stiffness also results in lower stress relaxation and higher chance of cracking (Mehta and Monteiro 2006). Finer cements and cements with high sulfate contents will reduce setting time and increase early strength/stiffness and therefore exhibit an increase in crack tendency. Low early-strength concretes made with type II cement should be preferred for bridge deck construction unless "open-early" is an issue (Hadidi and Saadeghvaziri 2005). Cavaliero and Durham (2010) compared a coarse-ground, Class G oil well cement (lower fineness) with Type II cement and concluded that the coarse ground cement developed early strength more slowly, developed less ultimate shrinkage strain, but cracked at earlier ages in comparison to Type II cement. In addition various transportation agencies have reported that the use of shrinkage-compensating (type K) cements mitigated early-age cracking for bridge decks (ACI 2001, Krauss and Rogalla 1996). Shrinkage-compensating cements attempt to balance autogenous and drying shrinkage with a designed expansion to prevent cracking.

Aggregate type: In order to reduce the ultimate shrinkage of concrete, the following properties of aggregates are sought: resistance to deformation and cracking, negligible shrinkage, high modulus of elasticity, and low absorption capacity (ACI 224R-01 2001, Krauss and Rogalla 1996). Light-weight aggregates have higher porosity and lower stiffness than normal-weight aggregates, however fine light-weight aggregates can be used for internal curing to reduce autogenous

shrinkage. Cavaliero and Durham (2010) found that fine light-weight aggregate concrete developed less ultimate micro-strain, developed early strength more slowly, had a higher durability factor (i.e., freeze-thaw resistance), and cracked at approximately the same age as normal fine normal-weight aggregate concrete. Jones et al. (2014) concluded the freeze-thaw resistance of internally cured (IC) light-weight aggregate concrete mixtures was comparable to standard normal-weight concrete mixtures as long as no more pre-wetted light-weight aggregate than required was used. Guo et al. (2014) predicted the service life of IC light-weight aggregate concrete mixtures in Indiana based on the concrete permeability, diffusion, and mixture proportions. The service life model presented in the study predicted a 3 to 4.5 times longer service life and 70% reduced life cycle costs for the IC light-weight aggregate mixtures in comparison to a conventional concrete mixture. McLeod et al. (2009) recommended the following characteristics for normal weight aggregates:

- For coarse aggregate, maximum absorption capacity should be less than 0.7%, and maximum deleterious substances should be: passing #200 sieve < 2.50%, shale < 0.50%, clay lumps and friable particles < 1.00%, coal < 0.50%.
- For fine aggregates, maximum deleterious substances should be: passing #200 sieve < 2.00%, shale < 0.50%, clay lumps and friable particles < 1.00%.
- Use TXDOT or MINNDOT optimized/blended aggregate methodology

In order to reduce the maximum allowable cement content, optimized aggregate blends are recommended. Shiltstone (1990) has proposed a method for blending the aggregate gradation in concrete, which can considerably reduce the cement content of concrete. Using blended aggregate gradation is currently permitted by some DOTs such as TxDOT (Tex-470-A 2006); however, PennDOT (2011) currently only permits the use of the AASHTO #57, #67, or #8 coarse aggregate gradations.

Riding et al. (2009) compared the effect of two types of coarse aggregates (i.e., dolomite limestone and siliceous river gravel) on the cracking of bridge decks. They concluded that the coarse aggregate with higher coefficient of thermal expansion (CTE) (i.e., siliceous river gravel) resulted in higher tensile stresses. As such, use of coarse aggregates with lower CTEs is recommended for the construction of bridge decks.

Supplementary cementitious materials (SCM): SCMs (formerly known as mineral admixtures) are often used in concrete as partial replacement for Portland cement. The uses of fly ash, ground granulated blast furnace slag (GGBFS), and silica fume have advantages for increasing the long-term strength and durability of concrete, and for lowering the heat of hydration. Riding et al. (2008) conducted experiments to determine the effect of fly ash mixtures on the early-age cracking of concrete. They concluded that using fly ash can improve crack resistance of concrete, due to lower heat of hydration, higher creep, and lower elastic modulus of the produced concrete. Lura et al.

(2001) and Lee et al. (2006) found that the use of ground granulated blast-furnace slag results in higher autogenous shrinkage in concrete and, as such, higher cracking risk.

In most studies, concretes containing silica fume were associated with increased cracking. Silica fume can increase the potential for plastic shrinkage (due to lack of bleed water) and autogenous shrinkage (due to pore size reduction) (Cohen et al. 1990, Mindess et al. 2003, Bentz and Jensen 2004). The increased early-age strength and stiffness can also cause less stress relaxation. Schmitt and Darwin (1999) observed an increased crack density on bridge decks made with concrete containing silica fume, and suggested that this is most likely due to the lack of bleed water. Krauss and Rogalla (1996) suggested that early-age cracking in silica fume concrete could be attributed to early higher elastic modulus and lower creep.

Chemical admixtures: McLeod et al. (2009) discouraged using any type of set-modifying admixtures for bridge deck concrete. In general, accelerators can increase shrinkage, early temperature rise, and early modulus of elasticity, all of which tend to increase the tendency of early-age cracking. In a lab experiment (Krauss and Rogalla 1996), specimens containing accelerators cracked 4 days earlier than the control specimens. They found that retarders lower the heat of hydration, which results in a decrease in thermal cracking. At the same time, retarders also delay setting, which leaves the concrete susceptible to plastic cracking for a longer period of time. Shrinkage reducing admixtures (SRA) are used to reduce the magnitude of both autogenous and drying shrinkage of a concrete mixture. They have been found to reduce shrinkage by up to 50% by reducing surface tension of the concrete's pore solution (Radlinska et al. 2008, Rajabipour et al. 2008, Weiss et al. 2008). Weiss et al. (1998) showed that SRA reduced drying shrinkage and increased the time to cracking initiation and reduced crack widths. Lura et al. (2007) studied the effect of SRA on plastic shrinkage cracking of mortars and found that mortars containing SRA exhibited fewer and narrower plastic shrinkage cracks than plain mortars when exposed to the same environmental conditions.

Fiber reinforcement: Several studies have shown that the use of fibers in concrete can greatly reduce plastic shrinkage and settlement cracking (Qi et al. 2003, Banthia and Gupta 2006) as well as the crack widths (Kim and Weiss 2003). Experiments using a restrained ring test by Gryzbowski and Shah (1989) have shown a delay of cracking and reduced crack widths. This is likely due to the effectiveness of fibers to bridge cracks, control crack opening (i.e., width), and prevent macro-crack propagation. In addition, Qi et al. (2003) and Banthia et al. (1995) found that fibers allowed multiple cracks to occur with smaller widths. Micro-fibers have been found to be more effective at reducing cracking than coarse fibers (Qi et al. 2003).

1.1.2.2 Effect of concrete mixture proportions

Cement paste and aggregate contents: Studies (Krauss and Rogalla 1996, Schmitt and Darwin 1999, Hadidi and Saadeghvaziri 2005) show that there is a strong positive relationship between

concrete cracking and increased cement paste content. This is because shrinkage mainly occurs in the cement paste and also because cement paste controls the heat of hydration (ACI-231 2010). Aggregates, on the other hand, don't shrink and provide internal restraint to reduce the overall shrinkage of concrete. McLeod et al. (2009) recommended that to prevent cracking in bridge decks, the cement content of concrete should be limited to a maximum of 540 lb/yd³ (5.75 sacks cement). Maximum paste volumes fraction of 27% (excluding air) have been recommended (Schmitt and Darwin 1995, Darwin et al. 2004). Higher crack densities were observed on monolithic bridge decks with paste volumes (excluding air) above 27.5%. Optimization of aggregate packing and particle size distribution in order to obtain a higher aggregate content has been suggested (Shiltstone 1990, McLeod et al. 2009) and is recommended.

Water content and water to cementitious materials ratio (w/cm): To minimize the cement paste content, water content must also be reduced proportionally with the cement content. Babaei and Purvis (1994) suggested a maximum water content of 323 lb/yd³. In addition, use of too low or too high w/cm must be avoided. High w/cm increases the risk of plastic shrinkage and settlement cracking and reduces the overall durability of bridge deck (Mindess et al. 2003). These concretes also tend to shrink more due to drying and carbonation (Krauss and Rogalla, 1996). Too low w/cm, also results in a high risk of cracking due to increased heat of hydration, increased self-desiccation, and increased stiffness (Brown et al. 2001) and reduced creep. A higher degree of cracking often observed for high strength (e.g., strengths higher than 5500 psi) concrete bridge decks (Darwin et al. 2004). Lower w/cm increases the need for proper moist curing due to lack of bleed water available during hydration of the concrete. Allowable w/cm in the range of 0.40-0.48 have been suggested (Kochanski et al. 1990, PCA 1970, McLeod et al. 2009).

1.1.2.3 Effect of concrete's fresh and hardened properties

Slump: Research (Dakhil and Cady 1975, Babaei and Hawkins 1987, Schmitt and Darwin 1995) has shown a clear correlation between concrete slump and its tendency to crack at early ages. By increasing slump, the settlement of fresh concrete over rebar can increase, which will cause cracking (Schmitt and Darwin 1995). Poorly consolidated high-slump concrete is especially prone to this type of cracking, since vibration from construction machinery and adjacent traffic lanes can cause further consolidation and settlement after finishing and result in cracking (Krauss and Rogalla 1996). Issa (1999) attributes increased cracking in higher-slump concretes to a decrease in bond strength between the reinforcing bars and concrete. The proposed values for the maximum allowable slump are 2 inches (PCA 1970), 2½ inches (Iowa DOT 1986), and 3½ to 4 inches (McLeod et al. 2009). Darwin et al. (2010) observed a significant increase in crack density when more than 70% of the samples taken from a bridge deck concrete exceeded a slump value of 3.5 inches.

Compressive strength: In order to increase compressive strength of concrete, increased cement content and reduced w/cm are required, which can result in: higher heat of hydration, higher

autogenous and drying shrinkage, higher modulus of elasticity and lower creep. These conditions contribute to higher stress development and higher cracking risk for concrete bridge decks. Frosch et al. (2003) found that strengths higher than specified by structural design are not only unnecessary but can potentially exacerbate deck cracking. Krauss and Rogalla (1996) related the increase in deck cracking since the 1970s to AASHTO's 1973 increase of the minimum concrete strength from 3000 psi to 4500 psi and lowering of the w/cm from 0.53 to 0.45.

Modulus of elasticity and creep: Higher modulus of elasticity was found to significantly affect cracking due to increased thermal and shrinkage stresses based on Hook's law (Krauss and Rogalla 1996). Concrete's tensile strain capacity is inversely proportional to its modulus of elasticity (ACI-224R 2001). In addition, creep and stress relaxation have been found to be inversely related to the Young's modulus. Creep is the ability of a concrete to continuously deform under a sustained stress. Relaxation is the gradual stress reduction under a sustained strain. Both creep and stress relaxation are due to the viscoelastic nature of concrete and are known to increase with the reduction of concrete's strength and elastic modulus (Mehta and Monteiro 2006).

Heat of hydration: Higher cement paste content results in higher temperature rise during the first 24 hours of hydration (ACI-231 2010) and higher potential for cracking. Several other factors affect the heat of hydration such as cement type, cement fineness, batching temperature, ambient temperature, and solar radiation (Riding et al. 2006). Lowering the heat of hydration lowers the thermal gradients within the concrete as well as the overall thermal contraction of concrete after setting. The heat of hydration can be reduced by using supplementary cementitious materials such as fly ash and GGBFS (Mindess et al. 2003).

Coefficient of thermal expansion (COTE) and thermal conductivity: Thermal expansion/contraction of concrete after setting is directly related to its coefficient of thermal expansion. The thermal conductivity of concrete is positively related to its aggregate content and moisture content, and negatively to its porosity (Mindess et al. 2003).

1.1.3 Effect of construction methods on early age cracking of concrete

Site ambient conditions: In general, placement of concrete for the bridge deck is recommended to be performed at an ambient temperature that is neither too high nor too low (Schmitt and Darwin 1995, Krauss and Rogalla 1996). The minimum range of ambient temperatures of 40-45°F (Cheng and Johnson 1985, French et al. 1999) and maximum range of 80-90°F (French et al. 1999, Krauss and Rogalla 1996) have been proposed. Concrete temperatures (at time of placement) of 55-70°F (McLeod et al. 2009) and girder temperatures of 55-75°F (Babaei and Purvis 1995) have been recommended. Current PennDOT specifications require that the girders be within 22 °F of the concrete at placement (PennDOT 2011). Furthermore, a research synthesis of the MDOT (2011) suggested placing bridge decks at temperatures between 45°F and 80°F, placing when the daily temperature fluctuation is less than 50°F, and limiting the differential temperature between the

deck and girders to 22°F for at least 24 hours after the concrete is placed to reduce thermal stresses. Similarly, Darwin et al. (2010) concluded that thermal cracking can be caused by placing warm concrete on cold girders, and can be reduced by limiting the ambient temperature range between 55°F and 70°F and by keeping the temperature differential of the deck and girders under 25°F. However, Schmeckpeper and Lecoultre (2008) concluded that a temperature differential limit is not sufficient to reduce cracking in integral abutment bridges and that maximum heat of hydration temperature has more of an effect on cracking.

Construction procedures: The procedures which can affect the cracking potential of bridge decks during constructions include the sequence and length of placement, consolidation, finishing, and curing. An increase in the placement length resulted in a delay in curing, in turn, causing an increase in early aged cracking. Ramey et al. (1997) suggested the following placement procedures:

- Place concrete for entire deck at one time when possible
- For simply supported single-span bridges, place concrete one span at a time. If the span is excessively long for a single placement the deck should be divided longitudinally and concrete placed one strip at a time. If this cannot be accomplished, it is recommended to start the placement of concrete at the center then move toward the supports.
- If multiple concrete placements are required for a continuous super-structure, the concrete should be first placed in the middle of each span and also, a 72-hour interval period should be considered between the placements of each section. The use of bonding agents was recommended to enhance bond at joints.

Insufficient vibration of concrete combined with inadequate concrete cover (<3") can increase plastic/settlement cracking (Issa 1999), particularly for concretes with high water content and high slump. Construction loads, spacing of reinforcement ties, vibration from traffic, and mixing revolutions in the concrete truck were found to have minor effects on early-age cracking (Krauss and Rogalla 1996). Furthermore, delayed finishing increases cracking and double-floated finishing results in less cracks in comparison to the standard float method (Krauss and Rogalla 1996)

Curing is a construction aspect that is considered to a significant effect on the development of early-age cracking in concrete bridge decks and delayed curing tends to increase the likelihood of cracking. Concretes with high cement content and low w/cm are more susceptible to delayed curing due to less bleeding observed in low w/cm concrete. When using wet burlap, it is recommended to apply the first layer of pre-soaked burlap 10 minutes after strike-off and apply a second layer within 5 minutes (McLeod et al. 2009). The application of an opaque curing compound to the surface of concrete after 14 days of wet curing is recommended (McLeod et al. 2009). Wet curing for a minimum of 7 days (Frosch et al. 2003) is required, however, some DOTs have specified a minimum of 14 days for bridge decks. For cold weather, curing should be

extended until the concrete has achieved sufficient strength. Krauss and Rogalla (1996) recommended the following for curing:

- Use of a fog nozzle water sprayer in hot weather in order to cool the concrete, steel and forms before placement.
- Application of water mist to keep mats wet or monomolecular film immediately after strike-off or early finishing.
- Application of white-pigmented curing compound as soon as bleed water diminishes.
- Application of pre-wetted burlap as soon as concrete resists indentation. The burlap must be continuously kept wet by sprinkling or by covering it with plastic sheeting and periodic sprinkling.
- [see additional recommendations in the executive summary]

1.1.4 Effect of structural design factors on early-age cracking

The effect of structural design factors on early-age cracking can be categorized into bridge deck design, girder and span configuration, and loading.

Bridge deck design: Some studies (Schmitt and Darwin 1995) did not find any significant relationship between cracking observations and the various structure types of steel super-structures, including continuous composite steel girder, continuous composite steel welded plate girder, haunched, and non-composite girder-deck systems.

However, a number of researchers (PCA 1970, Cheng and Johnson 1985, Krauss and Rogalla 1996, Frosch et al. 2002) have found that decks constructed on steel girders tend to crack more compared to those constructed on concrete girders. These researchers believe that concrete girders conduct heat slower than steel girders. As a result, lower temperature gradients and lower thermal stresses can be achieved in case of newly placed concrete bridge decks on concrete girders in comparison to steel girders. Additionally, Schmeckpeper and Lecoultre (2008) recommended maximizing girder spacing.

Studies (Poppe 1981, Kochanski 1990, Ramey et al. 1997, French et al. 1999, Schmeckpeper and Lecoultre 2008) have found that cracking decreases as deck thickness increases. Results of a finite element study (Saadeghaziri and Hadidi 2005) indicate that an increase in deck thickness reduces the stresses in the deck, with the exception of those integral with the abutments, i.e. those with a fixed-fixed boundary condition.

Furthermore, the thickness of the top cover of concrete affects the potential for cracking. If the top concrete cover is too low, the chance of settlement cracking increases and if it is too high, the effectiveness of the reinforcement in distributing stresses is reduced (Rajabipour et al. 2012). Studies recommend that the minimum top concrete cover be 2 in. and limit the maximum cover to 3 in. (Krauss and Rogalla 1996, AASHTO 2012, Ramey et al. 1997)

The literature suggests that increasing the size of the reinforcement bar increases cracking in bridge decks (Kochanski, 1990, Dakhil and Cady 1975, Schmitt and Darwin 1995). A maximum bar size of No. 5 is recommended (Kochanski et al. 1990, Ramey et al. 1997) and maximum bar spacing of 6 in. has been suggested (Frosch et al. 2003, Krauss and Rogalla 1996, Nielson et al. 2011). The NYSDOT (1995) recommends placing the longitudinal (shrinkage and temperature reinforcement) bars on top of the transverse bars in order to prevent transverse cracking. However, for a repair patch placed next to a deck's dam replacement, the transverse bars should be placed on top of longitudinal bars (when possible) in order to reduce longitudinal settlement cracking. In addition, the alignment of the top and bottom reinforcement should be staggered as to not create a vertical plane of weakness (Krauss and Rogalla 1996, Ramey et al. 1997). Epoxy-coated reinforcement has been found to increase cracking (Krauss and Rogalla 1996), due to the reduced bond strength between the concrete and the epoxy-coated bars in comparison to the bond achieved using uncoated bars. The AASHTO LRFD Bridge Design Specifications Section 5.10.8, specifies the shrinkage and temperature reinforcing requirements. . Furthermore, fewer studs with smaller rows and lengths have been recommended (French et al. 1999), however specific guidelines have not been provided.³

Girder spacing and type: In general, bridge superstructures integral with the abutments, i.e. fixed-end girders, exhibit increased cracking particularly in the end regions of bridge decks compared to simply supported, single span girders (Schmitt and Darwin 1995). French et al. (1999) found that simply-supported pre-stressed girder bridges have less cracking compared to continuous steel girder bridges due to the minimization of tensile stresses in the bridge superstructure and thus deck.

Due to varying stiffness and thermal properties between steel and concrete, steel girders have higher cracking potential (Krauss and Rogalla, 1996). Krauss and Rogalla (1996) found that cast in-place concrete girders and young pre-stressed girders have the best performance, while deep steel beams have performed worse in terms of the observed cracking in the bridge deck. The literature suggests that girder size and spacing be minimized (Schmitt and Darwin 1995, Saadeghvaziri and Hadidi 2005). In order to avoid uncontrolled cracking, contraction or control joints should be used (Bentz and Jensen 2004). Saadeghvaziri and Hadidi (2002) observed that the relative stiffness of the deck to the girder stiffness (ratio of deck to girder moment of inertia) is more critical than the type of girder in terms of cracking potential due to structural aspects. They recommend providing the required moment of inertia with more contribution from the deck.

1.1.5 Specifications to reduce early-age cracking

In the concrete industry, specifications related to materials and construction processes can be defined as prescriptive, performance-based, or a combination of the two (ACI 2010). A

³ see executive summary for additional items for consideration

prescriptive specification is one in which the material properties, mixture proportions, batching, mixing, transportation, and construction practices are detailed, while a performance-based specification defines the end results, performance judgment, and verification methods without implementing requirements for how the results are obtained (Russell 2013, ACI 2010).

The majority of State DOTs specifications are a combination of prescriptive and performance-based, with most of the specifications being comprised of prescriptive requirements (Russell 2013). A Transportation Research Board (TRB) study (Russell 2013) included a survey of State DOTs, which found that prescriptive specifications that are most effective at reducing early-age bridge deck cracking include a maximum water-cement ratio, minimum and maximum concrete placement temperature, maximum slump, minimum and maximum cement content, and minimum time to start wet curing methods. The Kansas DOT, along with 18 other State DOTs and the Federal Highway Administration (FHWA), implemented prescriptive contractual specifications for the construction of 20 low-cracking, high-performance concrete (LC-HPC) bridge decks during the first 6 years of an ongoing 10 year study (Darwin et al. 2010). The main features of the specification included a target water-cement ratio, a 10-minute time limit between concrete strike-off and wet curing, a qualification concrete batch, and a qualification slab (Browning et al. 2007, Browning et al. 2009, McLeod 2010, Darwin et al. 2010). Achieving the target water-cement ratio kept the concrete strength low (in the range of 4000 psi), while the qualification batch and slab were a means to ensure that the mix plant and contractor could produce the desired concrete quality (Browning et al. 2009, McLeod 2010). A 10 to 30 minute delay in the curing process was shown to increase the crack density by 0.06 to 0.08 ft/ft², which is more than five times the total crack density of a properly constructed LC-HPC deck (Browning et al. 2009).

The most common type of performance-based specification is a minimum concrete compressive strength, typically measured at 7, 28, or 56 days from concrete placement (Russell 2013). Other types of performance-based specifications include freeze-thaw resistance, deicer scaling resistance, chloride permeability, abrasion resistance, alkali-aggregate reactivity, and sulfate resistance (Russell 2004). Goodspeed et al. (1996) defined the performance of concrete using four material parameters that describe durability and four material parameters that describe mechanical properties (Table 2). Russell et al. (2006) revised the performance grades defined by Goodspeed et al. (1996) by (1) reducing the number of performance grades to three, (2) considering the grades as minimum performance levels, (3) adding alkali-silica reactivity, sulfate resistance, and flowability to the characteristics, (4) modifying several of the test procedures, and (5) using characteristics only when necessary for the specific application. Mokarem et al. (2005) suggested limiting the strain within concrete using the restrained shrinkage test (according to AASHTO PP34-98) to 200µε at 90 days. Additionally, Radlinska and Weiss (2012) introduced performance grades for concrete mixtures based on the magnitude of ultimate free shrinkage measured. Based on this model, shrinkage of the bridge deck concrete can be measured and a performance grade assigned (Figure 4). Alternatively, restrained shrinkage could be evaluated and potential for

cracking assessed via restrained ring test, ASTM C1581-09 (Radlinska et al. 2008a, Radlinska et al. 2008b). Following this approach concrete suppliers can receive incentives or penalties based on the predicted performance of concrete and its susceptibility to cracking (Figure 5). The material properties alone, however, cannot entirely define field performance and the field exposure conditions dependent on geographical location need to be taken into consideration (Barde et al. 2009).

Table 2. Grades of performance characteristics for high performance structural concrete (Goodspeed et al. 1996)

Performance Characteristic	Standard Test Method	FHWA HPC Performance Grade			
		1	2	3	4
Freeze/Thaw Durability (x= relative dynamic modulus of elasticity after 300 cycles)	AASHTO T 161 ASTM C 666 Proc. A	$60\% \leq x \leq 80\%$	$80\% \leq x$	—	—
Scaling Resistance (x= visual rating of the surface after 50 cycles)	ASTM C 672	X = 4,5	X = 2,3	X = 0,1	—
Abrasion Resistance (x= avg. depth of wear in mm)	ASTM C 944	$2.0 > x \geq 1.0$	$1.0 > x \geq 0.5$	$0.5 > x$	—
Chloride Permeability (x = Coulombs)	AASHTO T 277 ASTM C 1202	$3000 \geq x > 2000$	$2000 \geq x > 800$	$800 \geq x$	—
Strength (x = compressive strength)	AASHTO T 22 ASTM C39	$41 \leq x < 55$ MPa ($6 \leq x < 8$ ksi)	$55 \leq x < 69$ MPa ($8 \leq x < 10$ ksi)	$69 \leq x < 97$ MPa ($10 \leq x < 14$ ksi)	$x \geq 97$ MPa ($x \geq 14$ ksi)
Elasticity (x = modulus of elasticity))	ASTM C 469	$24 \leq x < 40$ GPa ($4 \leq x < 6 \times 10^6$ psi)	$40 \leq x < 50$ GPa ($6 \leq x < 7.5 \times 10^6$ psi)	$x \geq 50$ MPa ($x \geq 7.5 \times 10^6$ psi)	—
Shrinkage (x = microstrain)	ASTM C 157	$800 > x \geq 600$	$600 > x \geq 400$	$400 > x$	—
Creep (x= microstrain/pressure unit)	ASTM C 512	—	—	—	—

Table 3. Revised grades of performance characteristics for high performance structural concrete (Russell et al. 2006)

Performance Characteristic	Standard Test Method	FHWA HPC Performance Grade		
		1	2	3
Freeze-thaw Durability (F/T = relative dynamic modulus of elasticity after 300 cycles)	AASHTO T 161 (ASTM C666) Proc. A	$70\% \leq F/T < 80\%$	$80\% \leq F/T < 90\%$	$90\% \leq F/T$
Scaling Resistance (SR = visual rating of the surface after 50 cycles)	ASTM C672	$3.0 \geq SR > 2.0$	$2.0 \geq SR > 1.0$	$1.0 \geq SR > 0.0$
Abrasion Resistance (AR = average depth of wear in mm)	ASTM C944	$2.0 \geq AR > 1.0$	$1.0 \geq AR > 0.5$	$0.5 > AR$
Chloride Penetration (CP = coulombs)	AASHTO T 277 (ASTM C1202)	$2500 \geq CP > 1500$	$1500 \geq CP > 500$	$500 \geq CP$
Alkali-silica Reactivity (ASR = expansion at 56 d) (%)	ASTM C441	$0.20 \geq ASR > 0.15$	$0.15 \geq ASR > 0.10$	$0.10 \geq ASR$
Sulfate Resistance (SR = expansion) (%)	ASTM C1012	SR \leq 0.10 at 6 months	SR \leq 0.10 at 12 months	SR \leq 0.10 at 18 months
Flowability (SL = slump, SF = slump flow)	AASHTO T 119 (ASTM C143) and proposed slump flow test	SL $>$ 7-1/2 in. and SF $<$ 20 in.	20 in. \leq SF \leq 24 in.	24 in. $<$ SF
Strength (f'_c = compressive strength)	AASHTO T 22 (ASTM C39)	8 ksi $\leq f'_c <$ 10 ksi	10 ksi $\leq f'_c <$ 14 ksi	14 ksi $\leq f'_c$
Elasticity (E_c = modulus of elasticity)	ASTM C469	5×10^6 psi $\leq E_c <$ 6×10^6 psi	6×10^6 psi $\leq E_c <$ 7×10^6 psi	7×10^6 psi $\leq E_c$
Drying Shrinkage (S = microstrain)	AASHTO T 160 (ASTM C157)	$800 > S \geq 600$	$600 > S \geq 400$	$400 > S$
Creep (C = microstrain/pressure unit)	ASTM C512	$0.52/\text{psi} > C \geq 0.38/\text{psi}$	$0.38/\text{psi} > C \geq 0.21/\text{psi}$	$0.21/\text{psi} \geq C$

Furthermore, the Ohio DOT implemented a specification in which contractors must warrantee the performance of bridge decks based on spalling, scaling, and cracking criteria (Welter 2009). Contractors were required to perform remediation actions depending on the severity and extent of defects found during the two years following completion of construction, as summarized in

Table 4. Irrespective of the specification followed, the literature suggests that constant communication between owners, contractors, suppliers, and testing personnel is essential to the success of low cracking bridge decks (Browning et al. 2009, Darwin et al. 2010, McLeod 2010).



Figure 4. Assigning performance grades in performance related specifications (Radlinska and Weiss 2012)

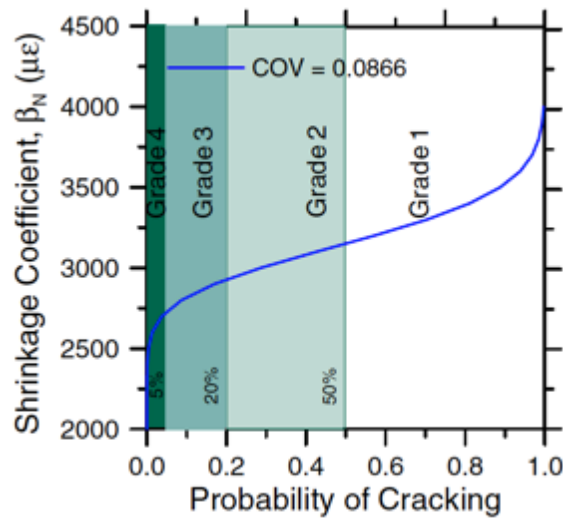


Figure 5. Allocating performance grades in shrinkage-based design approach (Radlinska and Weiss 2012)

Table 4. Contractual specifications based on bridge deck performance (Welter 2009)

Defect Found during Review	Required Remedial Action
Alligator or map cracking on 20% or less of deck area	Apply high molecular weight methacrylate resin (HMWM)
Alligator or map cracking on greater than 20% of deck area	Hydrodemolition of the surface of the entire deck, 1 in. deep and the placement of nominal 1 in. inlay with either latex modified concrete (LMC) or microsilica modified concrete (MSC)
Scaling less than 1/4 in. deep but greater than 1/8 in. deep and no more than 20% of deck area	Grind the defective area, saw cut transverse grooves, and seal the surface with non-epoxy sealer
Scaling greater than 1/4 in deep or spalling less than 32 yd ²	Diamond saw cut perimeter, hydrodemolition 1 in. deep, patch with LMC or MSC, and seal edges with HMWM
Scaling is more than 20% of deck area or spalling greater than 32 yd ²	Hydrodemolition of the entire deck 1 in. deep and place LMC or MSC

In addition to specifications, the contractor chosen for a particular project can significantly influence the performance of concrete bridge decks. McLeod et al. (2009) found that the average crack density varied from 0.027 to 0.2 ft/ft² for bridge decks constructed by different contractors. Similarly, Lindquist et al. (2005) studied the influence of the contractor on bridge deck overlay performance and found the average crack density to vary from 0.082 to 0.173 ft/ft² for silica fume overlays and from 0.07 to 0.249 ft/ft² for conventional overlays using several different contractors. McLeod et al. (2009) also researched the correlation of crack density with contractor experience, in terms of number of deck placements, but were unable to draw conclusions due to the number of parameters that influence each placement.

1.2 Effect of Cracks on Durability and Long-Term Performance of Concrete Bridge Decks

This section presents the deterioration processes related to concrete bridge decks and how cracks can reduce the service life by accelerating such processes. The durability of cracked concrete depends mainly on the effect of cracking on mass transport (e.g., moisture and chloride penetration) inside concrete, and on the corrosion rate of reinforcing steel. Literature regarding these topics is reviewed and the main findings are summarized. Furthermore, this section presents the existing modeling tools for prediction of the long-term performance of concrete decks. The models consist of two different types: (1) Service life models, which simulate the deterioration rate of concrete materials (i.e., micro-scale models) and (2) Performance prediction models, utilized by bridge management systems, which estimate the deterioration rate of the bridge deck as a whole (i.e., macro-scale models).

1.2.1 Deterioration mechanisms in reinforced concrete structures

Several mechanisms can cause degradation of reinforced concrete structures, including corrosion of reinforcing steel, freezing and thawing action (including deicing salt scaling), alkali-aggregate reaction (ASR), and sulfate attack (including physical salt crystallization damage, and chemical sulfate attack) (Mindess et al. 2003). Among these, corrosion of reinforcing steel is considered to be the most common cause of bridge deck deterioration, leading to the need for frequent maintenance and repairs (Virmani and Clemena 1998). In this section, the general mechanism of steel corrosion in concrete is presented. This is further linked, in the next section, with the effect of cracks on the initiation and propagation of corrosion damage. It should be noted that the corrosion mechanisms are similar in black versus epoxy-coated rebars. However, the main influence of epoxy coating is to protect the rebar surface and as such, much higher chloride concentrations are needed to initiate corrosion in epoxy-coated bars in comparison with black rebar. In addition, intact epoxy coating can electrically insulate the surface of rebar and as such, reduce the rate of electrochemical corrosion.

Corrosion causes a loss in the effective cross sectional area of rebar and a reduction in the bond between concrete and rebar. This leads to a reduction in load bearing capacity, serviceability problems (e.g., increased deformation and cracking), as well as possible failure and collapse. The resulting rust has a low density and can occupy up to 6 times more volume than the original steel (Bertolini et al. 2004). This expansion causes tensile stress development in concrete, which can lead to cracking and spalling of the concrete cover (PCA 2011).

The process of steel reinforcement corrosion is an electrochemical reaction and can be separated into anodic and cathodic reactions, as illustrated in [Figure 6](#). At the anode, iron oxidizes which results in the release of electrons and ferrous ions (Fe^{2+}). At the cathode, the electrons reduce water and oxygen and generate hydroxyl ions (OH^-). These ions then travel through the pore network of concrete and react with the ferrous ions and form ferrous hydroxide ($Fe(OH)_2$). In the

presence of oxygen and water, ferrous hydroxide converts to ferric hydroxide ($Fe(OH)_3$), which is a form of hydrated ferric oxide ($Fe_2O_3 \cdot nH_2O$), commonly known as rust. Unhydrated ferric oxide (Fe_2O_3) is approximately twice the volume of steel and can swell even more as it hydrates (PCA 2011).

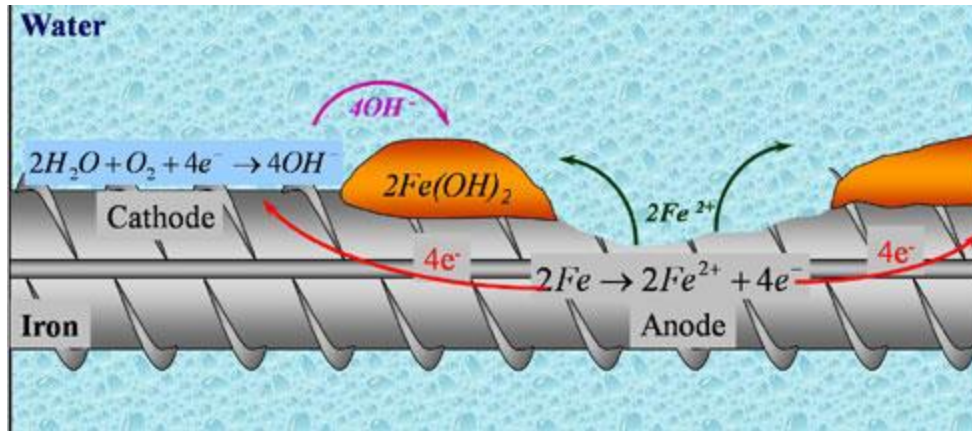
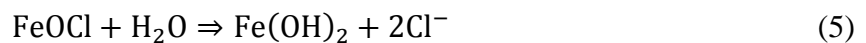
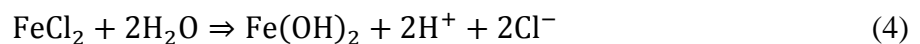


Figure 6. Reactions involved in the corrosion process of steel reinforcement (PCA 2011)

After the initiation of corrosion, due to the alkaline environment of the concrete, a thin but dense oxide layer (known as the passive layer) forms on the surface of the rebar. This passive layer prevents further corrosion by limiting the steel's access to oxygen and water (Mindess et al. 2003). Two types of mechanisms can destroy the protective passive layer in concrete: carbonation (i.e., reaction with ambient CO_2) and chloride attack. Carbonation-induced corrosion is not of much concern in bridge decks, and as such the focus of this section will be on chloride-induced corrosion. Equations 2-5 show the process in which chloride ions react with iron ions. These reactions remove the iron ions from the steel passive surface, causing an unstable and porous passive layer (Mindess et al. 2003).



In this process, the chloride ions are recycled and so the attack can continue. However, as long as the chloride concentration remains below a critical threshold, the passive layer can effectively restore itself when high pH (alkalinity) of concrete pore solution is maintained. The critical chloride threshold is defined as the chloride concentration in concrete at the level of rebar, which is required to depassivate the steel and restart the corrosion. This threshold value varies based on factors such as the type of reinforcement (uncoated or coated), temperature, cement composition and alkalinity, concrete w/cm and cement content, use of supplementary cementitious materials (SCM), and surface roughness of steel. Generally accepted chloride threshold values range between 1.0 and 2.0 lbs/yd³ of concrete for uncoated black steel reinforcement (Darwin and

Browning 2005) and are believed to be between 3.6 to 7.5 lbs/yd³ of concrete (Fanous et al. 2000) for other types of steel reinforcement (e.g., epoxy coated rebar).

In general, the corrosion process of reinforced concrete can be divided into two separate phases, corrosion initiation and corrosion propagation, as shown in Figure 7. During the initiation phase, chloride ions penetrate from the surface through the concrete cover, to reach the level of rebar. Chloride concentrations increase with time, however the reinforcement remains passive as long as the chloride concentration at the rebar level remains below the threshold necessary to depassivate the steel. Once the chloride threshold is surpassed, the rebar's passive layer is substantially degraded and the active corrosion propagation phase begins. The propagation phase ends when the consequences of corrosion (i.e., safety and serviceability concerns) can no longer be tolerated, and maintenance actions are necessary. The duration of the initiation phase depends primarily on the concrete cover thickness, chloride penetration rate (related to concrete porosity and diffusion coefficient), and the critical chloride threshold required to depassivate the steel. The corrosion rate during the propagation phase (e.g., slope of the line in Figure 7) depends on concrete's porosity and electrical resistivity, moisture content, oxygen availability, and temperature (Mindess et al. 2003).

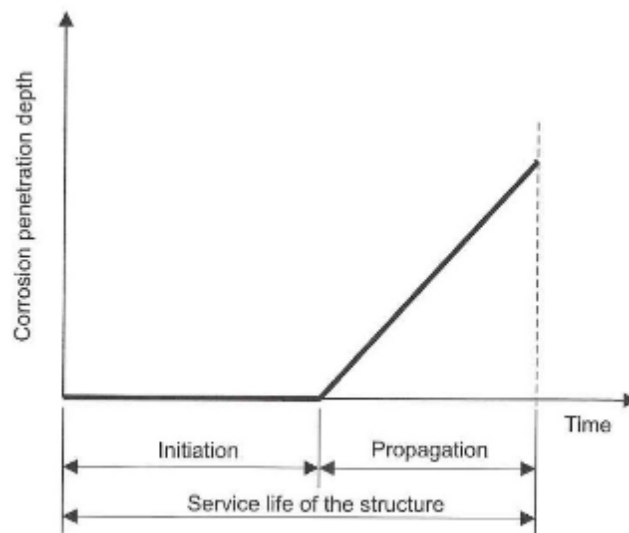


Figure 7. Initiation and propagation phases for corrosion in reinforced-concrete structure (Tuutti 1982)

Various protective systems (e.g., epoxy coated rebars, galvanized rebar, low slump concrete, waterproof membrane, overlays) can be used to extend the initiation period which results in the extended service life of the bridge deck. The following are some of the main findings of the #85-17 Bridge Deck Protective Systems Report (Malasheskie et al. 1988):

- Rebar coatings (i.e., epoxy-coated and galvanized rebars) are the most effective corrosion protection and can substantially increase the duration of the corrosion initiation period,

- Overlays can increase service life of a bridge deck if they are applied during the initiation period. Once the propagation phase begins their effect becomes less significant,
- Latex modified concrete overlays provide the best overall performance in terms of extending service life (i.e., duration of initiation phase) out of all overlay types.

Figure 8 shows an illustrative and schematic representation of factors that affect the corrosion rate of reinforcing steel (Scott and Alexander 2007, Otieno et al. 2010a). The availability of oxygen at the rebar level decreases with an increase in the cover depth, as represented by the ACE curve. This curve is also used to represent the corrosion rate because the cathodic reaction rates depend directly on the availability of oxygen. Corrosion is an electro-chemical reaction. As such, another factor that can limit the maximum corrosion rate is concrete electrical resistivity. The “PC resistivity” and “SCM resistivity” lines in Figure 8, which can be slanted to account for the variation in resistivity with cover depth, show how the maximum possible corrosion rate can be limited. For example, the maximum corrosion rate for PC (Portland cement) is determined by the BCE line and for concrete with SCM (supplementary cementitious material) is determined by the DE line.

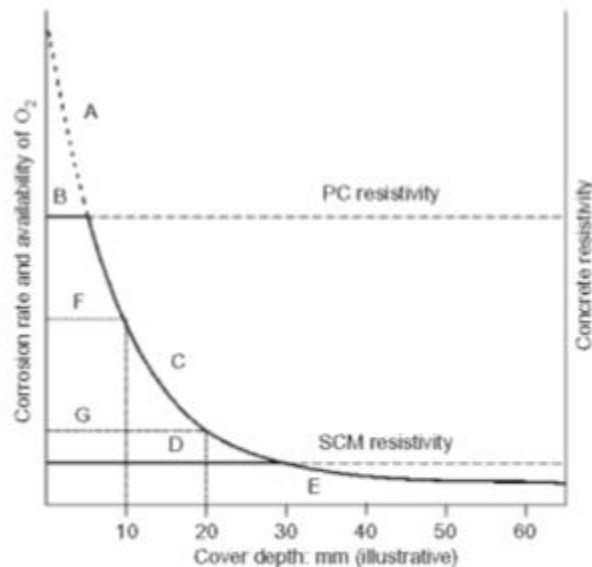


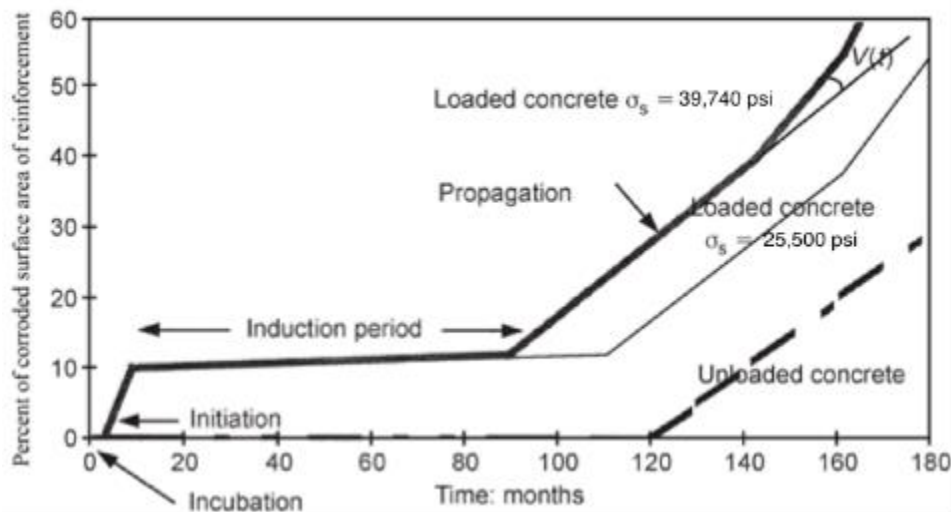
Figure 8. Schematic diagram of the relationship between corrosion rate, oxygen availability and resistivity (PC: ordinary Portland cement, SCM: supplementary cementitious materials) (Scott and Alexander 2007)

Concrete mass transport properties, such as water permeability and chloride ion diffusivity, significantly affect its durability against chloride ion penetration and the resulting corrosion. When the concrete cover is saturated (with respect to moisture), chloride ions can penetrate from the concrete surface towards the rebar by ionic diffusion through the concrete porosity or through cracks. In a dry concrete cover, in addition to diffusion, the water absorptivity and permeability of concrete also control the rate of chloride penetration; as moisture containing chlorides penetrates

into concrete. The diffusion mechanism is dominant at high degrees of saturation compared to the permeation mechanism (Richardson 2002). Cracking can accelerate both permeation and diffusion mechanisms, and the resulting steel corrosion, as described in the following sections.

1.2.2 Effect of cracking on corrosion of reinforcing steel

In cracked reinforced concrete, the corrosion initiation and propagation phases can be extended to four individual phases (Francois and Arliguie 1994). Figure 4 schematically illustrates these four phases and the percentage of corroded reinforcement area during the service life of cracked reinforced concrete. In Figure 9, the thin solid line represents a cracked concrete under flexural loads, the thicker solid line represents cracked concrete with higher flexural loads, and the dotted line represents uncracked concrete. The higher loads resulted in an increase in both surface cracks (crack widths and density) and bulk micro-cracks for the specimens that were evaluated (Francois and Arliguie 1994). As illustrated in Figure 7 and Figure 9, the corrosion process for uncracked reinforced concrete consists only of two phases, initiation and propagation (Tuutti 1982). However for cracked concrete, the “initiation” period is essentially divided into three separate phases: incubation, initiation and induction, as described below. For the cracked model (Francois and Arliguie 1994), the incubation and initiation phases are typically shorter than one year, and so the time to start of corrosion propagation depends mainly on the “induction” period.



[No metric units, how will protective systems affect this timescale?]

Figure 9. Schematic modeling of the corrosion process for cracked (loaded) and un-cracked (unloaded) concrete, (Francois and Arliguie 1994, Tuutti 1982)

- a) Incubation- Chloride ions penetrate through existing cracks to reach the level of steel reinforcement,
- b) Initiation- Chloride ion concentration reaches the critical threshold values at the level of rebar at the location of cracks and corrosion begins. The corrosion occurs along steel

reinforcement, in areas where steel have debonded from concrete (due to bleeding or mechanical debonding),

- c) Induction- Rust products form and seal the cracks and void spaces in debonded areas. Due to the sealing of cracks, the rate of corrosion is greatly reduced (Schiessel and Raupach 1997, Schiessel 1995). The volume of rust products in this phase is not enough to cause further cracking. This period ends when additional chloride ions penetrate through the uncracked concrete cover and critical chloride threshold values are reached at uncracked areas,
- d) Propagation- Corrosion restarts when most of the concrete cover is contaminated by chloride ions and the chloride concentrations at the rebar level exceed the critical threshold. Afterwards, the development of rust products causes tensile stress development, leading to secondary cracking and spalling of the concrete cover (Mindess et al. 2003). The end of the propagation phase represents the end of service life (i.e., the point in time when the extent of corrosion deterioration can no longer be tolerated due to safety or serviceability concerns). The extent of allowable deterioration, before any repair or replacement becomes necessary, is discussed in later sections (Section 1.4.2)

Figure 9 shows that corrosion propagation begins earlier in cracked concrete and for higher loads. In other words the “induction” period is shorter for higher loads because they increase the micro-cracking at the paste-aggregate interface and at the steel-concrete interface. These micro-cracks result in increased penetration rate of chloride ions through the concrete cover and can significantly decrease the time to start of corrosion propagation (Francois and Arliguie 1994). Similarly, wide surface cracks can facilitate faster penetration of chlorides and reduce the time to start of corrosion propagation. Furthermore, the defects or damages that are present at the concrete-steel interface also reduce the critical chloride threshold required for corrosion propagation (Buenfeld et al. 2004, Nygaard 2003, Nygaard and Geiker 2005). Once active corrosion starts, the rate of corrosion (i.e., the slope of the propagation lines in Figure 9) depends to a lesser extent on the cracking and microcracking condition of the concrete. As discussed before, the corrosion propagation rate primarily depends on concrete’s porosity and electrical resistivity, moisture content, oxygen availability, and temperature. Cracking can influence the propagation rate only when it affects one of these parameters.

The effects of crack size (e.g., crack width and effective depth), frequency and location on the time to corrosion propagation and the corrosion propagation rate are discussed further in the following paragraphs. As shown in Figure 10 and Figure 11, cracks clearly affect chloride concentrations at the location of cracks. Uncracked regions of bridge decks remain below the critical chloride threshold for corrosion propagation for many years. Whereas, at cracked sections, the majority of bridge decks exceed critical chloride thresholds within 2 years from construction (Lindquist et al. 2005, 2006). Figure 10 and Figure 11 highlight the significant difference in the chloride concentration levels at the rebar level (3.0in = 76.2mm) for adjacent cracked and uncracked

regions of bridge decks during the first 20 years after construction. In these figures, the 0.6 kg/m^3 (1.01 lbs/yd^3) limit is assumed to be the critical chloride threshold for the bridge decks.

Furthermore, the majority of available literature suggest that an increase in surface crack density and crack width reduces the time to start of corrosion propagation (Schiessel and Raupach 1997, Sagues et al. 2001, Berke et al. 1993, Francois and Arliguie 1999, Arya and Wood 1995, Beeby 1983, Bentur et al. 1997, Pettersson and Jorgensen 1996, Scott and Alexander 2007, Suzuki et al. 1990, Danilecki 1969, Otieno et al. 2010a,b). Qi et al. (2003) studied the effect of plastic shrinkage cracking using an accelerated corrosion test setup. They reported that, as crack width increased from 0.0098 to 0.0197 inches, corrosion propagation started earlier (from 50 to 15 days). Li (2001) studied the effect of crack width on the time to corrosion propagation for concrete beams which experience cycles of wetting and drying using 3.5% NaCl solution (Figure 12). For these specimens, the initiation time (i.e., time to start of propagation phase) significantly decreased until a crack width of 0.1 mm (0.004 in). The decrease of initiation times becomes more moderate for crack widths larger than 0.004 in.

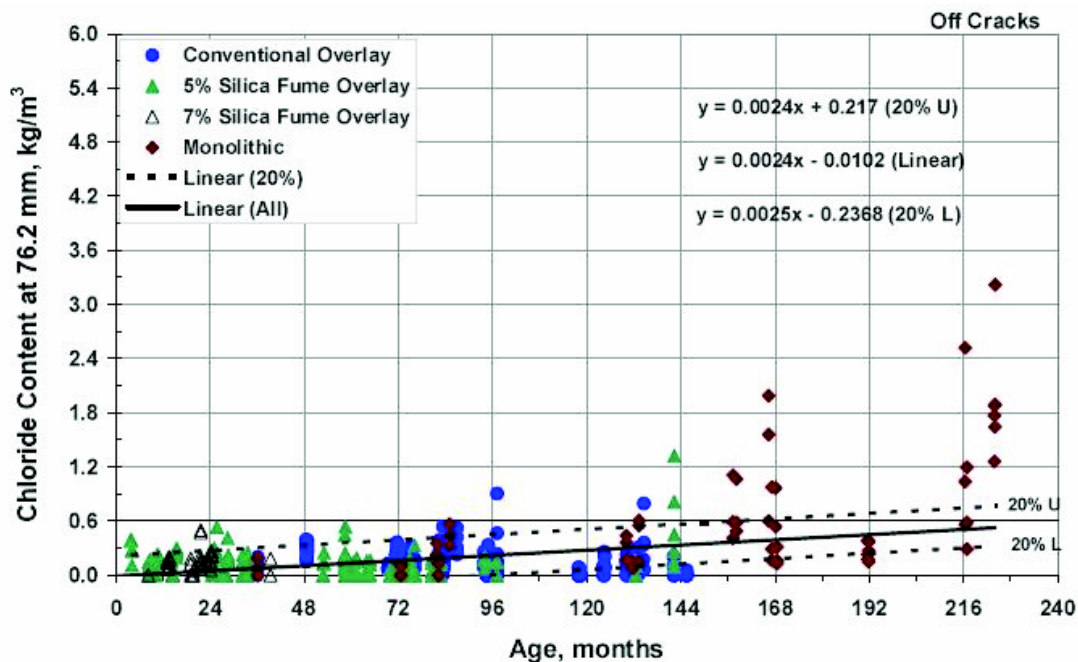


Figure 10. Chloride content at the rebar level ($3.0 \text{ in} = 76.2 \text{ mm}$) taken from uncracked regions of bridge decks versus age, $1 \text{ kg/m}^3 = 1.69 \text{ lbs/yd}^3$. (Lindquist et al. 2005)

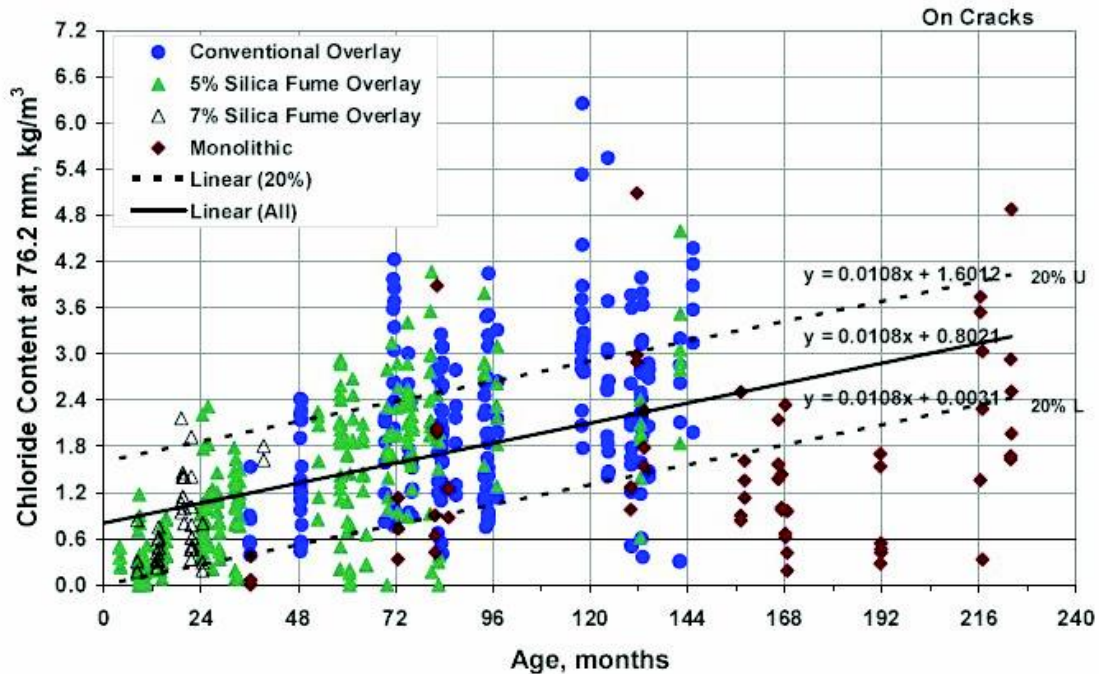


Figure 11. Chloride content at the rebar level (3.0in = 76.2mm) taken from cracked regions of bridge decks versus age, $1\text{kg/m}^3=1.69\text{lbs/yd}^3$ (Lindquist et al. 2005)

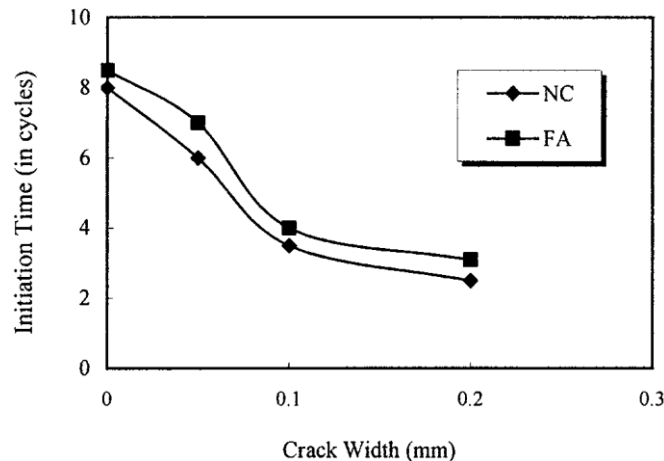


Figure 12. Initiation times (time to start of propagation phase) for cracked NC (normal cement) and FA (fly-ash blended) concrete beams, $0.1\text{ mm} = 0.00394\text{ in.}$ (Li 2001)

However, there are two schools of thought regarding the effect of crack width on corrosion propagation rate. Several studies argue that there is no correlation between crack width and the rate at which corrosion products develop in reinforced concrete (Schiessel and Raupach 1997, ACI 1985, Sagues et al. 2001, Berke et al. 1993, Francois and Arliguie 1999, Arya and Wood 1995, Beeby 1983, Bentur et al. 1997). These studies state that cracks may reduce the time to corrosion propagation, but have no effect on the rate of corrosion propagation (i.e., steel loss as a function of time). This can be explained by the sealing of cracks by the corrosion products during the induction phase, as illustrated in Figure 9 (Francois and Arliguie 1994). On the other hand, some

researchers have shown that larger crack widths ($> 0.0039\text{-}0.0157$ in.) do in fact increase the rate of corrosion during the propagation phase (Pettersson and Jorgensen 1996, Scott and Alexander 2007, Suzuki et al. 1990, Danilecki 1969, Otieno et al. 2010a,b). Overall, factors other than crack width (e.g., concrete quality, cover thickness, crack frequency, and type of rebar (coated or uncoated)) seem to dominate the corrosion propagation phase (Schiessl and Raupach 1997; Mohammed et al. 2002). The influence of concrete crack width, if any, diminishes with time (Schiessel 1976, Otieno et al. 2010a, 2010b, Schiessl and Raupach, 1997).

Otieno et al. (2010a,b) conducted an extensive investigation to evaluate the combined effect of crack width and concrete quality (represented as binder type and w/b ratio) on the corrosion rate of reinforcement during the propagation phase. [Figure 13](#) shows their results. They found that the presence of cracks increase corrosion rate, but the extent depends on the interaction of crack width, concrete quality and electrical resistivity. The following conclusions were made:

- Better quality concrete (i.e., lower w/b ratio, use of slag) can reduce the corrosion rate of cracked concrete,
- Even incipient cracks can greatly influence the corrosion rate, contradicting studies which state that crack widths below a certain threshold have no major effect on corrosion rates,
- Concretes containing ground granulated slag were found to be less prone to the accelerating effect of cracking on corrosion, in comparison with ordinary portland cement (OPC) concretes. This was attributed to a high electrical resistivity of concrete with slag, which tends to control the corrosion rate,
- Reloading of structures which are currently corroding was found to accelerate the corrosion by: reopening the self-healed cracks, increasing the loading level (i.e., stress in steel), widening existing cracks, and damaging aggregate-paste and concrete-steel interfaces.

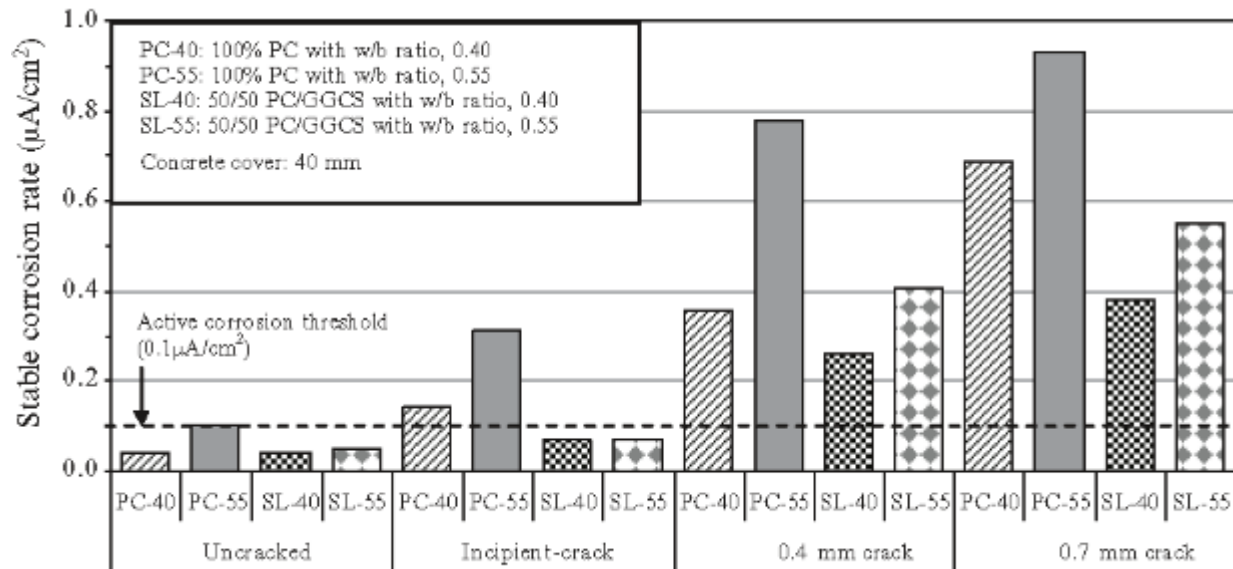


Figure 13. Effect of concrete quality and crack width on steel corrosion rate for PC (portland cement) and GGCS (ground granulated Corex slag) concrete specimens (Otieno et al. 2010a,b)

The cover thickness has also been found to affect the corrosion rates of cracked concrete (Scott and Alexander 2007). This is because an increased cover reduces the availability of oxygen at the reinforcement level by increasing the thickness which oxygen must pass through. This effect largely depends on the type of binder used, as shown in Figure 14. There is a dramatic reduction in corrosion rate for PC (Portland cement) concrete when concrete thickness is doubled from 0.787 to 1.575 in. However, increasing the concrete cover had a much smaller effect on the corrosion rate of concretes containing supplementary cementitious materials (SCMs). Scott and Alexander (2007) believe that the effect of cover thickness would have been equal for all the specimens; however, PC specimens show particular sensitivity because they have higher corrosion rates and thus require higher oxygen levels.

The crack frequency of concrete specimens also affects the corrosion rate of reinforcement. Arya and Ofori-Darko (1996) found that higher crack frequency (i.e., number of cracks in a specific length of specimen) results in increased corrosion, as shown in Figure 15. They also suggested that, since thicker concrete cover results in fewer (flexural) cracks, the frequency of cracks is a more fundamental factor which influences the amount of corrosion. They concluded that limiting the frequency of cracks intersecting the steel, instead of reducing surface crack widths, can be a more effective way to reduce corrosion.

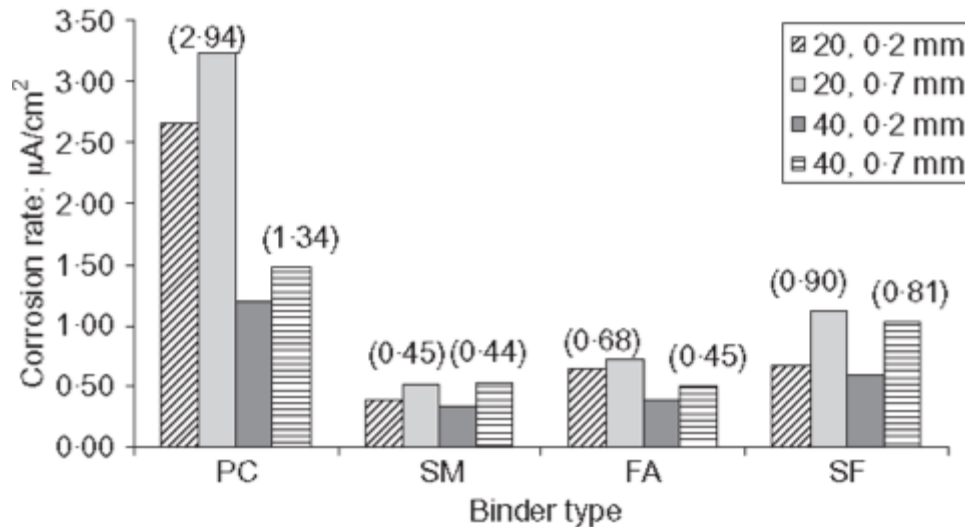


Figure 14. Effect of cover thickness (20 or 40 mm, 0.7874 to 1.5748 in.) on corrosion rates for PC (Portland cement), SM (50% slag replacement), FA (30% fly ash replacement), SF (7% condensed silica fume replacement) concrete specimens. (Values above the bars are averages for the two crack widths for the relevant cover depths) (0.2 or 0.7mm in the legend indicate crack widths; equivalent to 0.0079 to 0.0276 in.) (Scott and Alexander 2007)

Pease (2010) found that the damage (i.e., slip and separation due to flexural loads, settlement cracking) along the concrete-steel interface could lead to an increased probability of corrosion and higher propagation rates. If the damage at the steel-concrete interface is found to dominate the corrosion rate, current attempts at controlling surface cracks might not be as effective as previously believed. Mohammad et al. (2002) found that, in order to ensure long-term durability of reinforced concrete, not only surface cracks but also the voids present at the steel-concrete interface must be taken into consideration. Such voids are usually due to the settlement of plastic concrete as well as collection of bleed water underneath rebar. Generally, these voids form below horizontal steel bars, which are perpendicular to the casting direction. However, such voids can exist for bars oriented along the casting direction as a result of poor compaction (Mohammad et al. 2002).

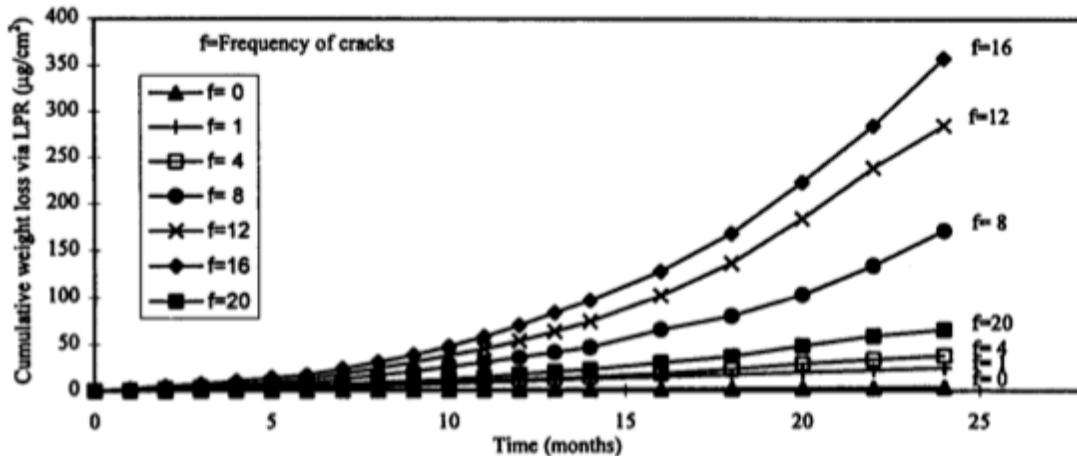


Figure 15. Effect of crack frequency on the cumulative weight loss due to corrosion based on linear polarization resistance (LPR) test, $1 \mu\text{g}/\text{cm}^2 = 0.1422 \mu\text{lb}/\text{in}^2$ (Arya and Ofori-Darko 1996)

Furthermore, Francois and Arliguie (1999) showed that the formation of microcracks, due to mechanical loads, can have a more significant effect on the initiation and propagation of corrosion, compared to surface cracks. Load-induced microcracking can affect the corrosion process in two ways. Firstly, due to the paste-aggregate interface damage, an increase in chloride penetration can be observed. Secondly, the steel-concrete interface damage can increase corrosion development on the tensile reinforcement. In order to account for the effect of microcracking, Francois and Arliguie (1999) suggested incorporating stress magnitudes (σ) with conventional parameters such as chloride diffusion coefficient of concrete (D) to estimate service life of reinforced concrete structures.

The crack depth, location and direction (parallel or perpendicular to rebar), and self-healing of cracks are also important parameters, which affect the corrosion of reinforcing steel. These effects are summarized below:

- A deeper and wider crack results in an increase in the percentage of surface area of steel that is exposed to corrosion for both coated and bare steel reinforcement (Sansone and Brown 2007),
- Cracks parallel to the reinforcement result in the largest amounts of corrosion, particularly when the cracks are located directly above the reinforcement. Cracks parallel but partly above the reinforcement contribute less to corrosion compared to those directly above; however they still cause more corrosion compared to perpendicular cracks (Sansone and Brown 2007, Mindess et al. 2003),
- The gradual self-healing of cracks as a result of calcite precipitation (further explained in section 2.4), can significantly reduce the permeability of cracked concrete, and can improve the protection of reinforcement against corrosion (Neville 2002).

In general, research regarding the combined effect of crack characteristics (e.g., width, density) and other concrete properties (e.g., type of concrete, cover thickness, type of reinforcement) on the

corrosion initiation and propagation of reinforcement in concrete has been limited and somewhat inconclusive. However, for the design of reinforced concrete structures, the maximum allowable crack width (line AC in Figure 16b) should be defined as the crack width, which is tolerable in terms of corrosion, by considering both cover depth and concrete quality (Otieno et al. 2010a). Figure 16 schematically illustrates the effect of crack width on the corrosion rate after considering other factors. Once a maximum crack width is defined, corrosion rates between zero (uncracked) and the maximum crack width can be found by using interpolation.

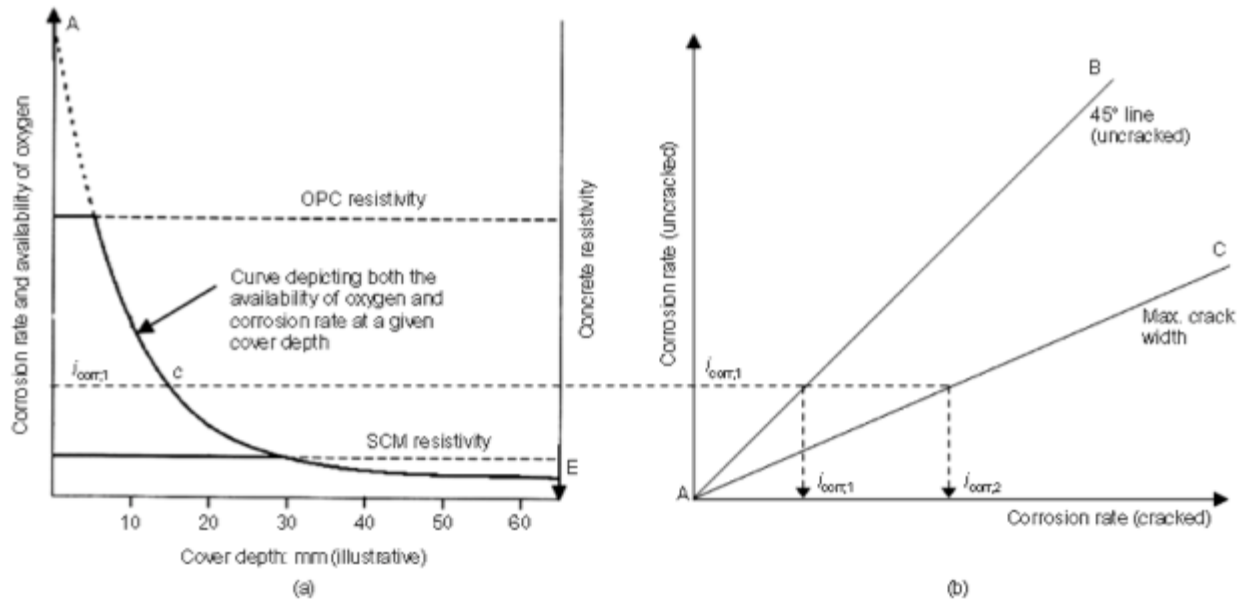


Figure 16. Schematic diagram of the relationship between corrosion rate, oxygen availability and resistivity, to account for crack width (PC: ordinary Portland cement, SCM: supplementary cementitious materials) (Otieno et al. 2010a)

In order to efficiently design reinforced concrete structures to ensure long-term durability, factors such as crack width, crack density, concrete quality, and crack reopening must be taken into consideration. Service life models should be modified accordingly to incorporate the combined effect of these factors, so as to provide predictions with higher accuracy. However, further studies are needed to obtain such a level of detailed design approach because of the many variables and uncertainties that are involved in such prediction models.

1.2.3 Effect of cracking on other deterioration mechanisms in concrete

Few studies have evaluated the effect of cracking on freezing and thawing (F-T) performance of concrete. Yang et al. (2004) assessed the influence of tensile damage (cracking and microcracking) on the freeze-thaw durability of concrete. Instead of measuring crack width or density, they characterized the damage (i.e., cracking) in concrete using acoustic emission (AE). They conducted cyclic freezing and thawing on sealed cracked specimens and used the relative dynamic elastic modulus (E/E_0 , ratio of the dynamic modulus at n^{th} F-T cycle over dynamic modulus at 0^{th}

cycle) to assess the extent of F-T damage. Figure 17 shows the results. The estimated stress level is calculated by dividing the stress at the point of interest by the maximum stress (i.e., stress at failure). The estimated strain level is calculated by dividing the strain at the point of interest by the maximum strain (i.e., strain at failure). The cumulative AE energy level was calculated by dividing the cumulative energy level at the stress level of interest by the maximum cumulative AE energy. The damage index (DI) combines the stress level, strain level, and cumulative energy level. DI represents the extent of load-induced damage (e.g., cracking and microcracking) after initial tensile loading of each specimen. The results show that specimens with higher estimated stress or higher damage indexes, tended to deteriorate at earlier ages (i.e., an earlier decline in the relative modulus). They also found that concretes with smaller number of wide and localized cracks are less durable than concretes with higher-density and narrower cracks.

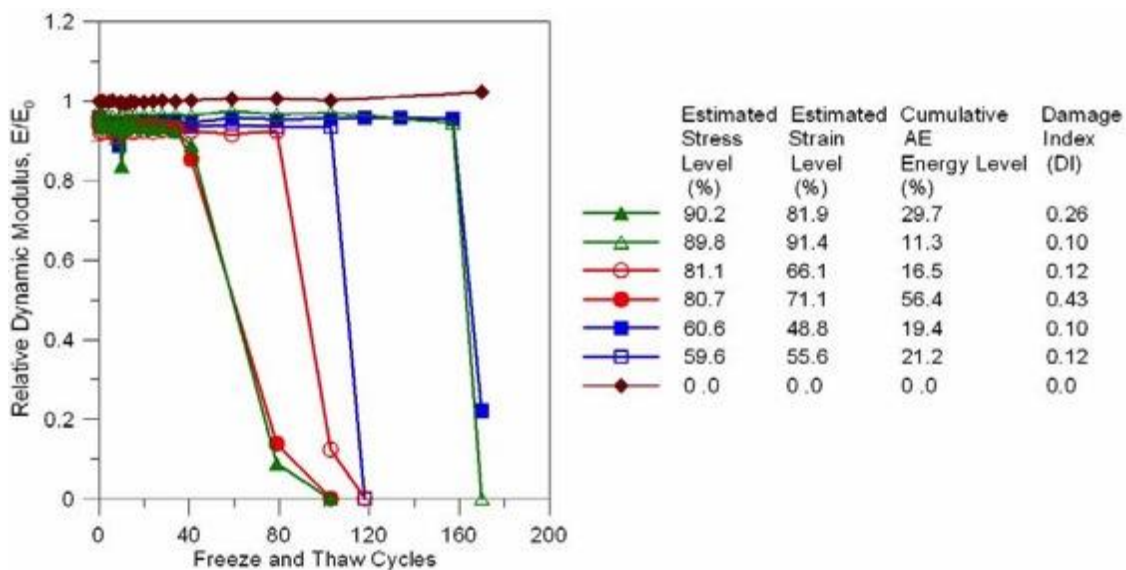


Figure 17. Degradation of dynamic modulus of elasticity of concrete with different load induced damage undergoing freezing and thawing test (Yang et al. 2004)

To the authors' knowledge, no studies have been reported in the literature on the direct effects of cracking on the alkali-aggregate reaction (AAR) or sulfate attack in bridge decks. However, given that water plays a critical role in the mechanisms of these reactions, it is anticipated that cracking can facilitate faster deterioration by allowing increased penetration of water and aggressive substances into concrete (Aldea et al. 1999). A chain reaction of "deterioration → cracking → more permeable/penetrable concrete → further deterioration" can eventually lead to destructive deterioration, which can result in structural failure or degraded serviceability (Mehta 2006). Therefore, the inter-relationship between concrete cracking and its mass transport properties (i.e., moisture and ion transport) is of great significance and plays a key role in the durability of concrete structures (Yang et al. 2004, Wang et al. 1997). This is discussed in the next section.

1.2.4 Effect of cracking on mass transport in concrete

The two main types of mass transport that affect the long-term durability of concrete are water permeation and chloride ion diffusion. The water permeability of concrete can be measured by determining the rate of water flow through a concrete sample under a pressure gradient. Diffusion is defined by the movement of ions through pores from the surface to internal areas due to the difference in concentration levels. Chloride ions diffuse only when dissolved in pore water (Bertolini et al. 2004). Most of the research for mass transport has been conducted for saturated concrete and as such, this section only considers mass transport in the saturated state of concrete. Research regarding mass transport in unsaturated concrete is limited and in its early stages (Bastidas-Arteaga 2011, Poyet 2011).

Cracking can increase both the water permeability and chloride diffusion in concrete. Earlier research suggested that cracks smaller than 0.002 to 0.004 inches do not affect the water penetration in concrete, partly due to a higher likelihood of self-healing in these cracks. However, larger cracks significantly increase the concrete permeability as shown in Figure 18 (Lawler et al. 2002, Wang et al. 1997, Aldea et al. 1999a, Clear 1985, Rapoport et al. 2002, Reinhardt and Jooss 2003, Edvardsen 1999).

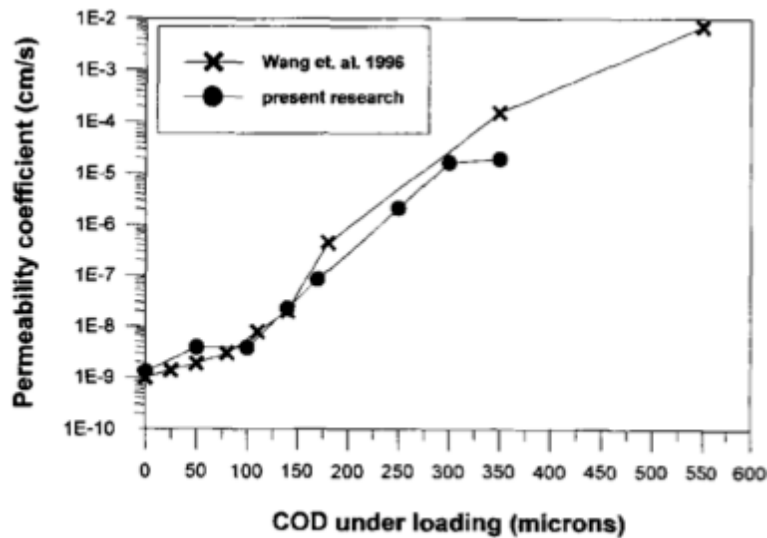


Figure 18. Effect of crack width under loading, which is represented as COD (crack opening displacement), on the water permeability of normal strength concrete, 100 microns=0.004in., 1 cm/s = 0.394 in./s (Aldea et al. 1999a, Wang et al. 1997)

Akhavan et al. (2012) evaluated the influence of crack width on the water permeability of cracks in plain and fiber-reinforced concrete. They found that the crack permeability is a function of crack width square and this trend agrees with theoretical predictions of laminar flow in smooth parallel plate gaps, as shown in Figure 19. However, the experimental values of permeability were found to be smaller than theoretical values by a factor of 4 to 6. This can be attributed to the effect of

crack tortuosity, crack surface roughness, and presence of fibers, which provide further friction against flow of water, and are not considered in the theoretical model.

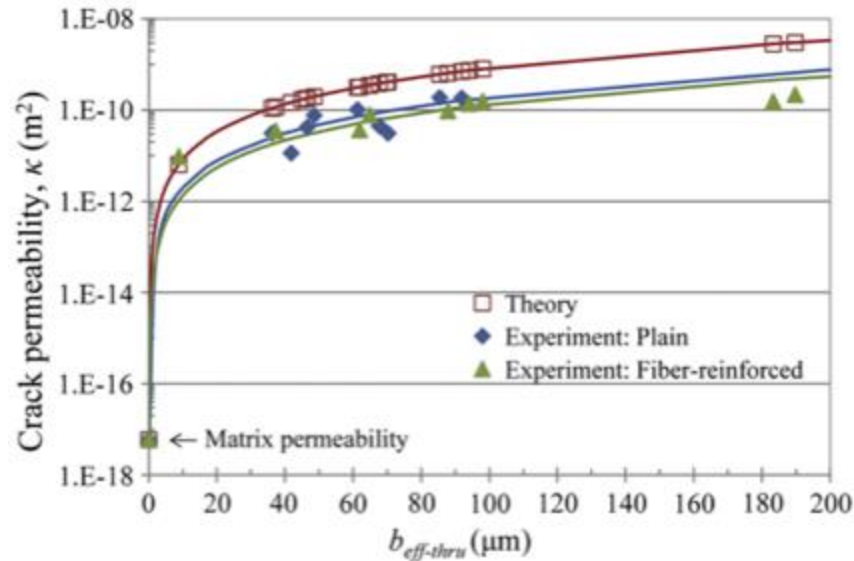


Figure 19. Theoretical and experimental values of crack permeability as a function of effective crack width, $100 \mu\text{m} = 0.004\text{in.}$ (Akhavan et al. 2012)

The majority of past studies have focused on the effect of dormant cracks on the water permeability of cracked concrete. Only a few studies (Desmettre and Charron 2013, Tawfiq et al. 1996) have focused on the effect of actively growing cracks (due to cyclic loading) on the permeability. These studies concluded that the cyclic loading of concrete in the presence of water resulted in two phenomena occurring: self-healing and crack propagation (i.e., increase in crack width, depth and length). Permeability due to such cracks can increase or decrease, depending on the relative importance of these two phenomena. In some cases (fiber reinforced concrete) the effect of self-healing overcame the damage due to cyclic loading.

The rate of chloride diffusion, which determines how fast chloride concentrations build up at the rebar level and reach the critical threshold, is dictated by concrete's diffusion coefficient. Diffusion coefficient is primarily related to concrete porosity, since ions can diffuse through water-filled pores but not through solids and air voids. Cracks when saturated can increase the diffusion coefficient by providing wide pathways for penetration of chloride ion. Aldea et al. (1999b) argued that diffusion is proportional to crack width, whereas, permeability is proportional to the square or cube of crack width (Wittke 1990). As such, the effect of crack width on the diffusion coefficient of concrete is less pronounced than the effect of crack width on permeability.

Several authors have defined a threshold crack width for chloride diffusion, below which cracks have little influence on ion diffusion coefficient of concrete (Gagne et al. 2001, Wang et al. 1997). The available literature considers this threshold to be between 0.002 and 0.0031 in. (Gagne et al.

2001, Djerbi et al. 2008). Above the threshold crack width, a linear correlation between crack width and the diffusion coefficient of cracked concrete has been found (Jacobsen et al. 1996, Aldea et al. 1999b). [Figure 20](#) (Djerbi et al. 2008) illustrates the effect of crack width of different types of concrete and shows the ratio of cracked diffusion coefficient to uncracked diffusion coefficient (D/D_0).

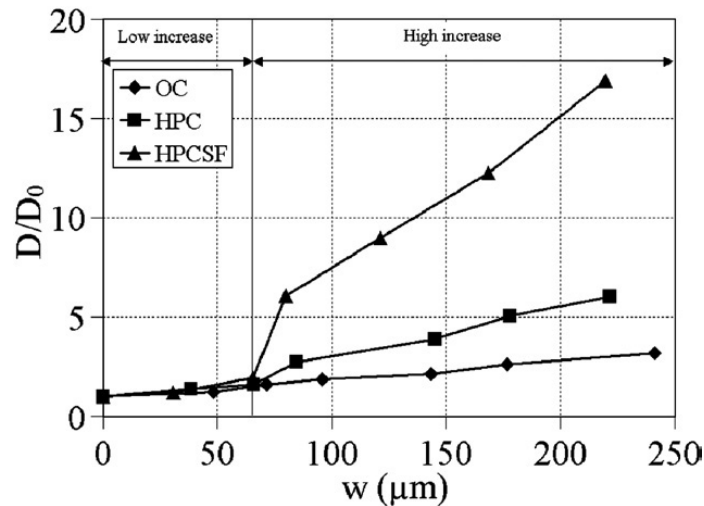


Figure 20. The effect of crack width on the ratio of diffusion coefficient of cracked concrete to uncracked concrete (D/D_0). The results are shown for OC (ordinary concrete), HPC (high performance concrete) and HPCSF (high performance concrete containing silica fume) $100 \mu\text{m} = 0.004\text{in.}$ (Djerbi et al. 2008)

[Figure 20](#) shows that the D/D_0 is lower for ordinary Portland cement concrete, which Djerbi et al. (2008) suggested is due to higher porosity and crack tortuosity of ordinary concrete compared to high performance concrete. Djerbi et al. (2008) believe that the effect of cracking on D/D_0 is more significant in denser materials, which have lower diffusion coefficient in uncracked state.

Recent research by Akhavan and Rajabipour (2013) suggests that the crack width could have minimal effect on the concrete diffusivity as long as the effect of crack tortuosity is accounted for. Instead they found that diffusivity is linearly related to the crack density or volume fraction (i.e., area fraction of cracks on the surface of a sample) as shown in [Figure 21](#). As a result, methods which reduce crack width (e.g., fiber reinforcement), but do not reduce the volume fraction of cracks, could have less benefits than previously anticipated for reinforced concrete (Akhavan and Rajabipour 2013).

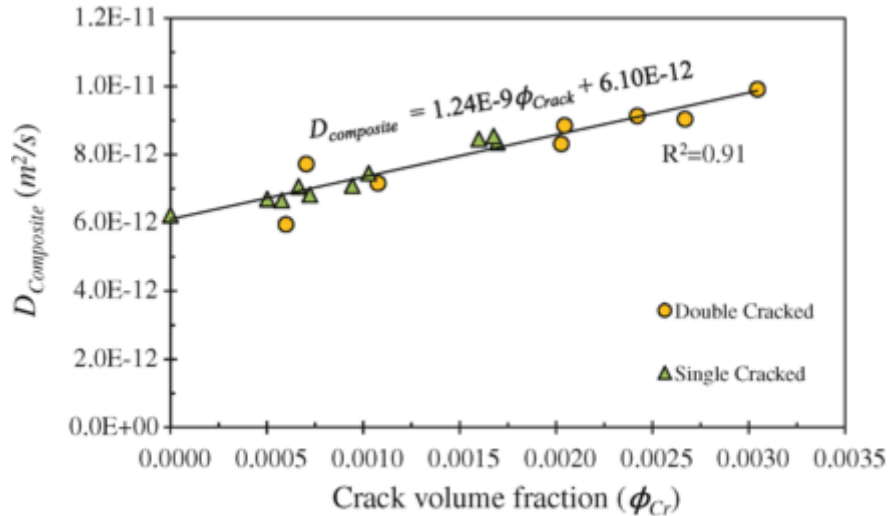


Figure 21. Estimated diffusion coefficient of cracked samples ($D_{composite}$) as a function of crack volume fraction, $1 \text{ m}^2/\text{s} = 10.764 \text{ ft}^2/\text{s}$ (Akhavan and Rajabipour 2013)

Mu et al. (2013) also found that the diffusion coefficient of water soluble chloride (WSC) varies linearly with the increase of crack density (i.e., feet crack length per square foot of surface), however, the same could not be concluded for acid soluble chloride (ASC) as shown in Figure 22. The diffusion of acid soluble chloride was found to increase exponentially until a crack density of 137.16 ft^{-1} and was constant for densities between 137.16 and 228.6 ft^{-1} .

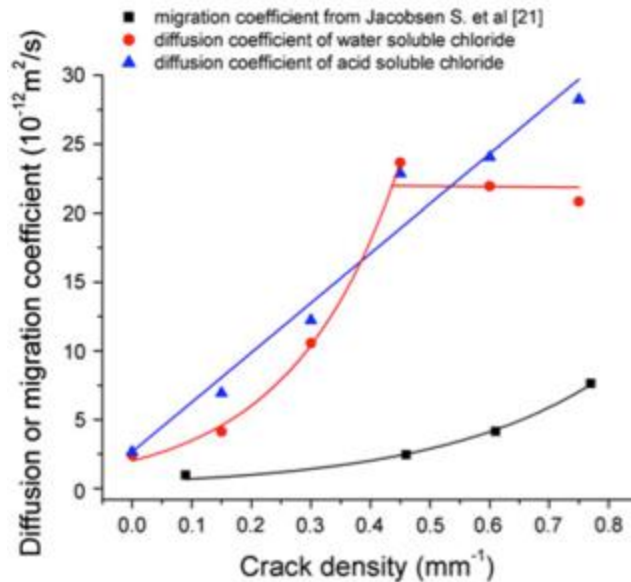


Figure 22. Effect of crack density on the diffusivity of water soluble chloride (WSC) and acid soluble chloride (ASC), $1 \text{ mm}^{-1} = 304.8 \text{ ft}^{-1}$, $1 \text{ m}^2/\text{s} = 10.764 \text{ ft}^2/\text{s}$ (Mu et al. 2013)

The self-healing of cracks can also affect the permeability and diffusion coefficient of cracked concrete. Self-healing refers to the concrete ability of healing cracks, which can involve processes

such as further hydration of cementitious material or the sealing of crack due to precipitation of calcite (calcium carbonate) (Jacobsen et al. 1998, Hearn 1998, Edvardsen 1999). Due to this phenomenon, minimally cracked concretes are potentially able to make a recovery of transport properties and become as durable as sound concrete. Li and Yang (2007) found that cracks can make a full recovery for crack widths below 0.002 in. and a partial recovery for crack widths between 0.002 and 0.006 in.

1.2.5 Modeling tools for prediction of long-term performance of concrete decks

The available modeling tools to predict the service-life performance of concrete bridge decks can be categorized into (1) service life prediction models and (2) performance prediction models. Service life models are based on the performance and deterioration of materials that are used in concrete bridge decks. Whereas the performance prediction models, which are used by bridge management systems, make holistic predictions about the deterioration state of a bridge deck at any given time. Service life models can be considered to be micro-scale (materials scale) whereas performance prediction models are macro-scale (structural scale).

1.2.5.1 Service life modeling

Several service life prediction models have been proposed to predict the durability of structural concrete and also estimate the time during which a concrete structure maintains a desired level of serviceability. The available models include DuraCrete (DuraCrete 2000), fib (fib Bulletin 34 2006), Life-365 (Ehlen et al. 2009, Life-365 Consortium II 2010), 4SIGHT (Synder 2001), HETEK (Nilsson et al. 1996, 1997; Frederiksen and Poulsen 1997), and STADIUM (SIMCO 2009). These models are mainly based on the simulation of rebar corrosion damage over time. The service life is assumed to be equal to the sum of the estimated duration of the corrosion initiation phase and the propagation phase until the tolerable level of corrosion is surpassed.

During the corrosion propagation phase, corrosion products expand within the concrete as the reinforcement cross-section reduces. The reduction in reinforcement cross section reduces load carrying capacity and can lead to structural failure, while the expansion of corrosion products results in cracking and spalling of the concrete cover. Despite extensive research on the effects of corrosion propagation for both reinforcement cross-section reduction (Hasegawa et al., 2004; Isgor and Razaqpur, 2006) and deterioration of concrete cover (Alonso et al., 1998; Liu and Weyers, 1998; Li, 2003; Vu et al., 2005; Ahmed et al., 2007; Li et al., 2008; Hwan Oh et al., 2009) various uncertainties still exist in predicting the propagation phase. This is because it depends on numerous factors including environmental conditions (temperature and relative humidity), loading conditions (dynamic or static), and change in material properties throughout years of service. As a result, service life models still require improvements in order to simulate time-dependent deteriorations of as-built reinforced concrete structures with higher accuracy. Most of the models are unable to consider the effect of cracking, as a result, they assume uncracked states for concrete. Due to the uncertainties involved in the propagation phase, the end of the initiation phase indicates

the end of the predicted service life for most of the available models. Some of the models are briefly described below:

Life-365 (Ehlen et al. 2009, Life-365 Consortium II 2010) does consider the propagation phase, however, the duration is not calculated based on user inputs. It is fixed and equal to 6 years for uncoated reinforcement and 20 years for epoxy-coated reinforcement. The user inputs for Life-365 (Life-365 Consortium II 2010) include geographic location, type of structure, nature of chloride exposure, thickness of concrete cover, water to cement ratio, type and quantity of admixtures (e.g., silica fume, fly ash, slag) and type of steel reinforcement and coatings. Richard's equation (Radcliffe and Simunek 2010) is used to model water flow and Nernst-Planck equation (Samson and Marchand 1999) is applied to describe ionic transport in unsaturated media.

STADIUM (SIMCO 2009), developed by SIMCO Technologies, can model unsaturated multi-ionic (OH^- , Na^+ , K^+ , SO_4^{2-} , Ca^{2+} , $\text{Al}(\text{OH})_4^-$, Mg^{2+} , Cl^-) transport in uncracked concrete. Inputs for material properties include: geometry of the concrete element, mixture proportion (such as type, quantities and densities of cement, supplementary cementitious materials, and aggregate), transport property (such as porosity, diffusivity, and conductivity) and exposure condition. The inputs for environmental conditions include: temperature, relative humidity, and exposure level.

4SIGHT (Synder 2001), developed by the U.S. National institute of standards and technology (NIST), can assess the durability of buried concrete structures. This model is similar to STADIUM but it also accounts for moisture flow within cracks and its effect on service life. Crack spacing, crack width, and crack depth can be input by the user. Alternatively flexural and shrinkage cracks can be predicted by the software based on simple structural analysis. This program provides concentration of various ions at any depth over a specified period of time as output. Cracks are modeled as smooth parallel walls with a gap equal to the observed crack width. Furthermore, tortuosity and roughness of cracks are not considered, as a result, the permeability is over-estimated.

Recent studies have used numerical modeling in order to consider the effect of cracking on the service life of concrete structures. Bentz et al. (2013) used software such as ANSYS and COMSOL to predict the service life of cracked concrete bridge decks. [Figure 23](#) shows the results of their proposed model which illustrates the effect of cracking on the reduction of the corrosion initiation period compared to uncracked bridge decks, based on the $C_{\text{rebar}}/C_{\text{ext}}$ (ratio of the chloride concentration at the surface of the bridge deck to the chloride concentration required to initiate corrosion at the rebar level). The highlighted area shows the typical range of $C_{\text{rebar}}/C_{\text{ext}}$ values (0.1-0.3) for the bridges in the field.

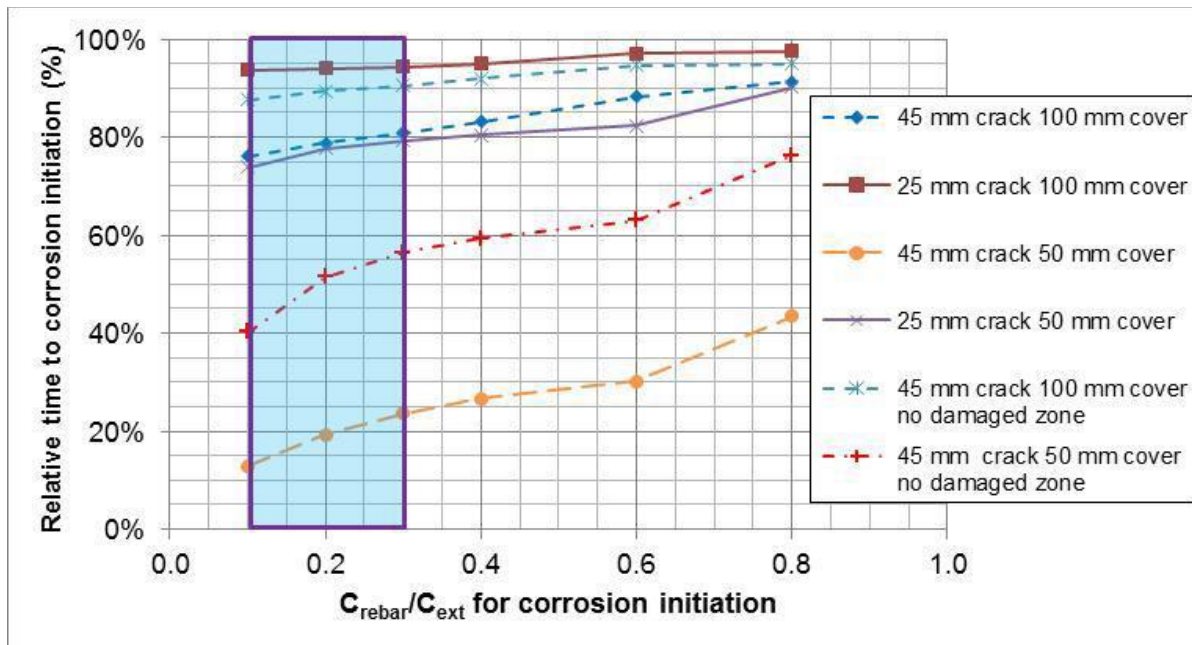


Figure 23. Predicted reductions in the corrosion initiation period for cracked concrete bridge decks (simulated using COMSOL by incorporating diffusion and binding) (Bentz et al. 2013)

1.2.5.2 Performance prediction models for bridge decks

Performance prediction models, also called deterioration models, play a significant role in determining the life-cycle cost of a bridge (Morcouc 2006). They estimate the deterioration rate using changes in the condition state over time, which are a measure of the condition of a bridge element and are assigned based on data obtained from bridge inspections. The deterioration model can be used to predict the service life of a deck and to determine when remediation actions should be performed. The role of deterioration models in bridge management systems is shown in Figure 24. Condition rating data is used as input for the models, which are capable of predicting future bridge performance and, in turn, allow transportation agencies to make bridge management decisions. Many forms of bridge management software, such as AASHTO's BrM (formerly Pontis) and BRIDGIT, implement performance prediction models to optimize remediation and repair decisions (Madanat et al. 1997, Mauch and Madanat 2001, Morcouc et al. 2002, van Noortwijk and Frangopol 2004, Agrawal et al. 2010, Huang 2010). There are several mathematical methods that have been used as the basis for performance prediction models, including deterministic, probabilistic, and artificial intelligence models (Morcouc 2006). Probabilistic models are the most commonly used model in bridge management software and, therefore, will be the main focus of this section. Please refer to Morcouc et al. (2002) and Morcouc (2011) for more information regarding deterministic models, and Flood et al. (1994), Tokdemir et al. (2000), Morcouc et al. (2002), and Huang (2010) for information related to artificial intelligence models.

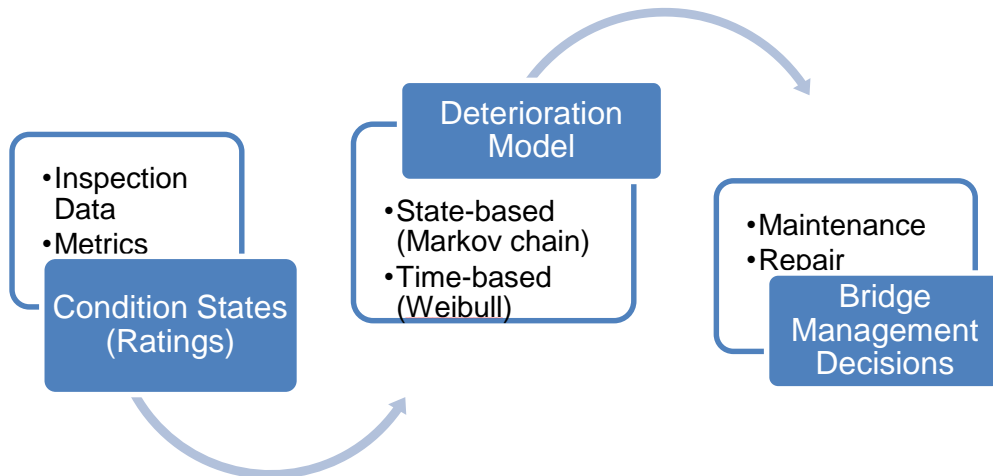


Figure 24. The role of deterioration models in bridge management systems

Probabilistic models, specifically the Markov chain model, have been used in bridge management systems to predict the deterioration of bridge elements using condition rating data. The Markov chain is a type of discrete-time, state-based model (Agrawal et al. 2010), in which the deterioration of a bridge element is modeled using the probability of a bridge element transitioning between condition states, called the transition probability, to develop a deterioration model. The transition probability is determined by the probability of the condition of an element transitioning from one condition state to the next over discrete time intervals (Morcouc 2006), and is expressed in a matrix form (Equation 6). The time interval is typically taken as two years to correspond with the frequency of bridge inspections. Each cell in the transition probability matrix represents the probability that the condition rating will transition from one rating to another.

$$P = \begin{bmatrix} p_{1,1} & p_{1,2} & \cdots & p_{1,n} \\ p_{2,1} & p_{2,2} & \cdots & p_{2,n} \\ \vdots & \vdots & \cdots & \vdots \\ p_{n,1} & p_{n,2} & \cdots & p_{n,n} \end{bmatrix} \quad (6)$$

Using the transition probability matrix P and the initial condition state vector $P(0)$, the future condition state vector $P(t)$ can be determined using Equation (7) (Collins 1975). In order to assemble the transition probability matrix P , an adequate amount of bridge deck condition state data is needed, otherwise, the use of expert judgment may be necessary (Morcouc 2006).

$$P(t) = P(0) * P^t \quad (7)$$

Several assumptions are often made in order to simplify the Markov chain model. The first assumption is that the time interval between inspections is constant over the life of the bridge. Bridges are required to be inspected every two years (Ryan et al. 2012); however, this does not mean that the inspection interval is precisely two years. Morcouc (2006) found that variations in the time interval between inspections can lead to a 22% error when predicting the service life of

bridge decks. The second assumption is that the future condition of a bridge element is dependent only on its present condition, making it independent of its past condition states. This assumption is referred to as the state independence assumption. Research has shown that the state independence assumption is valid for a 95% confidence interval, but only for individual bridge elements (Morcoux 2006).

The advantages of Markov chain models over deterministic models are that they account for the uncertainty in predicting deterioration and they use the present condition rating to predict the future condition rating (Morcoux et al. 2002). However, Morcoux et al. (2002) presents the following limitations of the Markov chain model:

1. The time intervals between inspections, bridge population, and transition probabilities are all assumed to be constant.
2. Deterioration predictions are only based on the present condition rating and not on the past condition ratings.
3. They only predict the deterioration for the “no maintenance” option due to the difficulty in accounting for various maintenance options.
4. They ignore interactions between individual bridge elements.
5. They are difficult to update as condition rating data is accumulated.

Many bridge management software programs, including BrM and BRIDGIT, have implemented the Markov chain model to predict deterioration rates and future bridge conditions; however, due to these limitations of the Markov chain model, changes to bridge management software are being implemented in an effort to increase their prediction capability (AASHTO 2013). AASHTO’s most recent version of bridge management software, termed BrM 5.2, which is set to be released in 2015 (AASHTO 2012), will use a hybrid system composed of Markov chain models and Weibull curve models (AASHTO 2013).

Unlike the Markov chain model, the Weibull curve model is a discrete-time, time-based model, for which the time that a bridge element is in a certain condition state is treated as a random variable (Agrawal et al. 2010). The Weibull curve model is capable of estimating the probabilities that an element will remain in a particular condition state for t years, will transition to the subsequent condition state in t years, or will remain in a particular condition state for an additional t_{t+n} years (Agrawal et al. 2010). BrM 5.2 will use the Weibull curve to model the deterioration process up to condition state 2 (AASHTO 2013). Once past condition state 2, the deterioration will follow the Markov chain model.

1.3 Bridge Inspection and Cracking Metrics

This section describes the current state-of-practice related to bridge deck inspection procedures, quantitative deck cracking metrics, and deck rating procedures. The National Bridge Inspection Standards (NBIS), contained in the Code of Federal Regulations, require each bridge to be inspected at a frequency no greater than 2 years (NBIS 2004). Routine inspections are the most common form of inspection and provide data critical to Departments of Transportation (DOTs) for bridge management (Phares et al. 2004). Routine inspections are used to determine the condition of bridges, to identify changes in the condition from previous inspections, and to ensure that the bridge meets service requirements; while in-depth inspections identify defects that are not readily detectable during routine inspections (NBIS 2004) and are typically performed less frequently (Graybeal et al. 2002). Pertaining to bridge decks, routine inspections are performed to generate data that is used to develop a numeric rating of the condition (Graybeal et al. 2002). Cracking metrics are numeric assessments commonly used to quantify the degree of cracking on the bridge deck and form the basis for most condition rating procedures. Cracking metrics are aggregated into a condition rating system, which is used to assign a numeric condition rating to the deck. Condition ratings are a means to quantify the in-situ condition of a deck relative to the as-built condition (PennDOT 2009) and, in turn, are used by DOTs to develop deterioration models to predict future performance (Huang 2010), make remediation and repair decisions (Phares et al. 2004), and determine monetary fund allocations (Madanat and Lin 2000). Current research has aimed at integrating all types of nondestructive evaluation (NDE) methods into bridge management software so that condition ratings are based on a cumulative evaluation of a bridge.

1.3.1 Bridge deck inspection

Bridge inspections follow standards set forth by federal agencies, such as the Federal Highway Administration (FHWA) and the American Association of State Highway and Transportation Officials (AASHTO). These standards establish the procedures for highway bridge inspections (and other transit structures though beyond the scope of this project) and the specifics of tests used for bridge deck inspection. The most common types of inspection are routine, which are used to assess the overall condition of a bridge, and in-depth, which occur less frequently (Graybeal et al. 2002) and are performed to evaluate deficiencies not detected in routine inspections (NBIS 2004). The types of evaluation methods used for inspection can be categorized as destructive or nondestructive. In regards to bridge decks, evaluation methods should identify locations of distress including cracking, scaling, spalling, and potholes (FHWA 1995, AASHTO 2008). The categories of evaluation methods and their relevance to bridge deck cracking are explained in the subsequent sections. However, prior to inspection, adequate planning should be undertaken.

Adequate planning includes reviewing previous inspection records, determining the evaluations to be performed, and preparing inspection forms (AASHTO 2008). In addition, the literature recommends that decks be clean and dry prior to inspection to avoid concealing defects (Darwin

et al. 2004, Pendergrass et al. 2011). Ganapuram et al. (2012) specifically recommended clearing the deck of debris using a leaf blower and spraying the decks with water prior to inspection to increase the visibility of cracks. Other pre-inspection procedures include the establishment of a rectangular global coordinate system (Figure 25) and a corresponding data collection grid (Figure 26), as required by the FHWA as part of their Long Term Bridge Performance (LTBP) program (FHWA 2013). Figure 25 shows the rectangular global coordinate system for several traffic variations with the origin denoted by the x - and y -axes. The implementation of a coordinate system allows for inspection data to be consistent from one inspection to the next.

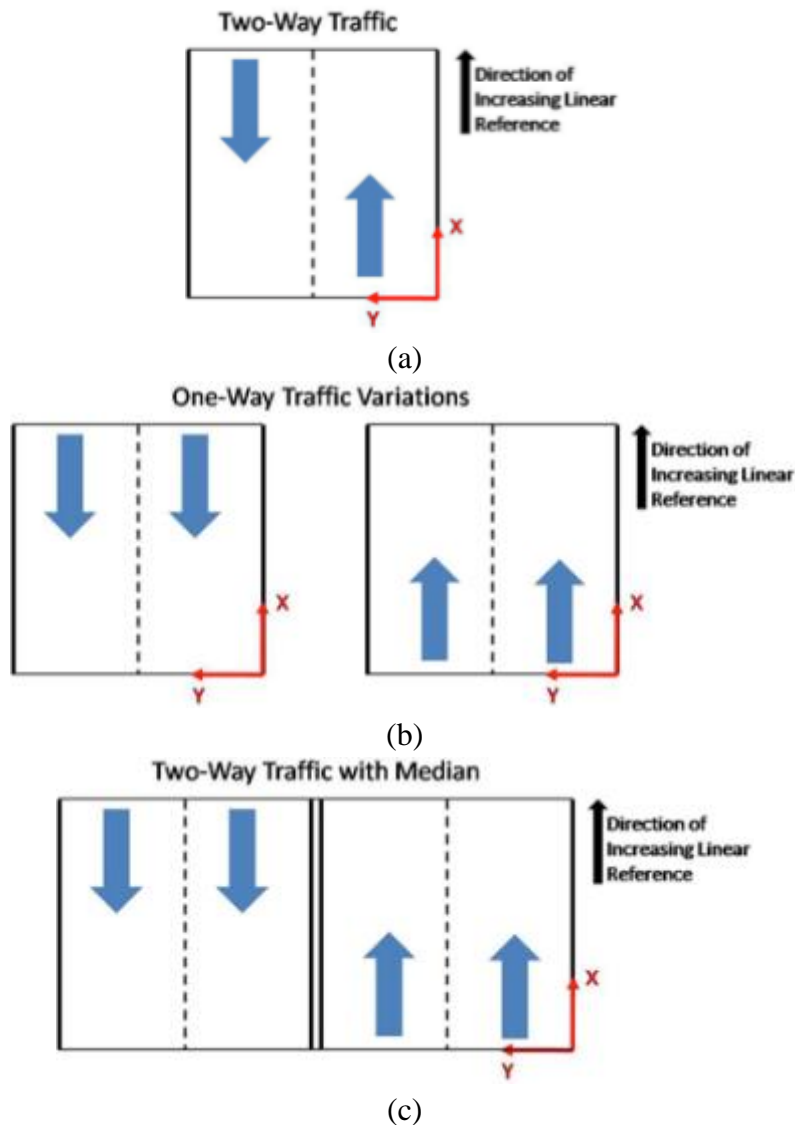


Figure 25. Recommended Global Coordinate System as denoted by x and y axis for (a) two-way traffic, (b) one-way traffic variations, and (c) two-way traffic with median (FHWA 2013).

Data collection grids, as shown in Figure 26, allow defects on the deck to be mapped consistently and aid in documenting the location of the evaluation performed. Similar grids have been used in

the past to create crack maps of the bridge deck during visual inspections (Schmitt and Darwin 1995, Darwin et al. 2004, Darwin et al. 2010, Pendergrass et al. 2011, Ganapuram et al. 2012). These maps provide detail documentation of the severity and extent of cracking facilitating in depth metrics that take into account the physical characteristics of each crack, such as length, width, and location.

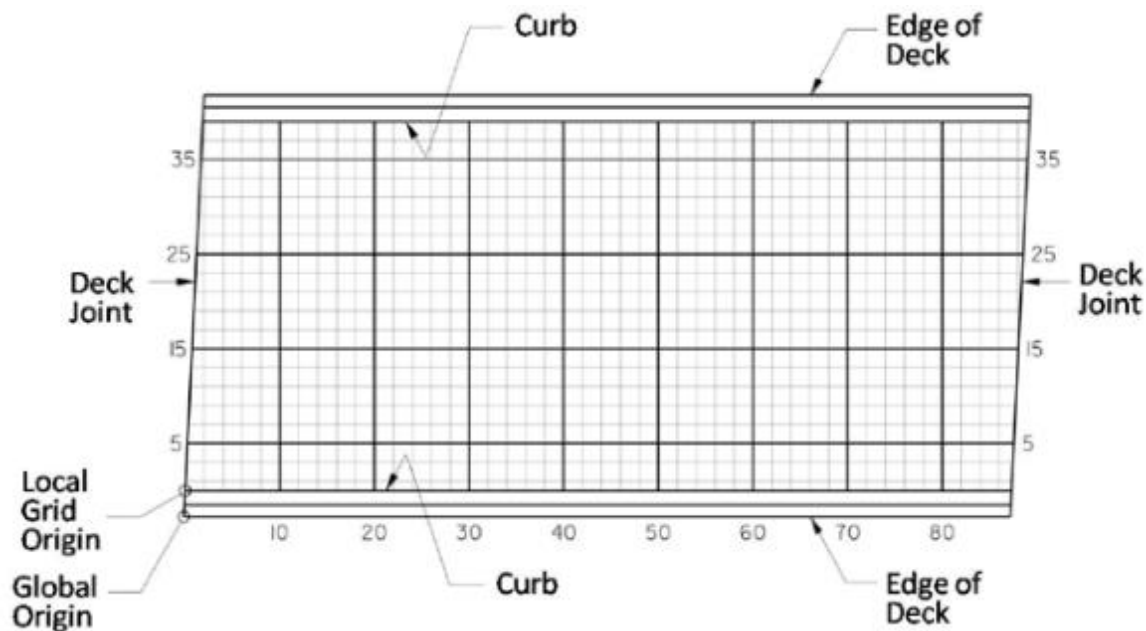


Figure 26. Data Collection Grid (FHWA 2013)

1.3.1.1 Nondestructive evaluation

Nondestructive evaluation (NDE) is the most common type of evaluation used in bridge deck inspections (Gucunski et al. 2013). NDE is defined by its ability to evaluate the condition of a structure over time without causing damage during testing (Van der Wielen et al. 20109). There are numerous types of NDE methods that are relevant to bridge deck condition assessment. Several studies have evaluated various NDE methods (McCann and Forde 2001, Scott et al. 2003, and Gucunski et al. 2013); however, an in depth review of each of these methods is beyond of the scope of this report. For this report, the most common methods are briefly discussed and relevant results from previous research are presented.

Visual inspection (VI) is the most common NDE technique used for routine inspections (Moore et al. 2001, Phares et al. 2004, Graybeal et al. 2002, Scott et al. 2003, Gucunski et al. 2011, Gucunski et al. 2013). VI is defined as all testing methods that use only the five senses of the inspector and basic hand-held tools or equipment, such as hammers, tape measures, plumb bobs, etc. (Moore et al. 2001). Visual inspection is most effective for locating distress on the surface of the deck. However VI is subject to the capabilities of individual inspectors, environmental conditions, etc., that introduces variability into the results of the inspection thus affecting the reliability and

accuracy (Lenett et al. 1999, Graybeal et al. 2002). Phares et al. (2004) found that 95% of condition ratings for individual bridge elements will vary within two rating points of the average, using the 0 to 9 scale established in the FHWA’s Recording and Coding Guide (FHWA 1995). Although the outcome of VI can be highly variable, VI is efficient, cost-effective, and requires only a moderate amount of skill by the inspector (McCann and Forde 2001).

Another type of NDE is sounding, that is used to evaluate delamination of the concrete from the reinforcing steel (AASHTO 2008). Sounding is commonly performed by dragging a chain, or series of chains, across the deck while the bridge inspector listens for acoustic variations (Scott et al. 2003, Yehia et al. 2008). The literature suggests that two inspectors perform the chain drag test in order to decrease variability in the results (Scott et al. 2003). FHWA protocols (2013) recommend a chain drag be used to determine the general area of delamination then hand-held hammers be used to define the boundaries of the delaminated area. The chain drag is a commonly used NDE method due to its simplicity of use; however, the results often vary depending on the number of inspectors, their experience (Scott et al. 2003). To increase the accuracy of chain drag evaluations, Scott et al. (2003) suggest increasing the time for the inspection and using a two foot grid to record the results.

Other types of NDE include impact echo (Shokouhi et al. 2011, Azari et al. 2012), ground penetrating radar (Yehia et al. 2008, Maser et al. 2012), and ultrasonics (Azari et al. 2012, Gucunski et al. 2013). [Table 5](#) summarizes the advantages, disadvantages, and cost of several types of NDE methods. The deck thickness, the depth of delamination, and the location of delaminated areas can be measured with the impact echo method (Azari et al. 2012). Ground penetrating radar is used to determine the location and depth of delamination (Yehia et al. 2008). Debonding of steel reinforcement, shallow cracking, and delamination can be detected using ultrasonic methods (Gucunski et al. 2013).

Table 5. Comparison of NDE methods (McCann and Forde 1997)

Inspection Method	Parameter Measured	Advantage	Disadvantage	Cost
Visual	surface condition	quick; modest skills required	possibility of subjective results	low
Impact Echo	reflected energy from mechanical impact	measures thickness and depth of defects	difficult to quantify data	moderate
Ultrasonics	wave velocities	can identify and locate specific flaws	can be slow; difficult to quantify data	moderate
Ground-penetrating Radar	electromagnetic wave velocity	efficient; subsurface characterization	requires skill to interpret data	moderately high

Some recent research on bridge deck evaluation has focused on decreasing the time required to inspect the bridge with the goal of reducing disruption to the traffic. One promising technology is

the use of robotics (Lim and La 2011). Robotic systems that use high resolution imaging have been developed to generate crack map images (Lim and La 2011). The advantages of the robotic system over traditional human-based visual inspections are increased accuracy by the elimination of human errors, the ability to autonomously inspect and map the entire deck, and decreased risk for the inspectors. Robotic inspection technology has been taken a step further by integrating multiple NDE methods into one robot (La et al. 2013, FHWA 2013). Robots have been equipped with GPS, electrical resistivity, impact echo, ultrasonics, and ground penetrating radar in addition to a high quality imaging camera as shown in the photograph of Figure 27. Others have implemented high resolution imaging for inspecting the underside of the superstructure using robotics (Oh et al. 2007, Lee et al. 2011), and for inspecting the deck using aerial photography (Bian et al. 2011, Chen et al. 2011).



Figure 27. Robotic Assisted Bridge Inspection Tool equipped with NDT technology (FHWA 2013)

In spite of significant advancements in NDE, specifically the underlying technology, the data produced is often too detailed to be directly input into bridge management software without proper interpretation (Hearn and Shim 1997, Madanat and Lin 2000). In light of this, research efforts have aimed at integrating NDE technologies into bridge management systems (BMS) (Hearn and Shim 1998, Rens et al. 2005, Gucunski et al. 2009). Recently, a study funded by the Strategic Highway Research Program (SHRP 2) is performing research towards the condition assessment and performance monitoring of bridge decks using NDE methods in an effort to improve decision-making, increase the efficiency of fund allocation for remediation and repairs, and to reduce traffic delays caused by interruptive inspections (Gucunski et al. 2013). The main goal of the project is to provide transportation agencies with resources that will allow them to integrate NDE methods into their codes of practice (Gucunski et al. 2013). To date, the research program has developed the NDToolbox website, which provides detailed information on the NDE methods and recommended applications. During the project, a number of NDE methods were evaluated using field validation testing and subsequently graded on a 1-5 scale (5 being excellent) based on the

type of deterioration using five weighted factors, as shown in Table 6. Table 4 summarizes the overall deterioration grades of several NDE methods based on the type of deterioration, which include delamination, crack depth, concrete deterioration, and corrosion. The grades assigned in Table 6 represent the performance of the individual NDE technologies based only on the deterioration type for which the technology was validated (Gucunski et al. 2013). The NDE methods were evaluated for accuracy, precision (repeatability), speed, ease of use, and cost, with each factor having an assigned weight.

Table 6. Deterioration grades for NDE methods based on validation testing (Gucunski et al. 2013)

NDE Technology	Deterioration Type	Accuracy	Precision (Repeatability)	Speed	Ease of Use	Cost	Overall Deterioration
		WF = 0.3	WF = 0.3	WF = 0.2	WF = 0.1	WF = 0.1	Grade (1 to 5 scale)
Impact echo	Delamination	2.8	4.0	2.3	2.1	3.0	3.0
Ultrasonic surface waves	Delamination	2.8	3.0	2.4	1.4	3.0	2.7
	Crack Depth	2.5	3.0	1.0	1.4	3.0	2.3
	Concrete Deterioration	3.8	4.0	2.4	1.4	3.0	3.3
Ground-penetrating radar	Delamination	2.1	4.0	3.9	2.2	3.0	3.1
	Corrosion	1.6	4.0	3.9	2.2	3.0	3.0
Half-cell potential	Corrosion	3.0	3.0	3.8	3.4	4.0	3.3
Galvanostatic pulse measurement	Corrosion	2.4	3.0	2.4	2.6	4.0	2.8
Electrical resistivity	Corrosion	3.0	4.0	3.8	3.6	4.0	3.6
Infrared thermography	Delamination	2.2	2.0	4.1	4.0	4.0	2.9
Chain dragging	Delamination	2.2	3.0	3.2	4.0	3.0	2.9

The NDE methods were then given an overall ranking determined from the sum of the individual grades for each deterioration type (Table 7). The rankings were assigned based on the cumulative grade from the four deterioration types, each having a corresponding weight factor. Gucunski et al. (2013) concluded that no single NDE method was the most effective at evaluating all four types of deterioration. Note that visual inspection was not included in the validation testing; however, based on the literature review performed by Gucunski et al. (2013), visual inspection was found to have the highest potential for vertical (i.e. through the deck thickness) crack characterization (Gucunski et al. 2013).

Table 7. Overall ranking of NDE methods based on validation testing (Gucunski et al. 2013)

Deterioration Type	Delamination	Corrosion	Vertical Cracks	Concrete Degradation	Overall Value	Ranking
	WF = 0.42	WF = 0.35	WF = 0.10	WF = 0.13		
Impact Echo	3.0	0.0	1.0	1.0	1.5	2
Ultrasonic surface waves	2.7	0.0	2.4	3.3	1.8	2
Ground-penetrating radar	3.1	3.1	0.0	1.0	2.5	1
Half-cell potential	0.0	3.3	0.0	0.0	1.2	3
Galvanostatic pulse measurement	0.0	2.8	0.0	0.0	1.0	3
Electrical resistivity	0.0	3.6	0.0	0.0	1.3	3
Infrared thermography	2.9	0.0	0.0	0.0	1.2	3
Chain dragging	2.9	0.0	0.0	0.0	1.2	3

1.3.1.2 Destructive evaluation

The most commonly used type of destructive evaluation is coring. Concrete core samples are taken from the bridge deck using a drill that is mounted to the deck (Dilek 2009). The required diameter of core samples is determined by the type of evaluation technique, e.g., compressive strength testing or chloride concentration testing, that will be performed on the sample following its removal from the deck (FHWA 2013). Traditionally, coring is used to confirm the results of prior NDEs, such as chain dragging, ground-penetrating radar, and impact echo (Scott et al. 2003, Yehia et al. 2008).

1.3.2 Cracking metrics and condition ratings

Data collected from inspections is used to establish a condition rating for the deck. Condition ratings are used to monitor the deterioration of bridge decks, select remediation and repair techniques, and efficiently allocate resources (Graybeal et al. 2002, Scott et al. 2002, Phares et al. 2004). As previously discussed, VI is the most commonly used inspection method. As a result, the majority of condition rating standards are formulated for the type of data produced from visual inspections. Cracking metrics serve as an intermediate step to translate data from visual inspections to a condition rating and serve as supplemental guidelines to simplify the condition rating process for individual bridge components (Ryan et al. 2012). Cracking data collected from visual inspections is aggregated into a metric, which, in turn, is used to assign a condition rating to a bridge component.

1.3.2.1 Types of cracking

Cracks are defined by their orientation on the bridge deck. Typically, multiple types of cracks are present on a bridge deck and are typically categorized as transverse, longitudinal, diagonal, or map (Figure 28).

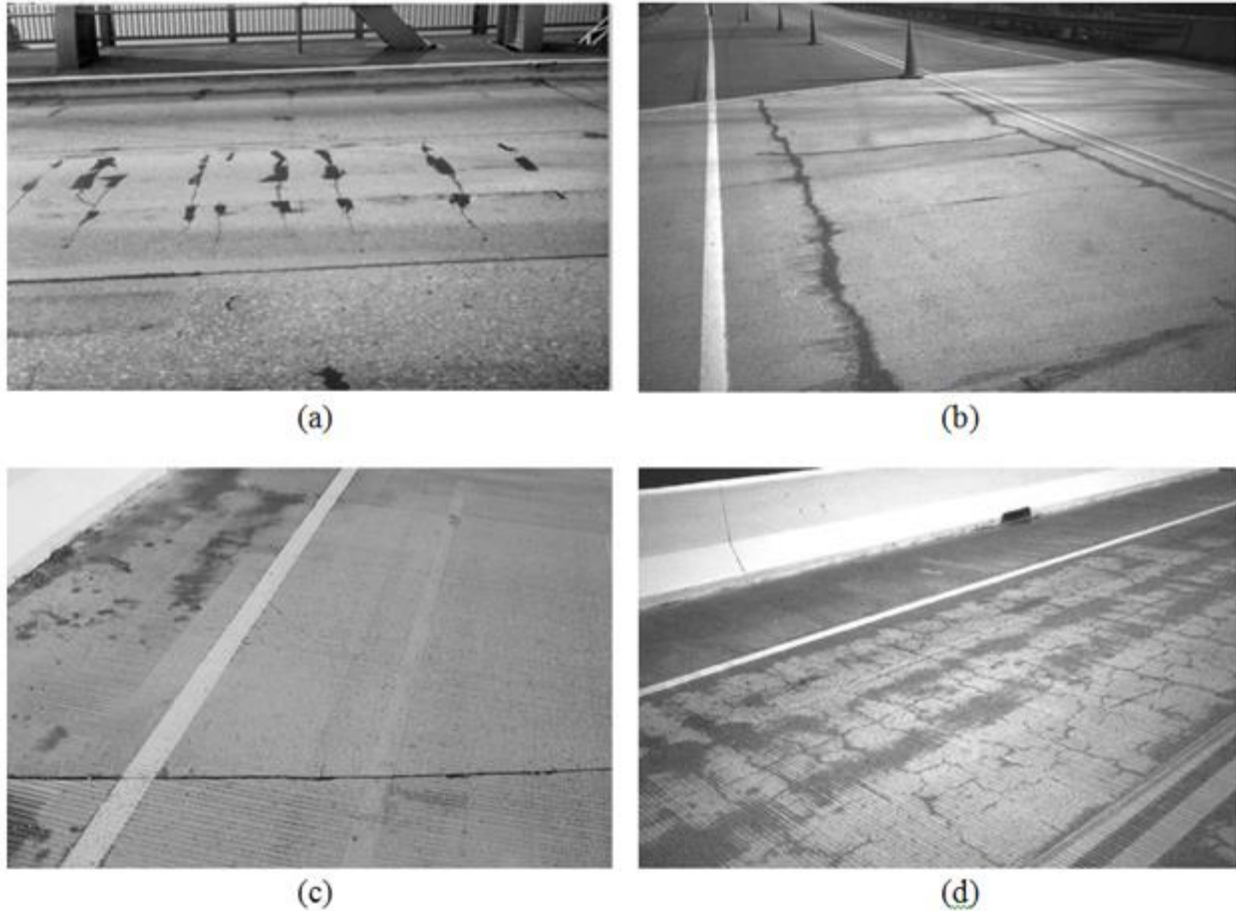


Figure 28. Types of bridge deck cracking: (a) transverse, (b) longitudinal, (c) diagonal, (d) map (TRB 2004)

Transverse cracks (Figure 28a) are oriented perpendicular to the longitudinal direction (direction of traffic) of the deck. The literature suggests that transverse cracking is the most prevalent form of cracking on concrete bridge decks (Ramey and Wright 1994, Saadeghvaziri and Hadidi 2002, Darwin et al. 2004). Transverse cracks form above the transverse reinforcement, providing a direct path for deicing chemicals from the deck's surface to the reinforcing steel. Therefore, transverse cracks critically affect the corrosion of the reinforcing steel. French et al. (1999) found that bridges with more than two spans, the interior (middle) spans typically experience more transverse cracking than exterior spans. Longitudinal cracks (Figure 28b) are parallel to the longitudinal direction of the bridge deck. Like transverse cracks, longitudinal cracks form above the steel reinforcement. Causes of longitudinal cracking can be linked to the movement of beams relative to one another for bridges with prestressed concrete box beams (Curtis and White 2007). Diagonal cracks (Figure 28c) are typically found at the corners and the ends of concrete bridge decks (Fu et al. 2007). Diagonal cracking is more prevalent on skewed bridges. (Fu et al. 2007).

Map cracking (Figure 28d) forms in a random pattern of intersecting transverse, longitudinal, and diagonal cracks. For this reason, map cracking is also referred to as pattern cracking. This type of

cracking has been attributed to the placement of fresh concrete on already cured concrete beams (Curtis and White 2007).

1.3.2.2 Cracking metrics

As previously stated, cracking metrics, such as width, length, and density, are used to quantify the severity (i.e. magnitude) or extent (i.e. prevalence) of cracking present on a bridge deck. The most commonly used metrics are established using data on the width, length, or density (spacing) of cracks. Crack measurements can be made by an inspector or obtained from post-processing of crack maps and crack images.

The width of the crack is often categorized as hairline, fine, and medium as shown in Table 8, or by a similar categorization system. The widths of cracks can be measured using a comparator card or other appropriate measurement device. Width limits are established so that cracks can be categorized and used in a condition rating procedure. Table 8 summarizes cracking categorizations used by three DOTs based on the measured width.

Table 8. Crack width definitions

Agency	Crack Width			
	Hairline	Narrow or Fine	Medium	Large
PennDOT (1988)	< 0.004 in.	0.004 in. to 0.007 in.	-	> 0.007 in.
OSIM (2008)	< 0.004 in.	0.004 in. to 0.012 in.	0.012 in. to 0.04 in.	> 0.04 in.
AASHTO (2010)	< 0.0625 in.	0.0625 in. to 0.125 in.	> 0.125 in.	-

Crack lengths can be measured using a steel tape or through computer analysis of crack maps (Darwin et al. 2004). Typically, crack length is not used alone to quantify cracking of bridge decks, but rather in combination with other measurements, such as the deck area (see Equation 8).

Crack density is a metric reflecting the extent of cracking that is present on a concrete bridge deck. Several metrics have been proposed and implemented to quantify crack density. Schmitt and Darwin (1995) quantified density using the total length of all cracks divided by the area of the deck as shown in Equation (8).

$$Crack\ Density = \frac{\sum crack\ length}{deck\ area} \quad (8)$$

Equation (7) has been adopted for a number of projects and State DOTs to quantify the extent of cracking (Darwin et al. 2004, Fu et al. 2007, Pendergrass et al. 2011, Ganapuram et al. 2012) during inspection. Others definitions for crack density have used the spacing between cracks (French et al. 1999, AASHTO 2010), the number of transverse cracks divided by the span length (PennDOT 1988), and the sum of the widths of cracks divided by the span length (Virginia DOT

2009). Crack density can also be calculated for sub-categories based on the type of cracks, i.e., transverse and longitudinal, or their location on a bridge deck, such as the positive and negative moment regions (see Appendix A).

Cracking metrics are used to establish the condition rating, or as a standalone quantity used to correlate cracking with selected parameters. Darwin et al. (2004) compared crack density measurements with factors such as the age of a bridge, concrete material properties, and structural design conditions. The results of this comparison showed that for certain parameters, such as age, water content, cement content, degree of girder end restraint, and type of overlay, crack density provided a direct correlation. Others have used crack width (Virginia DOT 2009) or combinations of crack width and density (PennDOT 1988) to determine remediation and repair decisions.

1.3.2.3 Condition rating

Condition rating standards are typically established as a means to assess the overall condition of a bridge, which is an aggregate of the condition of components, such as the deck, substructure, superstructure, and culvert (FHWA 2011). In addition to providing condition ratings for required bridge components, many state DOTs and other organizations have established their own condition rating criteria of individual bridge elements for use in their bridge management systems.

The Federal Highway Administration (1995) established a condition rating procedure to evaluate individual bridge components, using a scale of 0 to 9, 0 being failure and 9 being excellent. Supplemental guides have been developed by state DOTs to help in rating designations (PennDOT 2009). Condition ratings are used along with other parameters to establish a sufficiency rating of the overall condition of a bridge. The parameters are grouped into four categories, which are structural adequacy and safety, serviceability and functional obsolescence, essentiality for public use, and special reductions, each containing specific formulas to determine an individual sufficiency rating for the category (FHWA 1995). The sum of the four individual sufficiency ratings determines the overall sufficiency rating, between 0 and 100 (0 being the lowest possible rating and 100 the highest), of the bridge. The deck condition rating is one of the parameters used in the serviceability and structural obsolescence category. In addition, AASHTO has developed a rating procedure that evaluates the condition state of individual bridge elements and suggests remediation and repair decisions for each state. For bridge decks, there are four possible condition states, determined by the severity and extent of cracking, spalling, delamination, patching, and other factors, as summarized in [Table 9](#) (AASHTO 2010). Data gathered from inspections is used to establish metrics, such as crack width or density that are then used to assign a condition state. The condition states are incorporated into bridge management software as input for performance prediction models, and also used to recommend remediation and repair methods.

Table 9. Condition State Definitions (AASHTO 2010)

Defect	Condition State 1	Condition State 2	Condition State 3	Condition State 4
Cracking	None to hairline	Narrow size and/or density	Medium size and/or density	The condition is beyond the limits established in the condition state 3 and/or warrants a structural review to determine the strength or serviceability of the element or bridge
Spalls/ Delaminations/ Patched Areas	None	Moderate spalls or patch areas that are sound	Severe spalls or patched area showing distress	
Efflorescence	None	Moderate without rust	Severe with rust staining	
Load Capacity	No reduction	No reduction	No reduction	

Other rating procedures have been developed by state DOTs (Curtis and White 2007, Scott et al. 2002) to evaluate the condition state of bridge decks. The New York State DOT used a rating procedure based on crack width and density (Curtis and White 2007). The rating values were plotted against selected parameters suspected to contribute to cracking. Using the plots, Curtis and White (2007) identified concrete strength, concrete cover, and pour temperature as the most influential factors for bridge deck cracking; however, the researchers found little correlation between the ratings and reinforcing steel ratio, concrete temperature, deck age, and average daily truck traffic. Further, the University of Minnesota proposed a similar rating procedure based on crack width and density that was used to investigate correlations with material, construction, and design parameters (French et al. 1999). The results of the French et al. study identified correlations between cracking and the type of span (interior or exterior), type of bridge (straight or curved), size of reinforcing steel bar size, and degree of girder end restraint.

1.4 Management Practices for Remediation

It has been established that bridge deck cracking significantly affects the long-term performance of bridges. Therefore, it is important to utilize efficient remediation and repair techniques in order to extend the service life of bridges and delay deck repair and/or replacement. For best management of remediation methods, it is necessary to evaluate the cost of the remediation method, the age of the bridge, the condition of the bridge, the traffic volume, the rating of the deck, and its expected life (PennDOT Design Manual Part 4 2012).

1.4.1 Remediation method cost-effectiveness

There are a number of different types of remediation methods that can be used to repair bridge decks, such as Type-1 and Type-2 patching as shown in [Figure 29](#) (PennDOT Drawing BC-783M, 2010). If the deck repairs are extensive, overlays may be the most cost-effective long-term remediation technique. Epoxy overlays and Latex-Modified Concrete (LMC) overlays are

expected to last approximately 20-years. Bituminous overlays can entrap contaminated moisture beneath the overlay which can accelerate deterioration and, therefore, are not recommended (PennDOT Design Manual, Part 4, 2012). These remediation method materials are applied to the concrete surface in order to prevent the entry of deleterious ions that lead to corrosion of steel reinforcement. By applying treatment to the surface of the concrete deck, the ingress of chloride, moisture, and oxygen can be prevented. These factors contribute to corrosion and any method that is used to reduce their diffusion into concrete will subsequently slow down the deterioration of the deck (Ibrahim et al. 1999).

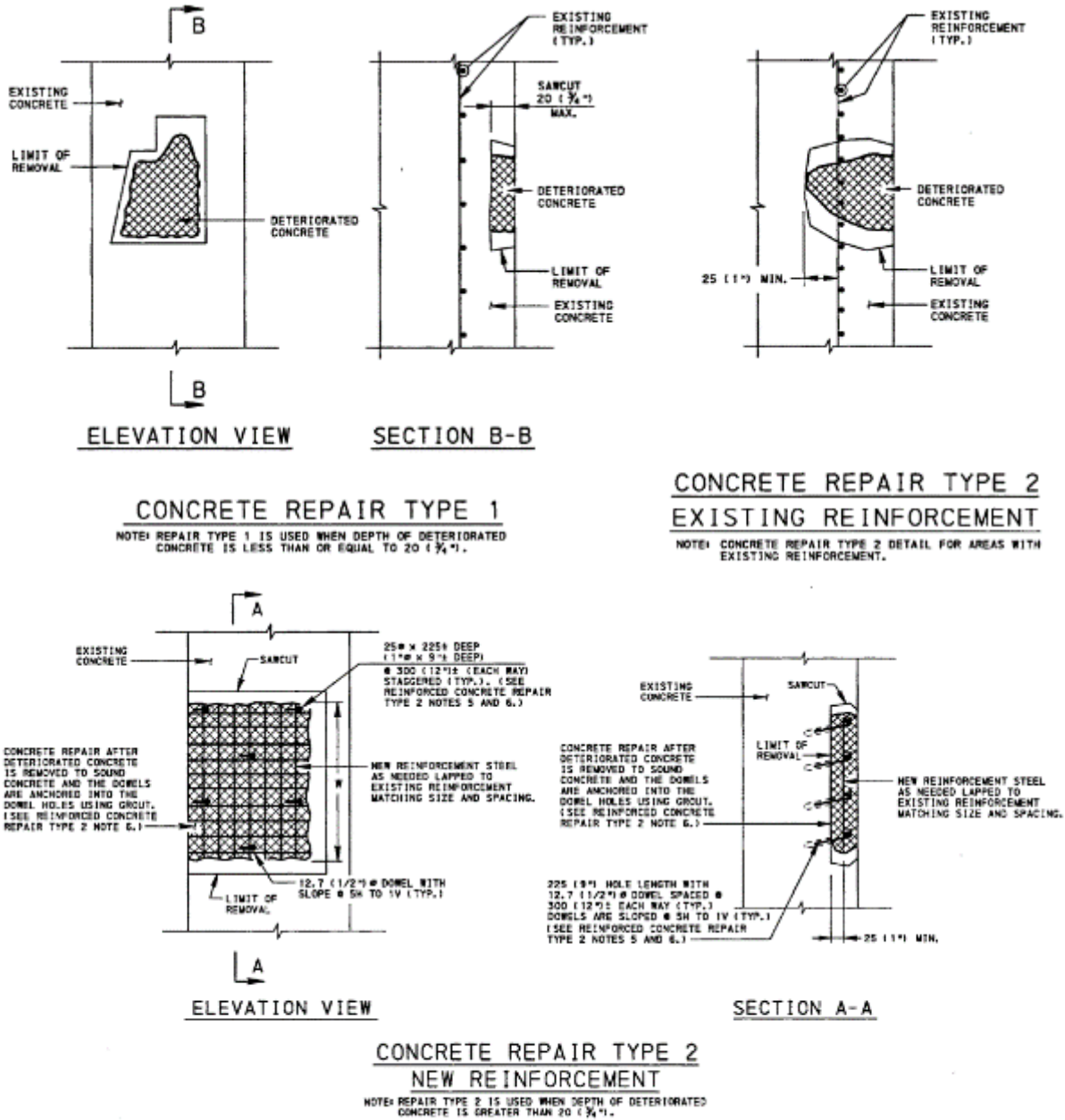


Figure 29. PennDOT Drawing BC-783M Type I & Type II Patching

According to the Bridge Deck Rehabilitation Guide (Figure 30) PennDOT prior to 2015 performed specific remediation methods based on a deck rating system. The new 2015 PennDOT Design Manual 4 (DM-4) also considers several other parameters (2015 DM-4 Figure D5.6.4.1-1/2). For decks that are rated as 8 or 9, no action is required for repair. It is recommended that decks with a rating of 7 should be sealed and decks with a rating of 5 or 6 should be remediated with LMC or epoxy overlay. Decks with a rating of 4 or less are considered structurally deficient. Type 1 or Type 2 patching can be used to remediate these decks, but typically deck replacement or partial depth reconstruction is necessary. The remediation decision is based on both visual and destructive testing (PennDOT Design Manual, Part 4, 2012).

Deck Cond (2)	9 - 7						6 (6)						5						4						≤ 3										
	< 3%			≥ 3%			< 3%			≥ 3%			< 3%			≥ 3%			< 3%			≥ 3%			< 3%			≥ 3%							
Deck Age (4)	Post 1976	1971-1976	Pre 1971																																
Rehabilitation/Replacement Strategies (5)																																			
(LO)	●	●	●	●	●	●	●	●	●	●	●	●	●	●	●	●	●	●	●	●	●	●	●	●											
(BP)																																			
(BO)																																			
(RO)								L	L																										
(RMO)								M	M		L	L																							
(R)							●			●																									
(RL)								H	H		M,H	M,H										M,H	M,H	M,H											
(RC)												H												M,H	M,H										
(RCMO)																								M,H	M,H										
(RCL)																								M,H	M,H										
(RPL)																								H		H	●	●	●	●	●	●			

KEY

Where options appear in more than one row, an economic evaluation is required and/or additional test data to support a decision.

- - Denotes action for all occurrences (level of service) of a given condition rating.
- - With concurrence of the District Bridge Engineer.
- L - On low volume routes (ADTT < 100)
- M - On medium volume routes (100 # ADTT # 500)
- H - On high volume routes (BPN + Exceptions) (ADTT > 500)
- - Shaded area is "gray area" where other factors must be considered.

NOTES

- (1) The Bridge Deck Rehabilitation Guide as such is for generalized usage. Exceptions will exist. These may include: monolithic deck systems, arches, concrete tee-beams, etc.
- (2) Refers to deck condition rating established using BMS2 Item 1A01.
- (3) Refers to measured entrained air content.
- (4) Dates were established based on coated steel versus uncoated steel. Pre-1971 black steel was used in PA. 1971-1976 both epoxy-coated and galvanized, Post 1976 epoxy-coated steel was utilized.
- (5) Rehabilitation, maintenance and replacement options are listed per the following code:
 - LO = Linseed oil or other surface treatment (silane, etc.) at prescribed maintenance intervals (maintenance activity)
 - BP = Bituminous patching only (maintenance activity)
 - BO = Bituminous overlay only (maintenance activity)
 - RO = Repair Types II and III, plus bituminous overlay
 - RMO = Repair Types II and III membrane waterproofing, plus bituminous overlay (maintenance activity)
 - R = Repair Types II and III
 - RL = Repair Types II and III, plus latex concrete overlay
 - RC = Repair Types II and III, plus cathodic protection
 - RCMO = RC plus membrane waterproofing and bituminous overlay
 - RCL = RC plus latex modified concrete
 - RPL = Replace the deck
- (6) Intuitively the Benefit/Cost ratio on lower volume roads will not support high cost rehabilitation options.

Figure 30. Pre 2015 Bridge Deck Rehabilitation Guide (PennDOT Design Manual, Part 4, 2012).

For concrete decks that experience cracks that are smaller than 0.007 in wide, repair methods do not yet need to be implemented because the cracks are still too small to allow the ingress of chloride ions (ACI 224R 1997). Other sources define small cracks as ranging from 0.001 to 0.004 in. as explained in section 2. However, if the bridge deck experiences larger cracks, the repair methods need to be considered (Wenzlick 2007). It is important to apply remediation methods before the concrete cover exceeds the chloride threshold limit required for corrosion initiation, in order to increase long-term effectiveness of the repair (Tabatabai et al. 2005).

1.4.1.1 Coatings

Coatings are applied to concrete bridge decks in one or more coats and their application is recommended before there are significant signs of corrosion damage (Sohanghpurwala et al. 2006). In general, coatings are applied to concrete surfaces in layers of approximately 0.03 in thick. Different types of coatings include epoxies, acrylics and urethanes. Epoxy coatings have a high adhesive strength and are resistant to abrasions, however are susceptible to UV light damage. An acrylic coating is hard but brittle and has low impact strength. Urethane coatings are characterized by high impact strength and can withstand weathering, however, have a low resistance to abrasion (Sohanghpurwala 2006, Radlinska et al. 2012.). In a report from the Kentucky Transportation Center (2006) it was noted that different states have implemented these coatings as repair methods and experienced several problems. For example, Ohio DOT has utilized epoxy-urethane systems but faced problems with respect to application and mixing. Michigan DOT utilized acrylic coatings for aesthetic purposes and concrete protection but issues regarding cold weather application and proper surface preparation were a concern (Palle 2006).

1.4.1.2 Overlays

Overlays are poured on to the bridge deck in order to form a layer that is approximately 0.25 in, or more, thick (Needham 2000). Once placed, overlays bond to the surface of concrete and prevent the intrusion of moisture and chlorides, which leads to improved long-term durability (Ahlborn et al. 2002, Silano 2003). Overlays provide protection to existing structures by decreasing moisture infiltration. However, its use in existing structures is not as effective because chloride ions are present (Ahlborn et al. 2002, Silano 2003). There are three different types of overlays that are commonly used to repair cracking. Type I is a multi-component polymer resin, considered to be the most economical and practical type of overlay (ACI 345R 1991) and typically used as a temporary repair. Type II is typically applied in 1.25 to 3 in. thick layers and is composed of high-performance Portland cement concrete. Type III is a combined system using asphalt and concrete (Shahrooz et al. 2000, Rahim et al. 2006).

Other types of overlays include latex-modified concrete and silica fume modified concrete. Latex-modified concrete overlays are expected to last up to 20 years (Ahlborn et al. 2002). However, they are susceptible to plastic shrinkage cracks and scaling and have a high material cost (Ahlborn et al. 2002). Silica fume overlays can be used in new construction and are typically applied in

layers of at least 1.25 inches. Silica fume reduces the size of pores within the concrete structure and is therefore capable of reducing permeability and increasing the strength (Abulshafi and Fitch 2005). It has been reported that this type of overlay has been effective in reducing the penetration of chloride ions in decks that have been exposed to salt-water (Ahlborn et al. 2002 , Radlinska et al. 2012).

1.4.1.3 Sealers

Concrete sealers can be used for sealing cracks as well as whole decks (Wenzlick 2007). The use of sealers is beneficial for surfaces that are exposed to wetting and drying cycles. Therefore, it is important to consider damp-proofing ability, breathability, resistance to chemicals, deterioration, resistance to freezing and thawing, and resistance to scaling when choosing a proper sealer (ACI 345-1R-06). The effectiveness of a sealer can be evaluated based on its ability to prevent chlorides from penetrating into the concrete, reach a penetration depth that is great enough to prevent UV degradation and corrosion under traffic, and to have a minimal need for reapplication (Rahim et al. 2006).

Sealers prevent liquid water from entering the concrete and can be used on bridge decks that experience early-age cracks with widths of 0.001 to 0.08 in. Sealers should be applied before the onset of severe damage in order to be effective. A nonwetable surface is created when penetrating sealers are applied and react with the pore structure of hardened concrete. Penetrating sealers do not degrade due to UV light and are generally abrasion resistant since they lay within the substrate of the concrete, however they have finite life and need to be resealed. Examples of penetrating sealers include silane, silicate, and siloxane materials (Ibrahim et al. 1999, Ahlborn et al 2002, Radlinska et al. 2012).

Investigations done by Ibrahim et al. (1999) revealed that silane coatings can result in a substantial reduction in corrosion in concrete specimens. Reactive silicates form precipitates when reacting with the concrete deck, which seal the open pores in the deck to reduce penetration of water and chloride. Silane and silane/siloxane can also be used in conjunction with topcoats. The use of an acrylic topcoat with Silane/Siloxane is most effective in reducing the damage due to sulfate attack. Furthermore, these sealers can be applied easily and do not require removal of previous layers before a new application (Ibrahim et al. 1999). However, one disadvantage to these treatments is that they must be reapplied periodically in order to maintain long-term effectiveness (Tabatabai 2009, Radlinska et al. 2012).

High Molecular Weight Methacrylate (HMWM) is another type of material that can be used to seal concrete decks. This type of sealer is capable of restoring structural bond strength (Rahim et al. 2006) and, according to research done by California Polytechnic State University, outperformed other tested material in regards to the restoration of flexural strength (Rahim et al. 2006). One particular HMWM, Sealate, can be used to fill fine surface cracks as well as wider cracks when

used in conjunction with sand. This prevents chlorides from penetrating the concrete structure and causing further damage (Transpo Insustries). HMWM is a low-viscosity material and is dependent on gravity in order to fill cracks. There also exists epoxy and urethane based materials that are similar to HMWM and can be categorized as gravity filling sealers. Gravity filling crack sealers are composed of two or more low-viscosity monomer or polymer components that harden into polymers when applied to the cracks. This seals the cracks and bonds to the crack walls to restore the flexural strength of the concrete (Sprinkel and Demars 1995). Urethane materials are similar to epoxies, except they are more flexible (Rahim et al. 2006).

1.4.1.4 Epoxy injections

Epoxy injections are generally utilized to repair larger bridge deck cracks to prevent moisture penetration and reestablish the structural integrity of the bridge deck (Keane et al. 2003). When the cracks are too deep for other conventional repair methods to be effective, epoxy injections can be used. The procedure of epoxy injections involves placing injection ports at intervals that measure no less than the depth of the crack itself. Epoxy is injected from one port to the exit of the adjacent port, so that the top and bottom of the crack is covered. This procedure is illustrated in [Figure 31](#). After crack repairs are made, an overlay may have to be placed over the deck for ride quality (VirginiaDOT 2009).



Figure 31. Epoxy Injection Procedure (VirginiaDOT 2009)

1.4.2 Maintenance

Most of the repair methods that have been described are not permanent and once applied to the structure, require periodic maintenance due to traffic loads, weathering, UV radiation, deicing chemicals, and other degradation processes (Sohanghpurwala 2006). Concrete coatings can last for 5 to 10 years before they need to be reapplied, but little information is available regarding both the cost of original application and cost of reapplication of these treatments. Overlays are generally more costly but several types, such as latex modified concrete overlays, are expected to last for

more than 20 years (Ahlborn et al. 2002). According to Rahim et al. (2006), the service life of a concrete sealer is a function of sealer material properties as well as service conditions related to sealer durability and chloride diffusion-related factors. It is expected that penetrating sealers will last approximately 3 years, although epoxy based sealers are generally ineffective after a year.

1.4.3 Optimization of rehabilitation methods and times to provide cost-effective outcomes

The intent of bridge deck remediation is to restore the structural integrity of the deck and extend its service life, i.e. the time to complete deck replacement. To effectively extend service life, State DOTs must have established strategies in terms of maintenance, repair, and remediation of concrete bridge decks. Bridge management strategies that balance preservation and replacement are more effective than those that allow bridges to deteriorate to the point of complete deficiency. It is important to apply the most appropriate treatment at the optimal time in order to lower the cost over the lifetime of the bridge (Ahmad 2011). The FHWA Preservation Guide suggests Systematic Preventative Maintenance (SPM) as a way to determine an effective remediation strategy. Figure 32 shows the steps involved in this program. The SPM program is a way for DOT's to determine the overall goal of preventive maintenance strategies as well as assess the needs, cost effectiveness, ability to accomplish the work (FHWA 2011).



Figure 32. Systematic Preventative Maintenance (FHWA 2011)

Due to the wide range of differences among DOTs and the environments in which the bridges are constructed there is no single “optimal” strategy. Rather, the literature has provided models (Huang et al. 2004, Hong and Hastak 2005, Robelin and Madanat 2007), bridge management systems (Guthrie et al. 2007, Robelin and Madanat 2007, PennDOT 2009), and rating systems as tools to aid DOTs in the planning and management large bridge inventories (Guthrie et al. 2007).

1.4.3.1 Models

In order to optimize maintenance, repair, and remediation of a bridge, different types of models are available for use. One model referred to as MEMRRES (Model for Evaluating Maintenance, Repair and Rehabilitation Strategies) is a spreadsheet tool that can be used to help choose optimal strategies. This model takes into consideration the effectiveness of the action, unit cost of maintenance, repair and remediation strategies, threshold performance levels, and the deterioration rate if the maintenance, repair, or remediation technique had not been applied. The MEMRRES is a convenient tool, however, it should be noted that some of the information that was used for its development is subjective information that was provided by responses of a questionnaire issued to 24 DOTs (Hong and Hastak 2005).

Robelin and Madanat (2007) proposed formulating a history dependent deterioration model using a Markovian process with an augmented state. Traditional Markovian-based models predict the future condition of an element, in this case bridge deck, based on the current condition and do not account for the condition history (Morcoux et al. 2002). They model the deterioration process using the probability that the deck will transition from one condition state to the next lower condition state over a discrete time interval, called the transition probability (Morcoux 2006). The augmented state Markovian model proposed by Robelin and Madanat (2007) is a modified form of the traditional Markovian process, in which the transition probability is based on the maintenance history and the time since the latest maintenance action in addition to the condition state. Using the augmented state Markovian model, optimal maintenance and replacement strategies can be implemented.

According to Huang et al. (2004), estimated service life and the timing of treatment are factors that contribute to the selection of the optimal treatment or maintenance of a bridge deck. In their studies, a mechanistic model of concrete deterioration (Babaei et al. 1996) is used to compute the relationship between the condition index and the age of the deck based on the percentage of spalled and delaminated areas, as well as chloride content. The estimated service life, in this model, is dependent on the original deck performance as well as the change in corrosion rate due to treatment performed on the deck. This model defines a K factor (the ratio of the slope of corrosion rate increase after treatment to that before treatment), which can be used to estimate service life of particular treatments. The estimated service life also depends on the time when the deck is expected to reach its maximum tolerable condition index. The overall conclusion of the studies of Huang et al. (2004) suggest that the estimated service life is strongly influenced by the timing in which treatment is applied. Early maintenance increases the estimated service life, while late maintenance can reduce the estimated service life (Huang et al. 2004).

1.4.3.2 Bridge management systems

Bridge management systems (BMS) have also been developed to assist agencies in the management of maintenance and rehabilitation by assessing current deck conditions, as well as

predicting future conditions (Guthrie et al. 2007, Robelin and Madanat 2007). Originally, bridge management systems utilized the National Bridge Inventory (NBI) database as the main source of information for bridge management decision-making. Later, the FHWA along with state DOTs developed Pontis, which provided decision support systems based on optimization (Thompson et al. 1998). PennDOT made changes to their original bridge management system that was based on NBI because it was not capable of predicting the cost of future deterioration and corrective actions (PennDOT 2009).

1.4.3.3 Rating systems

The National Bridge Inventory (NBI) rating system has been utilized nationwide and, as previously mentioned, has been used to develop bridge management systems (Phares et al. 2001). The NBI rating systems consists of a scale from 0 to 9 that rates the current condition of a bridge deck with 9 being excellent, like new, condition. However, because it is based on visual inspection, a consequence of the NBI rating system is a false sense of structural reliability. Inspectors often overestimate the quality of bridge decks, therefore, this rating system can be considered subjective (Phares et al. 2001).

Research studies conducted at Brigham Young University (BYU) (Guthrie et al. 2007) utilized visual inspection, sounding, Schmidt hammer testing, half-cell potential testing and chloride concentration testing to develop a deck rating system. The rating that a bridge deck received was utilized to determine the actions that should be taken. Based on a rating system from 0 to 100, preventative maintenance was recommended for ratings greater than or equal to 80, rehabilitation was recommended for ratings between 50 and 80, and replacement was recommended for a rating less than 50. Compared to the NBI system, this proposed system was better at distinguishing between different conditions of bridge decks and determining the best action required (Guthrie et al. 2007). [use the current system including FHWA protocols]

1.4.4 Life cycle cost analysis of bridge decks

Life-cycle cost analysis (LCCA) models analyze the costs related to all stages of an infrastructure application through-out its life cycle. Despite the considerable investment required for maintenance of bridges, Ozbaay et al. (2003) surprisingly found that only 12.5% of state DOT's apply any type of LCCA for bridges. The costs related to construction can be categorized into three types: agency costs, user costs and environmental costs. For a complete LCCA model, all three of these costs need to be considered. However, environmental costs are rarely considered in LCCA models and some LCCA studies (Enright and Frangopol 1999, Estes and Frangopol 2001, van Noortwijk and Frangopol 2004) neglect user costs as well. Agency costs include all costs related to construction, repair, rehabilitation, and replacement during the service life of the structure. Software for LCCA of bridge decks has been developed, such as BLCCA and BridgeLCC. In addition, discount rates will be described because they can affect the results obtained from LCCA

models. An integrated life-cycle assessment and life-cycle cost analysis (LCA-LCCA) model will also be reviewed.

User costs consist of three types: traffic delay, increased risk of traffic crashes, and increased vehicle operating costs due to construction. The majority of user costs are associated with user delay or time spent in traffic related to construction. User delay is calculated based on the additional time spent in construction related congestion compared to the time it would take to travel the same distance in normal traffic conditions. Traffic crashes due to construction work zones and due to the extended travel distance when a detour is taken, are also included in user costs. Costs due to traffic crashes can be calculated by assuming the relative risk of crashes is proportional to the additional distance traveled compared to the distance traveled on a roadway with no construction. Furthermore, increased fuel consumption by vehicles due to traffic conditions and longer detouring routes must also be considered when calculating user costs; even though fuel costs only make up 2% of total user costs (Kendall et al. 2008).

Environmental costs are due to the pollution damage inflicted during the construction processes including the emission of CO₂ from the energy consumption due to fossil fuel combustion, the chemical process in cement production, the electrical energy required for grinding of additive materials, the fuel consumption for the transportation of raw materials and final product. Damage costs due to pollution are difficult to calculate and all have considerable levels of uncertainty related to them, particularly damage due to pollutants which affect global warming (Kendall 2008). Banzhaf et al. (1996) was able to derive pollutant damage costs based on morbidity health values, mortality risks, and willingness to pay to avoid mortality risks. For greenhouse gases (GHG) costs, Tol et al. (2003) suggests a value of \$60 per metric ton of carbon (Tol 1999).

The software available for applying LCCA to bridges include: BLCCA (Bridge Life Cycle Cost Analysis) (Hawk 2002), developed by the National Cooperative Highway Research program and BridgeLCC (Ehlen 2003). Each of these software packages consider user and agency costs and have the capability to account for uncertainty modeling. BridgeLCC also allows the user to enter third party cost parameters such as environmental costs. These software packages have some disadvantages such as a complex user interface for BLCCA and a lack of detail in cost output for BridgeLCC.

The discount rate is an alternative measure of interest rate to the standard Annual Percentage Rate which can also affect the results obtained from LCCA models, particularly when analyzing structures with longer service lives. There are no specific rules regarding the selection of a discount rate for each model. Kendall et al. (2008) suggest that the discount rate can be based on values recommended by the United States Office of management and Budget (OMB) (Office of Management and Budget 2005), which estimates a real discount rate of 4% for user and agency costs.

Kendall et al. (2008) developed an integrated life-cycle assessment and life-cycle cost analysis (LCA-LCCA) model. They applied this model to a conventional concrete bridge deck and compared it to an alternative engineered cementitious composite link slab design. The LCA model evaluates the environmental performance of a product or process during its life cycle and provides the necessary data required to conduct a LCCA. Figure 33 illustrates the proposed integrated LCA-LCCA model framework.

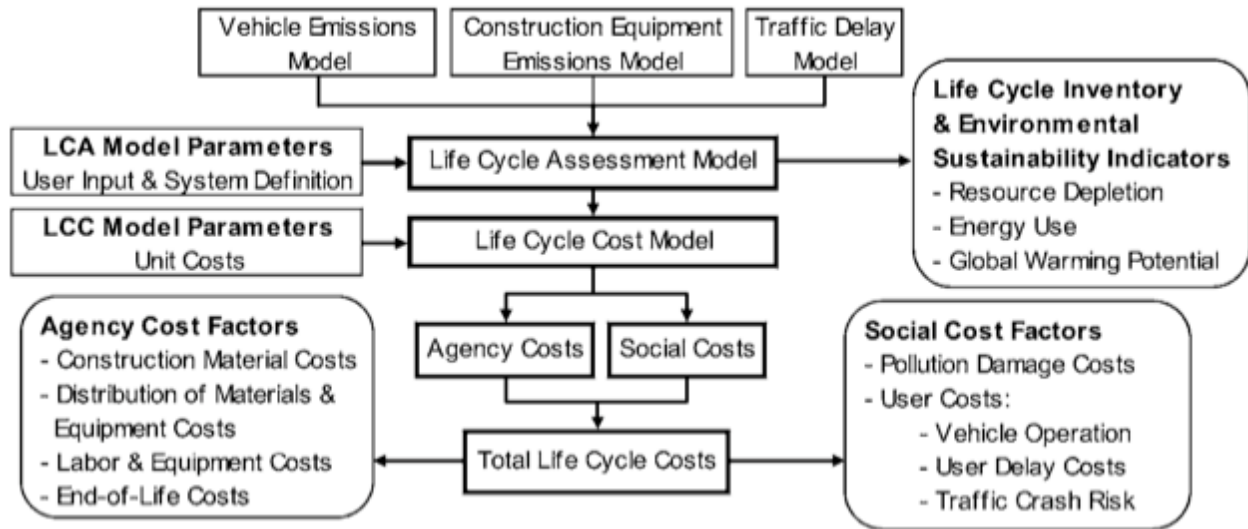


Figure 33. Integrated LCA-LCCA model flow diagram (Kendall et al. 2008)

Kendall et al. (2008) found that, for a particular bridge in Michigan with an annual daily traffic flow (AADT) of 35,000 vehicles, user costs comprised more than 90% of total life cycle costs. However, at lower traffic volumes, the agency and environmental costs played a significant role in the total cost results. Nonetheless, this emphasizes the fact that initial costs and agency costs are not always the majority of the total life-cycle costs.

CHAPTER 2 (TASK 2)

Interview PennDOT Personnel and Document Interview Data

2.1 Introduction

Task 2 efforts to design, launch, collect and analyze a survey for collecting information about the early-age bridge deck cracking are discussed in this chapter. The objective was to collect and document PennDOT personnel's detailed experience with early-age bridge deck cracking as it relates to long-term bridge deck performance. The intended recipients included PennDOT central office and district personnel representing design, construction, bridge inspection, and materials units.

The survey was intended to provide information on early-age cracking experience, preferred crack prevention methods, and deck cracking remediation methods/strategies. Information regarding the long-term performance of bridge decks with early-age cracking and the remediation methods were solicited as well. The survey was also structured to determine the recipients' area of expertise, and to identify other personnel who can provide additional information on the subject matter.

Upon completion of the development of the survey, it was disseminated to the intended recipients by PennDOT. The final steps were analyzing the responses and documenting them in this chapter.

2.2 Survey Design

A questionnaire in the form of an online survey was designed and reviewed by the project panel. While the survey questions are presented at the end of this section for reference, the original survey is included in the Appendix B.

The survey included three questions regarding the respondents' name, title, position, contact information, their role/unit within PennDOT, and their level of experience with bridge deck cracking.

A few questions covered crack detection and prevention methods to assist in understanding the responses. At PennDOT's suggestion, three questions regarding crack development and concrete placement during summer months were included in the survey. A couple of questions discussed short-term performance evaluation, and the effects of early-age cracking on the long-term performance of bridge decks. There were three questions about remediation methods, their selection, and their effectiveness.

The last question asked about the contact information for any other PennDOT experts who could discuss the subject further. As a result of this question, 10 additional contacts were identified and a request for additional information regarding the subject was sent to them. The additional contacts were asked to provide information (based on their experience with practices and policies) about:

- Reducing early-age cracking,
- Preferred prevention strategies in three subject areas: design, materials, and construction,
- Remediation methods for cracked decks, and their effectiveness, or lack thereof.

Of the 10 additional contacts, 9 responded to the request for information and 5 experts provided recommendations. Their responses are discussed in the analysis section of this chapter.

The Questionnaire:

<p>1. Respondent Information: Contact Name/Title: District: Phone No./Email:</p> <p>2. Which sections of PennDOT bridge construction projects do you represent? Please select all that apply Design Construction Bridge Inspection Materials Unit Other:</p> <p>3. Please indicate your level of experience with the following items pertaining to bridge deck cracking.</p> <table><tr><td></td><td>No</td><td>Experience</td><td>Some</td><td>Experience</td><td>Familiar</td><td>Very</td></tr><tr><td>Familiar</td><td></td><td></td><td></td><td></td><td></td><td></td></tr><tr><td>PennDOT Policies</td><td></td><td></td><td></td><td></td><td></td><td></td></tr><tr><td>Standard Drawing & Engineering Designs</td><td></td><td></td><td></td><td></td><td></td><td></td></tr><tr><td>Concrete Materials and Mix Design</td><td></td><td></td><td></td><td></td><td></td><td></td></tr><tr><td>Construction Practices & Specifications</td><td></td><td></td><td></td><td></td><td></td><td></td></tr><tr><td>Contractual Practices</td><td></td><td></td><td></td><td></td><td></td><td></td></tr></table> <p>4. Do you perform deck cracking surveys? Yes (indicate below the approximate percentage of District bridge deck surveys you perform) No Approximate percentage of District bridge deck surveys performed:</p>		No	Experience	Some	Experience	Familiar	Very	Familiar							PennDOT Policies							Standard Drawing & Engineering Designs							Concrete Materials and Mix Design							Construction Practices & Specifications							Contractual Practices						
	No	Experience	Some	Experience	Familiar	Very																																											
Familiar																																																	
PennDOT Policies																																																	
Standard Drawing & Engineering Designs																																																	
Concrete Materials and Mix Design																																																	
Construction Practices & Specifications																																																	
Contractual Practices																																																	

5. When do you typically observe initial cracking in a bridge deck?

0-28 days

1-3 months

3-12 months

1 year-end of life

Do not generally observe deck cracking

6. Please indicate the effectiveness of the following methods for preventing cracks from occurring. (1 being not effective and 5 being very effective)

1 2 3 4 5 Not Used

Mix Design

Structural Details

Construction Practices

Curing Techniques

Recommend any specific improvements that can be made to reduce deck cracking. Please provide references or links to construction specifications or information for the methods mentioned.

7. In your opinion, do you see more cracking during:

Hot summer months

Cooler fall/spring months

8. During the summer months, when does the placement generally occur?

Start time

Finish Time

9. In your opinion, do you think it would be beneficial to start summer placements about 7:00 PM so that as the superstructure cools and contracts during initial curing, the deck would see a slight compression?

Yes

No

10. In your opinion, what effect does early-age cracking have on the long-term performance of concrete bridge decks? (1 being no effect and 5 being significant effect).

1 2 3 4 5 N/A

Reduced bridge deck service life

Increased life cycle cost

Other effects (Please explain below)

Other effects:

11. Please indicate all remediation methods (strategies or techniques) for early-age cracking in your district and approximately the longevity of the remediation techniques.

Overlay

Epoxy injection/resin

Sealant

Latex modified bridge deck inlay

Asphalt overlay with waterproof membrane

Linseed oil

Other

12. Please rank and explain the 3 most successful remediation methods from Q11 based on cost and effectiveness. Why were these methods the most effective? Please provide references or links to specifications or information.

1.

2.

3.

13. What is the basis for selecting a particular remediation technique?

Prior Experience

Cost

Manufacturer

Other (please specify)

14. How do you evaluate a bridge deck's early (short-term) performance? Please select and explain all applicable methods used in your district.

Crack Survey

Material Testing

Structural Assessment

Other Methods

Other:

15. If there is someone other than yourself with who we should follow up for additional details, please provide their contact information below.

Contact Name/Title:

Phone No./Email:

2.3 Survey Distribution

As was mentioned in the previous section, an online survey tool was employed to solicit responses to the survey. A link to the online survey, along with a brief description of the project, was sent to PennDOT district offices and assistant district executives (ADEs) of construction by PennDOT via a transmittal email. The recipients were asked to respond and/or distribute to their staff with bridge construction experience.

2.4 Survey Response Data

The research team received 62 responses to the online survey. The survey responses are summarized in this section.

2.4.1 Respondents' Information

At least one person from each district responded to the survey with districts 2-0 and 12-0 having the largest numbers of respondents. The third largest number of responses came from different offices and bureaus within the central office, as seen in [Figure 34](#).

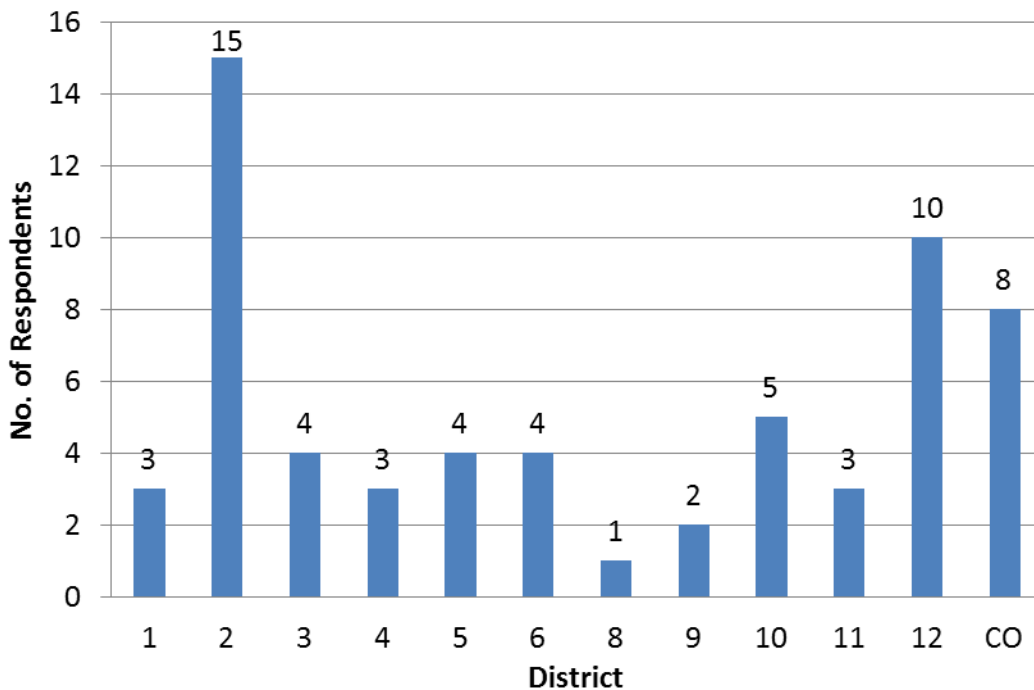


Figure 34. Number of Respondents from Each District (CO=Central Office)

As it was intended, the majority of respondents represented the construction unit. Some respondents had related experience in more than one unit within the PennDOT ([Figure 35](#)).

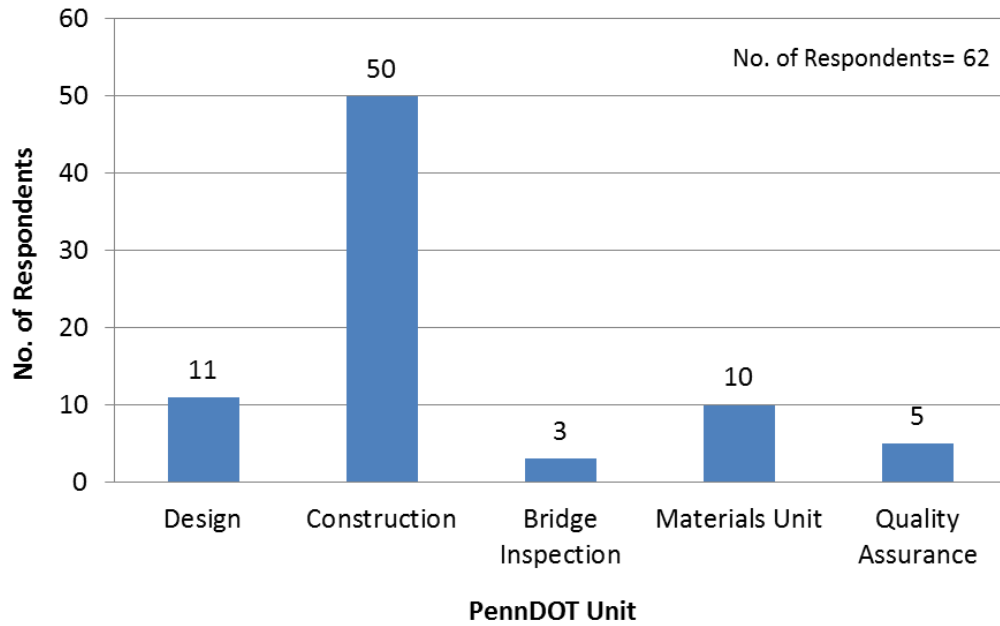


Figure 35. Number of Respondents from each PennDOT Unit

Regarding the respondents' level of experience with different items pertaining to bridge deck cracking, over 90% of respondents identified as being familiar or very familiar with PennDOT policies, standard drawings, construction, and contractual practices. With regards to concrete materials and mixture designs, 75% of the respondents identified as being familiar or very familiar with these subjects (Figure 36).

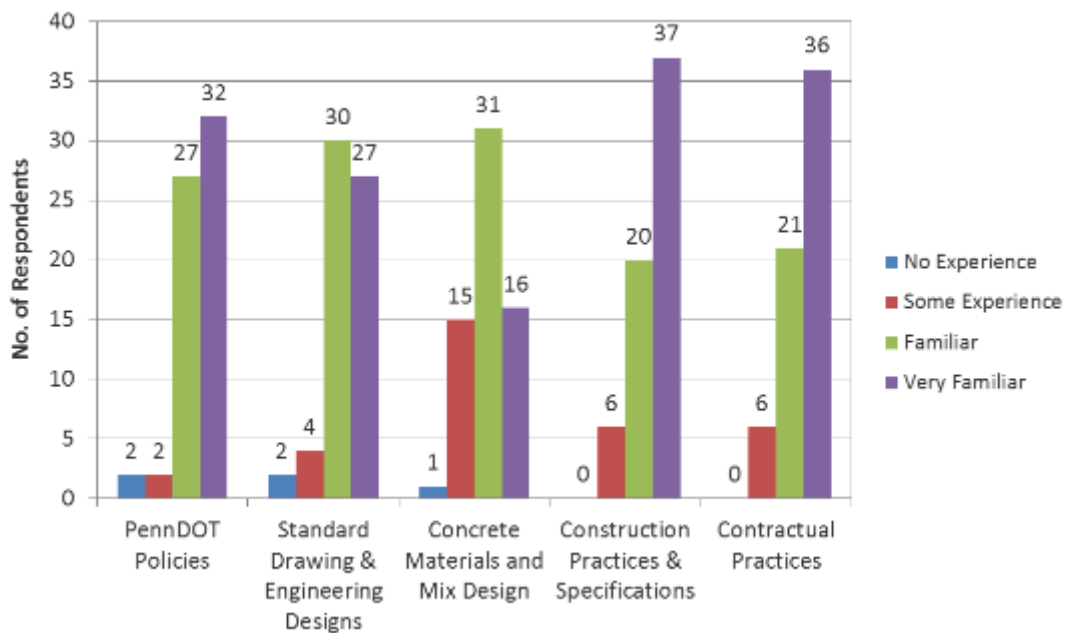


Figure 36. Respondents Level of Experience with Respect to Various Aspects of Bridge Deck Construction

2.4.2 Experience with Crack Detection

The respondents were asked whether they perform deck cracking surveys. They were also asked to provide the percentage of the bridges surveyed. Some of the responses represented the districts' practices, but some responses were individuals' response to the question. By examining the responses, it can be seen that early-age crack detection is done by construction units and it is typically assigned to structural control engineers (SCE) or material engineers. In one case, the design unit requested the materials unit to perform such surveys. Some of the districts (8-0, 11-0, and 12-0) indicated that they perform deck surveys on 100% of the bridges after their construction. All the representatives from two districts (4-0 and 6-0) answered "no" to the question.

The respondents were also asked when they typically observe initial cracks in decks and the majority indicated between 1 and 3 months after completion of deck concrete placement. However, about the same number of responses indicated observing cracks up to 28 days after a deck concrete placement, as shown in [Figure 37](#).

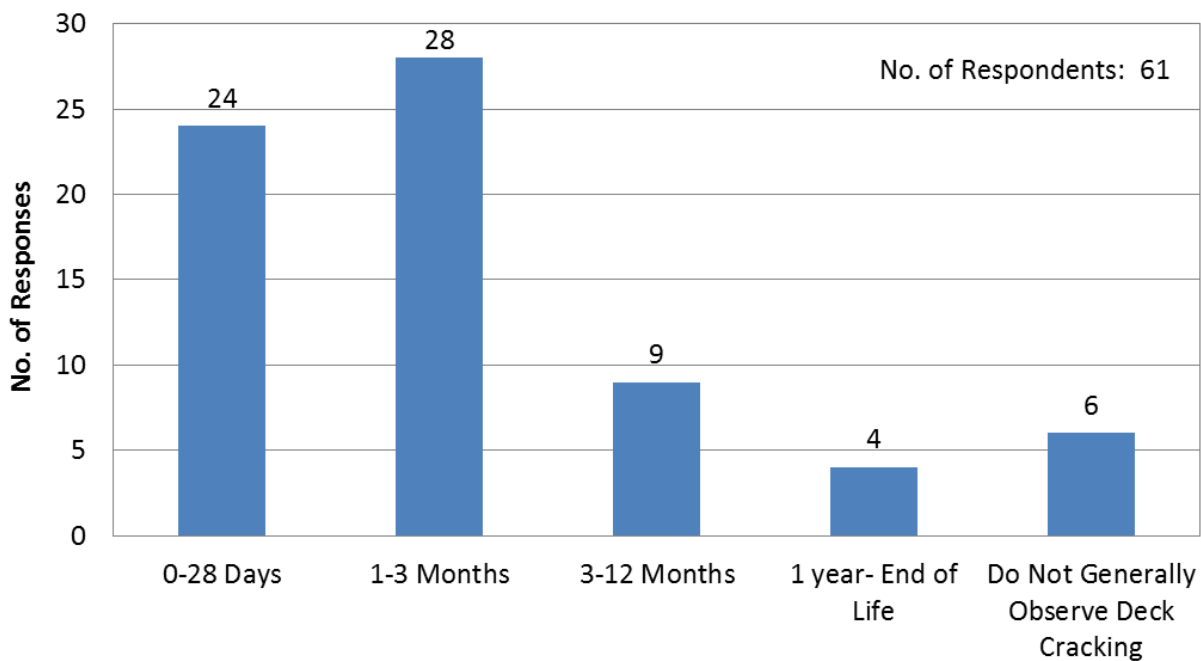


Figure 37. Respondents Observations of Initial Cracking

2.4.3 Experience with Summer Construction

PennDOT suggested three questions regarding crack detection and concrete deck placement during summer months.

On the subject of experiencing cracks during hot summer months versus cooler fall/spring months, 82% of the respondents indicated observing more cracks (can be interpreted as crack development) during summer months.

Regarding the time of deck placement during summer months, the majority of responses showed 4:00 AM as the start time and 10:00 AM as the finish time. The distribution of the responses is presented in Figure 38.

The respondents were asked whether it is beneficial to start summer placement around 7:00 PM in order to induce slight compression in the deck (due to superstructure contraction during curing). The majority of the responses (67%) showed agreement, however about one-third of the respondents (33%) suggested other times, usually at night, or early in the morning.

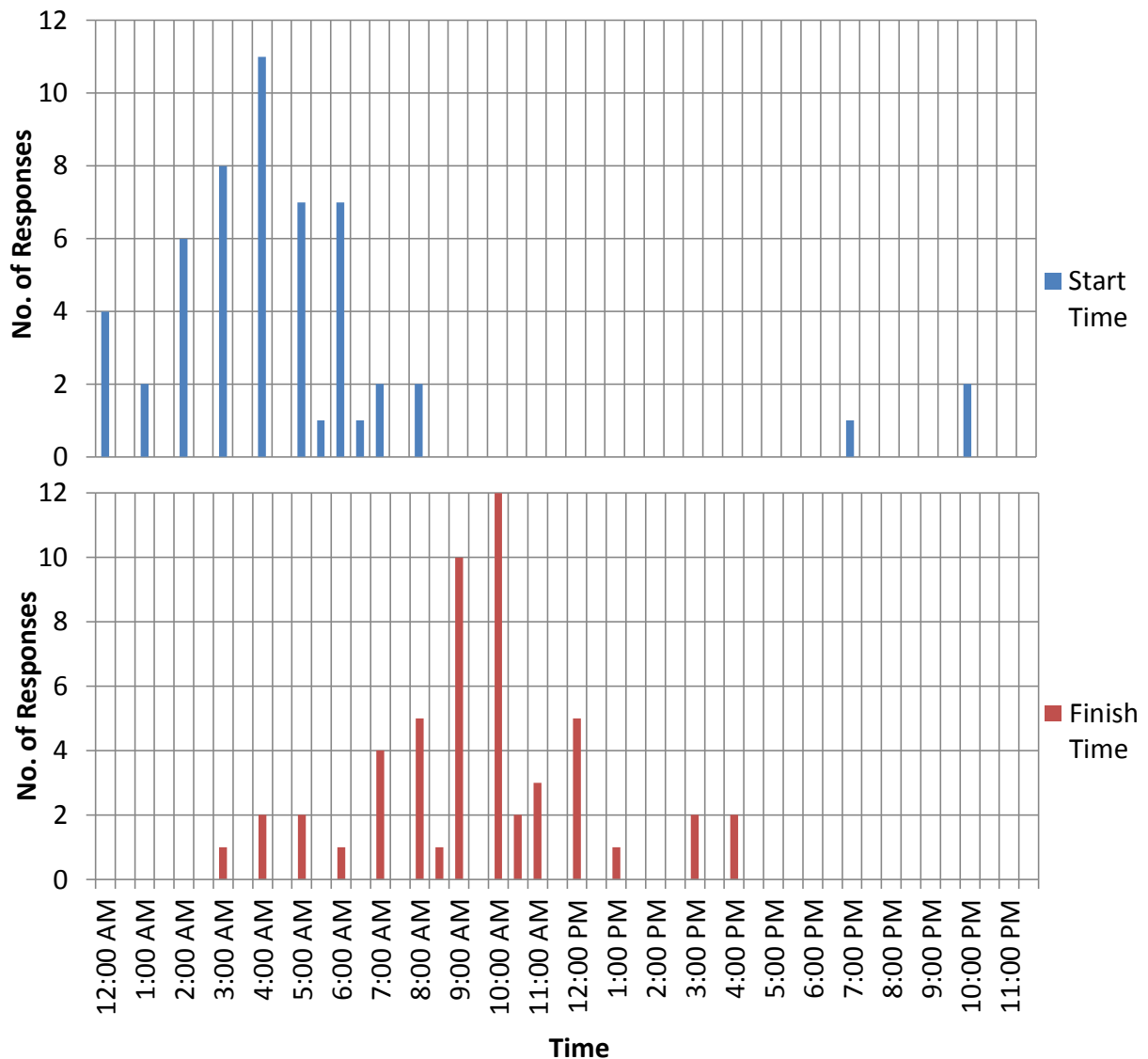


Figure 38. Respondents Past Experiences with Deck Placement Times

2.4.4 Crack Prevention Methods

The respondents were asked about the effectiveness of the following crack prevention methods: Mix design, structural details, construction practices, and curing techniques. As can be seen from Figure 39, curing techniques were indicated as “very effective” followed by construction practices, mix design, and structural details, respectively.

The respondents were also asked to provide their recommendations on specific improvements that can be made to reduce deck cracking. Table 10 presents these recommendations categorized by the area of improvement.

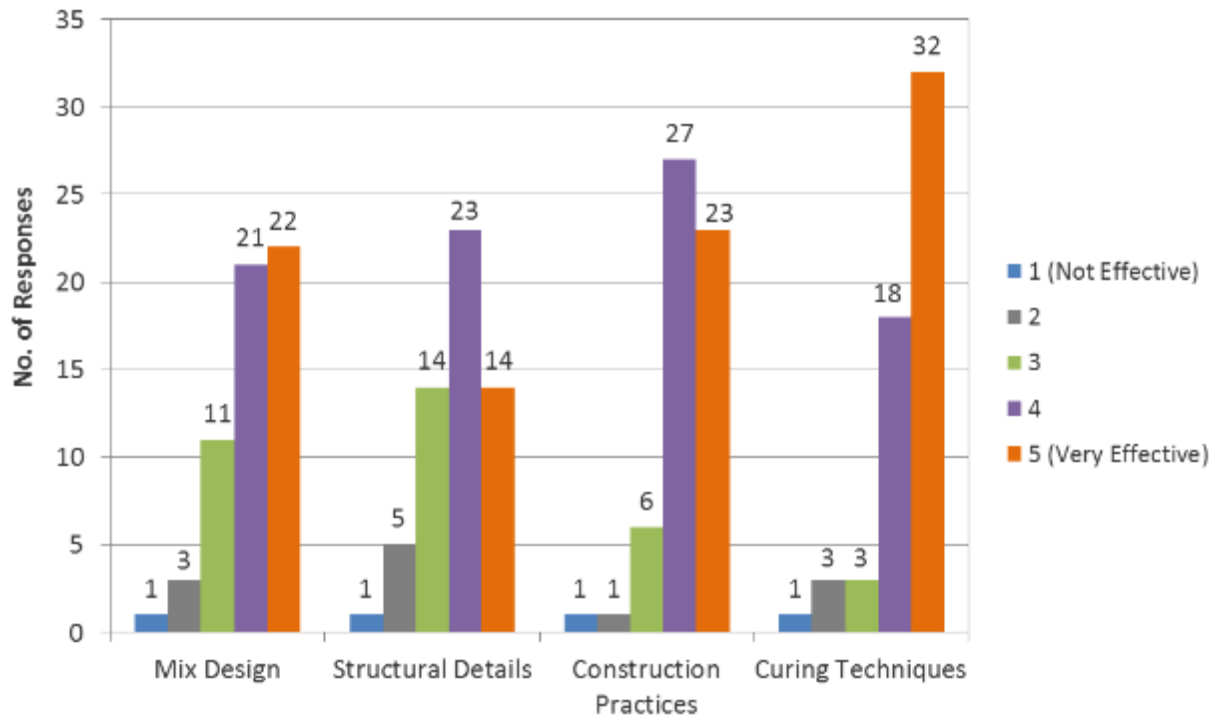


Figure 39. Respondents Opinion of Various Crack Prevention Methods

Table 10 Recommendations for Crack Prevention

Area of Improvement	Recommendations
Curing Techniques	<ul style="list-style-type: none"> • Apply curing as soon as possible and maintain curing for 28-days with wet burlap and weep hoses so deck remains saturated at all time. 14 day wet cure, plus 7 day wax membrane cure after. Require fogging behind placement.
Construction Practices	<ul style="list-style-type: none"> • Use conveyance systems instead of pumps for placing. • Insufficient wait time between positive and negative moment area placements. Evaluate simultaneous positive placements. • Cracking observed when deck is not poured according to sequence specified in design plans (deck poured from beginning to end without stopping). • Reduce number of construction phases. Vibration transmitted through Phase 1 transverse rebar into Phase 2 is conducive to cracking and possible reduction in concrete/rebar bond strength. • Stagger reinforcing bars between the top and bottom mats to reduce constraint. Consider filling SIP valleys with Styrofoam to further reduce the constraint. • To reduce the ultimate strength of the concrete, the current PennDOT penalty structure for the concrete along with the Road User Liquidated Damages need to be revised. • Finish bridge decks smooth to allow the immediate placement of wet burlap. Within 10 min. of finishing and within 10 to 18 feet behind the finishing equipment. • Mechanically groove surface texture. • Do not place concrete when the ambient air temperature is below 40°F or above 80°F. • Maintain the differential between mean beam temperature and the concrete mix temperature to under 22°F and for a minimum of 24 hours after placement (Summary Report for Research Project No. 89-01, Prevention of Cracks in Concrete Bridge Decks performed by Wilbur Smith Associates for PennDOT). • Minimize, slow down, or eliminate traffic on phased construction. • Detour traffic for 2-3 days during and after placing deck during half-width construction. • For prestressed decks, limit time between the beam fabrication and deck placement (differential creep and shrinkage). • Only pour decks at night & enforce “wet” cure wetness. (D-12) • Add penalty for cost of sealant/overlay if decks have cracking above __YD/SY. • Construct qualification slab to ensure mix can be pumped, worked, finished, and is low cracking.
Structural Details	<ul style="list-style-type: none"> • Study the effects of superstructure stiffness without the deck as it relates to deck cracking. • Consider requiring a latex overlay 1 year after placement of decks on adjacent box beam bridges. • Stagger studs and deck slab bars, revise BC-752M & BC-753M (CA, D-12).

	<ul style="list-style-type: none"> • Design “strain compatibility” during temperature differentials. i.e. design steel compression to offset shrinkage cracks w/o overstressing studs in very cold weather.
Mix Design	<ul style="list-style-type: none"> • Limit maximum concrete strength (5500 psi at 28 days). • Using lower strengths than the normal 4500 psi. • Slumps should be limited to lower values (<3.5 in.). • To gain strength quickly, less water is used, making mix brittle in hardened state. • The workability of AAA concrete is too high. • Use less brittle mix, such as A or AA with latex additive to increase flexibility. • Possible use of fibers in mix to control cracking. • Specify min. w/c ratio 0.40 to assure enough bleed water is present in the mix to allow proper finishing. • Use higher w/c (0.43) with AAA-P. • Modify coarse aggregate Pub.408, Section 704, Table A, note 7, to provide a min. of 35% passing the 1/2" sieve. • Use F.A. with FM range from 2.60 to 3.15. • Max. slag content not to exceed 35%. • Higher design plastic air content, 8.0% target. • Require aggregate optimization and cementitious material in mix designs. • Reduce the amount of chemical additives used in mixes. • Use “internal curing” via shrinkage reducing admixtures (SRA), saturated aggregate (>1%), and super-absorbent particles, such as HYDROMAX. • Concrete field values for strength have been found to be many times the design strength, resulting in brittle concrete.

The additional PennDOT experts provided recommendations regarding early-age crack prevention as well. These recommendations are presented in [Table 11](#).

Table 11- Additional PennDOT Experts' Recommendations for Crack Prevention

Area of Improvement	Recommendations
Curing Techniques	<ul style="list-style-type: none"> • Wet-curing decks for 14-days. • Burlap (2 layers) as soon as possible (within 10 min.) following finishing machine. • Require fogging during placement. • Soaker hoses placed over burlap then covered with white polyethylene plastic. • Liquid membrane cure applied after wet cure period. This should protect the deck from damage for 7 days and allow a slower/even drying of slab. • 21 days until open to traffic. Limit construction loading in accordance with Sec. 1001 of Pub. 408
Construction Practices	<ul style="list-style-type: none"> • Monitoring evaporation rates and mitigation as necessary. • Limiting the movement of freshly-placed concrete due to traffic on adjacent lanes in half-width construction by delaying construction of new diaphragms between phases or temporarily disconnecting existing diaphragms. • Restrict temperature difference between beam and plastic concrete to less than 22 degrees F. • For bridges with continuous steel girders, specify a minimum compressive strength of the positive sections prior to pouring the negative sections. • Stressing specification enforcement with construction inspection staff. • Avoiding over-finishing the concrete. • Avoiding placement when it is too windy or too hot. • Holding pre-pour meeting and discuss all aspects of the placement. • Phased pour sequences • No placement unless ambient air temp is 40° F and rising • Minimize hand finishing to prevent overworking • Placing the initial deck placements into tension on continuous structures. • Considering simultaneous placements of positive areas in adjacent spans.
Structural Details	<ul style="list-style-type: none"> • Calling out the proper pour sequence. • The shear studs in composite decks should be staggered to reduce the concentration of the restraint. • The top and bottom reinforcing bars should be staggered to reduce the concentration of the constraint. • Stay-in-place over removable deck forms has added constraint by their shape; perhaps fill the valleys with Styrofoam.
Mix Design	<ul style="list-style-type: none"> • Limit maximum concrete strength (5500 psi at 28 days) • Slumps < 4" at point of placement (settlement cracking). • Reducing the strength gain as much as possible. Slag mix designs normally have a slower strength gain; however, the slag mix designs can become a scheduling issue for the contractor in colder temperatures. • Utilizing HPC or AAAP mix designs. • For bridges with continuous steel girders, specify a minimum compressive strength of the positive sections prior to pouring the negative sections.

	<ul style="list-style-type: none"> • Lowering the cement content is the biggest change needed to prevent deck cracking. • Lowering cement content even more than that of AAAP mixes. • Perform Microstrain ASTM C-157 during mix design. < 500 microstrain • Prohibition of field addition of water to adjust slump. • Requiring ternary mix for slower strength gain and lower permeability (+/- 45% replacement) (RCP's < 1,200) • Increasing plastic air content 8% target • Max. cementitious 690 lb/cy • Max. W/C 0.43 • Decreased 28-day strength to 4,000 psi • Consider adding aggregate optimization in the future (TxDot, MinnDot, Shilstone, etc.).
--	--

2.4.5 Short-Term Bridge Deck Performance Evaluation

One of the questions in the survey was concerned with methods for evaluating short-term bridge deck performance. The options were crack survey, material testing, structural assessment, and any other possible methods practiced by the districts. The distribution of the responses is shown in [Figure 40](#) and it shows that performing a crack survey is the most common practice.

The following comments by some of the respondents provide more details on the evaluation methods:

- Obtaining concrete cylinders at the deck pour and testing them for rapid chloride permeability (RCPT).
- Visual bridge deck inspections consistent with the National Bridge Inspection Standards (NBIS) or district procedures.
- Inspection of the bridge deck texturing to evaluate skid resistance.

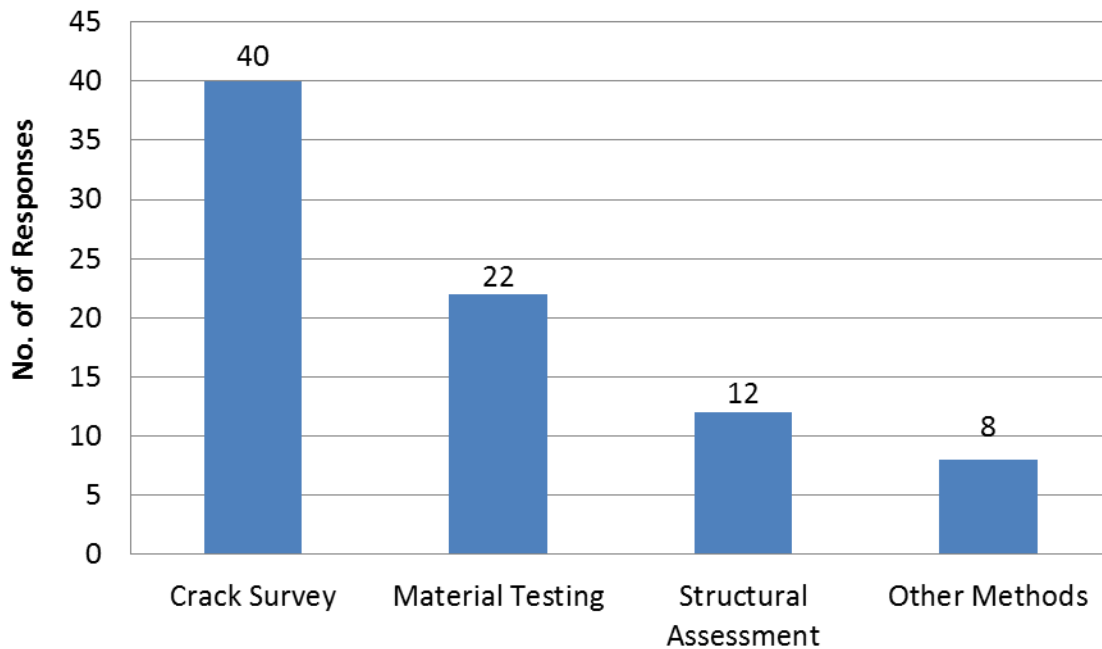


Figure 40. Evaluation Methods for Short-Term Bridge Deck Performance

2.4.6 Effect of Early-Age Cracking on Long-Term Bridge Deck Performance

The respondents' opinion was asked regarding the effects of early-age cracking on long-term bridge deck performance. The given effects were reduced bridge deck service life and increased life cycle cost, but they were also asked to provide any other possible effects. As is evident from [Figure 41](#), the respondents indicated early-age cracking to be effective or very effective in reducing bridge deck service life and increasing life cycle cost.

The other effects mentioned by the respondents were:

- Early-age cracking allows water and de-icing chemicals to penetrate into and possibly through the deck to the sub-structure.
- Early age deck cracking (~1-year) metrics can generally predict the deterioration rate for the deck. The shape of the deck cracking metric curves (yds/sy) is generally consistent, but the initial slope sets the deterioration rate and determines if the 45-year useful life can be attained.
- With early-age cracking, a maintenance crew must get involved earlier than anticipated.
- One comment relates to the effect of early-age cracking on public perception: “The public perception that PennDOT and its business partners cannot build a quality product.”

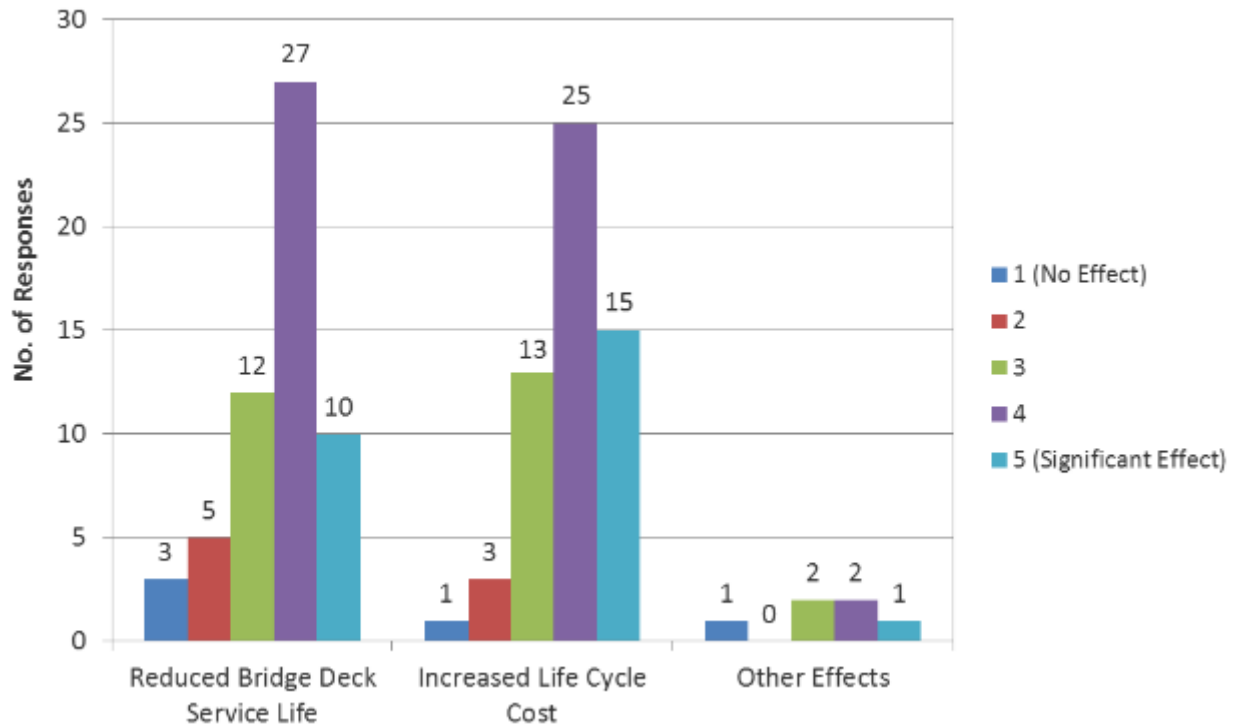


Figure 41. Effect of Early-Age Cracking on Bridge Deck Long-Term Performance

2.4.7 Crack Remediation Methods and Strategies

Three questions targeted remediation methods, their selection criteria, and their effectiveness.

The basis for selecting a particular remediation technique was one of the questions. The majority of the responses indicated prior experience as the basis for selection, followed by the cost, other criteria (listed below), and manufacturer (Figure 42).

The other bases for selection include:

- Performance over time.
- Depths, widths and quantities of cracking. Also, is cracking just localized or spread out over entire bridge.
- Scientific studies
- Value, deck life per unit cost

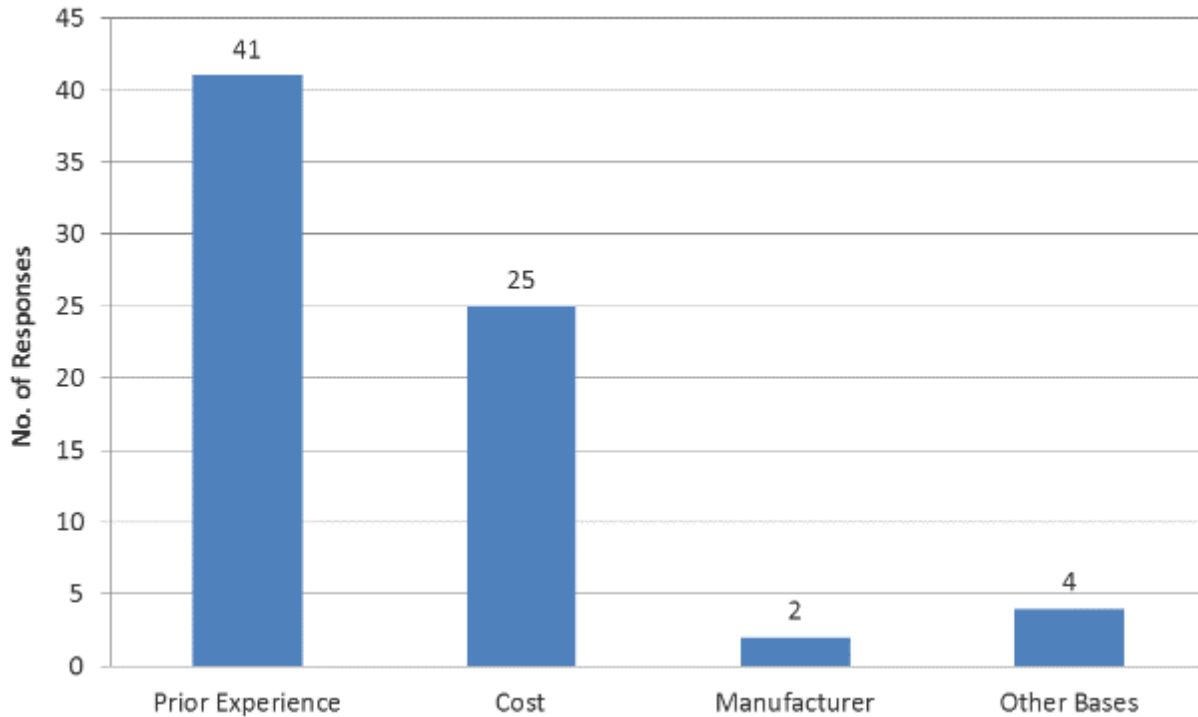


Figure 42. Selection Basis for Remediation Method

Another question asked about the remediation methods for early-age cracking in the district and the approximate longevity of the remediation techniques. The designated remediation methods were: latex modified bridge deck inlay, asphalt overlay with waterproof membrane, overlay, epoxy injection/resin, sealant, linseed oil, and any other possible remediation. For longer lasting remediation (5 to 10 years), latex modified bridge deck inlay was selected by most of the respondents followed by asphalt overlay with waterproof membrane, and overlay. For methods with shorter life (1 to 5 years), the use of sealant was indicated as the prevalent method followed by epoxy injection/resin. Use of linseed oil was indicated as the predominant method for remediation lasting less than 1 year (Figure 43).

Other remediation methods and comments are as follows:

- Use of penetrating sealer (Enviroseal® 40) placed on all decks after initial cure.
- Use of epoxy overlay (Polycarb’s Flexogrid, Euclid’s Flexolith, etc.).
- Preferred sealant is Methyl-Methacrylate penetrating sealer.
- Epoxy injection and latex last more than 10 years in most cases. Linseed oil effectiveness is dependent on its exposure to heat and UV (see Illinois DOT PRR 155).
- Asphalt overlays hide any future deterioration.

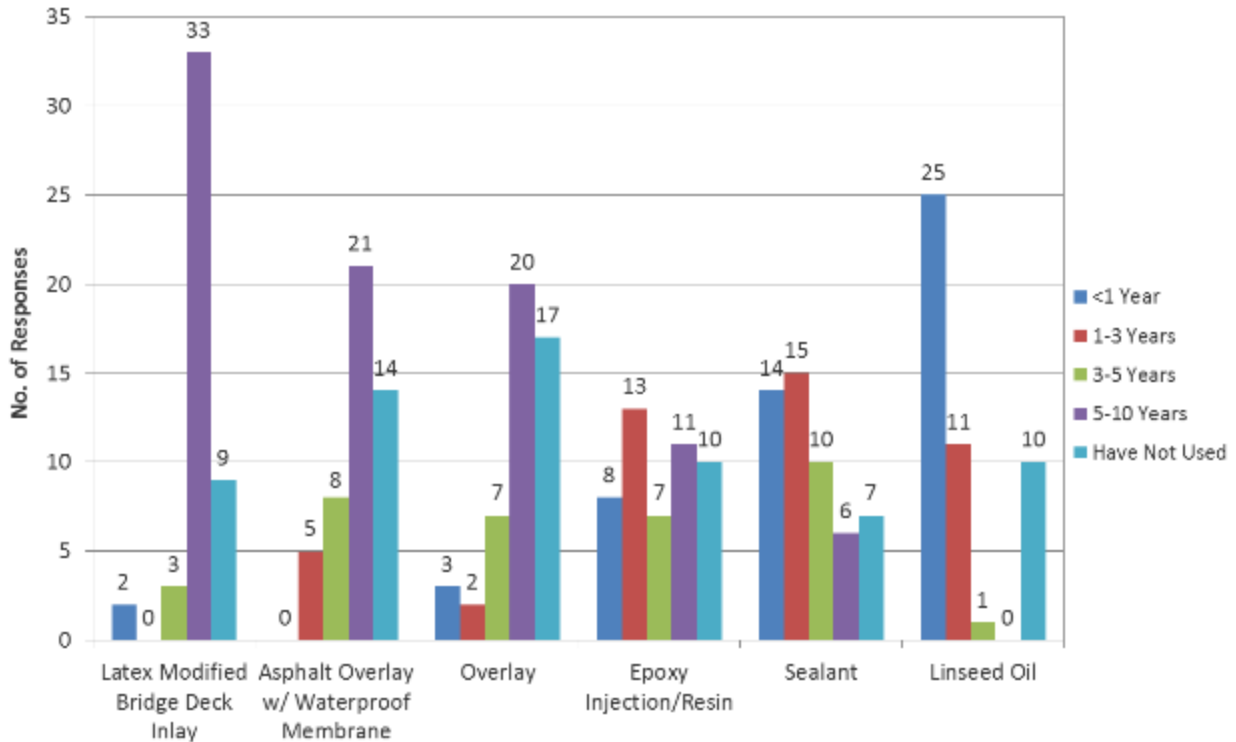


Figure 43. Remediation Methods and their Longevity

The last question regarding the remediation methods was a request to rank and explain the 3 most successful remediation methods based on cost and effectiveness. It should be mentioned that in the following discussion, “epoxy surface treatments” include epoxy overlays, epoxy aggregate overlays, and epoxy/resin injection. As can be seen from Figure 44, epoxy surface treatments and latex modified surface treatments were ranked first by a majority of the respondents. The use of sealants was ranked second, and asphalt overlay with waterproof membrane was ranked the third remediation method considering effectiveness and cost.

Some of the responses referred to specific compounds/brands of sealants such as Silane/Siloxane sealers, Enviroseal® 40, Methyl-Methacrylates, Transpo (T-70 and T-70 MX-30), and Sikadur 55.

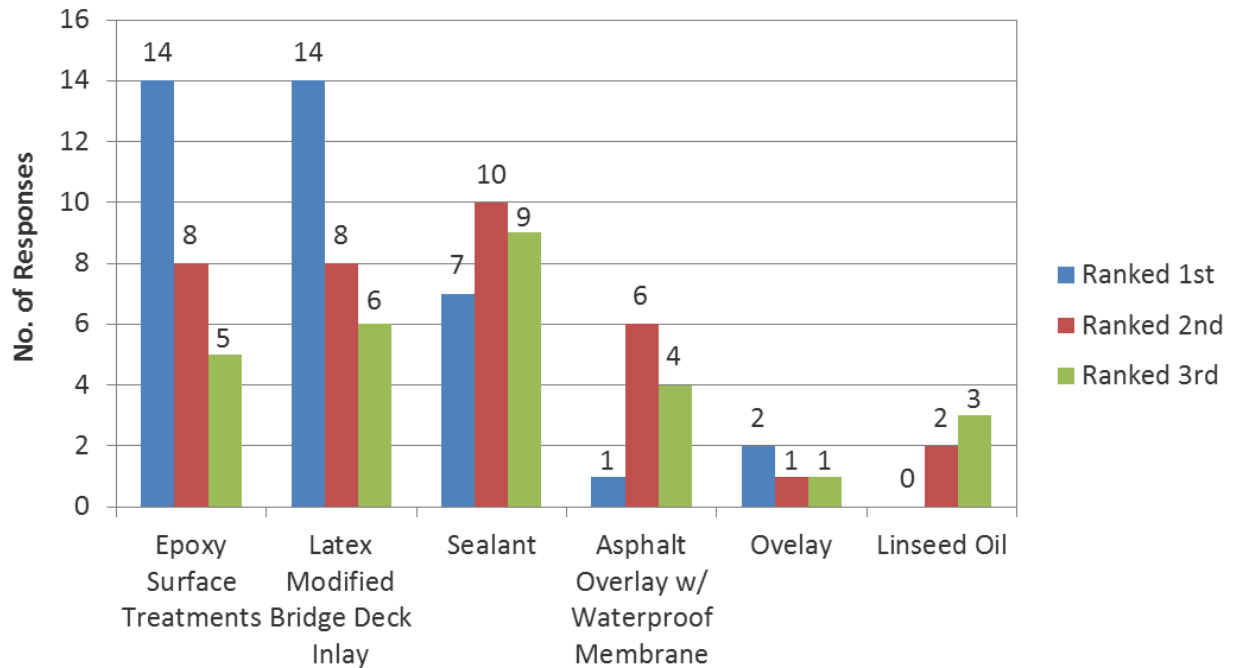


Figure 44. Ranking of the Remediation Methods

The additional PennDOT experts provided recommendations and comments regarding remediation methods as well. These recommendations are presented in the following section.

- Using a second coat of penetrating sealer for small cracks (0.007”) and methyl-methacrylate for larger cracks.
- Using epoxy injection.
- Using a thin epoxy overlay such as Poly-Carb’s Flexogrid system installed soon after construction (long-term effectiveness to be determined).
- Use of epoxy deck overlays or waterproofing membrane/bituminous overlays. Both overlay systems have performed well with no signs of deck cracking reflecting up through the overlay.
- There have been issues with latex cracking and failures in the past.
- For bridges constructed utilizing phase construction, using epoxy overlay placed as part of the original construction.
- Use of epoxy urethane overlays on bridge decks to extend the life of bridges.
- Performing hydro-demolition followed by 1-1/4” latex overlay to extend the decks life.
- Latex overlays generally last up to 25 years.
- Methyl Methacrylate: moderately effective. Some question of actual crack
- Use of penetration sealers such as Transpo T-70 or T-70 MX 30.

2.5 Summary

A survey emphasizing early-age cracking in concrete bridge decks was performed. The recipients were PennDOT personnel from districts and the central office. The findings of the survey can be summarized as follows:

- A couple of districts had less than 3 participants and another two districts had over 10 representatives, but the majority of districts had between 3 and 5 representatives.
- The majority of responses (39%) indicated typical observation of initial early-age cracks in decks between 1 and 3 months after completion of deck concrete placement. However, nearly as many responses (34%) indicated the occurrence of cracks up to 28 days after deck placement.
- Construction practices are perceived as an important factor in early-age bridge deck cracking, and the majority of the respondents represented construction units within PennDOT.
- Over 90% of respondents were familiar or very familiar with PennDOT policies, standard drawings, construction, and contractual practices.
- Eighty two percent (82%) of the respondents indicated observing the development of more cracks during summer months versus cooler fall/spring months.
- The majority of responses showed 4:00 AM as the start time and 10:00 AM as the finish time for deck placement during summer months.
- A majority of the respondents (67%) agreed that it is beneficial to start summer placement around 7:00 PM in order to induce slight compression in deck (due to superstructure contraction during curing). However, the remaining one-third of the respondents (33%) preferred a different time frame starting at night or early in the morning.
- Curing techniques were indicated as “very effective” in crack prevention, followed by construction practices, mix design, and structural details in this respective order. Most frequent recommendation was to apply curing as soon as possible, and to maintain the moisture level for at least 14 days.
- Numerous recommendations were given with regards to construction practices. Following the pour sequence (e.g. with regards to negative and positive moments) was one of the most recommended crack prevention methods. Limiting the movement of freshly-placed

concrete due to adjacent traffic was another recommendation, plus restricting the temperature difference between the concrete deck and beam to less than 22 °F.

- With regards to structural details, limiting the concrete deck restraints were the main recommendation.
- There were several recommendations concerning the mix design, and the most frequent one called for limiting the maximum 28-day compressive strength of the concrete (to varying magnitudes such as 4000 psi, 4500 psi or 5500 psi) through reducing the cement content, etc. Another recurring recommendation was limiting the maximum concrete slump (to varying magnitudes such as 3.5” or 4”). Reducing the concrete strength gain was another recommendation.
- Crack survey was the most often designated method of evaluating the short-term performance of bridge decks, followed by material testing, structural assessment, and other methods.
- With respect to the effects of early-age cracking on long-term bridge deck performance, early-age cracking was indicated to have significant effect in reducing bridge deck service life. It was also shown to be effective in increasing life cycle cost. Other long-term performance effects included the ingress of water and de-icing chemicals to the substructure and earlier-than-anticipated involvement of maintenance crew.
- The majority of responses indicated prior experience as the basis for selecting a particular remediation technique, followed by the cost, other criteria (listed below), and manufacturer. Other selection criteria included performance over time, scientific studies, and deck life per unit cost.
- For longer lasting remediation (5 to 10 years), latex modified concrete (LMC) overlay was indicated by most of the respondents as their districts’ remediation method followed by asphalt overlay with waterproof membrane and overlay. For methods with shorter life (1 to 5 years), the use of sealant was indicated as the prevalent method followed by epoxy injection/resin. The use of linseed oil was indicated as the predominant method for remediation lasting less than 1 year.
- Epoxy surface treatments (epoxy overlays, epoxy aggregate overlays, and epoxy/resin injection) and latex modified surface treatments were ranked first by the majority of respondents as the most successful remediation methods based on cost and effectiveness.

The use of sealants was ranked second, and asphalt overlay with waterproof membrane, was ranked third.

The results of this survey of PennDOT personnel have identified a number of interesting factors, which will be investigated as the study proceeds. Included among these is information about the timeframe during which early age deck cracking is observed, placement and curing requirements, effects on long term bridge performance, and suggestions for improvements in materials and construction practices. Since this information represents a compilation of in-house experience, it provides the research team with very useful information for conducting the remainder of this study.

CHAPTER 3 (TASK 3)

Review and Analysis of Bridge Condition Data

3.1 Introduction

Task 3 involved the visual inspection of 40 bridge decks, analysis of bridge inspection data, and development of a Deck Performance Database (DPD) in Microsoft Access. Sections 1.2 to 1.4 discuss the bridge deck selection process, visual inspection protocols, and material testing procedures. Chapter 2 presents the results of the bridge inspections, analysis of cracking data, and discussion of the findings. Chapter 3 summarizes the deck performance database.

3.2 Bridge Deck Selection Process and Field Inspections

Penn State and Quality Engineering Solutions, Inc. (QES) research teams performed visual inspections on 40 bridge decks throughout the state of Pennsylvania. An attempt was made to select bridges evenly distributed across the state, in order to evaluate bridges from each PennDOT District. District 6 was the only District not included in the study due to complex traffic control conditions. The locations of the inspected bridges are shown in [Figure 45](#).

The main objective of the visual inspections was to collect bridge deck cracking data and to assess the performance of different concrete types (i.e., AA, AAA, AAAP, and HPC concrete) and protective systems (i.e., epoxy-coated rebar, galvanized rebar, black rebar, and polymer impregnated concrete). Other objectives were to establish trends between bridge deck cracking and factors, including materials design, structural design, and construction practices. [Table 33](#) (Appendix A) presents the design factors included in the selection process and their corresponding values, adopted from PennDOT's BMS2 database. The goal of the selection process was to obtain a wide range of values represented for each design factor within the set of 40 bridges, which was accomplished through a number of iterations and quality control checks. As shown in [Table 33](#), the decks ranged in age from newly constructed to an age of 90 years. The average daily traffic (ADT) on the bridges varied from 89 to nearly 34,000 vehicles. Structural design factors included support conditions (simple or continuous) and girder material (steel or concrete). In addition, the number of spans ranged from 1 to 3, while the bridge lengths varied from 18 ft to 485 ft.

Included in the set of bridges inspected were a number of bridges from the “#85-17 Bridge Deck Protective Systems” investigation (Malasheskie et al. 1988) performed by PennDOT. The #85-17 study evaluated the performance of protective systems used in bridge decks. The protective systems that were evaluated in the 1988 study consisted of epoxy-coated rebar, galvanized rebar, waterproof membranes under bituminous layer, latex-modified concrete overlay, and low slump dense concrete overlay. The main findings of the #85-17 study were:

- rebar coatings (i.e., epoxy-coated and galvanized rebars) are the most effective corrosion protection and can substantially increase the duration of the corrosion initiation period;
- effective service life is directly related to initial chloride contamination, permeability of the concrete, and depth of cover over rebar. Latex modified concrete overlays provided the best overall performance based on the deterioration rate;
- coated rebar (i.e., galvanized and epoxy-coated) generally had excellent condition despite high chloride contents. The threshold value of corrosion for black steel was believed to be slightly less than 1.0 pound per cubic yards;

In general, the comparison of these protective systems can be problematic when they are used in conjunction with one another (e.g., LMC overlays are commonly applied to decks with epoxy-coated rebar). A preferred approach would have been to compare the effectiveness of rebar coatings and overlays separately.

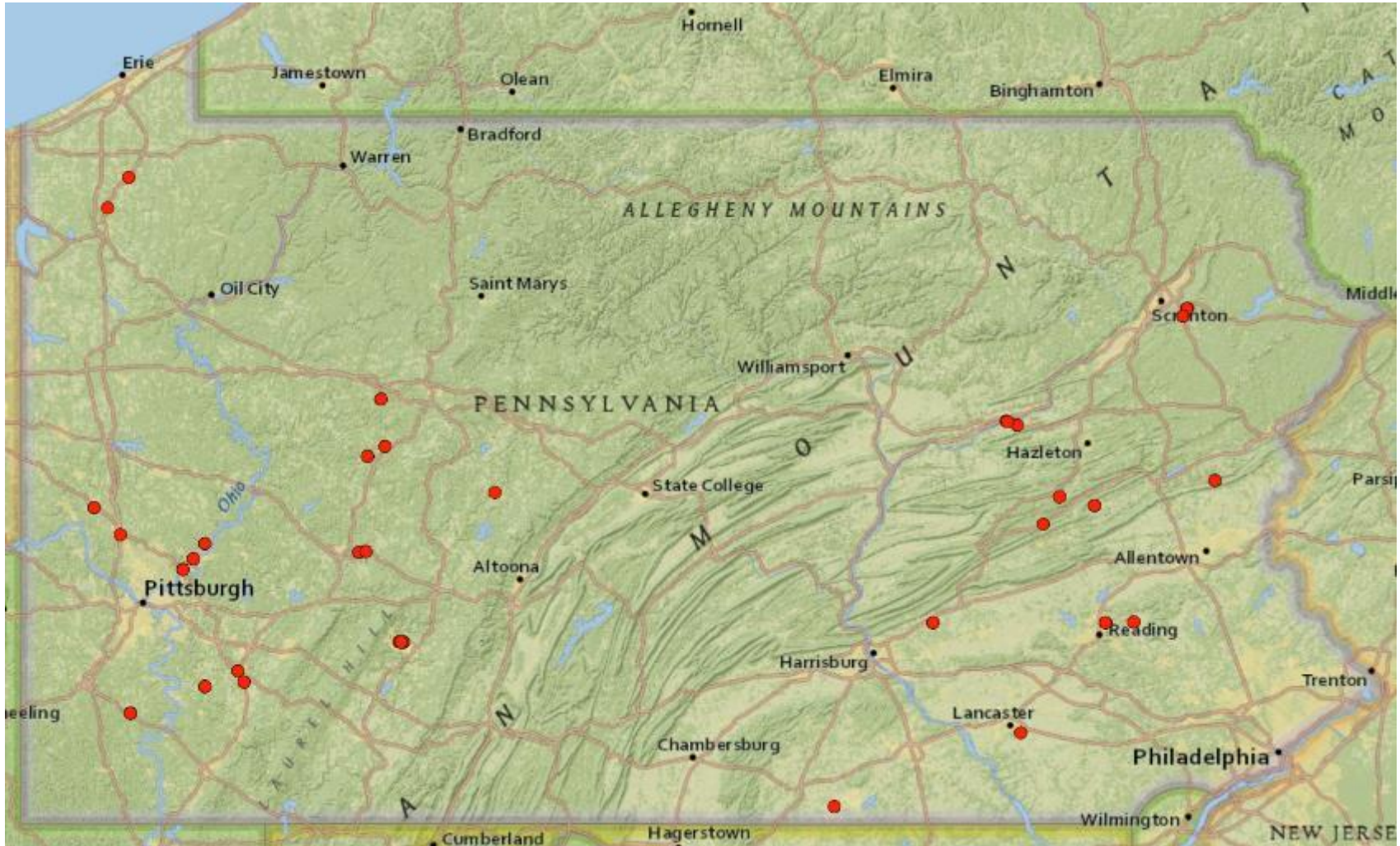


Figure 45. Locations of bridges (indicated by red circles) inspected in Summer 2014

In addition to the cracking data collected from the 40 bridge deck inspections (herein referred to as the 40 inspected bridge decks), cracking data from 163 newly constructed bridge decks was provided by PennDOT (herein referred to as the 163 new bridge decks). For the 163 new bridge decks, the data was collected from initial inspections – after construction and curing was completed – and follow-up inspections – approximately 1 year after bridge construction. Of the 163 new bridge decks, 100 used AAAP concrete, 42 used AAA concrete, and 21 were cast with HPC concrete. The cracking data from the 163 new bridge decks was included in the analysis of concrete classes and protective systems. The 163 new bridge deck data was also used to develop the DPD for future use to track deck cracking performance.

3.2.1 Bridge Deck Inspections

Bridge deck inspection protocols were established in order to ensure consistent data collection procedures for all 40 bridge deck inspections. Visual inspection protocols were written in an attempt to gather as much cracking information as possible, optimize the amount of time spent performing each inspection, and limit the subjectivity of inspections between different inspectors. A complete description of the visual inspection protocols can be found in the “Bridge Deck Inspection Protocols” (Appendix B). Cracking information was collected during each inspection using the “Bridge Deck Cracking Inspection Form” (Appendix B) and included the location, orientation (transverse or longitudinal), length, and width of all cracks on the deck surface.

Cores were extracted from 19 of the 40 inspected decks. For each deck cored, an attempt was made to take a core sample at a cracked location and at a uncracked location. The cores (3 inch diameter) were subsequently evaluated in Penn State’s laboratory to determine chloride content at the rebar depth and to determine the lack, or extent, of rebar corrosion. Chloride content information was used for the subsequent analyses of protective systems and concrete classes. A complete description of the coring procedure is included in Appendix B.

3.2.2 Concrete Core Evaluation and Chloride Content Testing

The cores obtained from field inspections were transferred to Penn State’s laboratory for materials testing. The main goal for the materials testing was to measure the total acid-soluble chloride content at the rebar level. Each core was drilled at the rebar level and powdered concrete was extracted as shown in [Figure 46](#). For LMC overlays, an additional powdered sample was also extracted from the LMC layer (close to the interface of two concrete types). The test samples were then prepared according to ASTM C 1152-04 for acid-soluble chloride ion measurements. After sample preparation, instead of using ASTM’s titration procedure for determining the chloride content of the sample, a chromatography test was carried out on a sample of the solution containing the powdered concrete. This procedure is discussed in more detail in Appendix C.



Figure 46. An example of a core with drill holes at the rebar level.

Concentration of chloride ions can be determined using conventional electrometric/titrimetric methods, however ion chromatography provides a single instrumental technique that may be used for rapid and sequential measurements of individual ions. Ion-chromatography is a method which separates ions based on their charge and their affinity to an ion-exchange resin. Each anion is identified based on their retention time and then measured by conductivity. Based on the peak values/areas of the “retention time-electric conductance graph”, the concentration (milligrams per liter) of each type of anion can be calculated for a given solution. For details regarding this method please refer to Standard Test 4110 (included in Appendix C).

The rebar within the concrete cores was also evaluated for any signs of corrosion. In order to evaluate the extent of corrosion, rebar from the cores were extracted by drilling and the percent effectiveness was determined for each rebar piece. Some rebar appeared to be more corroded than others and some rebar didn't show any signs of corrosion. Only the rebar showing signs of corrosion were tested in order to quantify the extent of their corrosion. For this purpose, ASTM G1-03: Standard Practice for Preparing, Cleaning, and Evaluating Corrosion Test Specimens was followed closely. A summary of the procedure is provided in Appendix C.

3.3 Results and Discussion

An attempt was made to correlate the extent of cracking to a number of variables related to concrete material design, structural design, and construction practices. [Table 12](#) lists and summarizes the parameters that were found to have an influence on deck performance based on the evaluation of cracking data from the 40 inspected bridge decks and 163 new bridge decks, analysis of the chloride content results from the core samples, and the results of the deterioration modeling.

Table 12. Summary of the variables that influenced deck performance (ordered from most influential to least influential)

Parameters	Summary
Concrete Type	Early-age cracking performance of AAAP and HPC concrete decks was better than AAA concrete decks. In terms of long-term performance, AA decks had an expected service life 4 years greater than the service life of AAA decks.
Protective System	Epoxy-coated rebar and galvanized rebar were more effective than black rebar in resisting corrosion. Black rebar corroded at lower chloride content levels and at earlier ages.
Concrete Mix	Early-age cracking performance was influenced by compressive strength and cementitious content. Mixes with lower compressive strength exhibited less cracking. Mixes with lower cement content and higher supplementary cementitious materials (SCM) content exhibited lower crack density.
Half width construction	Decks constructed using half width construction, on average, cracked approximately 4 times more than decks using detours.

3.3.1 Crack density results for 40 inspected bridge decks

Inspections were conducted according to the protocols described in Appendix B and C and the crack data was obtained for the 40 inspected bridge decks. The crack data was subsequently converted into crack maps (Appendix D) and crack density calculations were performed for each deck, as shown in [Table 36](#) and [Table 37](#) of Appendix D. The total crack density for each deck was separated into longitudinal/transverse crack orientations and negative/positive moment regions for subsequent analysis. The percentage of deck area that had been delaminated and spalled/patched was also recorded, as well as crack density values for decks with overlays (e.g., LMC, bituminous), as shown in [Table 36](#) and [Table 37](#).

[Figure 47](#) presents the crack density for the 40 inspected bridge decks based on their age. Due to significant variability in parameters that affect cracking, strong correlation between cracking and age were not observed. Furthermore, the data obtained for the 40 inspected bridge decks is one snapshot in time making the comparison of crack density values challenging due to the varying age of the decks. Ideally cracking data would be collected at intervals over a longer period of time for a specific bridge deck to more rigorously evaluate the performance of various protective systems and concrete classes.

Below are observations made regarding the 40 bridge inspections that are worth noting:

- general trends were not observed for crack density values with respect to protective systems;
- in general, the epoxy-coated rebar and galvanized rebar performed better than the other types of protective systems;
- most of the transverse cracks that were observed were not typically “full-width”. As a result, measuring crack densities by observing the cracks on the edge of the deck (over the parapet) would not be an accurate representative of the amount of transverse cracking on the decks surface, as they typically do not run through the whole deck’s width; therefore, this is not an effective way of comparing the crack densities of overlaid decks to monolithic decks. Also, counting the “number of transverse cracks” and multiplying by the decks width may significantly overestimate the crack density value;
- some decks had mainly longitudinal cracks whereas some had mainly transverse cracks. The type of bridges that displayed mainly longitudinal cracks also varied. The crack patterns were typically not uniform or consistent in any way. This includes the spacing of cracks occurring in both longitudinal and transverse directions. The crack maps included in Appendix D display these inconsistencies;
- inspecting the surface of the deck from the shoulder typically results in less detailed crack inspections and lower crack densities compared to inspecting the deck according to the protocols included in Appendix B (e.g., bending by the waist over the deck). This issue can cause significant variations in the measured crack densities and can lead to inconsistencies. As a result, care should be taken, so that data collected from multiple inspections for various decks over time are compatible and consistent.

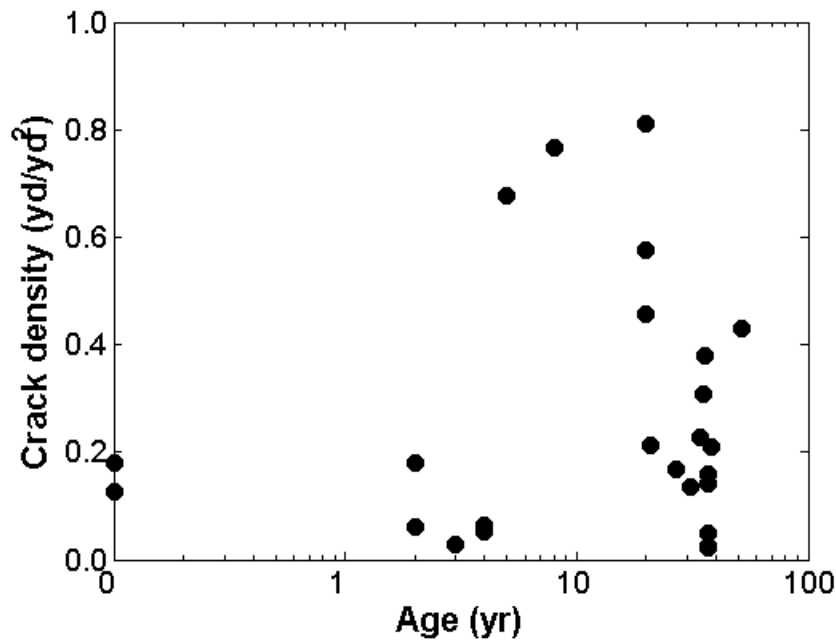


Figure 47. Raw crack density versus age (40 inspected bridge decks without overlays)

3.3.2 Concrete core data and chloride content results

The chloride content of each core was measured according to the procedures outlined in Section 1.4. Table 38 (Appendix D) lists the chloride content, sample depth, whether or not a surface crack was present depth of the crack, rebar type, condition of the rebar, and percent effectiveness of the rebar. Horizontal delamination cracks had caused some of the cores to split into two pieces (at the rebar level) during coring and this is also noted in Table 38.

Figure 48 presents photographs of the concrete and rebar condition for a sample of the cores. In some instances (such as Figure 48a) the rebar within the cores were completely intact. The rebar condition was noted as “No corrosion” in Table 38 for such cores. In other cases minor (Figure 48b) to extreme (Figure 48c and d) states of corrosion were observed. For rebar showing any signs of corrosion, the percent effectiveness was determined and is presented in Table 38. Two pieces of the extracted rebar (Figure 48) were too small to be accurately tested for percent effectiveness. Instead, a visual approximation for the extent of corrosion was made.

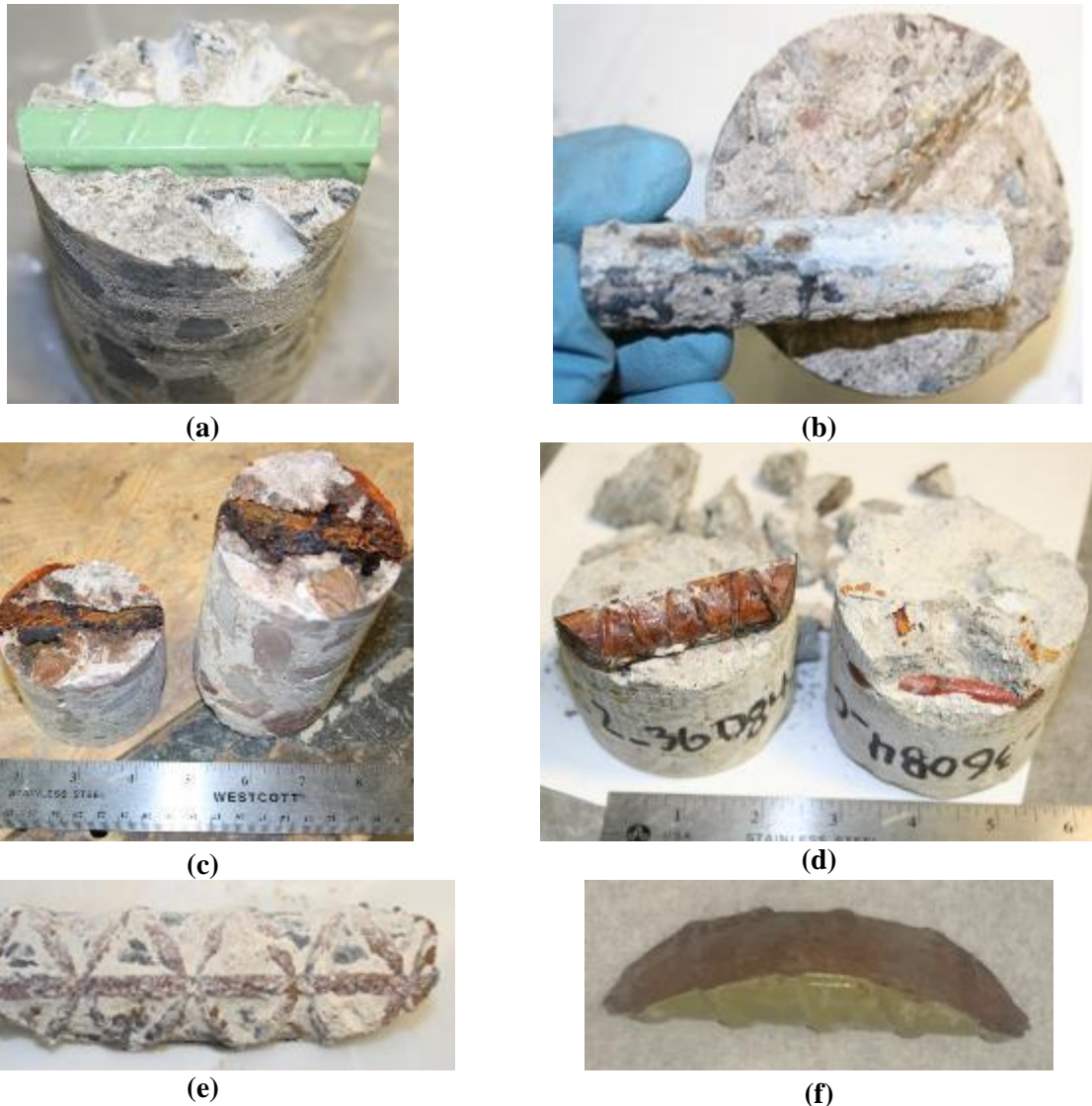


Figure 48. Examples of (a) a completely intact epoxy-coated rebar (Core C2_4908_NC); (b) a rebar with minor corrosion; (c) an extremely corroded black rebar (Core C1_20506_C); (d) a corroded epoxy coated rebar (Core C2_36084_C, 37 year old deck); (e) rebar sample No. 1 for which percent effectiveness was approximated (Core C1_652_NC); (f) rebar sample No. 2 for which percent effectiveness was approximated (Core C1_12905_C)

The chloride content measurements were made at different depths for different cores and directly comparing the chloride content results of one core to another could be misleading because the chloride content varies with depth for each core. In order to effectively compare the chloride content from core to core, in terms of their diffusion characteristic, a parameter called the “diffusion coefficient” was calculated and used as an indication of the rate of penetration of chloride at the core location. The higher the diffusion coefficient, the faster the chloride ions can penetrate through the concrete’s cover. In order to calculate the diffusion coefficient, the available data was fit to the most commonly used model for chloride diffusion: Fick’s second law of diffusion. Equation 1 shows the closed form solution to Fick’s second law, that was utilized to

calculate the diffusion coefficient in this study (shown in [Table 38](#)). By solving Equation (1) for a specific depth (x), time (t), surface chloride content (C_0), and chloride content (C) at a specified depth/time; the diffusion coefficient (D) was obtained. For each calculation, the surface chloride concentration was assumed to be 0.65%. This value is an average of the values recommended for highways in Pennsylvania (Life-365 Consortium II 2010).

$$C(x, t, D, C_0) = C_0 \times \left[1 - \operatorname{erf} \left(\frac{x}{2\sqrt{tD}} \right) \right] \quad (1)$$

where $C(x, t, D, C_0)$ is the chloride concentration at depth x and time t (% weight of concrete);
 C_0 is the chloride concentration at the surface of the deck (% weight of concrete);
 erf is the error function;
 t is the time (days);
 x is the depth (in);
 D is the diffusion coefficient ($\times 10^{-4}$ in²/day).

[Table 39](#) (Appendix D) presents the diffusion coefficients obtained from the chloride contents measured within the LMC layer of each applicable core. It is worth noting the date of application of the LMC overlays were unknown and the time (t) parameter used in the Equation (1) to calculate the diffusion coefficient for the LMC was assumed to be the same as the bridge deck's age. Several decks with LMC overlays have an age below 10 years, as a result, assuming a single time of application (e.g., 10 years) was not reasonable for these decks.

It is also worth noting one of the cores (C1_8407_C shown in [Figure 49](#)) appeared to have been injected with a type of sealer (possibly linseed oil). Even though high chloride content existed at the rebar level (0.352%), corrosion had not initiated for the embedded rebar; whereas 7 out of the 9 cores had experienced average to extreme corrosion had much lower chloride contents (0.1 to 0.326 % wt). This could be an indicator of the sealers effectiveness in delaying the initiation of corrosion by preventing further moisture and oxygen penetration.



Figure 49. The black material within the crack seems to be a sealer such as linseed oil (Core C1_8407_C)

The chloride content and diffusion coefficients were analyzed and compared for on-crack and off-crack locations. As expected, the chloride content and diffusion coefficient was generally much higher at the rebar level for on-crack cores compared to off-crack cores as shown in Figure 50a and b. There is typically a 1 to 4 times increase in the diffusion coefficient for on-crack locations which emphasized the effect of cracking in facilitating easier penetration of chloride.

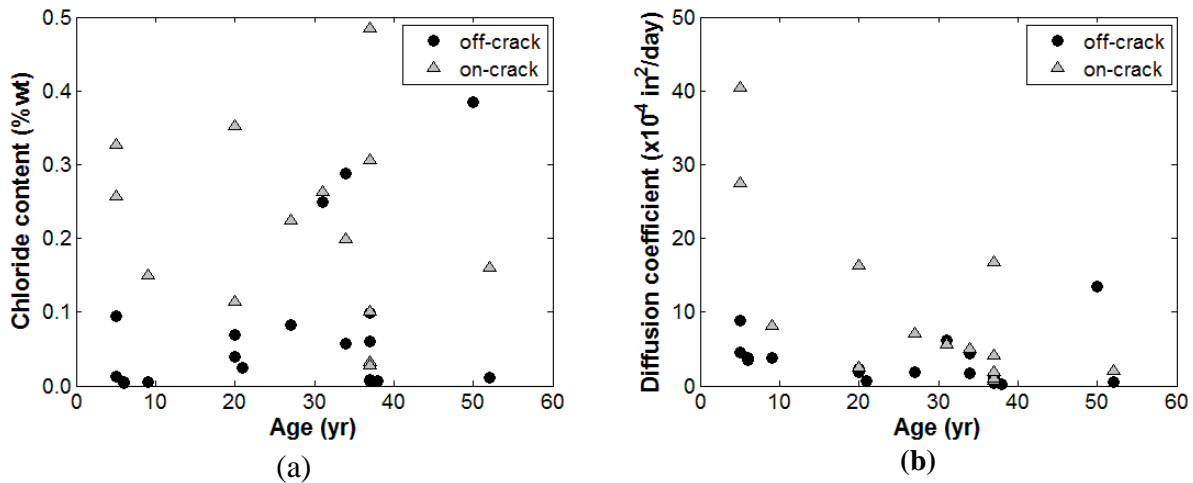


Figure 50. Comparison of off-crack and on-crack (a) chloride content (b) diffusion coefficient

For cores with LMC overlays, the chloride content was measured within the overlay at a depth close to the LMC-concrete interface. Figure 51 represents the effect of a LMC overlay on the diffusion coefficient. The LMC layer has a much lower calculated diffusion coefficient compared to the original concrete layer for younger cores. However at older ages (20-40 years), the LMC overlay has a higher diffusion coefficient. These results suggest that the LMC overlay is more effective in preventing chloride content penetration when applied at an early age. However, it

should be noted that the LMC was assumed to have the same age as the deck, which can cause inaccuracies when calculating the diffusion coefficient based on corresponding chloride content results. In order to efficiently analyze the effect of the LMC on the decks long-term performance, the dates of when the LMCs were applied are required.

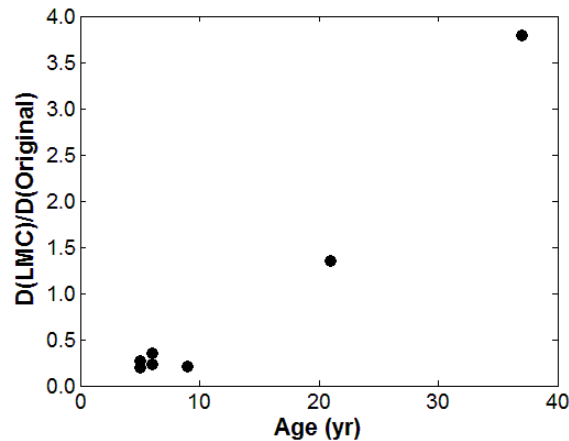


Figure 51. Ratio of diffusion coefficient of LMC overlay to the diffusion coefficient attributed to underlying concrete for the same core

3.3.3 Analysis of Protective Systems

The results of the chloride content testing and the crack density results gathered from the 40 inspected bridge decks were used to assess the performance of the various protective systems employed in the bridge decks. The protective systems analyzed in this study were black rebar (i.e., no protection), epoxy-coated rebar, galvanized rebar, and polymer impregnated concrete (i.e., latex modified concrete).

The performance of different protective systems (i.e., black rebar, epoxy-coated rebar, galvanized rebar, and polymer impregnated concrete) in terms of chloride content and corrosion initiation was evaluated using the extracted cores. Cores with intact rebar were identified as “not corroded” and if any sign of corrosion was observed it was assumed that corrosion had initiated; these were classified as “corroded.” From the results shown in [Figure 52a](#), corrosion was found to initiate at much lower chloride content (~0-0.1% wt) levels and at earlier ages (as low as 9 years) for black rebar compared to epoxy-coated rebar (0.2-0.3% wt). Furthermore, even though some cores did not have a surface cracks and the concrete cover was intact, corrosion had initiated on the black rebar as can be seen from [Figure 52a](#). For the black rebar cores it is possible the corrosion had begun at another location and propagated along the rebar via horizontal delamination cracks. [Figure 52b](#) shows 4 cracked cores and 1 uncracked core with epoxy-coated rebar had relatively higher chloride contents (0.15-0.35%), however the rebar for these cores did not show any sign of corrosion. This suggests the epoxy-coating can delay corrosion initiation by increasing the chloride content threshold required for the reinforcement to begin corroding. [Figure 52c](#) shows the chloride content

results for cores containing galvanized rebar. Two galvanized rebar samples displayed corrosion at early ages (< 10 years old) while an additional sample corroded at an off-crack location with low chloride content. The chloride content results for the polymer impregnated bridge decks are shown in Figure 52d. Only 2 polymer impregnated decks were cored so no definitive trends were observed. However, the 1 cracked core displayed higher chloride content in comparison to the un-cracked cores.

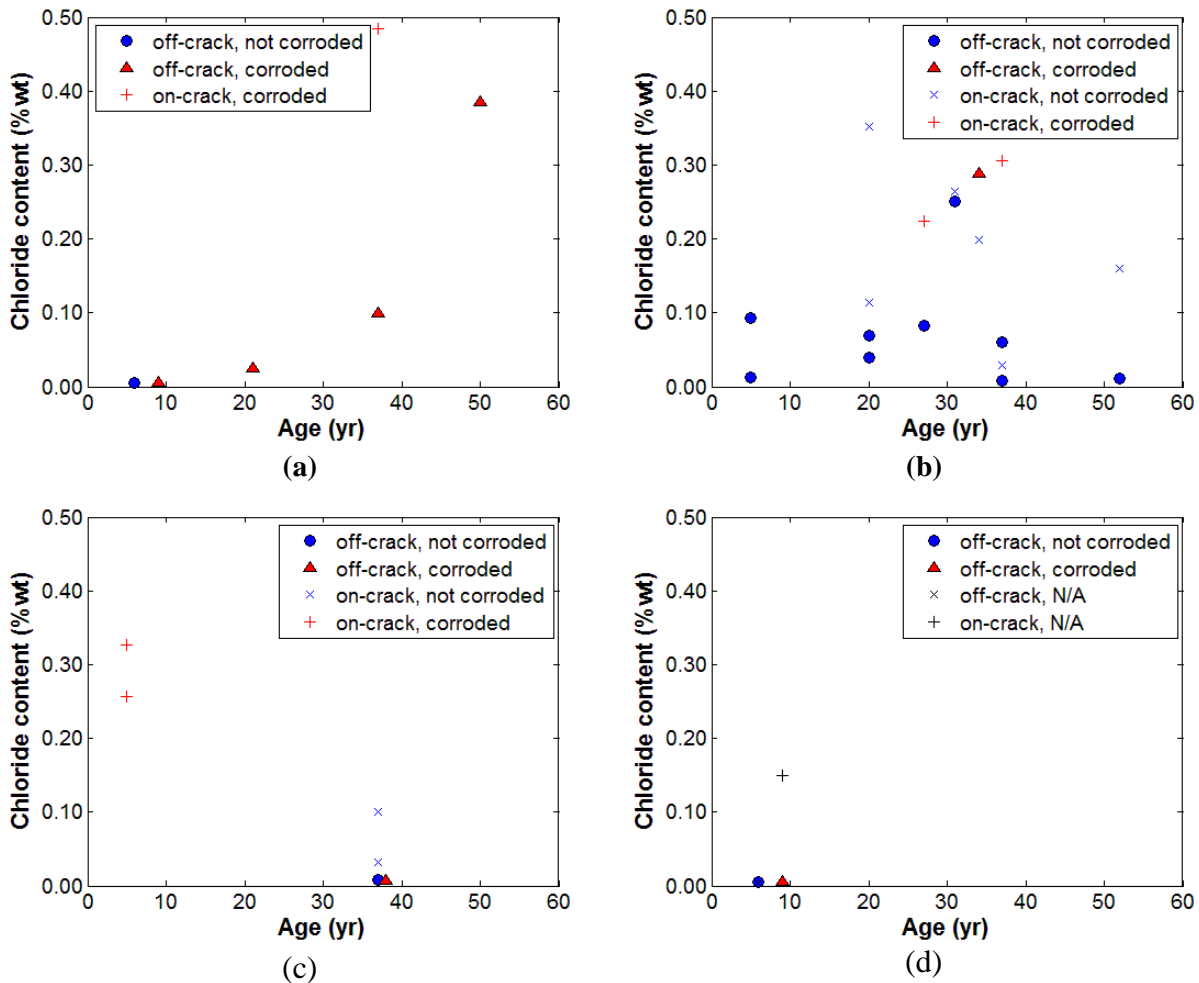


Figure 52. Chloride content results for (a) black rebar; (b) epoxy-coated rebar; (c) galvanized rebar; (d) polymer impregnated concrete

The percent effectiveness, in terms of mass loss, for the different rebar types in comparison to chloride content is presented in Figure 53a. In general, black rebar had lower effectiveness at higher chloride contents in comparison to epoxy-coated rebar and galvanized rebar. Several of the samples of epoxy-coated rebar and galvanized rebar had higher effectiveness values than samples of black rebar at lower chloride contents. This emphasizes the improved performance of epoxy coated rebar and galvanized rebar over black rebar.

The crack density results from the 40 inspected bridge decks were used in an attempt to evaluate the performance of the various protective systems. As shown in Figure 53b, no clear trends were found between crack density and protective system for the 40 inspected bridges.

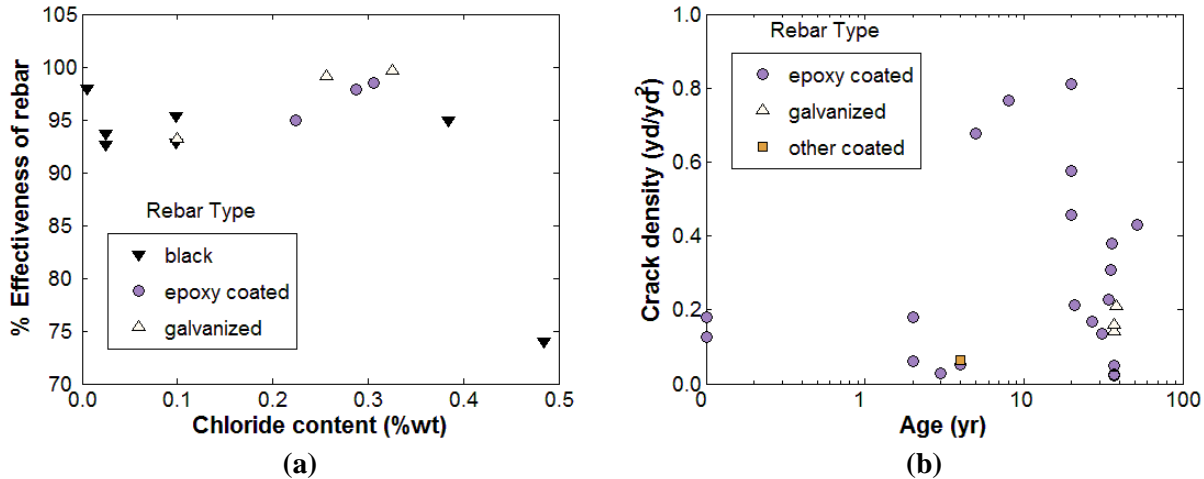


Figure 53. (a) Percent effectiveness versus chloride content for the various rebar types; (b) Crack density vs age for different protective systems (40 inspected bridge decks)

3.3.4 Analysis of Concrete Classes

The crack density results and chloride content results from the 40 inspected bridge decks as well as the cracking data provided by PennDOT for the 163 new bridge decks were used to assess the cracking susceptibility of the different concrete classes. The concrete classes included in the analysis were AA, AAA, AAAP, and HPC. It should be noted there were no HPC decks included in the 40 inspected bridge decks and there were no AA decks in the data for the 163 new bridge decks provided by PennDOT. The absence of AA bridge decks in the 163 new bridge deck data is due to AA concrete no longer being used by PennDOT for new bridge decks. In addition to analyzing the cracking susceptibility of the concrete classes, attempts were made to establish trends between the extent of cracking of the different concrete classes and various concrete materials design factors.

Cracking data from the 163 new bridge decks was recorded for initial and follow-up inspections. Initial inspections were performed post deck construction, prior to the bridge being opened to traffic. Follow-up inspections were carried out approximately 1 year after deck construction. A preliminary multivariate analysis was performed to determine whether the concrete type has an influence on the measured crack densities and, if so, to quantify the influence of each concrete type. To determine the influence of each concrete type on the measured crack density a one-way analysis of variance (one-way ANOVA) was performed. This analysis quantifies the similarity between the distribution of crack densities pertaining to a particular concrete type and the total distribution of crack densities, where all the concrete types are included. The ‘null hypothesis’ is

that the two distributions are very similar. The output parameter studied is the so-called p-value. If the p-value is equal to or smaller than the significance level (α), ANOVA suggests the data are inconsistent with the assumed null hypothesis (i.e., the subset distributions for individual concrete types would be ‘significantly’ different from the total distribution). For this analysis, significance levels of 1% (0.01) and 5% (0.05) were specified. The ANOVA results are presented in [Table 13](#) for the initial and follow-up inspection in terms of crack orientation (total, transverse, and longitudinal). Based on the ANOVA results, the influence of concrete type is significant for all crack density parameters except for longitudinal crack densities measured during the initial inspection and transverse crack densities measured during the follow-up inspection, for which the p-value is greater than or equal to 0.01. For all crack densities, the p-value is much less than both 0.01 and 0.05, indicating the strong influence of concrete type.

Table 13. ANOVA results for significance of all concrete types in relation to crack density (163 new bridge decks)

	Initial Inspection			Follow-up Inspection		
Crack Densities	Total	Transverse	Longitudinal	Total	Transverse	Longitudinal
p-value	0.0001	0.0014	0.0276	0.0024	0.0094	0.0004

A simple regression analysis reveals which concrete type has the greatest influence on each crack density orientation. It is reasonable to treat the three concrete types as independent ‘predictor variables.’ [Table 14](#) shows the results, in terms of regression coefficients for each of the concrete types, from a multivariate regression analysis. Total crack density values for both the initial and follow-up inspections are significantly higher for AAA concrete decks in comparison to AAAP and HPC decks. Although AAAP concrete decks displayed more cracking than HPC concrete decks at the initial inspection, the total crack density for HPC concrete decks was greater than AAAP at the follow-up inspection. During the initial inspection, AAA concrete decks had transverse crack density values one order of magnitude greater than those of AAAP or HPC. AAA had the highest transverse crack density values for the follow-up inspection as well, but the transverse cracking of HPC increased significantly and was about 20% less than AAA. Similarly, AAA concrete decks had the highest longitudinal crack density values for both initial and follow-up inspections.

Table 14. Regression coefficients for each concrete type from a multivariate regression analysis (163 new bridge decks)

		Initial Inspection			Follow-up Inspection		
		Total	Transverse	Longitudinal	Total	Transverse	Longitudinal
Regression Coefficient	AAA	0.058	0.041	0.017	0.082	0.052	0.030
	AAAP	0.008	0.003	0.004	0.014	0.022	0.007
	HPC	0.004	0.004	0.0001	0.043	0.042	0.001

Figure 54 presents the average crack density at the initial inspection for the various concrete classes and crack orientations. The data points plotted in Figure 54 indicate the average values while the range error bars encompass the minimum and maximum values. The AAA concrete exhibits the highest early-age cracking susceptibility, while the crack density for AAAP and HPC concrete is significantly lower. Based on total average crack density, AAAP cracked 84.7% less than AAA while HPC cracked 91.5% less than AAA and 44.7% less than AAAP. These values imply better performance at early ages for HPC. In addition to providing analysis of the different concrete classes, Figure 54 also presents the crack density based on crack orientation. For all three concrete types, transverse cracks contributed to total crack density more than longitudinal cracks. For initial inspections, the transverse crack density was 56.9%, 76.3%, and 96.2% greater than longitudinal crack density for AAA, AAAP, and HPC, respectively.

Concrete material design factors were investigated in an attempt to determine the difference in early-age cracking performance of the concrete types, and included compressive strength, cementitious materials content, and w/cm ratio. The average compressive strength for each concrete type is shown in Figure 55 along with range error bars for the 163 new bridge decks. On average AAA had the highest 7-day and 28-day compressive strengths, followed by AAAP and HPC. Based on the average crack densities for each of these concrete types, it can be concluded that an increase in compressive strength can result in an increase in early-age cracking. The improved initial performance of HPC and AAAP compared to AAA could be due to its lower cement and higher Supplementary Cementitious Material (SCM) contents. Figure 56 shows the cracking performance of the three aforementioned concrete types at the initial inspection versus the cement content. It is difficult to observe trends based on Figure 56. However, analyzing the concrete types based on average cement content and SCM content, as shown in Figure 57, illustrates the effect of cementitious materials on cracking performance. Shrinkage cracking is one of the main causes of early-age cracking and the majority of the shrinkage in concrete occurs in the cement component. As a result, lower cement content can lead to lower shrinkage cracking, which is supported by the initial early-age cracking performance of the three concrete types (AAA, AAAP, HPC). The w/cm ratio was compared to the extent of early-age cracking for AAA, AAAP, and HPC concrete types using the data from the 163 new bridge decks, as shown in Figure 58. For both AAA and AAAP concrete the crack density appears to increase with increasing w/cm ratio. The trend between the extent of cracking and w/cm ratio is not observed for HPC concrete. Additional research is needed

to provide recommendations for shrinkage reduction in bridge deck concrete mixtures and implementation of new testing techniques (i.e. ASTM C1581 Restrained Ring Test) that allow a comparison of cracking susceptibility of different concrete mixtures (Radlinska et al., 2008).

While the cracking data from the 163 new bridge decks was used to evaluate early-age cracking performance, the chloride content results and cracking data from the 40 inspected bridge decks was used to evaluate long-term cracking performance. Using the chloride content results from the concrete core samples, the ratio of diffusion coefficient for on-crack to off-crack locations were calculated for AA and AAA concrete decks which had cores at both locations as shown in [Figure 59](#). [Figure 60](#) presents the chloride content for off-crack locations separated by AA and AAA concrete types. The results presented in [Figure 59](#) and [Figure 60](#) suggest, on average, concrete type had little effect on diffusion coefficient and chloride content at the rebar level. It can be concluded that AA and AAA decks performed similarly in terms of chloride penetration. The average crack depth for the on-crack cores was measured during the evaluation of the cores. [Figure 61](#) presents the crack depth for the cracked cores over time based on the concrete type. Most AAA cores had cracks reaching the rebar level (2.5-3.5 in). However several of the cracks in AA cores did not propagate to the rebar level. The crack density of the AA, AAA, and AAAP concrete classes is plotted versus the corresponding deck age in [Figure 62](#). Little correlation is observed between crack density and age for the various concrete classes. However, there were several AA decks that showed better cracking performance than younger AAA decks. Due to the fact AAAP is a relatively new concrete class, it is difficult to evaluate its long-term performance at this time. In addition, the limited number of data points for AA (11) and AAA (18) make it difficult to draw conclusions regarding the long term performance of these concrete classes with numerous other design factors influencing the crack density.

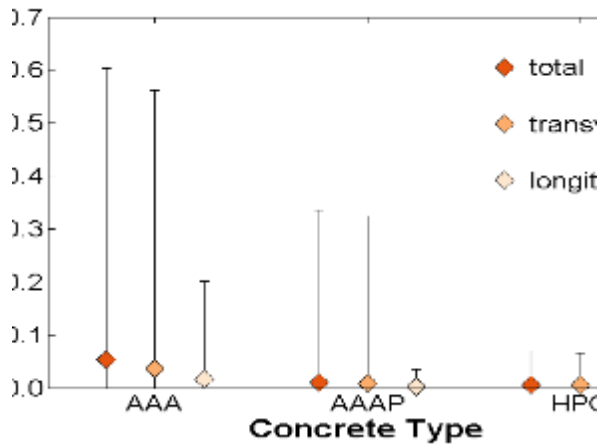


Figure 54. Average (data points) and range (error bars) of crack density for each concrete type at initial inspection (163 new bridge decks)

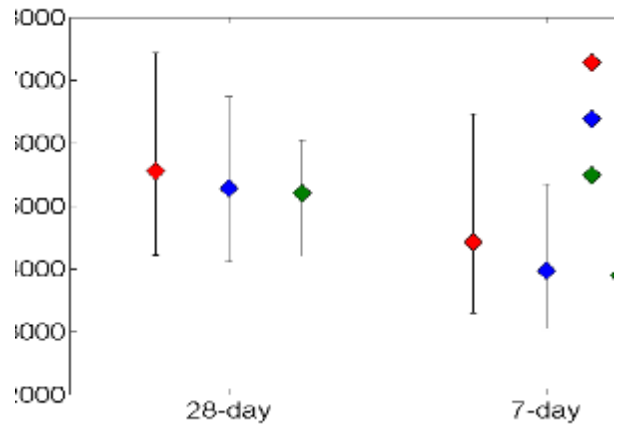


Figure 55. Average (data points) and range (error bars) of compressive strength for each concrete type at 28 and 7 days (163 new bridge decks)

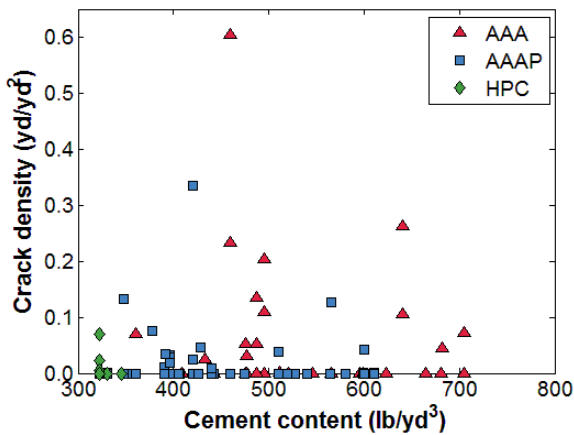


Figure 56. Crack density at initial inspection (163 new bridge decks) versus cement content

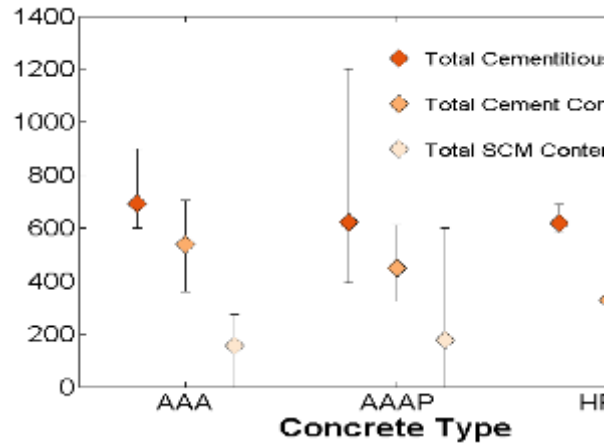


Figure 57. Average (data points) and range (error bars) of cementitious materials content for each concrete type (163 new bridge decks)

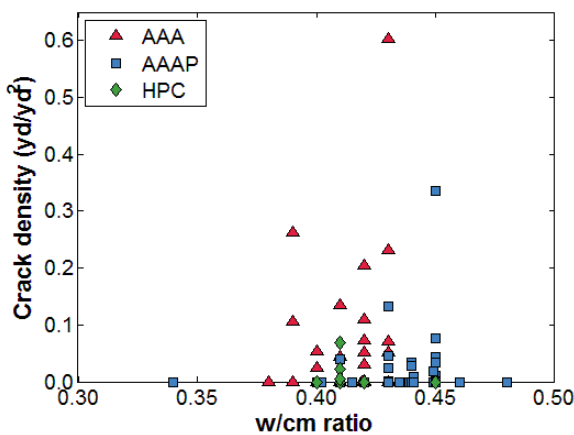


Figure 58. Crack density at initial inspection (163 new bridge decks) versus w/cm ratio

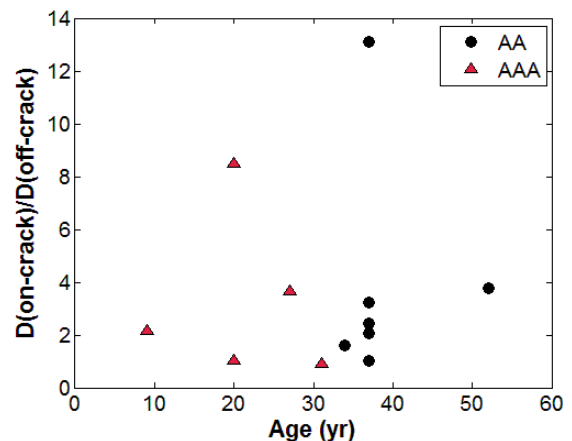


Figure 59. Ratio of diffusion coefficient for on-crack to off-crack cores

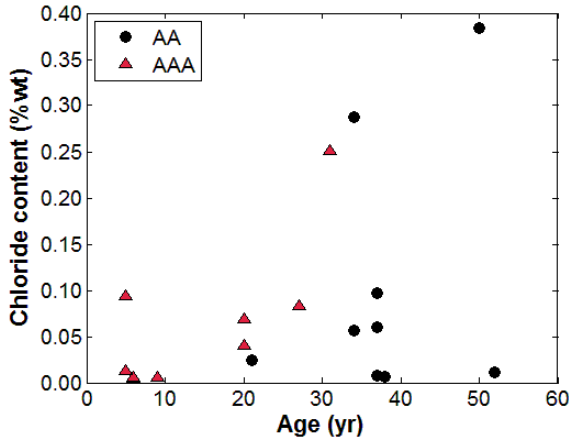


Figure 60. Comparison of chloride content based on concrete type for off-crack locations

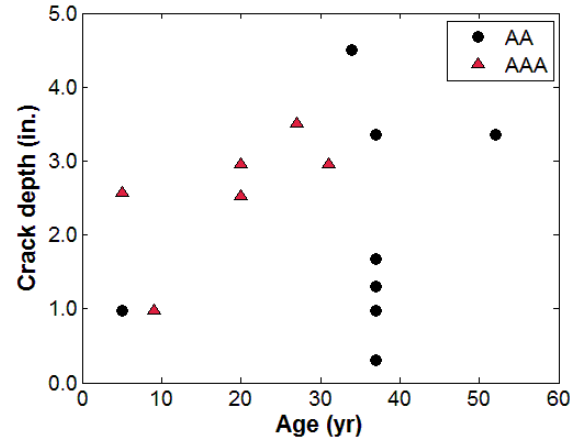


Figure 61. Crack depth over time for AA and AAA decks

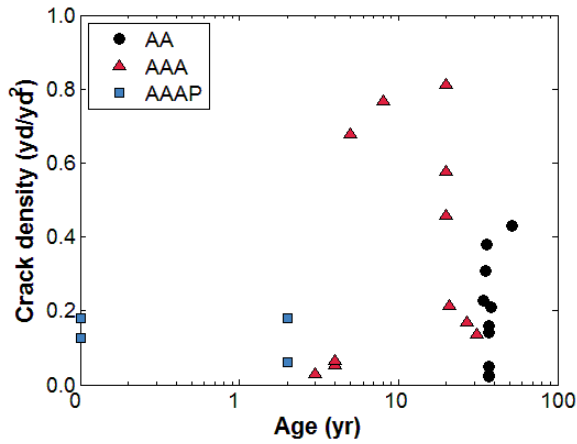


Figure 62. Crack density versus age for different concrete classes (40 inspected bridge decks)

3.3.5 Analysis of Other Variables

In addition to utilizing cracking data from the both the 40 inspected bridge decks and 163 new bridge decks to assess the performance of protective systems and concrete types, attempts were made to establish correlations between the extent of cracking and factors related to structural design and construction practices. The following sections discuss the findings of these correlation efforts.

The cracking data collected from the 40 inspected bridge decks and 163 new bridge decks was used to investigate the extent of cracking in relation to structural design factors such as girder material, moment region, number of spans, structure type, beam spacing, deck thickness, and bridge length. Crack density results from the 40 inspected bridge decks in terms of girder type is shown in [Figure 63](#). No observable correlations were established between the extent of cracking and girder type. Bridges with continuous supports are subject to negative moment regions, which create the potential for tensile stresses to develop within the concrete deck and thus cracking. The effect of the presence of negative moment regions on cracking for the 40 inspected bridge decks is shown in [Figure 64](#). No correlation was established between cracking and moment regions for continuous bridges.

The extent of cracking for various structural design factors using the cracking data from the initial inspections of 163 new bridge decks are presented in [Figure 65](#) through [Figure 70](#). The extent of cracking at initial inspections was similar for single and multi-span bridge decks ([Figure 65](#)), while steel girder bridges compared to prestressed concrete girders can be seen ([Figure 66](#)). The type of structural configuration utilized for the 163 new bridge decks was also investigated as a potential cause of deck cracking, as shown in [Figure 67](#). Adjacent box girder bridges displayed the highest average total deck crack density. However, there were only three decks with this structural configuration, so future data collection should be taken to confirm this observation. Additionally, adjacent box girder bridges were the only configuration for which longitudinal cracking was the majority contributor to total crack density. This problem has been recognized by PennDOT and design actions have been taken to address the issue (Zang 2010). Future inspections will determine the success of these design adjustments. [Figure 67](#) shows that steel I-beam configurations displayed significant cracking, particularly transverse cracking, while spread box girder bridges performed well in terms of crack density. The effect of beam spacing on early-age cracking is shown in [Figure 68](#). There appears to be more extensive cracking in bridges with spacing between approximately 75 and 125 inches, the latter being mostly spread box beam and I beam bridges. Crack density as a function of deck thickness is shown in [Figure 69](#). Eight inch thick decks displayed the highest crack density values, However, 8 inches was the most common thickness (126 decks). The other thicknesses with more than 5 bridges within the data set were 5 inches (12 decks) and 5.5 inches (10 decks). Bridge length is compared to crack density for the 163 new bridge decks in [Figure 70](#). As shown in [Figure 70](#), no correlation is apparent.

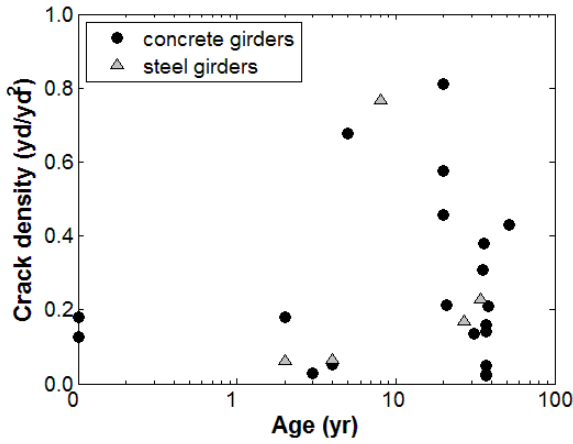


Figure 63. Crack density in terms of girder type (40 inspected bridge decks)

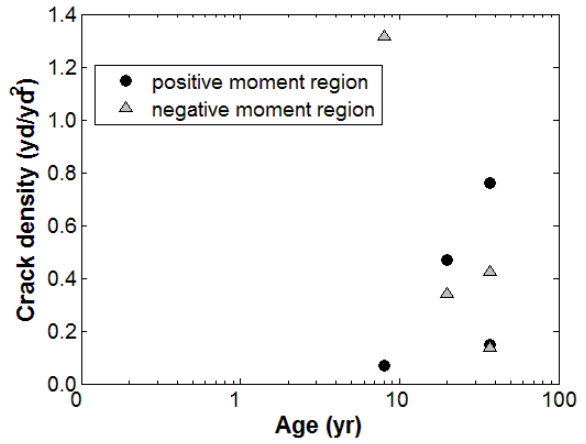


Figure 64. Comparison of crack density (40 inspected bridge decks) for positive and negative moment regions

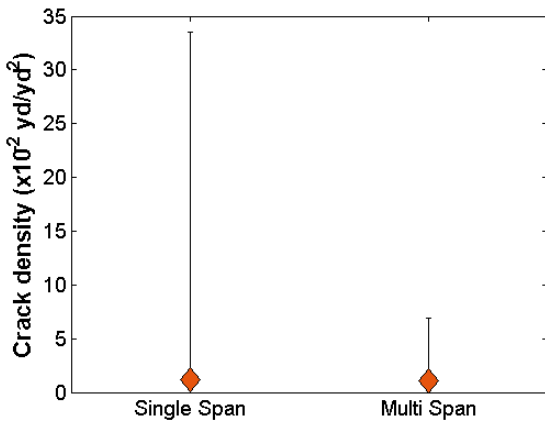


Figure 65. Comparison of average (data points) and range (error bars) of crack density at initial inspection (163 new bridge decks) between single and multi-span bridges

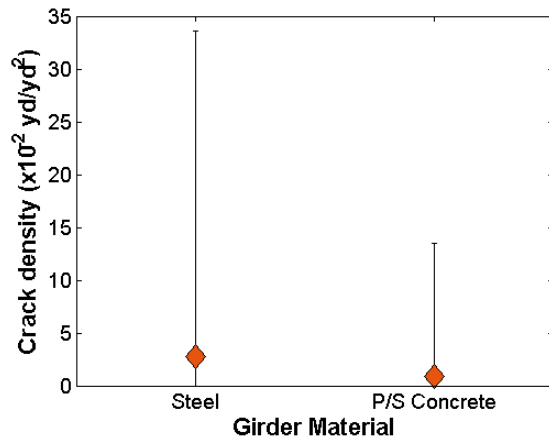


Figure 66. Average (data points) and range (error bars) of crack density at initial inspection (163 new bridge decks) in terms of girder material

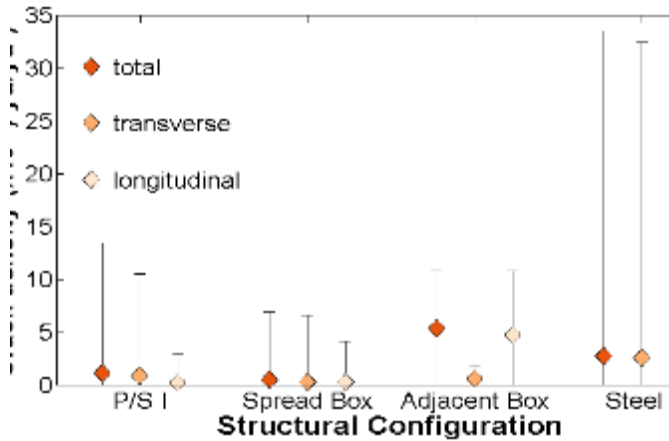


Figure 67. Average (data points) and range (error bars) of crack density at initial inspection (163 new bridge decks) in terms of structure type

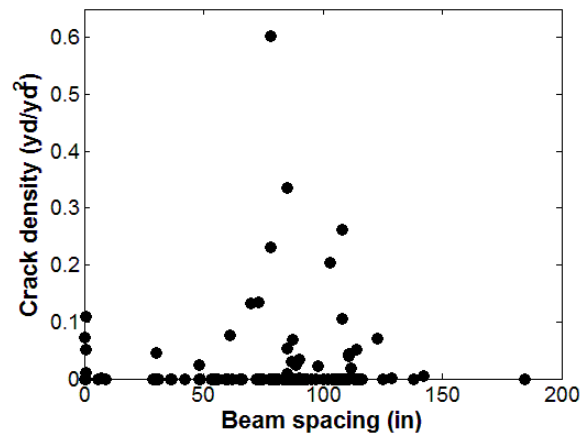


Figure 68. Crack density at initial inspection (163 new bridge decks) versus beam spacing

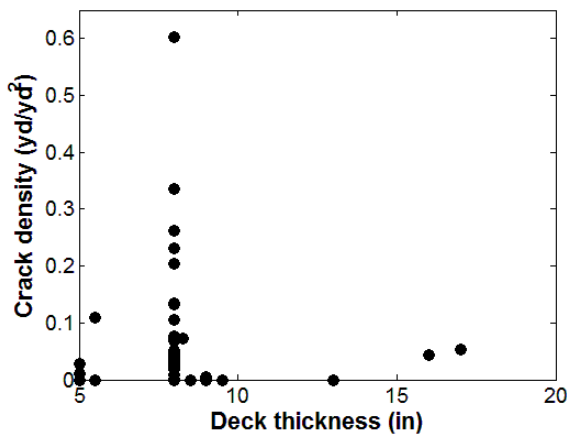


Figure 69. Crack density at initial inspection (163 new bridge decks) versus deck thickness

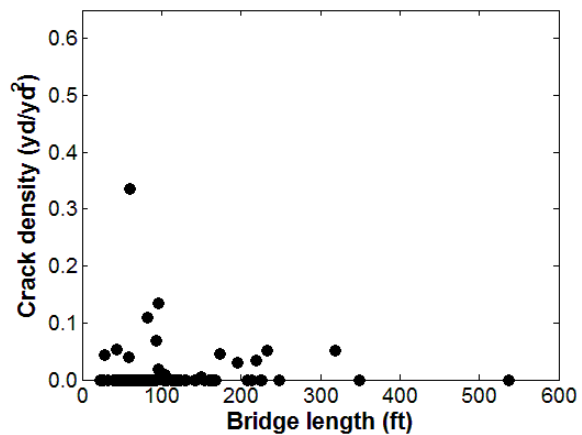


Figure 70. Crack density at initial inspection (163 new bridge decks) versus bridge length

Construction practices that were investigated in relation to early-age deck cracking included the curing duration, the construction procedure, the ambient temperature at time of placement, and the time of placement. The cracking data from the initial inspection of the 163 new bridge decks was used for the analysis. The early-age crack density in relation to curing duration is shown in [Figure 71](#). No observable apparent correlation was established. The effect of construction procedure, in terms of half width construction, on early-age cracking is shown in [Figure 72](#). Decks placed using a half width construction procedure showed an average crack density more than four times greater than decks poured in a full width construction procedure. The reasons for this observation could be the influence of adjacent traffic during placement or the effect of a cold joint.

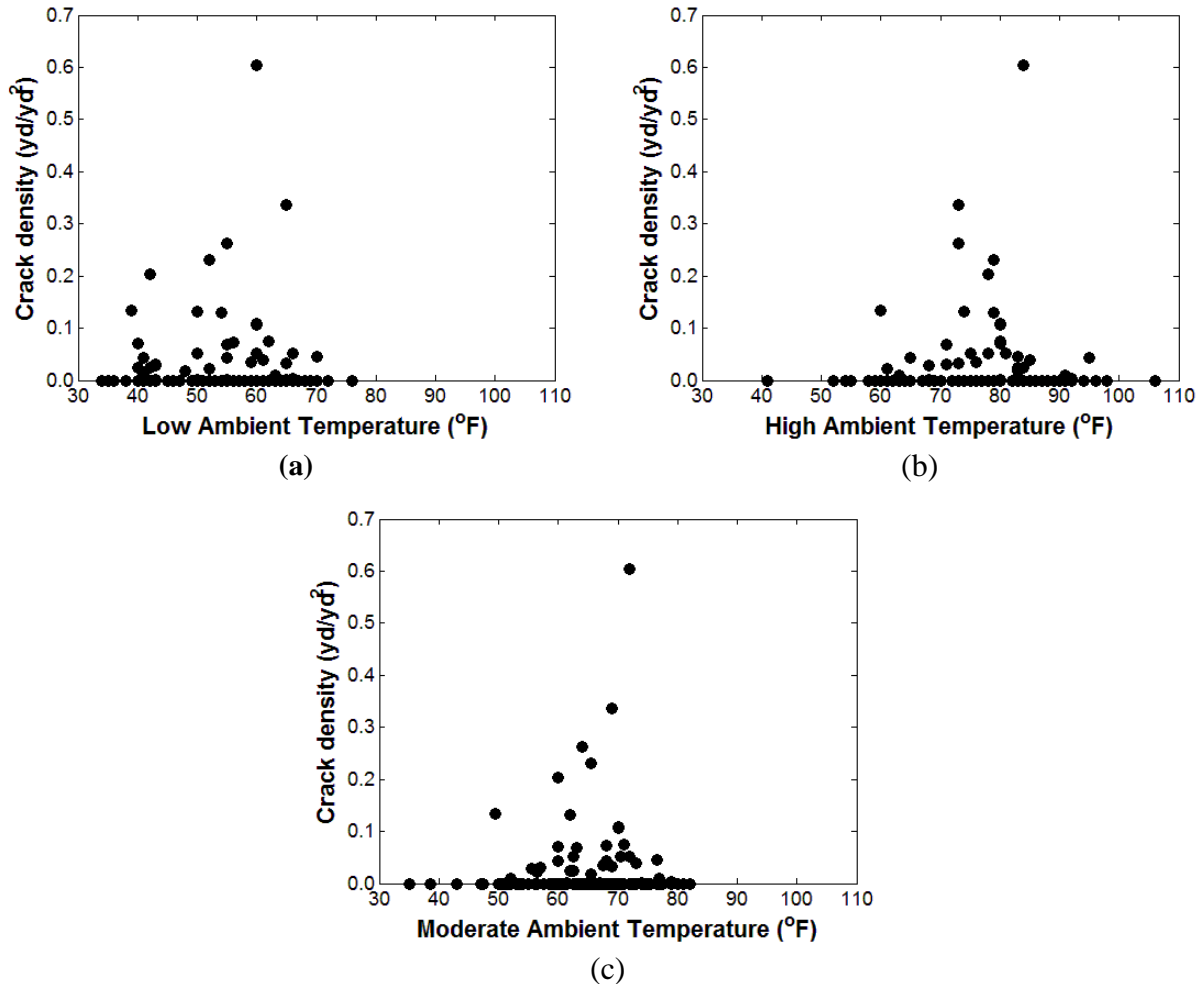


Figure 73. Crack density at initial inspection (163 new bridge decks) in terms of (a) low ambient temperature (b) high ambient temperature (c) moderate ambient temperature.

The average early-age crack density corresponding to the month of placement is shown in [Figure 74](#). There is no distinguishable correlation between the month of placement and deck cracking. However, additional data is needed to confirm this observation. In particular data for the Winter and Spring months (December through May) for which the current analysis had a limited number of placements in this timeframe.

The service level of a bridge deck, in terms of average daily traffic (ADT) and average daily truck traffic (ADTT), was also investigated as a potential contributor to cracking. [Figure 75](#) shows early-age crack density versus ADT and ADTT for the 40 inspected bridge decks, respectively. For both ADT and ADTT, the early-age crack density does not appear to be correlated to the service level.

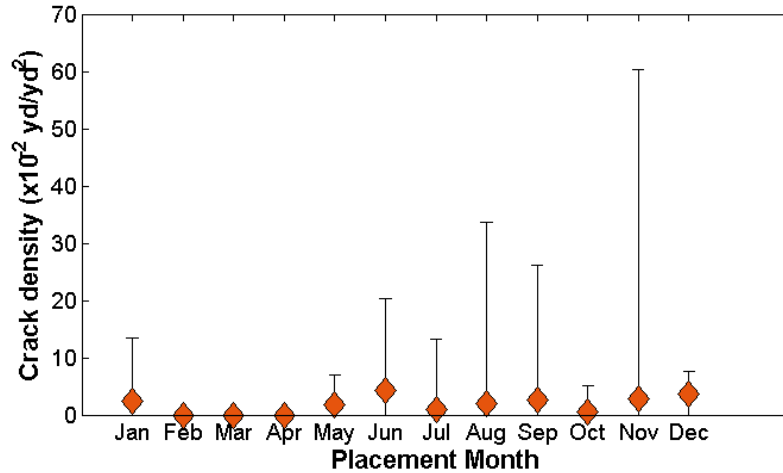


Figure 74. Average (data points) and range (error bars) of crack density at initial inspection (163 new bridge decks) in terms of placement month

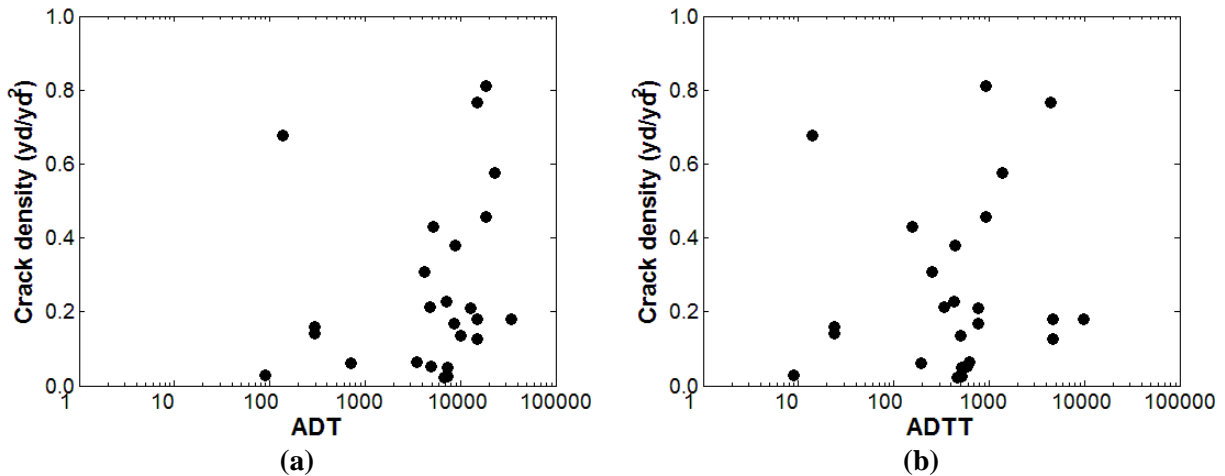


Figure 75. Effect of traffic on early-age cracking (40 inspected bridge decks) in terms of (a) ADT; (b) ADTT

3.3.6 Comparison of 85-17 Study and Current Study

Twelve of the 40 inspected bridge decks were also inspected in the “#85-17 Bridge Deck Protective Systems” investigation performed by PennDOT (Malasheskie et al. 1988). The bridges included in both the current and past #85-17 studies are listed in Table 40 (Appendix E). The objective of the study performed by Malasheskie et al. (1988) was to evaluate the effectiveness of protective systems used in bridge decks in Pennsylvania, specifically epoxy-coated rebar, galvanized rebar, waterproofing membranes underneath bituminous overlay, latex-modified concrete overlay, and low slump dense concrete overlay (w/c= 0.33 max), many of which are no longer used by PennDOT. The study involved the inspection of 169 bridge decks, categorized by the detail of inspection performed. Twenty one “Level A” decks were inspected visually as well as using physical testing, including half-cell potential, electrical resistance, and core sampling to determine

concrete permeability and chloride content. An additional 148 “Level B” decks were only visually inspected.

The decks considered in the present study were all Level B decks. Level B decks were assigned a condition rating from 9 (best) to 0 (worst) according to PennDOT’s Structural Inventory Record System Bridge Inspection Manual for the 85-17 study using the results of the visual inspections. In addition, a Deterioration Factor (D.F.) was correlated to condition rating and assigned to each of the decks according to Equation (2) (Malasheskie et al. 1988).

$$D.F. = Structure\ Age + \frac{ADT}{5000} + \frac{ASTM\ Weathering\ Index}{100} + \frac{Average\ Annual\ Freeze-Thaw\ Cycles}{10} \quad (2)$$

The Deterioration Factors assigned to each deck during the #85-17 study are presented in Table 15 below (also as Table 40 in Appendix E). Comparing the Deterioration Factor from the #85-17 study to the crack density results from the current study (Figure 76a) shows a counterintuitive correlation, in which decks with high crack densities have low Deterioration Factors. The lack of data points is due to 7 of the 12 decks being replaced or overlaid since the #85-17 study. Comparing the Deterioration Factor to the current condition rating for the decks that were not replaced since the #85-17 study (Figure 76b) shows some degree of correlation. The three decks with highest Deterioration Factors (i.e., high potential for deterioration) have low current condition ratings. This indicates that the Deterioration Factor is a good indicator for the performance of these decks.

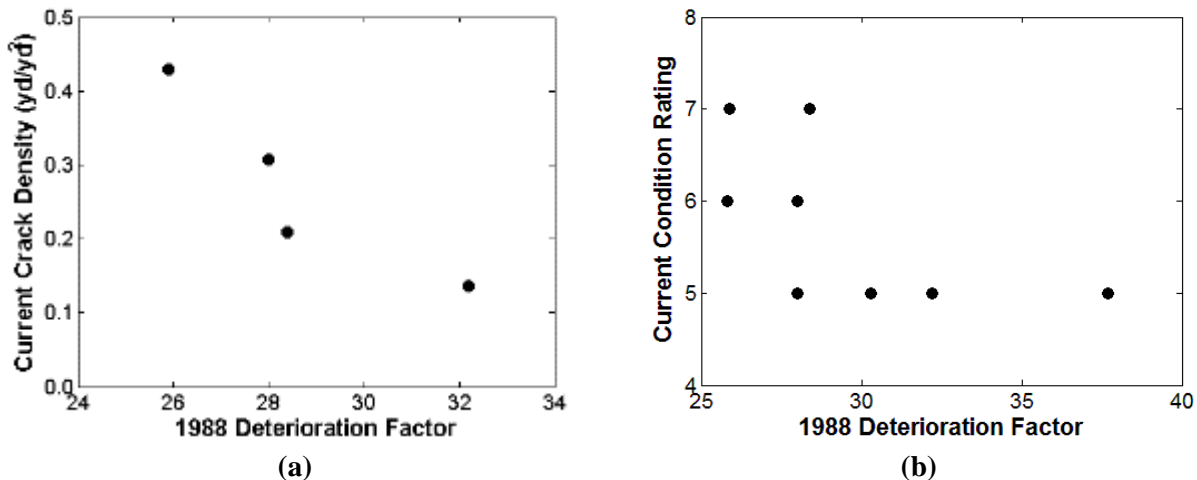


Figure 76. Comparison of 1988 Deterioration Factor to (a) current crack density; (b) current condition rating (for decks that were not replaced since #85-17 study)

Table 15 List of bridge decks included in both the #85-17 Study and the Current Study

Bridge Number	1988 Protective System (Current)	Original Concrete Type (Current)	Current Wearing Surface	Year Built	Year Rebuilt	Age (years)	Deterioration Factor (#85-17)	Current Condition Rating
20613	Latex-Modified Concrete (None)	AA (AA)	LMC	1978	-	36	37.7	5
20507	Latex-Modified Concrete (None)	AA (AA)	LMC	1977	1993	21	28.0	6
20506	Latex-Modified Concrete (None)	AA (AA)	LMC	1977	-	37	28.0	5
30752	Galvanized Rebar (None)	AA (AA)	Bituminous	1924	-	90	25.8	6
4908	Low Slump Concrete (Epoxy-coated Rebar)	AA (AA)	Original	1962	-	52	25.9	7
30643	Epoxy-coated Rebar (Epoxy-coated Rebar)	AA (AA)	Original	1937	1979	35	28.0	6
19551	Epoxy-coated Rebar (Epoxy-coated Rebar)	AAA (AAA)	Original	1983	-	31	32.2	5
19724	Epoxy-coated Rebar (Epoxy-coated Rebar)	AAA (AAA)	Epoxy Overlay	1984	-	30	23.4	-
20588	Galvanized Rebar (Galvanized Rebar)	AA (AAA)	LMC	1975	2009	5	31.6	7
20589	Galvanized Rebar (Galvanized Rebar)	AA (AAA)	LMC	1975	2009	5	31.6	7
26993	Galvanized Rebar (Galvanized Rebar)	AA (AA)	Original	1976	-	38	30.3	5
21651	Galvanized Rebar (Galvanized Rebar)	AA (AA)	Original	1976	-	38	28.4	7

3.3.7 Correlation of Condition Rating to Crack Density

The current PennDOT rating system for concrete bridge decks considers various parameters such as the area of delamination/spalling, electrical potential of concrete, and chloride content (as shown in

Table 16). Using the crack densities (from the 40 inspected bridge decks and the 163 new bridge decks) and condition ratings for corresponding decks (provided by PennDOT), attempts were made to establish correlations between the condition ratings and crack densities. However there is a large amount of scatter in crack densities for each condition rating. As a result, the ranges of crack density for each condition rating have significant overlap, as shown in [Figure 77](#). This suggests

that a meaningful range or even a median/mean cannot be defined for each condition ratings with the current data.

Table 16. PennDOT (2009) condition rating system for concrete bridge decks

Category Classification	Rating	Condition Indicators					
		Deck Area		Electrical Potential	Deck Area	Chloride Content (#/CY)	Deck Area
		Visible Spalls	Delamination				
Category 3 Light Deterioration	9	none	none	0.0	none	0.0	none
	8	none	none	$0.0 < EP < 0.35$	none	$0.0 < CC < 1$	none
	7	none	< 2%	$0.35 < EP < 0.45$	≤ 5%	$0.0 < CC < 2$	none
Category 2 Moderate Deterioration	6	< 2% spalls or sum of all deteriorated and/or contaminated deck concrete (≥ 2 #/CY Cl) < 20%					
	5	< 5% spalls or sum of all deteriorated and/or contaminated deck concrete 20% to 40%					
Category 1 Extensive Deterioration	4	> 5% spalls or sum of all deteriorated and/or contaminated deck concrete 40% to 60%					
	3	> 5% spalls or sum of all deteriorated and/or contaminated deck concrete > 60%					
Structurally Inadequate Deck	2	Deck structural capacity grossly inadequate					
	1	Deck has failed completely - repairable by replacement only					
	0	Holes in deck - danger of other sections of deck failing					

Notes: Rating 9 - no deck cracking exists, Rating 8 - some minor deck cracking is evident

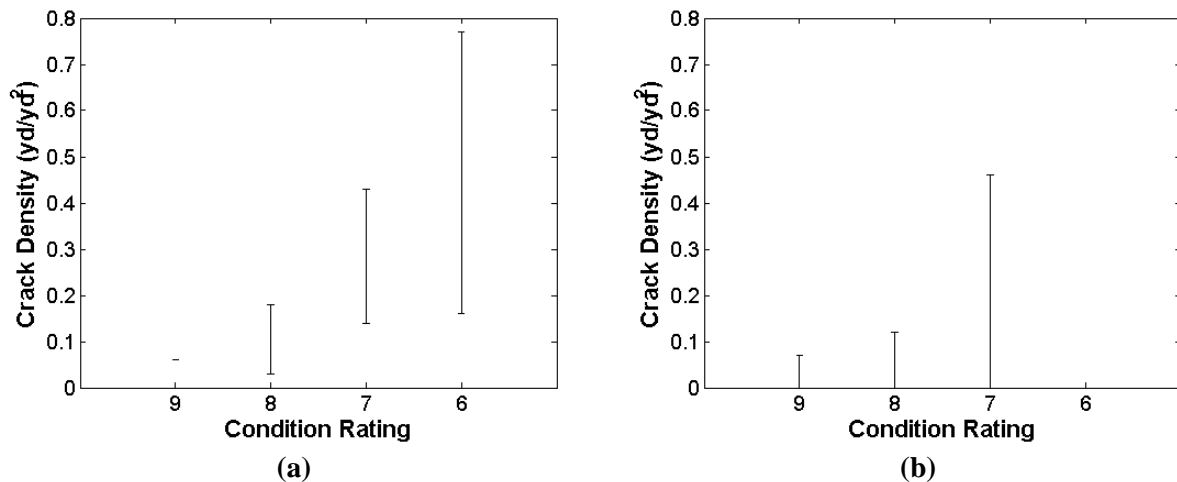


Figure 77. Ranges of crack density values for each condition rating based on (a) 40 deck data (non-overlaid); (b) 163 deck data.

Without additional data (crack densities) from various bridge decks for each rating over time, attempting to predict the crack density of decks solely based on deck condition rating is not recommended at this time. Even with additional condition rating data to categorize the crack density data, establishing a trend might not be feasible since the PennDOT condition rating system

is based on phenomena other than surface cracking (e.g. corrosion and delamination), for which other performance criteria are used (e.g., chloride content and electrical resistivity). Instead, the ratings history data is most useful for prediction of useful life (as discussed in subsequent deterioration modeling section). Table 17 shows an analysis of crack density ranges and averages for each condition rating based on deck cracking data from the 40 inspected bridge decks and the 163 new bridge deck. The raw data used to calculate these values is included in Appendix F.

Table 17. Correlation of bridge deck condition rating to crack density (Poisson distribution assumed for confidence intervals)

40 Inspected Bridge Decks (non-overlaid)				
Deck Condition Rating	No. of decks	Corresponding Crack Densities (yd/sy)		
		Range	Mean	Median
9	1	0.06	0.06	0.06
8	4	0.03-0.18	0.10	0.12
7	4	0.14-0.43	0.29	0.21
6	4	0.16-0.43	0.36	0.31
163 New Bridge Decks				
Deck Condition Rating	No. of decks	Corresponding Crack Densities (yd/sy)		
		95% Conf. Intervals	Mean	Median
9	75	0.00-0.07	0.01	0
8	48	0.00-0.12	0.02	0
7	8	0.00-0.46	0.05	0

3.4 Deck Performance Database (DPD) and PSU Bridge Deck Life software

This chapter explains the two software packages developed by PSU. The first is DPD (Deck Performance Database) which is a database to store inspection records from crack inspections conducted every two years for each bridge deck in Pennsylvania. Screenshots of DPD are included as a User Manual as well. The second developed software is PSU Bridge Deck Life which is a service life prediction and deterioration modeling software for bridge decks in Pennsylvania. The underlying deterioration model for PSU Bridge Deck Life is also explained in this chapter.

3.4.1 DPD Description and User Manual

A Deck Performance Database (DPD) was developed in order to store the cracking and related data for bridge decks in Pennsylvania. Information related to the structure, construction and placement of the decks is entered and stored in the DPD. Inspection data, including the amount of cracking observed in each inspection, can be input repeatedly with subsequent inspections. The DPD performs calculations in order to obtain the crack density (yd/sy) for each inspection and stores the calculated values. A “report” function is also built into the DPD allowing users to filter the list of bridge contained in DPD and export data to excel worksheets. In the subsequent section the various pages included in DPD are described including associated computer screenshots.

Main Menu: DPD starts with the Main Menu page as shown in [Figure 78](#).

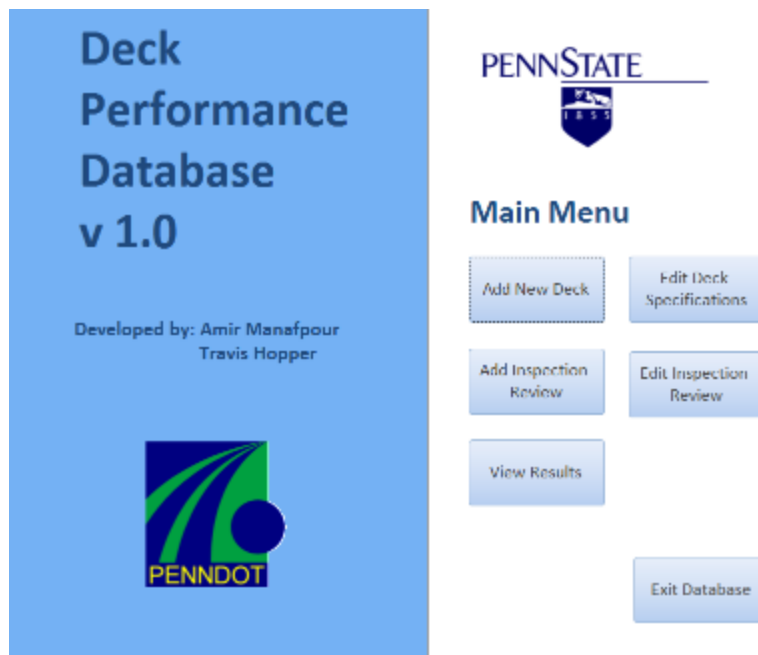


Figure 78. Main Menu page of Deck Performance Database

Add New Deck:

Figure 79 shows the page for the entry of a new deck into the database. The BMS and BrKey numbers are required for each deck and this form checks the database for duplicate IDs. The form will not allow duplicate entries for BMS and BrKey numbers.

New Deck Entry

Please enter the identification data below

BMS#: *Required

BrKey: *Required

ECMS#:

SR/Section:

Cancel Enter Bridge Specs

Figure 79. New Deck Entry page

After clicking “Enter Bridge Specs” the user is taken to the Decks Specifications page where the information is entered for the deck as shown in Figure 80. On the “Enter Bridge Specs” page the Construction Type, Concrete Type, and Placement Date are required and the form cannot be submitted without these inputs.

After clicking “Enter Inspection Data” the user is taken to the Inspection Form as shown in Figure 81. The rows in the crack table of this page expand as the data is entered, so several spans and rows of data can be entered for one inspection. This form requires the Inspection Data to be entered before the form is submitted. After clicking “Submit Inspection” the DPD calculates and stores the total and longitudinal and transverse crack densities.

The other input on the Main Menu page (Edit Deck Specifications, Add Inspection Review, Edit Inspection Review) requires the user to first select the considered deck (using the BMS#) then edit the data accordingly. The user can change the bridge ID data (i.e., BMS#, BrKey, ECMS#) by clicking “Edit Bridge ID Data” in the “Edit Deck Specifications” menu.

Deck Specifications

BMS#: 11-1111-1111-1111

BrKey: 111

ECMS#:

SR/Section:

Structure Information

Construction Type:

Beam Spacing: inches
(Center-to-center)

Deck Thickness: inches

Concrete Mix Design

Please input the following information based on the corresponding mix design form

Concrete Type:

Supplier Name:

Mix Design JMF#:

Cement Content: pcy

Slag/GGBFS Content: pcy

Fly Ash Content: pcy

Silica Fume Content: pcy

Select the admixtures that were used:

Water Reducer

Air Entrainment

Retarder

QC Target Slump: inches

Water/Cement Ratio:

28-day Design Strength: psi

28/7 Day Ratio:

Concrete Placement Data

The temperatures below include curing time

Ambient Temperature High: °F

Ambient Temperature Low: °F

Actual Curing Duration: days

Date Opened to Traffic:

Actual Slump: inches

Placement Date:

7-day Avg. Break Strength: psi

28-day Avg. Break Strength: psi

28/7 Day Ratio:

Half-width Construction?

Yes No

Additional Construction Data

Max. Concrete Temperature: °F

Corresponding Top Flange Temp: °F

Temp. Difference b/w Deck_Girder: °F

Approximate Pour Start Time:

Approximate Pour End Time:

Placement Method:

(Enter manually if not in list)

Comments:

Cancel and Return
to Previous Menu

Save Specs

Enter
Inspection Data

Figure 80. Deck Specifications page

Inspection Form

BMS#:

BrKey:
 ECMS#:
 SR/Section:

Date of Inspection(mm/dd/yyyy):

Select checkbox for initial inspection (before opening to traffic):

Inspection Performed By:

Comments:

Please input crack data in the table below for each span

	Span No.	Span Length (ft)	Span Width (ft)	Moment	Transverse Crack Length (yd)	Longitudinal Crack Length (yd)
▶	0	1	1	Positive	0	0
				Negative	0	0

Figure 81. Inspection Form page

3.4.2 Service Life Prediction and Deterioration Modeling

The most commonly used probabilistic model used in bridge management systems to predict the deterioration of bridge elements using condition rating data is the Markov chain model. A proposed procedure for applying a semi-Markov model to the PennDOT condition rating data for over 20,000 bridges will be explained in this section. The Weibull distribution will be used to define the probability distribution functions for the sojourn times of each condition. Using the proposed model’s results, the service life and deterioration behavior over time for these decks can be obtained.

3.4.2.1 Data Collection

Beginning approximately in 1985, PennDOT initiated biannual (every two years) inspections of bridges across Pennsylvania. From each inspection, condition ratings are assigned to each element of the bridge (e.g., deck, superstructure, substructure). In this study, the deck CR historical data for more than 22,000 bridge decks from 1985 to 2014 and their corresponding specifications data were collected, analyzed and employed. The criteria used to assign a CR to a deck is summarized in Table 18. The ratings range from CR9 to CR0, where 9 represents the best possible condition and 0 the worst. The deck specifications data were obtained from Bridge Management System 2 (BMS2, PennDOT 2009) to evaluate the effects of each factor on the deterioration of the considered decks. These variables and definitions were slightly modified to suit this study and are listed in Table 18.

Table 18. Transformed BMS2 variables used in analysis and their definitions (PennDOT 2009)

Variable	BMS2 Variable Name	Variable Description
DISTRICT	5A04	Location of deck based on district: 1 to 6 and 8 to 12
INTERACT	6A28	Type of Span Interaction for Main Unit: 1 = simple, non-composite; 2 = Simple, composite; 3 = Continuous, non-composite; 4 = Continuous, composite; 9 = Other
REBARTYPE	6A42	Type of Deck Reinforcement Bar Protection: 1 = Bare reinforcement; 2 = Galvanized; 3 = Epoxy; 9 = Other
SURFTYPE	5B02	Deck Surface Type: 1 = Concrete; 2 = Concrete overlay; 4 = Low slump concrete; 5 = Epoxy overlay; 6 = Bituminous; 9 = Other
SPANNUM	5B11	Total Number of Spans in Main Unit: 1 = single-span; 2 = multi-span
MAINPHYSICAL	6A27	Physical Makeup of Primary Load Carrying Members for Main Unit: 1 = Reinforced; 2 = Pre/Post-tensioned; 6 = Rolled sections; 9 = Other
NHS	5C29	National Highway System: 0: Route is not on NHS; 1: Route is on NHS
ADTT	6C27	Average Daily Truck Traffic (CONTINUOUS VARIABLE)
LENGTH	5B18	Total Overall Structure Length in feet (CONTINUOUS VARIABLE)

3.4.2.2 Data Preprocessing

To implement the CR history data into a specific model, the dataset had to be preprocessed. Basic filtering/preprocessing algorithms were applied in order to remove the effects of miscoding, typos, bridge accidents leading to substantial damage, and inspector subjectivity as follows:

- miscoded data (e.g., “-“ or blanks), non-applicable data (e.g., “N” rating) and mismatching duplicate entries (e.g., same inspection dates different ratings) were eliminated;

- decks with unusual drops in ratings (i.e., more than 2-ratings possibly due to impacts of trucks/ships, traffic accidents, etc.) were omitted;
- rating histories for bridge with less than 3 inspection points were not included in the analysis;
- mistyped or out-of-place ratings such as a 0-rating in the middle of series of ratings (i.e., 6,6,6,5,5,0,5,5) were corrected/modified accordingly;
- deck was required to remain at any given CR for at least two consecutive inspections in order to be considered as a sojourn time in the sojourn time extraction procedure;
- the CR history of some decks were modified to account for possible inspector subjectivity. For example, if an unusual increase/drop of 1 CR was observed while the deck had remained at the same rating 4 years before and 4 years after the increase/drop, then the increase/drop inspection point was considered to be a subjective inspector error and was eliminated.

3.4.3 Estimation algorithm for placement date of most recent deck

Construction and reconstruction data is available from the BMS2 database, however the accuracy of this data is a concern. For most bridges, an increase in rating typically corresponds to the BMS2 construction or reconstruction date. However, occasionally the construction data may not have been updated or may not be related to the deck. In order to improve the accuracy in estimating the placement dates for the decks under review, an algorithm was developed which utilizes the construction date, reconstruction date as well as the rating history for each bridge to determine the placement date of the most recent deck for that bridge. The framework of this algorithm is shown in [Figure 82](#).

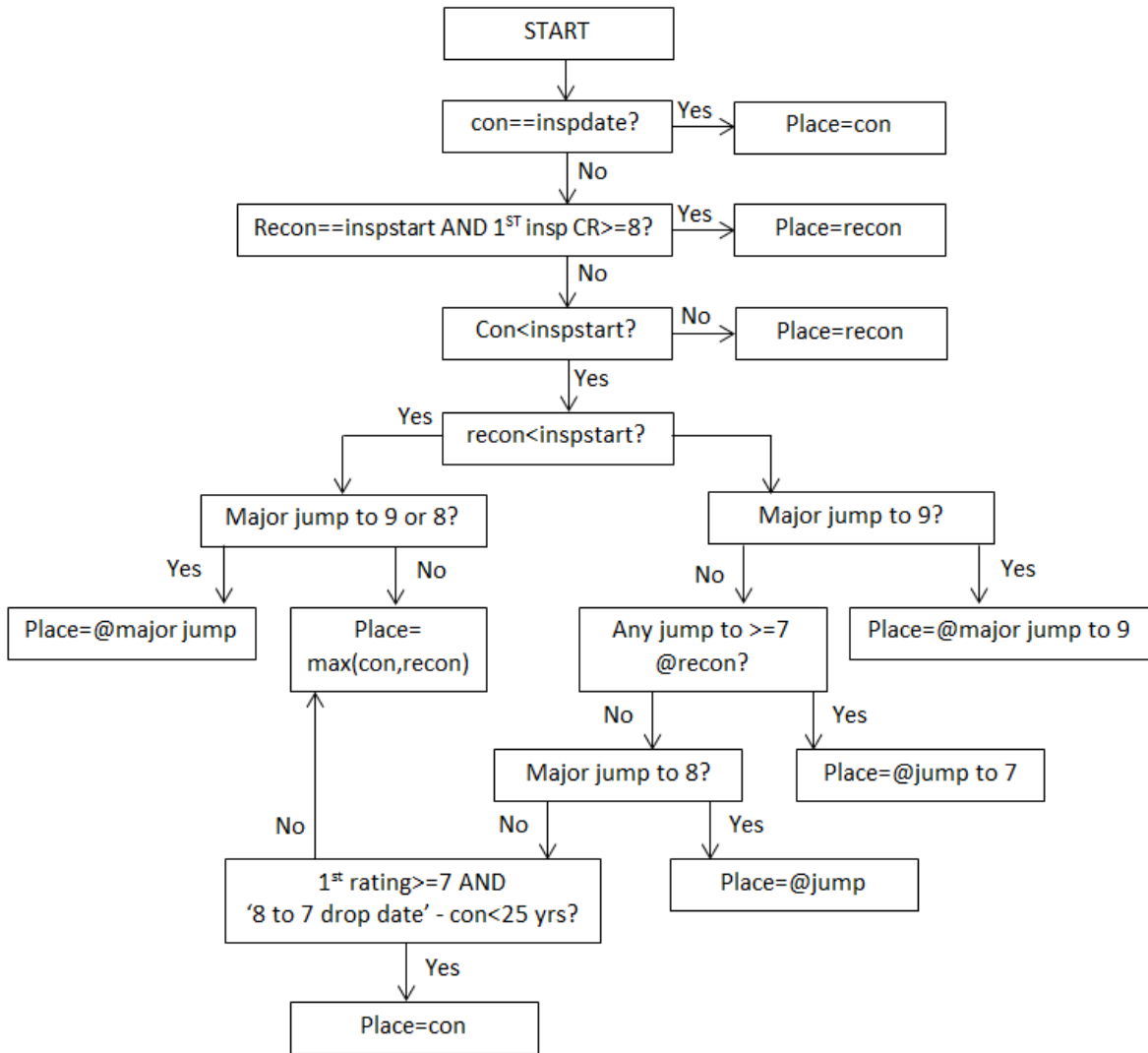


Figure 82. Algorithm used to improve placement date data accuracy. “con” is BMS2 construction date, “Recon” is BMS2 reconstruction date, “place” is the placement date which is the output for this algorithm, “CR” is condition rating, “inspstart” is the date of first inspection

3.4.3.1 Sojourn time extraction and Weibull Fitting

The sojourn time for a particular condition rating i is defined as the amount of time spent at that condition rating i before transitioning to a lower rating $i-1$ (Sobanjo 2011). For example, if a deck rating transitioned from a CR (Condition rating) 9 to a CR 8, stayed at CR 8 for 14 years and then transitioned to a CR 7; the sojourn time for CR 8 for this particular deck is $T=14$ years. Various types of PDFs (probability distribution functions) have been used to represent the distribution of sojourn times. In this study the Weibull distribution will be used to estimate the transition probabilities in a semi-Markov process. The details of the proposed semi-Markov process are described in the following sections.

After preprocessing the CR dataset, feature extraction procedures were applied to the CR historical data set in order to extract the information required to develop a deterioration model. The feature

of interest in this study is the sojourn time, defined as the time spent at a specific CR i before transitioning to a lower CR $i - 1$. When extracting sojourn times from the CR historical data, some were observed till the decks transition to a lower state and their exact duration at a given CR is known. However, the deck may not have transitioned to a lower state by the end of the observation period and the observation period may have ended before the exact duration at a given CR is known. The former is referred to as a complete or uncensored observation and the latter is defined as a right-censored observation.

Right-censored sojourn times reflect a situation where the observed sojourn time is known to be less than the actual sojourn time (Allison 1998). One reason studies might include censored data points, is to maintain a population in the dataset. However, studies have demonstrated that improved fit was obtained to the probability distribution functions when censored CR data was disregarded (Sobanjo et al. 2010, Sobanjo 2011). Sobanjo et al. (2010) attribute this to “the nature of the data and the inability to adequately fit the available censored data to a suitable probability distribution”. Due to large population of the CR dataset (approximately 22,000), this study was able to rely upon only uncensored/complete sojourn time data. After removing complete data, a total of 7,537 sojourn times were successfully extracted from the original dataset for CR3 to CR9. Also, during the extraction of sojourn times, the start and end of each sojourn time was approximated to occur half-way between the two inspection times corresponding to the CR drops.

During the sojourn time extraction procedure it was observed that there were essentially two types of uncensored sojourn times, as shown in [Figure 83](#). Type I: a drop in CR is observed at the start of the sojourn time and Type II: a jump (due to remediation) in CR is observed at the start of the sojourn time. In order to incorporate the differences between these two types of sojourn times, another variable (not included in the BMS2 data of [Table 18](#)) called SojType was developed to identify the type of each sojourn time and was included in the statistical analysis when estimating AFT Weibull-fitted parameters.

Essentially, Type II sojourn times only capture the “remediated” deterioration rate; whereas Type I sojourn times largely correlate to the “unremediated” deterioration rate, even though most of them will have been at least mildly affected by prior remediation. Type I sojourn times do not necessarily correspond to “unremediated” decks, because it is possible that the deck was remediated earlier in its life. However, if the deck had been remediated in the past, the remediation is expected to have a less pronounced effect on Type I deterioration rate compared to Type II. In general, the majority of the decks have had some remediation by the time they transition below CR6. [Table 19](#) classifies sojourn times into the two types for each CR. The highest CR is CR9 and bridge decks cannot transition to CR9 from a higher CR (because CR10 does not exist), as a result, Type I sojourn times do not exist for CR9.

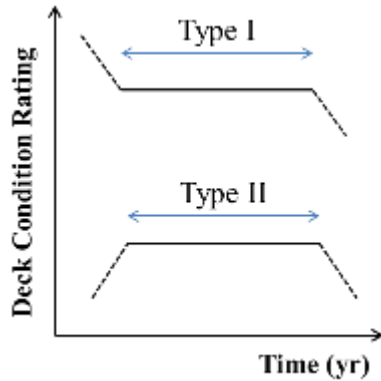


Figure 83 Difference between Type I and Type II sojourn times observed from PennDOT bridge deck data

Table 19. Number of Type I and Type II sojourn times

Condition Rating	Number of observed uncensored sojourn times		
	Total	Type I	Type II
3	17	16	1
4	144	127	17
5	835	639	196
6	2063	1289	774
7	2537	1226	1311
8	1577	291	1286
9	204	0	204

Statistical analysis was conducted on the extracted sojourn times using the statistical software Stata (StataCorp 2013). The maximum likelihood estimate (MLE) method was used to estimate the AFT Weibull-fitted parameters (i.e., β covariates and p -parameter). In order to evaluate the significance of the exogenous variables listed in Table 18, a series of dummy variables were generated based on the possible input values for each variable. The statistical analysis of the sojourn times and the deck specifications data provided p-values for each of the dummy variables, which identified their significance in estimating sojourn times. Subsequently, a variable selection process was conducted until all remaining dummy variables were significant at the chosen significance level (either p-value < 0.05 or 0.10).

3.4.3.2 AFT Weibull Distribution and Semi-Markov process

The Weibull model is commonly used to define the probability of failure or sojourn times for infrastructure and bridges (Mishalani and Madanat 2002, Agrawal et al. 2010, Sobanjo et al. 2010, Sobanjo 2011). Sobanjo (2011) compared the Weibull, exponential and lognormal distributions and found the Weibull distribution was the best fit for the majority of sojourn times for bridge condition states. Assuming T is a continuous nonnegative random variable describing the sojourn time of a deck at a specific CR, the cumulative distribution function (CDF) $F(t)$ and the Weibull PDF $f(t)$ are shown in Eqs. (1) and (2).

$$F(t) = 1 - \exp[-(\lambda t)^p] \quad (1)$$

$$f(t) = \frac{dF(t)}{dt} = \lambda p (\lambda t)^{p-1} \exp[-(\lambda t)^p] \quad (2)$$

where λ and p are constant Weibull model parameters. The survivor function $S(t)$ describes the probability a deck will last at least t years at the current CR before transitioning to a lower CR, as shown in Eq. (3). The hazard rate function $h(t)$ represents the instantaneous risk that a deck will experience a drop in CR having lasted at the current CR for t years, as shown Eq. (4).

$$S(t) = 1 - F(t) = \exp[-(\lambda t)^p] \quad (3)$$

$$h(t) = \frac{f(t)}{S(t)} = \lambda p (\lambda t)^{p-1} \quad (4)$$

Eq. (5) can be used to calculate $E(T)$, the average expected sojourn time for the Weibull distribution.

$$E(T) = \frac{1}{\lambda} \Gamma\left(1 + \frac{1}{p}\right) \quad (5)$$

where Γ is the gamma function. Detailed information regarding the stochastic duration model functions and relationships presented in Eq. (1) to Eq. (5) can be found in Greene (1997).

The hazard rate function $h(t)$ identifies the effect of age on the nature of the deterioration being modeled. A constant hazard rate (i.e., $p = 1$) suggest regardless of how long the deck has spent at a given CR, the probability of transitioning out of that CR remains constant over time. Such processes are known to “lack memory” and this characteristic is referred to as duration independence. An increasing hazard rate over time (i.e., $p > 1$) reflects positive duration dependence and implies the probability of transitioning from the current CR increases, as the deck spends more time in that CR. A decreasing hazard rate over time (i.e., $p < 1$) reflects negative duration dependence. As a result, the hazard function rates can be utilized to evaluate duration dependence and test whether or not a process possesses the Markovian property (i.e., memoryless property).

Bridge deck deterioration is expected to depend on a series of exogenous, and independent, factors such as those listed in Table 18. In order to incorporate the effect of these variables on the deterioration rate, the constant parameter λ can be replaced by a function dependant on the exogenous variables. To ensure that λ remains positive, an exponential form is adopted as shown in Eq. (6), resulting in an AFT Weibull model.

$$\lambda = e^{-\beta X} \quad (6)$$

where X is a column vector of exogenous variables and β is a row vector of constant parameters to be estimated. X also includes the value 1 in order to capture the constant term. Weibull AFT models assume the effect of a covariate is to increase or decrease the deterioration rate of a given process by a constant and are typically used for processes with a known sequence of intermediary states (Kalbfleisch and Prentice 2002). Substituting Eq. (6) into Eq. (2) results in Eq. (7), an exogenous variable-dependent AFT Weibull PDF.

$$f(t) = \frac{p}{t} (e^{-\beta X t})^p \exp[-(e^{-\beta X t})^p] \quad (7)$$

Eq. (7) is a PDF used to describe the sojourn times and applied to a proposed semi-Markov model which defines the stochastic nature of deck deterioration (CR transitions) as discussed in the following section.

Semi-Markov Model Development

A semi-Markov process is a stochastic process which estimates the probability of being at a specific CR and includes parameters which depend on the current CR, the visited CRs and the next CR (Ross 1970, Cinlar 1975). The transition probabilities of semi-Markov models can be duration dependent, unlike Markov chain processes which are duration independent or “memory less.” To calculate the semi-Markov transition probabilities (probability of transitioning from CR i to a lower CR), various methods have been proposed (Cinlar 1975) and researchers have studied their applications in bridge deterioration (Ng and Moses 1998, Kallen and Noortwijk 2005).

Sobanjo (2011) conducted an extensive study developing transition probabilities for bridge deterioration based on Weibull-fitted parameters describing sojourn times. Sobanjo utilized approximation solutions suggested by Permen et al. (1997), Black et al. (2005), and Kallen and Noortwijk (2005) to formulate transition probability equations for the semi-Markov process. Sobanjo (2011) developed transition probability for up to 3-step transitions (e.g., from CR9 to CR6). In this study, formulation for up to 5-step transitions (e.g., from CR9 to CR4) were developed and computationally calculated. A complete explanation of the formulation is included in Appendix A and only the key the resulting equations presented herein for brevity.

In this study, the sojourn time PDF for CR i is represented by f_i and the CDF is represented by F_i . Two main assumptions were made in the development of the proposed semi-Markov model: 1) there can only be an instantaneous drop of 1 in CR throughout the service life of the deck (e.g., CR9 must transition to CR8 before transitioning to CR7); and 2) no remediation that could potentially increase the CR is conducted throughout the service life of the deck. The effect of remediation is incorporated by modifying AFT Weibull parameters is addressed later on in this paper.

The deck is initially assumed to be at CR9 at the time of deck construction ($t = 0$) for simplification. Before proceeding the following notations is defined: $P_{9,j}(t)$ is the probability of a deck being at exactly CR j at time $t > 0$ assuming the deck was at CR9 at $t = 0$. Whereas, $P_{9,j...}(t)$ is the probability of being at CR j or lower having initially started at CR 9. First, the probability of

remaining at CR 9 after time t (i.e., $P_{9,9}(t)$) will be calculated. For CR9, this is simply the survival function, as shown in Eq. (8).

$$P_{9,9}(t) = S_9(t) = 1 - F_9(t) \quad (8)$$

The next step is to calculate the probability of starting at CR9 and ending up at CR8 (i.e., $P_{9,8}(t)$) which depends on $P_{9,9}(t)$ and $P_{9,7...}(t)$. By implementing approximation methods and assuming only one drop in CR at a time as described in Appendix A, $P_{9,7...}(t)$ is calculated as follows:

$$P_{9,7...}(t) = \sum_{a=1}^t f_9(a) \cdot F_8(t - a) \quad (9)$$

Eq. (9) essentially considers all the possible combinations of reaching CR7 from CR9 using discrete state summations. By decreasing the time increments used to calculate the sum in Eq. (9), the approximation accuracy increases. For example, in order to calculate $P_{9,7...}(t = 4 \text{ years})$ using 1-year increments, Eq. (9) can be expanded as follows

$$P_{9,7...}(t = 4) = f_9(1) \cdot F_8(3) + f_9(2) \cdot F_8(2) + f_9(3) \cdot F_8(1) \quad (10)$$

Finally, it is assumed that

$$P_{9,8}(t) = 1 - P_{9,9}(t) - P_{9,7...}(t) \quad (11)$$

The next step is to calculate $P_{9,7}(t)$ which depends on $P_{9,9}(t)$, $P_{9,8}(t)$, and $P_{9,6...}(t)$. The following formulation (derived in Appendix A) can be used for this purpose:

$$P_{9,6...}(t) = \sum_{b=a}^t \sum_{a=1}^t f_9(a) \cdot f_8(b - a) \cdot F_7(t - b) \quad (12)$$

$$P_{9,7}(t) = 1 - P_{9,9}(t) - P_{9,8}(t) - P_{9,6...}(t) \quad (13)$$

It can be noticed that each $P_{9,j}(t)$ depends on $P_{9,j-1}(t)$ and all intermediate $P_{9,k}(t)$ where $j < k < 9$. The same methodology can be applied to obtain all $P_{i,j}(t)$ probabilities, that assume the bridge deck enters CR $i < 9$ at time $t = 0$. The formulations of other transition probabilities as well as the derivations of the presented formulations are described further in Appendix A.

The transition probabilities calculated in Eq. (8) to (13) can be compiled into one transition matrix $P(t)$ as shown in Eq. (14). Assuming an initial CR vector as shown in Eq. (15), the transition matrix can be used to estimate the probabilities of a deck being at each CR at any given time t , as shown in Eq. (16). Using the RATINGS vector shown in Eq. (17), the average expected CR at time t can be obtained by calculating the product of $CR_{prob}(t)$ and the transpose of the RATINGS vector as shown in Eq. (18). It is worth noting that the last element in the transition matrix is always equal to 1, because we assumed a minimum CR of 3. This essentially makes the last CR an absorbing state (i.e., the deck never transitions out of CR3).

$$P(t) = \begin{bmatrix} P_{9,9}(t) & P_{9,8}(t) & P_{9,7}(t) & P_{9,6}(t) & P_{9,5}(t) & P_{9,4}(t) & P_{9,3\dots}(t) \\ 0 & P_{8,8}(t) & P_{8,7}(t) & P_{8,6}(t) & P_{8,5}(t) & P_{8,4}(t) & P_{8,3\dots}(t) \\ 0 & 0 & P_{7,7}(t) & P_{7,6}(t) & P_{7,5}(t) & P_{7,4}(t) & P_{7,3\dots}(t) \\ 0 & 0 & 0 & P_{6,6}(t) & P_{6,5}(t) & P_{6,4}(t) & P_{6,3\dots}(t) \\ 0 & 0 & 0 & 0 & P_{5,5}(t) & P_{5,4}(t) & P_{5,3\dots}(t) \\ 0 & 0 & 0 & 0 & 0 & P_{4,4}(t) & P_{4,3\dots}(t) \\ 0 & 0 & 0 & 0 & 0 & 0 & 1 \end{bmatrix} \quad (14)$$

$$CR_{initial} = [p_9(0) \quad p_8(0) \quad p_7(0) \quad p_6(0) \quad p_5(0) \quad p_4(0) \quad p_3(0)] \quad (15)$$

$$CR_{prob}(t) = CR_{initial} \times P(t) \quad (16)$$

$$RATINGS = [9 \ 8 \ 7 \ 6 \ 5 \ 4 \ 3] \quad (17)$$

$$CR_{EXPECTED}(t) = CR_{prob}(t) \times RATINGS^T \quad (18)$$

where $CR_{initial}(0)$ is the initial CR vector; $p_i(0)$ is the probability of being at CR i at $t = 0$; $CR_{prob}(t)$ is the vector probabilities of being at each CR at time t ; $CR_{EXPECTED}(t)$ is the average expected CR at time t ; $RATINGS^T$ is the transpose of the ratings definition vector. To summarize, by computing the transition probability matrix and assuming a $CR_{initial}$, a deterioration curve for the predicted CR can be generated.

The calculation process for all remaining transition probabilities $P_{9,8}(t)$ to $P_{9,4}(t)$ are as follows:

$$P_{9,7\dots}(t) = \sum_{a=1}^t f_9(a) \cdot F_8(t - a) \quad (4)$$

$$P_{9,8}(t) = 1 - P_{9,9}(t) - P_{9,7\dots}(t) \quad (5)$$

$$P_{9,6\dots}(t) = \sum_{b=a}^t \sum_{a=1}^t f_9(a) \cdot f_8(b - a) \cdot F_7(t - b) \quad (6)$$

$$P_{9,7}(t) = 1 - P_{9,9}(t) - P_{9,8}(t) - P_{9,6\dots}(t) \quad (7)$$

$$P_{9,5\dots}(t) = \sum_{c=b}^t \sum_{b=a}^t \sum_{a=1}^t f_9(a) \cdot f_8(b - a) \cdot f_7(c - b) \cdot F_6(t - c) \quad (8)$$

$$P_{9,6}(t) = 1 - P_{9,9}(t) - P_{9,8}(t) - P_{9,7}(t) - P_{9,5\dots}(t) \quad (9)$$

$$P_{9,4\dots}(t) = \sum_{d=c}^t \sum_{c=b}^t \sum_{b=a}^t \sum_{x=1}^t f_9(a) \cdot f_8(b - a) \cdot f_7(c - b) \cdot f_6(d - c) \cdot F_5(t - d) \quad (10)$$

$$P_{9,5}(t) = 1 - P_{9,9}(t) - P_{9,8}(t) - P_{9,7}(t) - P_{9,6}(t) - P_{9,4\dots}(t) \quad (11)$$

$$P_{9,3\dots}(t) = \sum_{e=d}^t \sum_{d=c}^t \sum_{c=b}^t \sum_{b=a}^t \sum_{x=1}^t f_9(a) \cdot f_8(b - a) \cdot f_7(c - b) \cdot f_6(d - c) \cdot f_5(e - d) \cdot F_5(t - e) \quad (12)$$

$$P_{9,4}(t) = 1 - P_{9,9}(t) - P_{9,8}(t) - P_{9,7}(t) - P_{9,6}(t) - P_{9,5}(t) - P_{9,3\dots}(t) \quad (13)$$

For more details of the calculation process discussed above please refer to Sobanjo (2011).

3.4.3.3 Deterioration Modeling Results

The estimates of fitted AFT Weibull distribution parameters (i.e., β covariates and p -parameters) obtained from statistical analysis for each CR are shown in Table 43 (Appendix G). LENGTH was the only continuous variable and all other variables had discrete inputs as listed in Table 18. A series of dummy variables were generated for each of the discrete variables and each dummy variable had a baseline value as shown in the shaded headers for each variable in Table 43. Based on the statistical analysis, only the dummy variables that were significant at the chosen significance levels are listed in Table 43. All other dummy variables were not significant and were grouped together with the baseline values during analysis.

The DISTRICT variable was statistically significant for all condition ratings which highlights the effect of location on the deterioration rate of decks. The location of the deck may inherently consider the effect of several other variables such as: 1) traffic variations (urban areas have higher traffic volumes); 2) construction and maintenance practices (quality and standard may vary across districts); and 3) slight changes in climate. In addition, the estimated parameters for the LENGTH coefficients for CR 8 and CR9 were negative, which indicated that the longer a deck is, the shorter the estimated sojourn time. One possible explanation for this could be that an increase in deck length can lead to an increase in maximum deflection which typically leads to higher cracking.

It is worth noting that the Average Daily Truck Traffic (ADTT) was found to have p -values higher than 0.10 for all CRs. This does not necessarily mean that ADTT has no effect on the deterioration rate of decks. Instead, it is possible that other variables are “picking up” the effect of ADTT as a result of endogeneity bias (Ramaswamy and Ben-Akiva 1990). For example, it would be intuitive to say that the traffic volumes for decks on interstates differ from those on non-interstates. Also, ADTT may vary across different districts based on the location of main traffic routes.

3.4.3.4 Interpretation of AFT Weibull Parameter Estimations

The p -parameters for all CRs were larger than 1 which reflects positive duration dependence. These p -parameters were intuitively correct as we would expect the probability of a deck transitioning from its current CR i to a lower CR $i - 1$, would increase the longer the deck spends at CR i . Furthermore, a positive estimated parameter for the exogenous dummy variables results in a decrease in the λ -parameter and an increase in the average expected sojourn time $E(T)$. The interpretation of these parameter estimations will be discussed in this section.

The parameter estimation values vary for each CR, which can be attributed to the nature of deck deterioration, as well as the definition of each CR within the rating system. For example, a CR change for a deck at higher CRs may be mainly controlled by the chemical processes (i.e., chloride penetration and corrosion initiation); whereas for lower ratings, the mechanistic processes (i.e., delamination and spalling) are also incorporated into the rating system. As a result, the

deterioration model predictions for different CRs were expected to vary, as observed in [Table 43](#) (Appendix G). Based on the estimation parameters, the sojourn times for CR 8 and 9 mainly depend on: the length of the deck, the type of rebar protection, single or multi-span, and interstate or non-interstate bridges. The main factors that affected sojourn times for CR7, CR6, CR5, and CR4 were type of span interaction, type of physical makeup including any remediation, and surface wear type. All other variables were statistically insignificant for these sojourn times.

In order to better understand the value of the estimated parameters [Table 43](#) (Appendix G), the ratios of average expected sojourn times were calculated according to the Equation below.

$$\frac{E(T)_2}{E(T)_1} = \frac{\lambda_1}{\lambda_2} = e^{-\beta(x_1-x_2)}$$

If the only difference between $E(T)_1$ and $E(T)_2$ is due to a change in a single dummy variable j , then the ratio of average expected sojourn times simplifies to e^{β_j} for a discrete variable, where β_j is the covariate value for dummy variable j . [Table 44](#) (Appendix G) shows the ratios of average expected sojourn times to the baseline average. The empty cells in this table represent a value of 1.00 which essentially means that the dummy variable's effect is the same as the baseline. [Figure 84](#) illustrates the effect of some of these variables on the average expected sojourn time ratios. The dashed lines in these figures represent the baseline dummy variable.

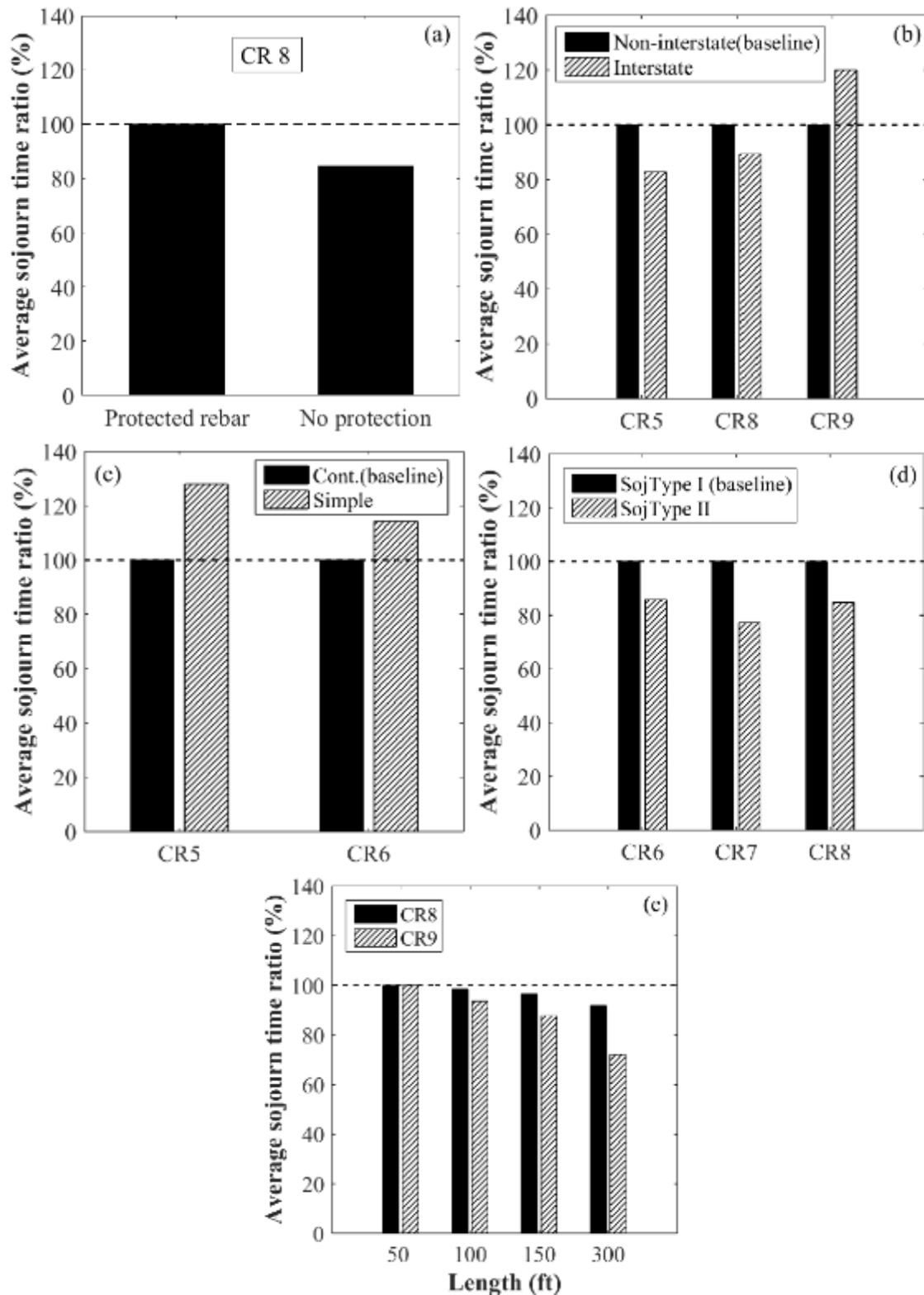


Figure 84. Ratio of average expected sojourn time to the baseline average expected sojourn time based on (a) Whether the rebar is protected or not; (b) Whether the deck is located on an Interstate or Non-interstate; (c) The type of span interaction; (d) Type of sojourn time. Dashed lines on figures represent baseline

Non-interstate decks last 20% and 12% longer at CR5 and CR8 compared to decks on interstate routes, respectively, as shown in Table 44. One possible reason for this could be the effect of higher traffic volumes for interstate routes which leads to faster deterioration rates and shorter sojourn times. On the other hand, interstate decks last 20% longer at CR9 compared to non-interstate decks. This contrast in initial performance might be attributed to the higher quality of construction and design for decks situated on highways compared to those on rural routes. Another reason could be the material behavior of concrete used in decks, as explained in the following paragraph.

Several studies have shown the tensile stresses due to mechanical loading (i.e., traffic loads) of bridges are far smaller than those caused by restrained shrinkage (Schmitt and Darwin 1995, Krauss and Rogalla 1996, Frosch et al. 2003, Hadidi and Saadeghvaziri 2005). The majority of restrained shrinkage occurs at early-ages and thus the majority of shrinkage cracking occurs at early-ages as well. Early-age shrinkage cracking can be mitigated using better construction practices, such as applying proper curing for longer periods of time. In summary, construction quality can have a higher impact on early-age deterioration compared to traffic volumes, which have a more pronounced affect at later ages. The results presented here support this claim regarding decks located on interstate routes compared to those on rural routes.

Bridge decks with protected rebar (e.g., epoxy-coating or galvanized) last about 18% longer at CR8 compared to those without any rebar protection, as shown in Table 44. The transition from CR8 to CR7 depends heavily on corrosion initiation within the deck, which is monitored using electrical potential in deck inspections. The higher the measured electrical potential of a deck, the more likely that corrosion has initiated. The main objective of rebar protection is to offset corrosion initiation. The results presented here support the claim that rebar protection extends the service life of decks compared to those with bare rebar.

Decks with simply supported spans last 28% and 14% longer at CR5 and CR8, respectively, compared to those with continuous spans (Table 44); additionally, the single-span decks last 12% longer at CR7 compared to multi-span decks (Table 44). These differences may be due to the lack of negative moment stresses in simply supported spans which lead to lower surface cracking compared to continuous spans.

Type II sojourn times at CR6, 7, and 8 were 14%, 23% and 15% shorter, respectively, compared to Type I sojourn times as shown in Table 44. The shorter Type II sojourn times can be explained by focusing on the effect of remediation on the deterioration behavior of decks. After applying remediation, a CR jump of 1 or 2 is typically observed. However, the analysis results indicate that the rate of CR-reduction increases after the remediation is applied (i.e., shorter Type II sojourn times). There were two possible reasons for this.

First, the visually observed CR can exaggerate or over-estimate the effectiveness of the remediation due to subjective or inaccurate inspections. The actual improvement in deck performance may not be as high as anticipated for a specific remediation procedure. Second, the accumulated damage due to underlying deterioration processes (such as corrosion and freeze and thaw) is not fully recovered after remediation is applied. Compared to a younger and healthier deck, shorter sojourn times would be expected after remediation for the same CRs without remediation. The results for the effect of surface type on the sojourn time at CR7 also confirm that faster deterioration rates were observed (i.e., shorter duration times) after remediation (overlays) is applied. Studies by Hatami and Morcouc (2012) also found that decks with overlays had faster deterioration rates compared to original monolithic decks.

3.4.3.5 Deterioration Curve Development: Example Case Analysis

To evaluate the stochastic nature of the deterioration problem, an example case will be used to generate deterioration curves and results. The deck specifications used are shown in the list of variable values (Table 20). The average expected sojourn times for each CR were calculated according to Eq. (5) and the results are shown in

Table 21. The sojourn times were calculated using Type I as the SojType in the deterioration model and recalculated for Type II. The two types were equal for CR3, CR4, and CR5 because SojType was not identified as a significant parameter for these CRs. CR9 did not have any Type II. The differences observed between Type I and Type II sojourn times are discussed in detail in the “Effect of Remediation” section. The remainder of this section will only consider an unremediated deck using the corresponding Weibull-fitted parameters for Type I sojourn times for CRs below 8.

Variable	Example case values
DISTRICT	8
INTERACT	Simple
REBARTYPE	Protected rebar
SURFTYPE	No overlay
SPANNUM	Single span
MAINPHYSICAL	Reinforced
NHS	Interstate
LENGTH	100 ft (30.5 m)

Table 21. Average expected sojourn times calculated using Eq. (5) for example case shown in Table 20

CR	Average Expected Sojourn Times (yrs)	
	Type I	Type II
9	-	1.7
8	5.6	4.8
7	8.7	6.7
6	8.0	6.8
5	6.5	6.5
4	1.4	1.4
3	5.6	5.6

The PDF, CDF and survival functions for the example case (Table 20) are shown in Figure 85. CR9 and CR4 have highly concentrated probability distributions. In contrast, the distributions for CR8 to CR5 were significantly spread out which highlighted the stochastic nature of deck deterioration and supported the need for probabilistic as opposed to deterministic modeling for bridge deck deterioration. As a result, average expected values (

Table 21 and Figure 85) should be used with caution in order to avoid inaccurate conclusions regarding the deterioration and remaining service life of bridge decks.

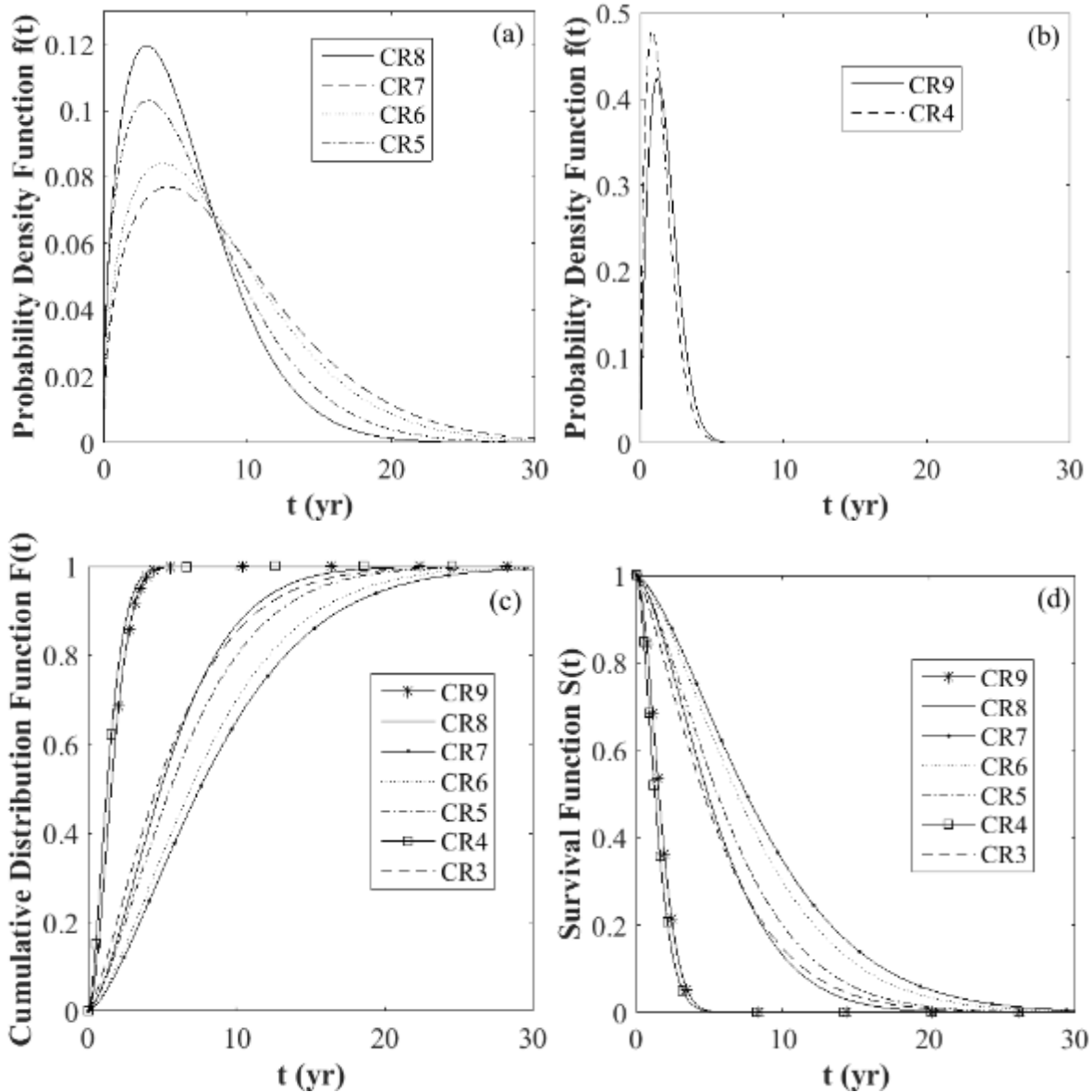


Figure 85. Probability functions for example case define in Table 20 and using Type I sojourn times: a) PDF for CR 8 to CR5; b) PDF for CR9 and CR4; c) CDF for CR9 to CR3; d) survival functions for CR9 to CR3

The hazard rate functions shown in Figure 86 graphically depict the positive duration dependence characteristic. If the Markovian property were valid, these functions would have been constant (indicating duration independence). All the hazard rates in Figure 86 clearly increase with time, however a slower increase rate can be observed for CR7 and lower CRs for longer periods at that CR. In conclusion, the Markovian property does not hold for any of the CR sojourn times for the bridge decks evaluated in this study.

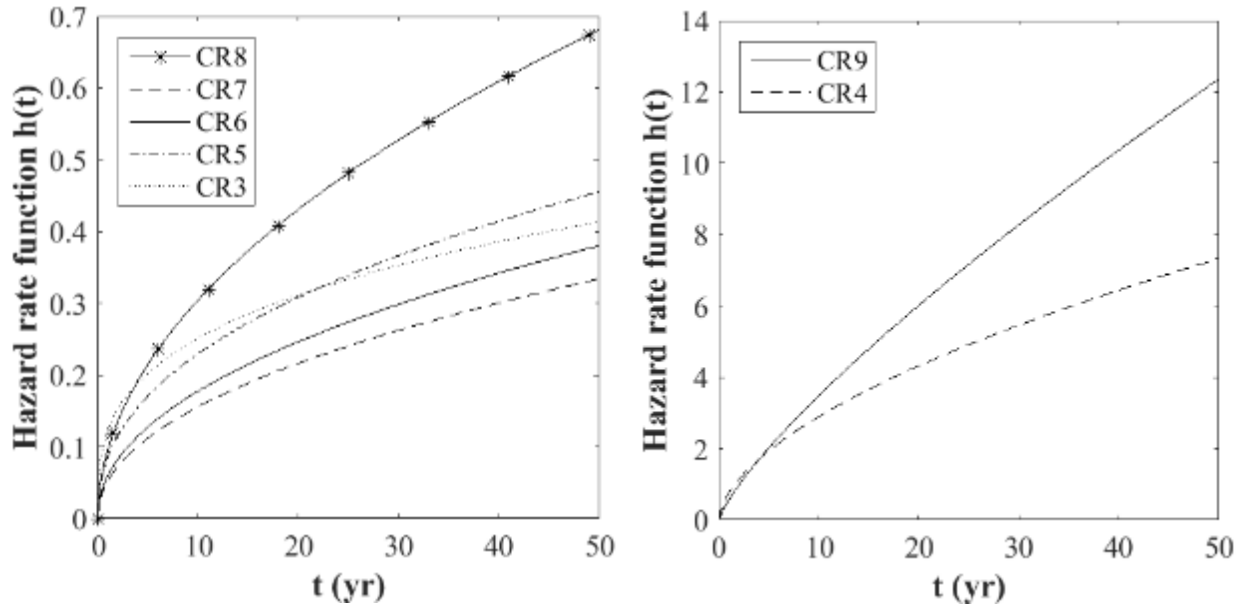


Figure 86. Hazard rate functions for example case as defined in Table 20 and using Type I sojourn times

The transition probabilities $P_{i,j}(t)$ were calculated according to the semi-Markov formulation mentioned in the Methodology section. A time increment of 0.25 years was used to approximate the transition probabilities according to the presented formulation. Once a deck enters CR4, it is typically considered for immediate replacement. As a result, decks reaching CR4 or less were assumed to fail and the corresponding probability of failure is illustrated by $P_{9,4...}$ in transition probability plots (Figure 87 and Figure 88).

Figure 87 illustrates the transition probabilities assuming that a newly constructed deck started at $i = \text{CR9}$. The probability of remaining at CR9 ($P_{9,9}$) quickly decreases within the first few years after construction to almost 0 by the fifth year. Within the same period, the probability of transitioning to and being at CR8 ($P_{9,8}$) rapidly increases and peaks at about 4 years. After 5 years from construction, there is a 67% chance of being at CR8, 30% chance of being at CR7, and only 2% chance of being at CR6. As time progresses, the probabilities for each CR peaks and then decreases. After 30 years of service, there is a 5% chance that the bridge deck will be at CR7, 19% chance for CR6, 25% chance for CR5, and 51% chance of failing (i.e., reaching CR4 or less).

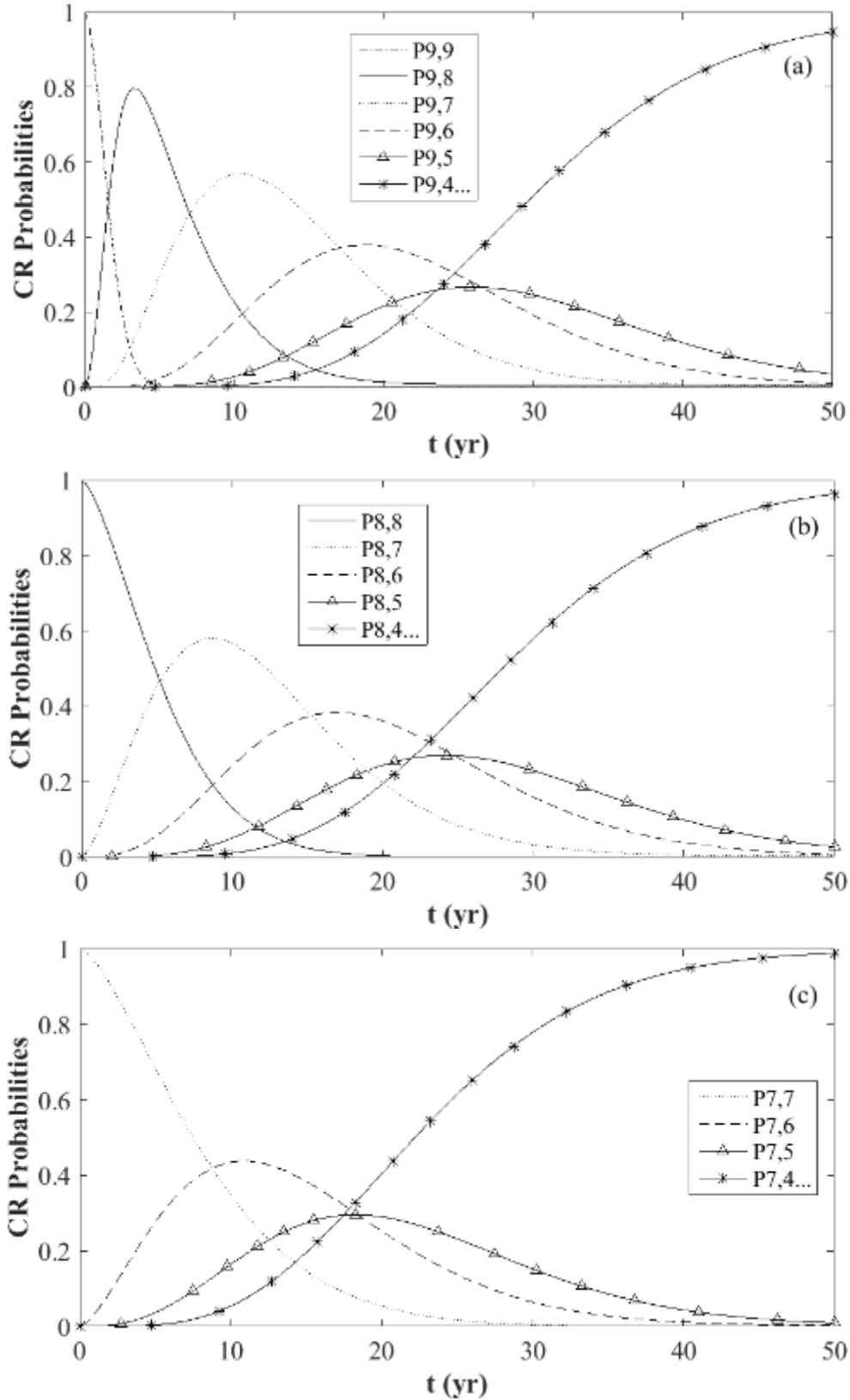


Figure 87. CR probabilities for deck entering (a) CR9, (b)CR8, (c)CR7 at time $t = 0$ for example case as defined in Table 20 and using Type I sojourn times

Figure 87 illustrates the transition probabilities assuming the deck entered CR8 at $t = 0$. The graphical representation of these transition probabilities is similar to those with an initial CR of 9 as shown in Figure 87. However, there were clear differences observed for the transition probabilities when the deck is known to enter CR7 and CR6 at $t = 0$, as shown in Figure 87 and Figure 88. The probabilities of being at CR5 and CR6 become less dispersed (i.e., width of distribution decreases while height increases) from Figure 87a to Figure 87c and Figure 88. A closer look at how these transition probabilities were formulated can explain this phenomenon. For example, if the deck entered CR9 at time $t = 0$ (Figure 87), the probability of being at CR5 depends on the PDFs of CR9, CR8, CR7, CR6, and CR4. Whereas, if the deck entered CR6 at time $t = 0$ (Figure 88), the probability of being at CR5 only depends on the PDF of CR6 and CR4. As a result, higher uncertainties were involved when calculating transition probabilities for the former case.

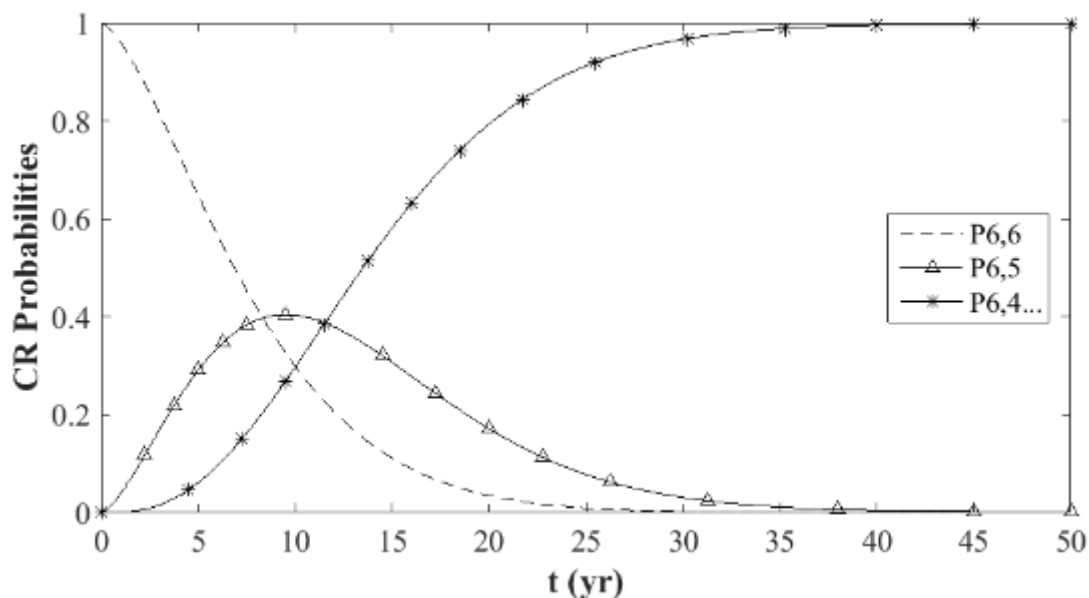


Figure 88. CR probabilities assuming deck entered CR6 at time $t = 0$ for example case as defined in Table 20 and using Type I sojourn times

It is also worth mentioning that the probabilities of the bridge deck being at CR6, CR5, and CR4 or less have very similar values at certain years for each of the figures shown above (approximately around the 25, 24, 18, and 10 year marks for Figure 87 to Figure 88, respectively). This means that the probability of being at any one of CR6, CR5, and CR4 is almost equal for these years and CRs. This highlights the high uncertainty corresponding to the CR estimations for these time periods and is mainly due to the wider distributions of PDFs when moving from CR9 to CR5. The user should exercise care when using the average expected CR deterioration curve when the uncertainty of prediction is so high. Particularly, if the type and cost of remediation/maintenance to be applied significantly varies for each of these CRs which could lead to high inaccuracies when estimating life cycle cost.

The transition probabilities shown in [Figure 87](#) and [Figure 88](#) were used to calculate the expected CR over time according to Eq. (18). A quarter year time interval was used for summation approximation purposes such as those shown in Eq. (9) and (12). The resulting deterioration curves are shown in [Figure 89](#) for various initial CRs without remediation. The dashed horizontal line at CR4 in this figure shows the minimum acceptable level of performance or the failure level. The remediated deterioration curves are also included in this figure and will be explained in the Effect of Remediation section.

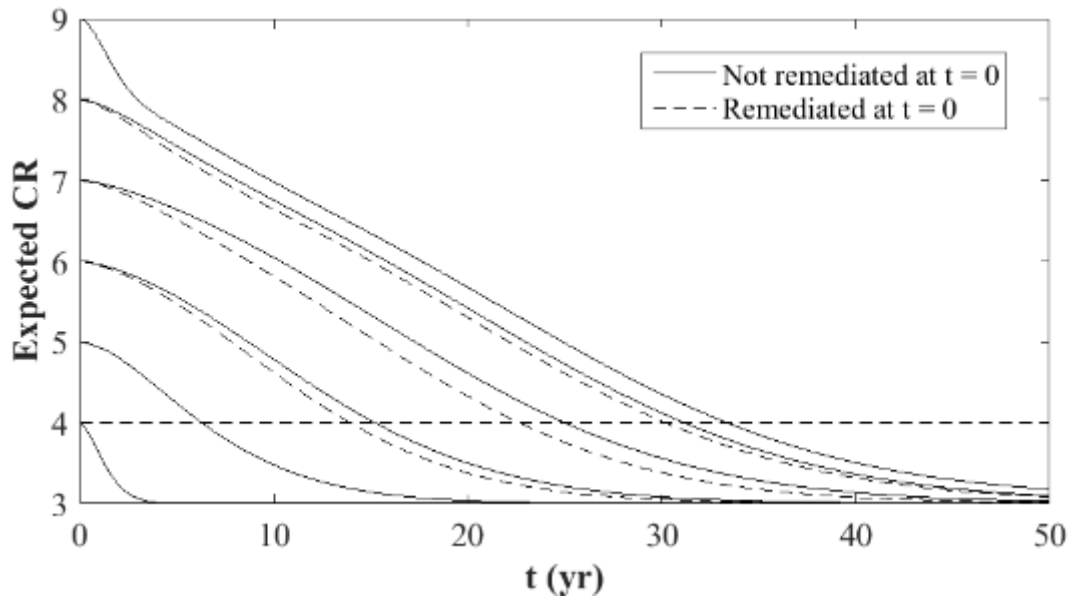


Figure 89. Semi-Markov process deterioration curves for various initial CRs for example case. Dashed horizontal line at CR4 represents minimum acceptable performance

These deterioration curves seem to asymptote at CR3 which is mainly characteristic of the deterioration curve obtained from Markov chain models. The likely reason for this, is that CR3 behaves like a limiting state because it is the lowest considered CR. As a result, the probability of reaching CR3 will never reach 1 and the expected CR will never reach exactly 3 using Eq. (18). In summary, the deterioration curves shown in [Figure 89](#) were reliable for CR predictions from CR9 to CR4, whereas they will be overestimating the amount of time taken to reach CR3 from CR4. In order to expand the prediction capabilities to CR3, the probability distribution of CR2 must also be known. However, it is extremely rare for a deck to be allowed to reach CR2 or CR1 and as a result there is a lack of adequate data for sojourn times can be extracted for CR2. As such, attempting to fit an AFT Weibull distribution to such a small dataset may result in significant errors due to over-fitting of data and was not possible based on the available data in this study.

3.4.3.6 Effect of Remediation

In this section the proposed deterioration model is used to evaluate the effects of remediation on the deterioration curve. In the example case (defined by variable values shown in [Table 20](#)) so far,

the effect of remediation on the deterioration rate was ignored and only Type I sojourn times were used to obtain the unremediated solid-line deterioration curves in Figure 89. In this section, attempts will be made to incorporate the effect of remediation on the deterioration curve by utilizing Type II sojourn times. For this purpose, a hypothetical problem is defined as follows.

Case 1 Remediation Problem Statement: Consider a new deck with the same specifications as the previous example case as listed in Table 20. The initial CR for this deck is CR9 at the time of construction ($t = 0$). It is anticipated that the deck will be remediated once CR6 is reached. For the sake of example, it will be assumed that the scheduled remediation is 80% effective in restoring a deck to a CR7 from a CR6. No further remediation is scheduled for this deck and it is allowed to naturally deteriorate to CR4 before being replaced. The average expected deterioration curve for this deck's service life (i.e., until it reaches CR4) is desired.

First, the effect of remediation on the deterioration rate must be addressed. Considering the definitions of Type I and Type II sojourn times (Figure 83) the following assumptions can be made: 1) The deterioration curve before remediation can be assumed to be the same as the one developed in the previous section (solid line Figure 89) which was based on Type I sojourn times. 2) The deterioration curve after remediation can be developed by utilizing Type II sojourn time distributions only for the first CR immediately after remediation (i.e., CR7 for this example) and Type I sojourn times for all following CRs (i.e., CR 6 to CR4). Table 22 better illustrates the sojourn types that were used to develop the deterioration curves for the unremediated and remediated cases. The Case 1 Remediation starts at CR7, as a result, the CR8 and CR9 distributions were not utilized for Case 1.

Table 22. The sojourn time distribution types (I or II) used to develop each curve shown in Figure 90

CR	Unremediated curve	Case 1: Remediated to CR7	Case 2: Remediated to CR8
9	Type II*	-	-
8	Type I	-	Type II
7	Type I	Type II	Type I
6	Type I	Type I	Type I
5	Type I	Type I	Type I
4	Type I	Type I	Type I
3	Type I	Type I	Type I

*Note: Type I sojourn times do not exist for CR9

By expanding the same concept to decks with different initial CRs at $t = 0$, all deterioration curves for decks that have been remediated at time $t = 0$ can be obtained, as shown by dashed lines in Figure 89. Type II sojourn times were used for the starting CR and Type I for all following CRs in order to develop the remediated dashed curves which are slightly steeper compared to the solid-

line unremediated curve. As a result, the difference between the remediated and unremediated curves was mainly during the starting CR and afterwards, the curves were almost parallel.

Next, the importance of remediation effectiveness (80%) must also be evaluated. One interpretation of this value is that the remediation improved 80% of the deck area to CR7, whereas 20% of the deck remained at CR6 after remediation. This can be easily incorporated into the proposed deterioration model by assuming an initial CR vector as shown in Eq. (19). By multiplying the $CR_{initial}$ by the $RATINGS$ vector (Eq. (17)) the initial CR for the deck after remediation is estimated at 6.8.

$$CR_{initial} = [0 \quad 0 \quad 0.8 \quad 0.2 \quad 0 \quad 0 \quad 0] \quad (19)$$

Finally, the remediated transition matrix (Eq. (14)) must be compiled using the Type II transition probabilities for CR7 and Type I transition probabilities for all other CRs. Using the remediated transition matrix and initial CR vector, the deterioration curve can be generated for the deck after it has remediated back to a CR7. By combining the deterioration curves before (solid-line starting at CR9 in Figure 89) and after remediation (similar to dashed line starting at CR7 in Figure 89), the Case 1 Remediation curve is obtained, as shown in Figure 90.

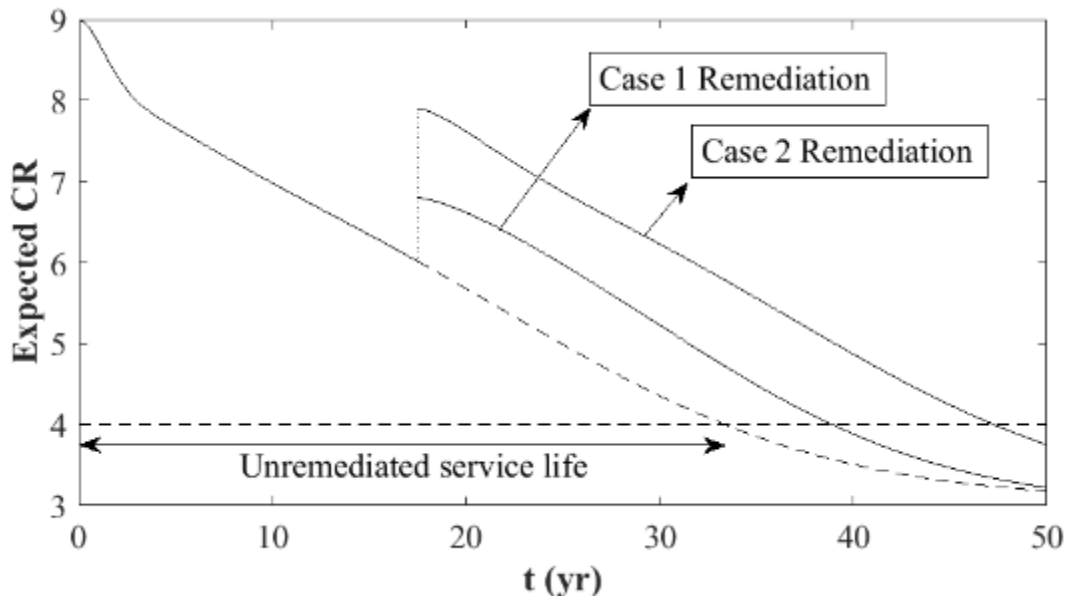


Figure 90. Deterioration curve for example deck with case 1 and 2 remediation

The Case 2 Remediation in Figure 90 shows another scenario where the remediation occurs at CR6 again, but this time the deck performance increases to a CR8 with an effectiveness of 95%. The initial CR vector for this case, shown in Eq. (20), indicates that 95% of the deck successfully increased to CR8 whereas 5% remained at CR6. Similar to the previous case, a remediated deterioration curve is obtained by using Type II sojourn times for CR8 and Type I for all other CRs, as shown in Table 22 for Case 2 Remediation. The Case 2 remediation starts at CR8, as such the CR9 distribution was not utilized for Case 2.

$$CR_{initial} = [0 \quad 0.95 \quad 0 \quad 0.05 \quad 0 \quad 0 \quad 0] \quad (20)$$

The overall service life (time from CR9 to CR4) for the unremediated case was approximately 33.2 years. The case 1 and case 2 remediation resulted in an increase of approximately 5.5 and 14 years, respectively, compared to the unremediated case. These results illustrate the potential effect of remediation on extending the service life of bridge decks. Actual deterioration rates after remediation were obtained from in-service performance data, however, the actual increase in performance due to the remediation will depend on the effectiveness of the specific type of remediation that is being applied. Very limited maintenance/remediation records for the 22,000 evaluated bridges were available to the authors at the time of analysis, as a result, hypothetical values were used to represent increase in condition rating. Further research is required to quantify the actual increase in performance (condition rating) corresponding to each type of remediation in order to further improve the prediction accuracy of the proposed model.

3.4.3.7 PSU Bridge Deck Life software (Deterioration Modeling Software)

The Weibull distribution parameters for each condition rating were implemented into a functioning excel deterioration model called PSU Bridge Deck Life. The user can select the input for each variable available in the user input page and view the expected condition rating prediction over time and probability of reaching a CR 4 (end of service life).

CHAPTER 4 (TASK 4)

Best Practice Decision Methodology, Matrix, and Guideline

4.1 Introduction

Life-Cycle Cost Analysis (LCCA) was utilized to generate tables and graphs for comparing alternative bridge deck treatments and their sequences. Agency costs were evaluated in the analysis. Treatment types, their cost, and their expected service life were obtained from the “rehabilitation guide” spreadsheet provided by PennDOT. The spreadsheet includes categorized service life and cost information based on the age of bridge decks and deck inspection rating. This information was used in the Federal Highway Administration’s (FHWA) Real Cost life cycle cost analysis program to compare alternative treatment scenarios over a defined analysis period of 50 years. A one hundred analysis period year scenario was also considered.

4.2 Remediation Treatments (2013 Baseline Costs per ECMS)

Bridge deck remediation treatments that were evaluated in this study include:

- Epoxy Based Surface Treatment (base cost of \$60/SY)
- Latex Modified Concrete or LMC (base cost of \$80/SY)
- Waterproofing Membrane & Bituminous Overlay (base cost of \$50/SY)

The PSU team has only limited qualitative information on Methyl Methacrylate (MMA) sealers and no real in-service data or cost data, so this was not included in the investigation.

Two separate age categories are defined based on Business Plan Network (BPN) highway classifications used by PennDOT. The BPN classifications are 1=interstate, 2=NHS non-interstate, 3=non-NHS >2000 ADT, and 4=non-NHS ADT<2000.

The age categories for BPN 1 and 2 are:

- Less than 15 years
- 15 to 30 years
- Over 30 years

For BPN 3 and 4, the age categories are:

- Less than 15 years
- 15 to 40 years
- Over 40 years

Remediation treatments were considered for deck condition levels 7, 6, 5, and 4. Design Manual Part 4 Volume 1 (5.6.4) should be consulted for specific information regarding remediation for bridge decks with a rating of 4 and also for deck replacement recommendations.

4.3 Software

The FHWA RealCost software was used for the LCCA. The analysis period was 50 years with a discount rate of 4%. The cost is represented in different forms, but the method of interest is the “present value” (PV) which carries initial and future dollar costs to a single point in time; the present. Another LCCA form of interest for transportation projects is the equivalent uniform annual cost (EUAC), which represents the investment on the basis of an annual investment.

The analysis includes calculating the remaining service life (RSL) if the alternatives have service lives that exceed the analysis period. The value of RSL is calculated based on project cost and the percentage of design life remaining at the end of the analysis period and is the prorated share of the last rehabilitation cost.

4.4 Treatment Matrix

Different treatments and treatment sequences were considered for each age group and deck rating. The broad age groups (e.g., <15 yrs, 15-30 yrs, and >30 yrs for BPN 1 and 2) in the Design Manual Part 4 Volume 1 (5.6.4) “rehabilitation guide” ([Table 23](#)) were further broken down into five-year intervals for the analysis since the treatment sequences vary based on the deck age within each of the three age categories. [Table 23](#) and

Table 24 show the recommended treatments based on deck age and deck rating for BPN 1&2 and BPN 3&4, respectively. The following notes accompany Tables 22 and 23, which were provided by PennDOT, with the yellow highlighted recommended treatments added based on lowest LCCA cost:

- (1) Refer to Figures 5.6.4.3.2-1 & 5.6.4.3.2-2 for Concrete Deck Overlay Decision Trees, based on Business Plan Network
- (2) For deck rating of 9 "no action" is recommended, for deck rating of 8 either "no action" or apply epoxy based surface treatment
- (3) Add penetrating sealer if surface cracks in deck (shallow map cracking) due to improper finishing or severe cracking in LMC overlays, expect ~3-years service life
- (4) For deck rating of ≤ 3 full deck replacement is recommended, for deck rating of 4 use section DM-4 Remediation Guideline / Deck Replacement Section 5.5.2.3
- (5) Use Type II and Type III patching as required
- (6) Unit costs do not include traffic control and road user delay costs which may significantly affect unit costs, these additional costs should be included to determine actual construction and service life costs.

It should be mentioned that section D5.6.4.2 of the Design Manual Part 4 calls for Types II and III patching in conjunction with other treatments where required. It has been assumed that the amount of patching remains the same regardless of the treatment sequence, and since it has the same effect on all alternatives, it can be omitted from the calculations in accordance with LCCA method.

The deck rating changes as deck remediation treatments are executed and also as the deck ages. Three scenarios for the change in deck rating were investigated:

- In the first scenario, deck ratings are assumed to increase immediately after any given remediation but decrease by one unit at the end of each remediation's service life.
- In the second scenario, deck ratings are assumed to increase immediately after any given remediation, but decrease by one unit relative to the previous deck rating at the end of its remediation service life.
- The third scenario assumes that deck ratings increase immediately after any given remediation but decrease over the service life of the remediation method according to a deck deterioration model based on data collected in earlier project tasks.

With this approach, different treatments and sequences can be compared with each other for each age and deck rating. These three scenarios were developed, and the third scenario, based on bridge deck deterioration rates determined in Task 3, was selected for further development.

Table 23. Recommended treatments based on deck age and deck rating for BPN 1 and 2

BPN 1 & 2														
Deck Age -->			< 15 Years				15 - 30 Years				> 30-Years			
Current Deck Rating -->			7	6	5	4	7	6	5	4	7	6	5	4
Remediation Category	Base cost/SY (2012 dollars)	Remediation Service Life Metric	Yellow highlighted options are recommended				Yellow highlighted options are recommended				Yellow highlighted options are recommended			
Epoxy Based Surface Treatment	\$60	Service Life, Yrs.	10	8			10	8		Note-4	10	8		Note-4
		\$/SY/YR	\$6.00	\$7.50			\$6.00	\$7.50			\$6.00	\$7.50		
Waterproofing Membrane & Bituminous Overlay	\$50	Service Life, Yrs.		15	15			15	15	Note-4		15	15	Note-4
		\$/SY/YR		\$3.33	\$3.33			\$3.33	\$3.33			\$3.33	\$3.33	
Latex Modified Concrete	\$80	Service Life, Yrs.	25	20	15	10	25	20	15	Note-4	25	20	15	Note-4
		\$/SY/YR	\$3.20	\$4.00	\$5.33	\$8.00	\$3.20	\$4.00	\$5.33		\$3.20	\$4.00	\$5.33	
Type II Patching			X	X	X	X	X	X	X	X	X	X	X	X
Type III Patching					X	X			X	X			X	X

Table 24. Recommended treatments based on deck age and deck rating for BPN 3 and 4

BPN 3 & 4														
Deck Age -->			< 15 Years				15 - 40 Years				> 40-Years			
Current Deck Rating -->			7	6	5	4	7	6	5	4	7	6	5	4
Remediation Category	Base cost/SY (2012 dollars)	Remediation Service Life Metric	Yellow highlighted options are recommended				Yellow highlighted options are recommended				Yellow highlighted options are recommended			
Epoxy Based Surface Treatment	\$60	Service Life, Yrs.	10	8			10	8		Note-4	10	8		Note-4
		\$/SY/YR	\$6.00	\$7.50			\$6.00	\$7.50			\$6.00	\$7.50		
Waterproofing Membrane & Bituminous Overlay	\$50	Service Life, Yrs.		20	20			20	20	Note-4		20	20	Note-4
		\$/SY/YR		\$2.50	\$2.50			\$2.50	\$2.50			\$2.50	\$2.50	
Latex Modified Concrete	\$80	Service Life, Yrs.	25	20	15	10	25	20	15	Note-4	25	20	15	Note-4
		\$/SY/YR	\$3.20	\$4.00	\$5.33	\$8.00	\$3.20	\$4.00	\$5.33		\$3.20	\$4.00	\$5.33	
Type II Patching			X	X	X	X	X	X	X	X	X	X	X	X
Type III Patching					X	X			X	X			X	X

4.4.1 The Selected Scenario Based on the Bridge Deck Deterioration Model

In this scenario, deck ratings increase immediately after any given remediation but decrease over the service life of the remediation method. The initial increase in deck rating and the reduction in deck rating at the end of each remediation's service life were extracted from a deterioration model based on results of the bridge deck surveys and bridge deck database analyses carried out in Task 3.

Table 25 shows deck condition ratings and the average time that a bridge deck remains at specific deck ratings according to Task 3 results.

Table 25. Average time at specific deck condition ratings for remediated and unremediated decks

BPN 1&2		
Rating Transition	Avg. Duration (Years) Unremediated at start of transition period	Avg. Duration (Years) Remediated at start of transition period
4 to 3	3.7	3.7
5 to 4	5.0	7.9
6 to 5	7.3	5.8
7 to 6	7.5	4.9
8 to 7	4.1	3.9
9 to 8	2.0	2.0
BPN 3&4		
Rating Transition	Avg. Duration (Years) Unremediated at start of transition period	Avg. Duration (Years) Remediated at start of transition period
3 to 2	3.5	3.5
4 to 3	6.2	7.4
5 to 4	7.8	6.8
6 to 5	7.3	6.0
7 to 6	8.0	5.7
8 to 7	6.4	4.8
9 to 8	2.0	2.0

The remediated column values should only be used for the rating duration immediately after remediation. Once remediation is applied and after the deck drops by 1 rating level, one should revert back to the "Unremediated" values. For example, if a deck is at a 5 and is remediated to a 7, the transition duration for 7 to 6 should be taken from the remediated column, but the subsequent transitions (6 to 5, 5 to 4, 4 to 3) should be taken from the unremediated columns. This approach

was selected to consider the effect of the remediation treatment and the ongoing deterioration of the deck.

Service lives for the remediation treatments are presented in [Table 23](#) and

Table 24. By considering each treatment’s service life and the deck rating at the time of treatment, changes in ratings –the immediate increase after application of treatments and the reduction during the service live– at the end of each treatment’s life were approximated. These approximate reductions are presented in [Table 26](#).

The PennDOT team informed the research team that for bridge decks 30 years or older and with deck ratings of 6 or 5, the best remediation option is to use waterproofing membrane and bituminous overlay and this was considered in the analysis.

Table 26. Changes in deck ratings

BPN 1&2			
Rating before remediation	Treatment (approximate service life in years)	Rating immediately after treatment	Expected rating at end of service life (rounded to nearest rating)
7	Epoxy (10)	8	6
	LMC (25)	8	4
6	Epoxy (8)	7	6
	LMC (20)	8	5
	Bituminous (15)	8	5
5	LMC (15)	7	5
	Bituminous (15)	7	5
4	LMC (10)	6	4
BPN 3&4			
Rating before remediation	Treatment (approximate service life in years)	Rating immediately after treatment	Expected rating at end of service life (rounded to nearest rating)
7	Epoxy (10)	8	6
	LMC (25)	8	4
6	Epoxy (8)	7	6
	LMC (20)	8	5
	Bituminous (20)	8	5
5	LMC (15)	7	5
	Bituminous (20)	7	5
4	LMC (10)	6	4

The PennDOT team also informed the research team that when a deck rating becomes 4, on average, 6 years pass before the deck is replaced and this was included in the analysis.

Different treatments and sequences were considered for the LCCA and the results can be compared with each other in order to select the most appropriate treatment type and sequence. They are discussed in the following sections.

4.4.2 Treatments for New Bridge Decks

According to [Table 25](#), a bridge deck with rating of 9 will become a 7 in 5.9 and 6.8 years for BPN 1&2 and BPN 3&4, respectively. The PennDOT experience approximates this time to 5 years. Therefore, examining a bridge deck with deck age of 5 years at different ratings (7, 6, 5, and 4) seems appropriate. The concept of preservation as illustrated in [Figure 91](#) by the FHWA calls for application of treatments at more frequent intervals (compared to major rehabilitation for structural damage) for extending the service life and a better investment. The same concept can be applied to bridge decks as well.

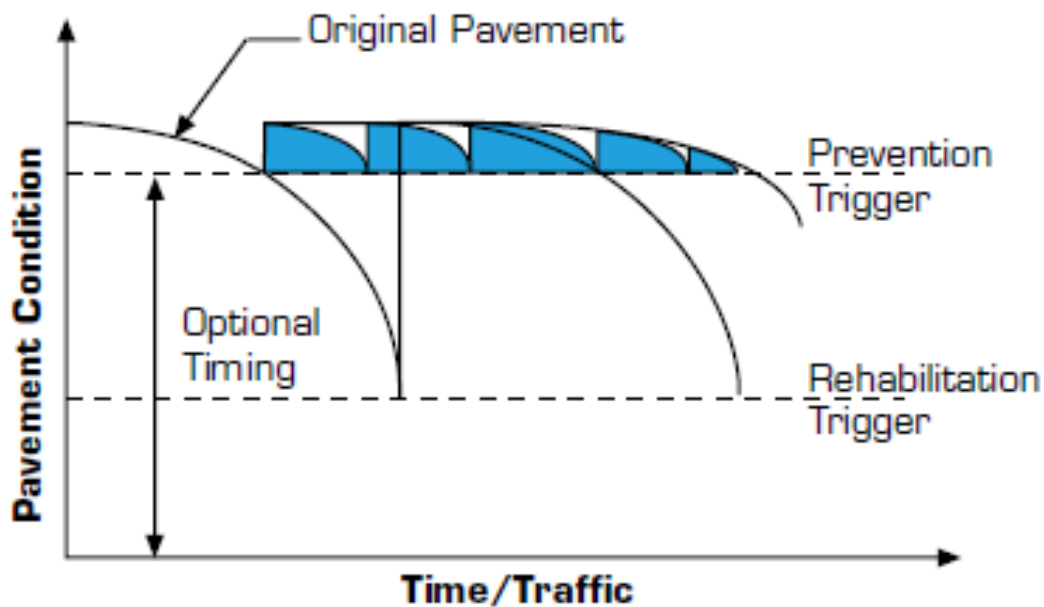


Figure 91. Extending the Useful Life of Pavement (Optimizing Highway Performance: Pavement Preservation, Federal Highway Administration, <http://www.fhwa.dot.gov/construction/fs00013.pdf>)
Note that the effect of preservation illustrated delays, but does not replace rehabilitation.

[Figure 92](#) shows treatment sequences for a BPN 1&2 bridge with deck age of 5 years along with the associated life cycle costs. In this figure, E stands for “Epoxy Based Surface Treatment,” L stands for “Latex Modified Concrete,” and B stands for “Waterproofing Membrane and Bituminous Overlay.”

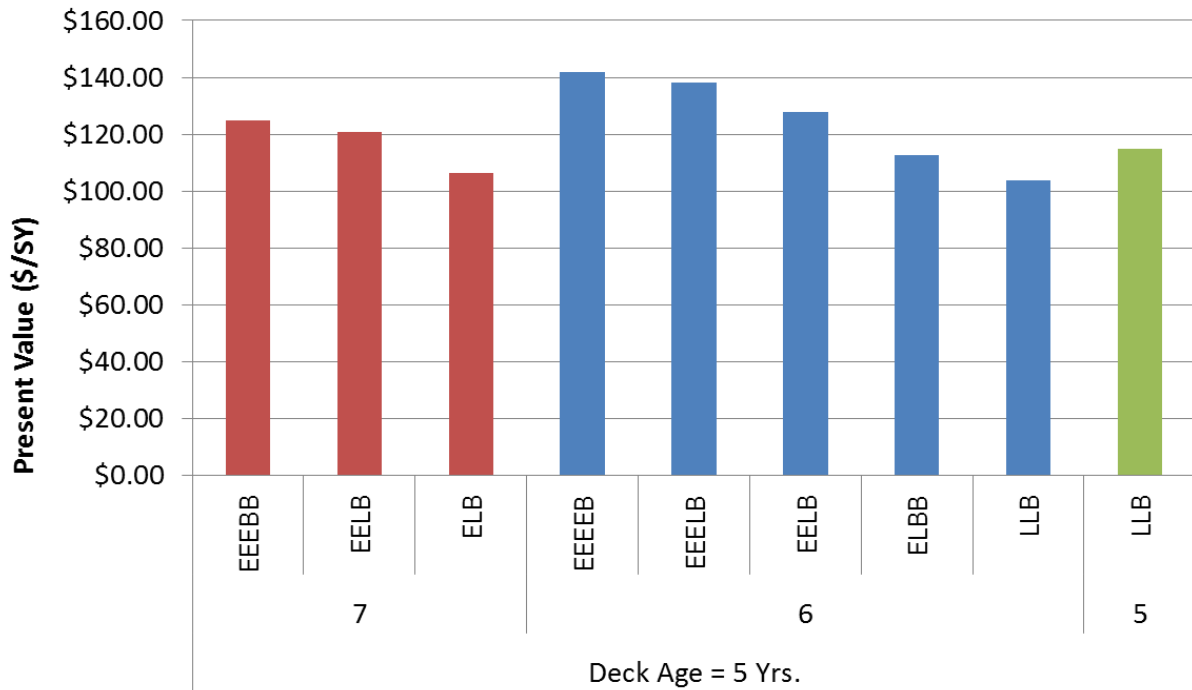


Figure 92. Treatment Sequences and Life Cycle Costs for a BPN 1&2 Bridge with Deck Age of 5 Years

It can be observed that using longer lasting treatments is the most cost-effective option followed by using a combination of the longer lasting treatments and other treatments where applicable. However, when combining two different treatments to preserve a deck, their sequence governs the life cycle cost and if the longer lasting treatments are used sooner, the cost is less than when they are used later in the sequence. These observations are consistent with the philosophy of preventive treatments.

Table 27 shows details of the treatments, their service lives and the sequences for a bridge in BPN 1&2 category.

Table 27. Remediation Guideline at deck age of 5 years (BPN 1&2)

Deck Age (Yrs)	Deck Rating Before Treatment	1st Treatment			Deck Rating Before Treatment	2nd Treatment			Deck Rating Before Treatment	3rd Treatment			Deck Rating Before Treatment	4th Treatment			Deck Rating Before Treatment	5th Treatment			Present Value (\$/SY)
		Treatment (Service Life, Yrs)	Deck Rating After Treatment	Deck Age (Yrs)		Treatment (Service Life, Yrs)	Deck Rating After Treatment	Deck Age (Yrs)		Treatment (Service Life, Yrs)	Deck Rating After Treatment	Deck Age (Yrs)		Treatment (Service Life, Yrs)	Deck Rating After Treatment	Deck Age (Yrs)		Treatment (Service Life, Yrs)	Deck Rating After Treatment	Deck Age (Yrs)	
5	7	EP (10)	8	15	6	EP (8)	7	23	6	EP (8)	7	31	6	WB (15)	8	46	5	WB (15)	7	61	\$124.87
5	7	EP (10)	8	15	6	EP (8)	7	23	6	LMC (20)	8	43	5	WB (15)	7	58					\$120.60
5	7	EP (10)	8	15	6	LMC (20)	8	35	5	WB (15)	7	50									\$106.41
5	7	LMC (25)	8	30	4	6 years b	N/A	34	3	Full Deck Replacement											N/A
5	6	EP (8)	7	13	6	EP (8)	7	21	6	EP (8)	7	29	6	EP (8)	7	37	6	WB (15)	8	52	\$141.70
5	6	EP (8)	7	13	6	EP (8)	7	21	6	EP (8)	7	29	6	LMC (20)	8	49	5	WB (15)	7	64	\$138.08
5	6	EP (8)	7	13	6	EP (8)	7	21	6	LMC (20)	8	41	5	WB (15)	7	56					\$127.66
5	6	EP (8)	7	13	6	LMC (20)	8	33	5	WB (15)	7	48	5	WB (15)	7	63					\$112.58
5	6	LMC (20)	8	25	5	LMC (15)	7	40	5	WB (15)	7	55									\$103.83
5	5	LMC (15)	7	20	5	LMC (15)	7	35	5	WB (15)	7	50									\$114.94
5	4	LMC (10)	6	15	4	6 years b	N/A	21	3	Full Deck Replacement											N/A

4.4.2.1 Cells with N/A in the “Present Value” Column

It should be mentioned that in the context of this investigation, LCCA cannot be performed for treatment sequences that do not extend the deck life to 50 years (two instances in [Table 27](#)) without appropriately redefining the analysis period. In these two cases, deck ages at rating of 4 are 30 and 15 years, respectively. After the 6-year period before the next remediation is applied, the ages will be 36 and 21 years, respectively. Therefore, LCCA cannot be performed for the full 50 year analysis period for these cases. Analysis could be performed for an analysis period of 21 years, including using salvage life for the 36 year case.

Another approach is to assess the LCCA for these cases, using different scenarios that include “deck replacement” and that extend the deck service life well beyond 50 years. A single analysis time (e.g., 100 years) should be selected and potential remediation treatments after deck replacement should be included in the analysis. This process will produce a large matrix by itself, so it is recommended that this be done for individual cases for which the district pavement managers have a narrowed-down list of treatments to be included in the LCCA.

4.4.3 Treatments for Bridge Decks with Varying Ages and Deck Condition Ratings

Similar to what is shown in [Figure 92](#) and [Table 27](#), the LCCA was carried out for a matrix of different deck ages and condition ratings. The results are presented in graph and table formats in the appendix. The appendix is in the form of an Excel file accompanying this report. Examples in this section will demonstrate methods to employ the data in the appendix in assessing treatment options for bridge decks.

The presented graphs and tables can be referenced in order to compare different alternatives for treatment sequences. The tables present detailed information such as deck age at the time of remediation, treatment service lives, changes in the deck rating for each alternative, and cost.

If the goal is to compare different alternatives for a deck with known age and rating, the following procedure can be employed. For each age category (i.e., age of the deck at the time of remediation) and deck rating at the time of remediation, different alternatives (treatment sequences) are presented along with the present value for each alternative’s cost per square yard. Generally, the alternative with the lowest present value is the preferred one, although factors other than cost (practicality, availability, logistics, incorporation with other planned work, available funding, etc.) must be considered. This may result in another alternative being the best alternative. An example can be found in the previous section for the case of a deck age of 5 years and deck rating of 7 (BPN 1&2). In this case, there are several treatment sequences as shown below.

Deck Age	Deck Condition Rating	Treatment Sequence	Present Value (\$/SY)
5 Years	7	EEEEBB	\$124.87
		EELB	\$120.60
		ELB	\$106.41

Figure 93 shows the expenditure stream for the three alternatives for the undiscounted sum values. The lowest present value cost is for a treatment sequence of epoxy overlay, followed by a LMC overlay and a waterproofing membrane and bituminous overlay application.

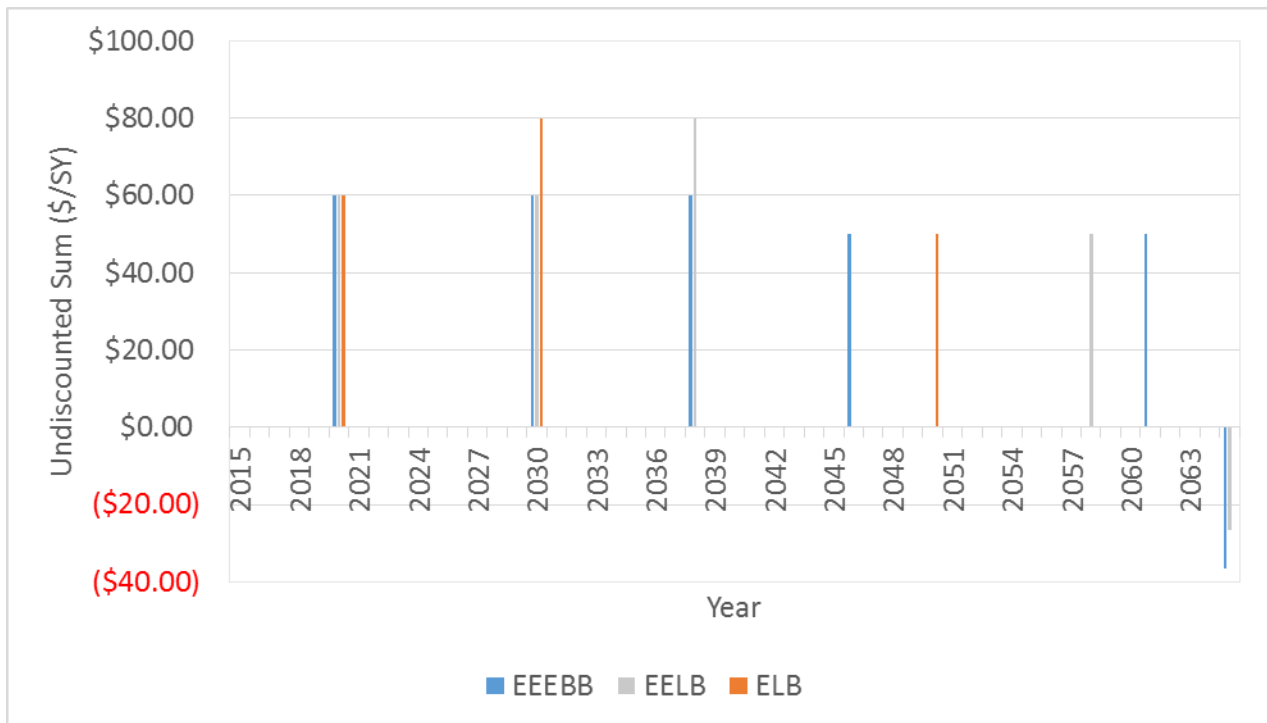


Figure 93. Expenditure Stream for the Three Alternatives

If the goal is to compare alternatives for different deck ages and ratings, the following procedure can be used. This is a case in which deck age and rating are known for a particular bridge, and the goal is to see how much the cost will be if remediation is performed at a later date (which results in a decreased rating). To do this, the alternatives (and their costs) for the particular bridge with known deck age and rating can be extracted from the tables (presented in the appendices) and the present values can be compared with those of the alternatives for the estimated future deck age and rating.

Regarding the cells with N/A in the “Present Value” column, the same discussion at the end of the previous section (4.2.1) is valid and should be followed.

An example of such analysis is presented in this section. For this example, approximate times for transitions between unremediated deck ratings were extracted from [Table 25](#). The “bridge deck deterioration model” can be used to predict these times more accurately.

4.4.3.1 An example:

For a bridge with deck age of 10 and condition rating of 7 (BPN 1&2), the following treatment alternatives are available:

Deck Age	Deck Condition Rating	Treatment Sequence	Present Value (\$/SY)
10 Years	7	EEEB	\$99.64
		EELB	\$96.11
		ELB	\$85.11

The alternative with lowest present value is epoxy overlay followed by an LMC application and a waterproofing membrane and bituminous overlay. If it is desired to wait for 5 years and to look at the treatment alternatives for the same deck at the age of 15 years, [Table 25](#) is examined. It can be seen that the rating of 7 does not change after 5 years, so the same treatment alternatives will be recommended.

If investigating the alternatives after 5 more years is desired, [Table 25](#) shows that the deck rating will drop to 6 and the following alternatives are recommended:

Deck Age	Deck Condition Rating	Treatment Sequence	Present Value (\$/SY)
20 Years	6	EEB	\$59.11
		ELB	\$55.57
		LB	\$44.58

The alternative with the lowest present value is LMC overlay followed by a waterproofing membrane and bituminous overlay application.

If waiting for 5 more years is of interest, the same process can be followed. The following is the only alternative for a deck age of 25 years and rating of 5 which is the same as the previous case, but the present value is different due to timing of the remediation application:

Deck Age	Deck Condition Rating	Treatment Sequence	Present Value (\$/SY)
25 Years	5	LB	\$38.08

Similar types of analyses can be performed for different deck age and condition rating scenarios. If deck ages between the 5-year intervals (in the appendix tables) are to be investigated, the closest age in the tables/graphs can be considered. If the exact ages are to be investigated, LCCA using FHWA's RealCost is recommended for individual cases.

4.4.4 Example of a 100-Year Analysis

In keeping with PennDOT's philosophy of 100 year bridge life, the following example of 100-year analysis was developed. In this example, the initial deck rating is 7 at deck age of 5 years. The base cost of removing and replacing the deck (Deck R&R) is \$1,450/SY.

For this example, a treatment sequence of epoxy (10 yrs.), LMC (20 yrs.), and waterproofing membrane & bituminous overlay (15 yrs.) is considered. It was assumed that the deck has to be removed and replaced after 50 years. The deck rating is assumed to become 9 immediately after the deck replacement and to be 7 after 13 years (according to the deck deterioration model). If the same treatment sequence will be applied to the deck, the present value will be \$320.85 per square yard.

Error! Reference source not found. shows details about this example. For this example, it was assumed that the deck was replaced as shown in treatment 4 of the table. Subsequent deck rehabilitation of the replaced deck enabled the scenario to reach the 100 year analysis period desired. These assumptions were made to illustrate the application of the LCCA to a 100 year analysis period. Other scenarios could be considered for this analysis period, and results compared as a planning tool. However, it is always unlikely that the exact assumed scenario will be carried out during the life of any specific bridge.

Table 28. Example of a 100-Year Analysis

	Deck Age (Yrs)	5
	Deck Rating Before Treatment	7
1st Treatment	Treatment (Service Life, Yrs.)	E (10)
	Deck Rating After treatment	8
	Deck Age (Yrs)	15
	Deck Rating Before Treatment	6
2nd Treatment	Treatment (Service Life)	L (20)
	Deck Rating After treatment	8
	Deck Age (Yrs)	35
	Deck Rating Before Treatment	5
3rd Treatment	Treatment (Service Life)	B (15)
	Deck Rating After treatment	7
	Deck Age (Yrs)	50
	Deck Rating Before Treatment	N/A
4th Treatment	Treatment	R&R
	Deck Rating After treatment	9
	Deck Age (Yrs)	63
	Deck Rating Before Treatment	7
5th Treatment	Treatment (Service Life)	R&R
	Deck Rating After treatment	9
	Deck Age (Yrs)	63
	Deck Rating Before Treatment	7
6th Treatment	Treatment (Service Life, Yrs.)	E (10)
	Deck Rating After treatment	8
	Deck Age (Yrs)	73
	Deck Rating Before Treatment	6
7th Treatment	Treatment (Service Life)	L (20)
	Deck Rating After treatment	8
	Deck Age (Yrs)	93
	Deck Rating Before Treatment	5
8th Treatment	Treatment (Service Life)	B (15)
	Deck Rating After treatment	7
	Deck Age (Yrs)	108
Cost	Present Value (\$/SY)	\$320.85

4.4.5 Benefit of Starting Remediation Later in the Deck's Life

The following table (Table 29) illustrates the benefit of starting remediation later in the deck's life, such as 15 or 25 years instead of 5 years. By examining the present values for bridge decks with

the same rating and different ages, it can be observed that the longer a bridge deck is maintained at (or extended to) an 8 or 9 rating, the remediation cost-effectiveness increases.

Table 29. Benefit of Starting Remediation Later in the Deck’s Life

Deck Age	Rating	1st Treatment			Rating Before 2nd Treatment	2nd Treatment			Rating Before 3rd Treatment	3rd Treatment			Present Value (\$/SY)
		Service Life	New Rating	Deck Age		Service Life	New Rating	Deck Age		Service Life	New Rating	Deck Age	
5	7	E(10)	8	15	6	L(20)	8	35	5	B(15)	7	50	\$106.41
5	6	L(20)	8	25	5	L(15)	7	40	5	B(15)	7	55	\$103.83
5	5	L(15)	7	20	5	L(15)	7	35	5	B(15)	7	50	\$114.94
15	7	E(10)	8	25	6	L(20)	8	45	5	B(15)	7	60	\$67.19
15	6	L(20)	8	35	5	B(15)	7	50					\$57.09
15	5	L(15)	7	30	5	B(15)	6	45	5	B(15)	7	60	\$72.96
25	7	L(25)	8	50									\$30.01
25	6	L(20)	8	45	5	B(15)	7	60					\$33.88
25	5	L(15)	7	40	5	B(15)	7	55					\$38.08

E=Epoxy, L=LMC, B=Waterproofing Membrane and Bituminous Overlay

This may be achieved either by reducing deck cracking or by performing remediation at a rating before the initiation of corrosion for epoxy coated bars.

4.5 A brief Overview of the LCCA Method and FHWA’s RealCost

Life Cycle Cost Analysis is a valid tool for comparing alternatives over a defined analysis period. This technique provides decision makers with improved insight into long term budget management strategies for maintaining infrastructure assets. A variety of alternative asset management strategies or optional treatments can be compared to determine the relative cost either excluding or including user costs. The cost of alternatives is compared over the defined analysis period on the basis of present value, or equivalent uniform annual costs.

Performing a life cycle cost analysis requires the determination of several important input factors including:

- Determination of an appropriate analysis period
- Identification of an appropriate discount rate (discount rate is the difference between interest rate and inflation)
- Determination of estimated performance life for various alternatives
- Estimated costs for the various treatments included in the analysis during the analysis period

The analysis period is typically selected to reflect the number of years for which asset performance is expected, and for which competing alternatives can be effectively compared. For the bridge deck remediation analysis work carried out, an analysis period of 50 years has been identified as the most reasonable starting point.

Historically, a discount rate of 4% has been found to be a reasonable value for government assets. With the recent drop in interest rates, a lower discount rate in the range of 2% has been valid during recent years. However, it must be remembered that this discount rate is applied to the entire analysis period, so therefore, the use of the more representative long term discount rate is probably more reasonable.

Historical treatment performance life is the best source of information for estimating the performance of individual treatment strategies. This information can be obtained from asset management information. However, if it is not available from a reliable data source, the use of estimated values provided by experienced experts (“expert opinion”) provides a viable source of information until additional actual data can be collected.

Historical treatment cost information can be obtained from the PennDOT ECMS price history for treatments which have been actually constructed. For new treatments for which price history does not yet exist, suppliers can typically provide a reasonable cost estimate for the installed treatment.

The LCCA may be used to compare the effect on life cycle cost of applying treatments at different times throughout the analysis period, or of different treatments.

The FHWA has developed the RealCost software for conducting LCCA for highway and bridge assets. It is available on the FHWA website. The software can be used to perform either deterministic (fixed value) or probabilistic analyses. While the deterministic analysis relies on fixed input information, such as estimated cost or performance life, the probabilistic analysis considers the variability of the input information and provides the user the additional insight into the relative reliability of options considered.

As previously discussed several inputs are necessary to run the RealCost program. For the bridge deck mitigation treatment analysis, example RealCost analysis have been provided. For these examples a fixed analysis period of 50 years has generally been used. This analysis period has been used assuming that a typical bridge performance deck life with no remediation, such as shown by Minnesota data indicating a performance life of 35 years, can be extended to approximately 50 years by the application of deck remediation treatment strategies. Any anticipated performance beyond the 50 year analysis period is treated as salvage value and included in the present value calculation. The present value analysis includes the sequential application and costs of potential deck remediation treatments. The anticipated costs are all brought forward to a present value by the application of present worth factors to the various time series events. Several examples of this analysis and summary comparison of those results are provided. It is clear to users that the earlier

in the performance period a cost is incurred, the greater impact it has on the present value since the present worth factors increasingly diminish the effect of anticipated future year costs.

Using the RealCost tool, it is very feasible to develop analyses for any analysis period, considering additional remediation treatments and treatment application timing during the analysis period.

Similarly, new treatments can be added, or “what if” scenarios can be tested for changing the application timing of various treatments. For a given bridge deck situation, this approach can be used to determine the optimum approach to achieving the maximum performance benefit from the cost invested in remediation treatments. It can also be used to assess treatment cost effectiveness if a different performance life is considered.

CHAPTER 5 (TASK 5)

Draft Changes to PennDOT Printed Resources

The findings from Task 1 through 4 identified causes of early-age cracking in concrete bridge decks and methods to mitigate cracking, assessed the effect of cracking on the long-term durability and performance of bridge decks, and identified the most cost-effective remediation practices to extend the life of bridge decks. The following sections provide a summary of the Project findings and present recommendations for PennDOT printed materials to prevent and remediate cracked concrete bridge decks.

5.1 Factors Relevant to Bridge Deck Cracking and Deterioration Rates Considered/Addressed by the Project

Table 30 summarizes the factors that were investigated over the course of the Project in relation to bridge deck cracking and deterioration. Factors related to design, concrete materials, and construction practices are listed, along with the rating of the factors effect on cracking, based on the analysis of cracking data, testing of concrete cores, and deterioration rates of Pennsylvania bridge decks. Herein, CR refers to Condition Rating.

Table 30. Project summary of factors relevant to bridge deck cracking and deterioration.

Factors Causing Deck Cracking	Effect on Deck Cracking				Comments	Source
	Major	Moderate	Minor	None		
Materials						
Concrete type	✓				The highest early-age cracking was observed in AAA, followed by AAAP and HPC.	163 new bridge decks
Compressive Strength	✓				High 7 and 28 days compressive strength correlates with high cracking.	163 new bridge decks
Cement content	✓				Higher total cementitious materials content leads to higher cracking.	163 new bridge decks
SCM content		✓			Higher SCM content resulted in lower early-age cracking.	163 new bridge decks
Slump		✓			Excessive slump (> 5 in.) results in settlement cracking on top of rebar, especially for small cover thickness.	literature
Cement type		✓			Type III and other cements with high heat of hydration, fine particle size and rapid hardening/stiffening result in higher cracking. Several transportation agencies reported successful use of type K shrinkage compensating cements.	literature
Water/cement ratio			✓		No clear correlation as long as w/c is maintained in the range of 0.40 to 0.45.	163 new bridge decks

Design						
Continuous/simple span		✓			Simply supported spans remain at CR5 and CR8 28% and 14% longer, respectively, compared to continuous spans.	Deterioration modeling
Reinforcement type	*			*	Rebar type does not affect cracking, however protected rebar (e.g., epoxy-coated and galvanized) last 18% longer at CR8 by comparison to unprotected black rebar. Improved performance with regard to corrosion resistance is observed for protected rebar. Corrosion initiation threshold for the epoxy coated rebar was found to be 7x higher than the black rebar.	Deterioration modeling; 40 inspected bridge decks
Rebar design		✓			Cover thickness must be within 2 to 3 inches; use max. rebar size of #5 and max. rebar spacing of 6 in. Place longitudinal bars on top of transverse bars and stagger shear studs and deck slab bars to prevent a weak plane.	
Traffic volume (ADT & ADTT)			✓		Interstate decks last 20% longer at CR9. Non-interstate decks last 20% and 12% longer at CR5 and CR8, respectively.	Deterioration modeling
Girder spacing			✓		Girder spacing had minimal influence on cracking, and the influence of girder spacing varied from one girder type to another.	163 new bridge decks
Deck thickness			✓		Decks with an 8 inch thickness cracked more than other 5.5 inch thick and 12 inch thick decks.	163 new decks
Construction						
Moist curing	✓				Proper and timely moist curing has a major impact on early-age cracking. Curing must start no later than 15 min after finishing.	literature
Water evaporation rate	✓				Not to exceed 0.1 lb/ft ² per hr, to eliminate the risk of plastic shrinkage cracking.	
Half-width construction	✓				On average, decks constructed using half-width construction methods showed approximately 4 times more early-age cracking than decks constructed with detour routes.	163 new bridge decks
Location/District		✓			The location/district can inherently consider the effect of other variables such as: (1) traffic variations (urban areas have higher traffic volumes); (2) construction	Deterioration modeling

					and maintenance practices (quality and standard may vary across districts); and (3) slight changes in climate.	
National Highway System		✓			Non-interstate decks remained at CR5 and CR8 20% and 12% longer, respectively by comparison to interstate decks. However non-interstate decks remained at CR9 17% less compared interstate decks.	Deterioration modeling
Remediation		✓			Decks remained at CR6, CR7 and CR8, 14%, 23%, and 15% less time, respectively, immediately after remediation compared to unremediated deterioration.	Deterioration modeling
Ambient conditions		✓			Do not place concrete at air temperature below 45F (thermal cracking) or above 90F (plastic shrinkage cracking)	163 new bridge decks, literature
Concrete temperature and girder temperature at placement		✓			Must be between 55-75F.	literature
Sequence of pour		✓			In continuous span bridges pour the positive moment regions ahead of negative moment regions	163 new bridge decks, literature
Proper consolidation			✓		Proper consolidation is important to minimize the risk of settlement cracking.	literature

5.2 Findings from Tasks 1 thru 4

The sections below summarizes the key findings from Task 1 through 4 related to concrete materials, design, construction practices, and protective systems that affect concrete bridge deck cracking and bridge deck deterioration.

Task 1

- a) To minimize early-age cracking:
 - i. Limit total cementitious materials (paste) content, 28-day strength, and slump.
 - ii. Optimize aggregate gradation.
 - iii. Use SCM to reduce heat of hydration (in summer) + increase concrete resistivity.
 - iv. Enforce proper moist curing.
 - v. Limit rebar size and spacing.
- b) Cracking shortens corrosion initiation time. The chloride content at rebar level builds up quickly to high levels that are needed for corrosion to begin. However, this localized (at crack) corrosion comes to halt soon as the corrosion products seal the crack. Further corrosion of rebar will not resume until chlorides build up at off crack locations to significant levels (known as a critical chloride threshold) that are needed for the entire bar

to start corroding. The critical chloride threshold for black rebar has been reported as 2 lbs/cy (0.05%). For epoxy coated rebar this value could be 8 lbs/cy (0.2%) as reported in Task 3.

- c) To reduce corrosion risk: Min 2” cover, use SCM.
- d) Remediation must take place before active corrosion starts; in other words, before chlorides at the entire rebar level reach their critical threshold. This level of chlorides corresponds with transition between condition rating of 7 to 6.
- e) concentration needed for corrosion propagation.

Task 2

- a) Initial time of cracking:
 - i. 73% of responses indicated that cracking occurs within the first 3 months after construction of bridge deck.
- b) Prevention:
 - i. Structural details: limit the concrete deck restraints.
 - ii. Materials: limit the maximum 28-day compressive strength of the concrete (e.g. 4000 psi to 5500 psi).
 - iii. Curing techniques were indicated as “very effective” in crack prevention, followed by other construction practices, mix design, and structural details.
 - iv. Frequent recommendation to apply curing as soon as possible and maintain moisture level for at least 14 days.
 - v. 82% of the responses indicated observing more cracks during summer months versus cooler fall/spring months.
- c) Performance:
 - i. Early-age cracking was indicated to reduce bridge deck service life by accelerating deterioration mechanisms.

Task 3

- a) Chloride content and corrosion analysis:
 - i. Epoxy-coating was found very effective in delaying corrosion initiation, as compared to black rebar. An increase in the critical chloride concentration (required for corrosion propagation) from 0.05% (2 lbs/cy) for black bars to 0.20% (8 lbs/cy) for epoxy-coated bars was observed. Further the use of supplementary cementitious materials (SCM) can reduce the permeability of concrete, which in turn increases the time needed for chlorides to build up to critical levels at the rebar.
- b) Crack density analysis:
 - i. Higher compressive strength correlated with higher crack density. Possibly limit max strength at 7 or 28 days.

- ii. Lower total cementitious materials content and higher portland cement replacement with SCM resulted in less cracking. Limit max CM to 620 lbs/cy and use SCM to reduce heat, increase resistivity, and prevent ASR.
 - iii. Decks constructed using half-width procedures cracked 4 times more than decks constructed using detours.
- c) Sojourn time is the average number of years a deck remains in a certain condition rate (e.g., 6 yrs at CR8):
 - i. Coated rebar results in longer Sojourn times.
 - ii. Shorter, simply-span and non-interstate bridges have longer Sojourn times.
- d) At present, it is not possible to determine effect of deck cracking on Sojourn times; however this will be possible in future with the aid of DPD developed in this project.
- e) Deterioration model can be used to assess the effect of remediation on deck service life.

Task 4

- a) Life cycle cost analysis (LCCA) is effective in evaluating bridge deck performance:
 - i. Useful for comparing alternative remediation strategies
 - ii. Comparison of remediation sequences
 - iii. Process is flexible, can vary analysis period, adjust to changing economics, etc.
 - iv. Can consider user cost impacts
 - v. RealCost software can provide deterministic or probabilistic analysis results.
- b) In general, fewer remediation treatments applied during the performance period results in lower LCC.
- c) This can be achieved by:
 - i. Extending the time before remediation is needed (e.g., using routine preventative maintenance).
 - ii. Use of longer performing remediation treatments.
- d) Latex overlay and combination of latex and bituminous with waterproof membrane appear most cost effective for most circumstances.

5.3 Draft Recommendations to PennDOT Printed Material

The following recommendations are based on the Project findings from Task 1 through 4. In addition, recommendations from concurrent PennDOT sponsored projects as well as PennDOT supported recommendations are included.

a. Major recommendations for inspection protocols and data management

- i. Strict measures should be taken to maintain inspection consistency for crack density measurements:
 - Significant cracks (larger than 0.004 in) can be identified when the inspector bends at the waist and observes the surface directly from above. Observations

made from the shoulder (especially for wider decks) can lead to significant under-estimations of cracking compared to those observed directly from above.

- The type of cracking (i.e., transverse, longitudinal, diagonal, map cracking) should also be considered when evaluating the “crack density” value
- ii. Centralized method for proper maintenance/remediation tracking protocols should be developed and adapted
- In order to evaluate the effect of various types of remediation on the long-term performance the following historical data is required: (1) performance over time (such as condition ratings) and (2) remediation application types and dates. Without readily accessible and available remediation information or a centralized method to gather such data, it will be difficult to develop accurate statistics from which inferences about remediation effectiveness can be made.

b. PennDOT construction practices for bridge deck replacement

- i. Project supported improvements:
- Total cementitious materials (CM) content should be limited to max 620 lbs/cy.
 - Use SCM to reduce concrete resistivity and heat of hydration. The min SCM dosage must be determined based on PennDOT specifications for AAAP concrete (Publication 408, Section 704) and AASHTO PP-65 document for ASR mitigation, whichever is greater.
 - Do not use silica fume in bridge decks.
 - A max compressive strength limit is advised: 4000psi at 7 days or 5000psi at 28 days.
 - Proper and timely water curing is very important. Curing must start no later than 15 minutes after texturing and should continue for 14 days.
 - Do not exceed an evaporation rate of 0.10 lbs/ft².hr from freshly placed concrete.
 - Avoid half width construction when possible or ensure the construction quality matches full-width construction practices or induced vibrations are minimized.
 - Determine the differences in standards/procedures for deck construction for each District causing variability in deterioration rates of decks in different Districts.
- ii. PennDOT ProTeam supported improvements: Concurrent to this research project, a separate group of PennDOT engineers recommended improvements to reduce deck cracking. These recommendations are published in an Standard Special Provision (SSP) to “pilot” the improvements during 2015-2017 to determine if the recommendations should be incorporated. The items proposed by the ProTeam that are supported by PSU include:
- Aggregate Optimization (limits past volume, improves workability)
 - Air content of 7%

- Adequate vibration and use of foggers
 - Max w/c ratio of 0.45 and max slump of 5”
 - Contractor required to seal cracks with methyl-methacrylate sealer
- iii. PennDOT supported recommendations:
- Restore past practice of restricting deck construction during winter months
 - Consider warm (>80 °F) weather pours to start/end time and to cool the concrete to minimize thermal stresses between concrete and girders.
 - Cold (< 50 °F) weather pours consider tenting girders and control temperature differential between setting concrete and the girders.

c. Use of alternative materials to reduce deck cracking

i. Project supported improvements:

- Limit maximum total cementitious content.
- Use SCM content as high as possible without sacrificing early age strength development. Be especially cautious in colder construction season.
- Limit 28-day compressive strength.

ii. PennDOT supported recommendations:

- FLWA: Use fine lightweight aggregate to promote internal curing. Estimated reduction in shrinkage cracking is 23%
- SRA: Use shrinkage reducing admixtures to reduce shrinkage cracking by an estimated 20%.
- Consider use of Type II cement, estimate reduction in shrinkage cracking by 25%.
- Reduce maximum cementitious content from 690 pcy to 620 pcy. Current deck concrete has an average field strength of 6,100 psi, which should be lowered to about 5,000 psi. Restrained ring testing confirms that 600 pcy to 610 pcy cracks much less than 690 pcy.

d. Design Recommendations to PennDOT Standards

i. PennDOT supported recommendations to Publication 218, BD Standards:

- BD-601, Make the top mat the longitudinal bars, and stagger transverse and longitudinal bars vertically to eliminate weak planes in the deck where cracks could form.
- BD-628, Type 3, reduce restraint and cracking in deck by eliminating the tie bar between the deck and the approach slab.
- BD-656, Type 3 approach slabs, reduce restraint and cracking in deck by eliminating the tie bar between the deck and the approach slab.
- BD-660, require the “alternate deck placement sequence” and use the new “transverse construction joint detail, including crack control” recommended for BC-752 to reduce deck cracking.

- BD-667, D11.6.4.6P addresses thermal movements for integral abutments, but the tie bar between the deck and approach slab appears to restrain the deck causing excessive cracking. Integral Abutments have a serious cracking problem (ref TRB 13-3348), and eliminating the longitudinal restraint should reduce deck cracking significantly.
- ii. PennDOT supported recommendations to Publication 219, BC Standards
- BC-752, Add transverse construction and crack control joint detail. Similar to designing a long concrete retaining wall, periodic crack control joints are required to reduce cracking. See BD-660 above, joints are at inflection points where pour joints are located for continuous decks only.
 - BC-753, add note and/or detail to stagger stud rows transversely across deck. FEA has shown that aligned stress concentrations can cause transverse cracks.
- e. Publication 15M, Design Manual Part 4 (Design Items)**
- i. PennDOT supported recommendations:
- 11.6.4.6P addresses the thermal movements for integral abutments, but BD-667 uses a tie bar that restrains the movement and causes deck cracking. Revise details and criteria to allow thermal movements.
 - 5.4.2.2 specifies the coefficient of thermal expansion for deck concrete. Consider AC5.4.2.2 and the range of COTE based on the aggregate mineral (such as dolomite vs limestone) and use the least advantageous COTE for design. Design/space the crack control joints for continuous spans for the expected shrinkage without cracking.
 - 14.3, define the “ ξ_{sh} ” installation temperature range.
- f. Proposed specifications and standards for new materials**
- i. PennDOT supported recommendations:
- Publication 408, Sections 106 & 110, revise acceptance criteria for deck slabs as per the NDOR (704.05) methodology whereby the basis is solely on the actual average break strengths and does not include any increase for standard deviation. Current practice has $f'c$ of 4,000 psi and remove and replace below 3,850 psi, which is only 150 psi.
 - Publication 408, section 704, reduce the maximum cementitious from 690 pcy to 620 pcy in conjunction with removing the 350 psi standard deviation for acceptance, thereby lowering the removal limit from 3,850 psi to 3,500 psi.
 - Publication 408, section 1001, consider restricting winter deck pours, or requiring that the thermal design spreadsheet be used to reduce the potential for deck cracking.
 - Consider piloting or adding a new SSP for polyester polymer overlay in order to avoid the cracking issues from using LMC overlays.

g. Guide for repair and remediation of severely cracked (AAA) decks

i. PennDOT supported recommendations:

1. Publication 15M, Design Manual Part 4 (Remediation Items): Consider the addition of polyester polymer overlays as an equal or alternate to LMC overlays.
- New pilot SSP requires contractors to seal cracks with methyl-methacrylate sealer. This is the first remediation step after the deck is poured and not open to traffic. This should also be re-visited 12-months after placement.
 - Use the new Deck Performance Database (DPD) and the included “Decision Matrix” including deterioration modeling and Life-Cycle Cost Analysis (LCCA) to determine when and which type of remediation is the most cost-effective.
 - The DPD will be used to store the remediation histories for the BMS2 bridges to develop and confirm cost-effectiveness.

CHAPTER 6 (TASK 6.3)

Cost Analysis for each Approved Design and Construction Recommendation

6.1 Introduction

A final life cycle cost analysis will consider the potential impact of recommended changes to PennDOT's bridge policy. The base case presented will be a life cycle cost analysis representing recent past bridge deck performance identified during the study. Based on observations from the LCCA work presented in Task 4, an overall approach for improving the life cycle cost of bridge decks is to minimize the number of deck remediation treatments applied during the analysis period. Considering the currently used PennDOT bridge deck remediation strategies, it was recommended in Task 4 that one of the more effective ways to reduce the number of deck remediation treatments is to increase the time before the application of the first remediation treatment. In keeping with this recommendation, a strategy of sealing deck cracks early to delay the onset of serious reinforcement corrosion damage is included in the LCCA here. Additional analyses are provided for the anticipated improvement resulting from example improvements resulting from recommendations for both "no cost" and "at additional cost" changes in practice.

6.2 Basis for the Analyses

To provide the basis for these analyses, the key value of the time to the beginning of serious corrosion damage was predicted for these several cases using the LIFE-365 prediction model. The difference in the time after initial construction to the onset of serious corrosion damage between two cases are used for comparison of the effects of the recommendations included as examples in this section. For example, the difference in time to reinforcement deterioration from corrosion between decks containing epoxy coated bars with different concrete cover thickness, or decks for which cracks are not sealed, as opposed to those kept sealed to limit chloride intrusion into the deck. A summary of the results used in this section are provide in Table 31.

Table 31. Summary of LIFE-365 Corrosion Initiation Results

Concrete	Rebar	Cracked?	Concrete Cover (in)	Corrosion Initiation (yrs)
AAA	epoxy	N	2	20.8
AAA	epoxy	Y	2	13.5
AAA	epoxy	Y	3	22.2
AAAP	epoxy	Y	2	19.1

6.3 Scenarios

Several of the recommendations have previously been implemented by the Department, and therefore are currently considered "no cost" enhancements since the cost is already included in

recent project costs. A good example of this is the use of epoxy coated reinforcement bars in bridge decks. While epoxy coated reinforcement bars have generally been used in PennDOT bridge decks, this report provided information about the improvement in deck life that results. Performance predictions using the LIFE-365 model indicate that the onset of corrosion deterioration in AAA bridge deck concrete is increased from approximately 8 years to approximately 20 years as a result of changing from black reinforcement bars in decks to epoxy coated bars. Other recommendations from the project include techniques which are expected to increase the cost of bridge deck construction. Examples of recommendations which are expected to increase deck construction cost are techniques such as increasing the reinforcement cover in bridge decks, and potentially improving curing techniques to delay the onset of corrosion damage. The potential effect of these additional deck construction cost on the total LCCA over the analysis period is of interest.

Several enhancement scenarios based on these recommendations were considered. Results of these recommended enhancements are presented along with the base case in the following section. For these analyses, it has been assumed that the remediation treatments are applied a few years before the predicted onset of serious corrosion damage, with the objective of preventing this critical threshold from being reached since it is understood that applying a deck remediation treatment after serious corrosion damage has begun will not effectively protect the deck, and deterioration will continue to occur at a rate more similar to that identified during Task 3 as the expected deterioration rate for cracked bridge decks.

6.3.1 Base Scenario

The base case considered in this section is a deck strategy with a good life cycle cost based on Task 4 results. A fifty year life cycle cost analysis is presented here beginning with the construction cost of a bridge deck at time zero. The LCCA for the base scenario can then be compared with the other recommended cases discussed to illustrate potential improvements in the life cycle cost over the fifty year analysis period. For the recommended cases, the time to serious corrosion of reinforcement is delayed in the analysis in accordance with the results from the LIFE-365 analysis model. The subsequent sequence of remediation treatments for these cases remains the same as evaluated during Task 4.

For the following examples, a 100-foot long bridge deck, 40 feet wide was assumed. The initial construction cost was assumed to be the same as deck removal and replacement cost from the previous task since it is consistent with most of the current deck construction practices. The treatment sequence for this base case is as follows.

Deck Age (Yrs)	Deck Rating Before Treatment	1st Treatment			Deck Rating Before Treatment	2nd Treatment			Deck Rating Before Treatment	3rd Treatment		
		Treatment (Service Life)	Deck Rating After Treatment	Deck Age (Yrs)		Treatment (Service Life)	Deck Rating After Treatment	Deck Age (Yrs)		Treatment (Service Life)	Deck Rating After Treatment	Deck Age (Yrs)
5	7	Epoxy (10 Yrs)	8	15	6	LMC (20 Yrs)	8	35	5	WM&B (15 Yrs)	7	50

6.3.2 Sealed versus Unsealed Scenario

An example showing different practices is shown in this section. It compares a deck with sealed cracks versus a deck with unsealed cracks. It was assumed that the deck has 400 linear feet of cracking. The cost of sealing the cracks was obtained from the literature and is the average of several materials. The average cost was estimated to be \$0.40 per square foot for the material plus the same rate for application of the sealers. The treatment sequence is as follows.

Practice	Deck Age (Yrs)	Deck Rating Before Treatment	1st Treatment			Deck Rating Before Treatment	2nd Treatment			Deck Rating Before Treatment	3rd Treatment		
			Treatment (Service Life)	Deck Rating After Treatment	Deck Age (Yrs)		Treatment (Service Life)	Deck Rating After Treatment	Deck Age (Yrs)		Treatment (Service Life)	Deck Rating After Treatment	Deck Age (Yrs)
Unsealed	11	6	LMC (20 Yrs)	8	31	5	WM&B (15 Yrs)	7	46	5	WM&B (15 Yrs)	7	61
Sealed	18	5	LMC (15 Yrs)	7	33	5	WM&B (15 Yrs)	7	48	5	WM&B (15 Yrs)	7	63

6.3.3 AAA versus AAAP Mixture Design

Another example indicates that changing from AAA to AAAP concrete in a cracked deck is expected to delay the onset of serious corrosion damage from 13 to 19 years. It was assumed that no additional cost is associated with using the AAAP mixture design. The treatment sequence is as follows.

Practice	Deck Age (Yrs)	Deck Rating Before Treatment	1st Treatment			Deck Rating Before Treatment	2nd Treatment			Deck Rating Before Treatment	3rd Treatment		
			Treatment (Service Life)	Deck Rating After Treatment	Deck Age (Yrs)		Treatment (Service Life)	Deck Rating After Treatment	Deck Age (Yrs)		Treatment (Service Life)	Deck Rating After Treatment	Deck Age (Yrs)
AAA	11	6	LMC (20 Yrs)	8	31	5	WM&B (15 Yrs)	7	46	5	WM&B (15 Yrs)	7	61
AAAP	17	6	LMC (20 Yrs)	8	37	5	WM&B (15 Yrs)	7	52				

6.3.4 Increased Cost Case of Two-inch Concrete Cover versus Three-inch Concrete Cover

As an example, increasing deck cover of reinforcement steel from 2 inches to 3 inches in a cracked deck is expected to delay the onset of serious corrosion damage from 13 years to 22 years. The additional cost for the extra concrete was estimated to be \$11 per square yard for this example. The treatment sequence is as follows.

Practice	Deck Age (Yrs)	Deck Rating Before Treatment	1st Treatment				2nd Treatment				3rd Treatment		
			Treatment (Service Life)	Deck Rating After Treatment	Deck Age (Yrs)	Deck Rating Before Treatment	Treatment (Service Life)	Deck Rating After Treatment	Deck Age (Yrs)	Deck Rating Before Treatment	Treatment (Service Life)	Deck Rating After Treatment	Deck Age (Yrs)
2" cover	11	6	LMC (20 Yrs)	8	31	5	WM&B (15 Yrs)	7	46	5	WM&B (15 Yrs)	7	61
3" cover	20	5	LMC (15 Yrs)	7	35	5	WM&B (15 Yrs)	7	50				

6.4 LCCA Results for the Examples

Results of the LCCA for the examples discussed in the previous section are presented in Table 32. It can be seen that the recommended practices to prolong bridge deck life and delay the maintenance activities produce smaller present values and therefore are better options economically as well.

Table 32. LCCA Results for the Examples

Practice	Present Value	Undiscounted Sum	EUAC
Base Scenario	\$691,737	\$728,889	\$32,200
Unsealed	\$675,493	\$708,148	\$31,444
Sealed	\$669,078	\$705,505	\$31,146
AAA	\$675,493	\$708,148	\$31,444
AAAP	\$667,487	\$699,259	\$31,072
2" Cover	\$675,493	\$708,148	\$31,444
3" Cover	\$671,192	\$707,111	\$31,244

6.5 Conclusions

Conclusions from the fifty year life cycle cost analysis results for the example recommendations indicate that each of the recommendations evaluated will potentially improve the life cycle cost of bridge decks if implemented. In each of the examples, the recommended action results in a reduction in the total life cycle cost when compared with the current practice. It is interesting to note that the improvement in life cycle cost for the three cases presented in Table X2 produce savings of similar magnitude. Among these examples, increasing the reinforcement cover from 2" to 3" results in the greatest savings. Other recommendations from this report are expected to produce additional cost reduction as well, and in some cases compounded saving may be realized.

References

- AASHTO LRFD Bridge Design Specifications, 6th Edition (2012). American Association of State Highway and Transportation Officials, Washington, DC
- Abdulshafi, O. A., and Fitch, M. G. (1995). *Field and Laboratory Evaluation of Silica Fume Modified Concrete Bridge Deck Overlays in Ohio*. No. FHWA/OH-95/027.
- ACI (1985). Debate: Crack Width, Cover, and Corrosion. *Concrete International*, May, p. 20.
- ACI Committee 345R (1991), Guide for Concrete Highway Bridge Deck Construction, ACI Manual of Concrete Practice, American Concrete Institute, Detroit, MI
- ACI 308R-01 (2001). Guide to Curing Concrete. American Concrete Institute. Farmington Hills, MI.
- ACI 224R-01: (2001). Control of Cracking in Concrete Structures. American Concrete Institute. Farmington Hills, MI.
- ACI 231-10: (2010). Early-Age Cracking: Causes, Measurement, and Mitigation. American Concrete Institute. Farmington Hills, MI.
- ACI 345-1R-06 (2006). Guide for Maintenance of Concrete Bridge Members, American Concrete Institute, Farmington Hills, Michigan,
- Agrawal, A., Kawaguchi, A., Chen, Z. (2010). Deterioration Rates of Typical Bridge Elements in New York. *ASCE Journal of Bridge Engineering*, 15(4), 419-429.
- Ahlborn, T.M., Kasper, J.M., Aktan, H., Koyuncu, Y., and J. Rutyna (2002). Causes and Cures of Prestressed Concrete IBeam End Deterioration. Report No. CSD 200202, Center for Structural Durability, Michigan Tech Transportation Institute, and Michigan Department of Transportation Report RC1412, Lansing, MI.
- Ahmad, A. (2011). Bridge Preservation Guide – Maintaining a State of Good Repair Using Cost Effective Investment Strategies. FHWA Publication Number: FHWA-HIF-11042.
- Ahmed, S. F. U., Maalej, M., and Mihashi, H., (2007) Cover cracking of reinforced concrete beam due to corrosion of steel. *ACI Materials Journal*, 104 (2), 153–161,

- Akhavan, A., Shafaatian, S.M.H., Rajabipour, F. (2012). Quantifying the effects of crackwidth, tortuosity, and roughness on water permeability of cracked mortars. *Cement and concrete research*, ELSEVIER, 42, 313-320
- Akhavan, A., and Rajabipour, F. (2013). Evaluating ion diffusivity of cracked cement paste using electrical impedance spectroscopy. *Materials and Structures* 46:697-708, DOI 10.1617/s11527-012-9927-x
- Aldea, C.-M., Shah, S.P., and Karr, A. (1999a). Permeability of Cracked Concrete, *Materials and Structures*, Vol. 32, June, pp.370-376
- Aldea, C.-M., Shah, S.P., ASCE, Member and Karr A. (1999b). Effect of cracking on water and chloride permeability of concrete. *Journal of Materials in Civil Engineering*, Vol. 11, No. 3, August
- Alonso, C., Andrade, C., Rodriguez, J., and Diez, J. M. (1998). Factors controlling cracking of concrete affected by reinforcement corrosion. *Materials and Structures*, 31 (211), 435– 441,
- American Association of State Highway and Transportation Officials (AASHTO) (2008). *The Manual for Bridge Evaluation*, Washington, D.C.
- American Association of State Highway and Transportation Officials (AASHTO) (2010). *Bridge Element Inspection Guide Manual*, Washington, D.C.
- American Association of State Highway and Transportation Officials (AASHTO) (2012). *AASHTOWare Bridge Update*. AASHTO SCOBS General Session. Austin, TX.
- American Association of State Highway and Transportation Officials (AASHTO) (2012). *LRFD Bridge Design Specifications*, 6th Edition. Washington, DC
- American Association of State Highway and Transportation Officials (AASHTO) (2013). *AASHTOWare Bridge Management Product Update*. Taken from <http://aashtowarebridge.com/2013/04/25/product-update/>
- American Concrete Institute (ACI) (2010). *Report on Performance-Based Requirements for Concrete*. ACI Report ITG-8R-10. Farmington Hills, MI.
- American Concrete Institute *Manual of Practices* (1997). Edition ACI 224R, 4.4, Table 4.1 Crack Widths in Concrete Bridge Decks

- Arya, C., and Wood, L.A., (1995). The Relevance of Cracking in Concrete to Corrosion of Reinforcement. The Concrete Society, Camberley, Surrey, Technical Report No. 44.
- Arya, C., and Ofori-Darko, FK. (1996). Influence of crack frequency on reinforcement corrosion in concrete. *Cement and Concrete Research* 26(3): 333–353.
- ASTM D4580-12 (2013) Standard Practice for Measuring Delamination in Concrete Bridge Decks by Sounding. Current edition approved Dec. 15, 2012. Published May 2013. Originally approved in 1986.
- Azari, H., Yuan, D., Nazarian, S., Gucunski, N. (2012). Sonic Methods to Detect Delamination in Concrete Bridge Decks: Impact of Testing Configuration and Data Analysis Approach. *Journal of the Transportation Research Board*, No. 2292, 113-124.
- Babaei, K., and Hawkins, N. (1987). Evaluation of Bridge Deck Protective Strategies. *Transportation Research Record*, NCHRP Report 297, Washington, D.C.
- Babaei., K., and Purvis, R. (1994). Prevention of Cracks in Concrete Bridge Decks: Report on Laboratory Investigation of Concrete Shrinkage. Research Project No. 89-01, Pennsylvania Department of Transportation, Harrisburg, PA.
- Babaei., K., and Purvis, R. (1995). Prevention of Cracks in Concrete Bridge Decks: Report on Observation of Bridge Deck Construction. Research Project No. 89-01, Pennsylvania Department of Transportation, Harrisburg, PA.
- Babaei, K., Purvis, R. L., Clear, K. C., and Weyers, R. E. (1996). Methodology for concrete removal, protection, and rehabilitation. *Rep. Prepared for the U.S. Department of Transportation, Federal Highway Administration*, Wilbur Smith Associates, Falls Church, Va.
- Banthia, N., and Gupta, R. (2006). Influence of Polypropylene Fiber Geometry on Plastic Shrinkage Cracking in Concrete. *Cement and Concrete Research*. 36(7). 1263-1267.
- Banzhaf, H. S., Desvousges, W. H., and Johnson, F. R. (1996). “Assessing the externalities of electricity generation in the Midwest.” *Resource Energ. Econ.*, 18, 395–421
- Barde, V., A. Radlinska, M. Cohen, and W. J. Weiss (2009). Relating Material Properties to Exposure Conditions for Predicting Service Life in Concrete Bridge Decks in Indiana. Publication FHWA/IN/JTRP-2007/27., Indiana Department of Transportation and Purdue University, West Lafayette, Indiana. doi:10.5703/1288284313444.

- Bastidas-Arteaga, E., A., Chateauneuf, M., Sánchez-Silva, Ph., Bressolette, F., Schoefs, A. (2011). Comprehensive probabilistic model of chloride ingress in unsaturated concrete. *Engineering Structures*, Volume 33, Issue 3, March 2011, Pages 720–730
- Battaglia, I., Whited, G., and Swank R. (2008). Eclipse shrinkage reduction product evaluation: Final report. Research study # FEP-02-01, Report # FEP-01-08, Wisconsin DOT Technical Services
- Beeby, A., (1983) Cracking, cover and corrosion of reinforcement. *Concrete International* 5(2): 35–40.
- Bentur, A, Diamond, S, and Berke, N. (1997). *Steel Corrosion in Concrete, Fundamentals and Civil Engineering Practice*. E & FN Spon, London, pp. 41–43.
- Bentz, D. P., and Snyder, K. A., (1999). Protected Paste Volume in Concrete-Extension to Internal Curing Using Saturated Lightweight Fine Aggregate. *Cement and Concrete Research*, V. 29, pp.1863-1867.
- Bentz, D.P., and Jensen, O. (2004). Mitigation Strategies for Autogenous Shrinkage Cracking. *Cement and Concrete Composites*, 26(6), 677-685.
- Bentz, D.P., Lura, P., and Roberts, J.W. (2005). Mixture Proportioning for Internal Curing. *Concrete International*, Feb 2005, 35-40
- Bentz, D., P. Halleck, A. Grader, and J. Roberts. (2006). Water Movement during Internal Curing: Direct Observation Using X-Ray Microtomography. *Concrete International*, Vol. 28, No. 10, pp. 39-45.
- Bentz, D.P., and Weiss, W.J. (2011). Internal Curing: A 2010 State-of-the-Art Review. NISTIR 7765. U.S. Department of Commerce. February 2011
- Berke, N.S., Dellaire, M.P., Hicks, M.C., and Hoopes, R.J. (1993). Corrosion of Steel in Cracked Concrete. *Corrosion*, Vol. 49, 1993, p. 934.
- Bertolini, L., Elsener, B., Pedferri, P., Polder, R. (2004) *Corrosion of steel in concrete*. WILEY-VCH Verlag GmbH & Co. KGaA, Weinheim, ISBN 3-257-30800-8
- Bian, H., Chen, S., Watson, C., Hauser, E. (2011). Bridge Deck Joints Evaluation using LiDAR and Aerial Photography. *Proceedings of SPIE*, 7983(79831L), 1-12.
- Bridge Inspection and Rehabilitation A Practical Guide. Ed. Silano L.G., John Wiley & Sons, (1993).

- Brown, M., Sellers, G., Folliard, K., and Fowler, D. (2001). Restrained Shrinkage Cracking of Concrete Bridge Decks: State-of-the-art Review. Texas Department of Transportation.
- Browning, J., Darwin, D., Hurst, K. (2007). Specifications to Reduce Bridge Deck Cracking. HPC Bridge Views, Issue No. 46.
- Browning, J., Darwin, D., Hurst, K. (2009). Specifications to Reduce Bridge Deck Cracking. HPC Bridge Views, Issue No. 55.
- Buenfeld N, Glass G, Reddy B, Viles F (2004) Process for the Protection of Reinforcement in Reinforced Concrete. United States Patent # 6685822, Alexandria, VA, USA
- Cavaliero, R., and Durham, S. (2010). Examination of Cement and Aggregate Type on the Crack-Resistance of Colorado's Bridge Deck Concretes. Transportation Research Board (TRB) Annual Conference Proceedings.
- Chen, S., Rice, C., Boyle, C., Hauser, E. (2011). Small-Format Aerial Photography for Highway-Bridge Monitoring. ASCE Journal of Performance of Constructed Facilities, 25(2), 105-112.
- Cheng, T.T., and Johnson, D.W. (1985). Incident Assessment of Transverse Cracking in Bridge Decks: Construction and Material Consideration. Report No. FHWA/NC/85-002, Vol. 1. Federal Highway Administration, Washington, DC.
- Clear, C. A. (1985). The Effects of Autogenous Healing upon the Leakage of Water through Cracks in Concrete. Technical Report 559, Cement and Concrete Association, 31 pp.
- Cohen, M.D., Olek, J., and Dolch, W.L. (1990). Mechanism of Plastic Shrinkage in Portland Cement and Portland Cement-Silica Fume Paste and Mortar. Cement and Concrete Research, 20(1), 103-119.
- Collins, L. (1972). An introduction to Markov chain analysis, CATMOG, Geo Abstracts, Univ. of East Anglia, Norwich, U.K.
- Curtis, R., White, H. (2007). NYSDOT Bridge Deck Task Force Evaluation of Bridge Deck Cracking on NYSDOT Bridges.
- Cusson, D., Z. Lounis, and L. Daigle. Benefits of Internal Curing on Service Life and Life Cycle Cost of High-Performance Concrete Bridge Decks: A Case Study. Cement and Concrete Composites, Vol. 32, No. 5, 2010, pp. 339-350.
- Dakhil, F.H., and Cady, P.D. (1975). Cracking of Fresh Concrete as Related to Reinforcement. ACI Journal. 72(8) 421-428

- Danilecki, W. (1969). An investigation into the effect of crack width on the corrosion of reinforcement in reinforced concrete. RILEM Symposium on the Durability of Concrete. Prague.
- Darwin, D., Browning, J., Lindquist, W. (2004). Control of Cracking in Bridge Decks: Observations from the Field. *ASTM Journal of Cement, Concrete, and Aggregates*, 26(2), 148-154.
- Darwin, D., Browning, J., O'Reilly, M. and Xing, L. (2007). Critical Chloride Threshold for Galvanized Reinforcing Bars,” research report 07-2 submitted to the International Lead Zinc Research Organization, Inc. by University of Kansas, December.
- Darwin, D., Browning, J., Lindquist, W., McLeod, H., Yuan, J., Toledo, M., Reynolds, D. (2010). Low-Cracking, High-Performance Concrete Bridge Decks: Case Studies over First 6 Years. *Journal of the Transportation Research Board*, No. 2202, 61-69.
- Demis, S., Efstathiou, M.P., Papadakis, V.G. (2013). Computer-Aided Modeling of Concrete Service Life, Cement & Concrete Composites, doi: <http://dx.doi.org/10.1016/j.cemconcomp.2013.11.004>
- Desmettre, C., Charron, J.P. (2013). Water Permeability of Reinforced Concrete Subjected to Cyclic Tensile Loading”, *ACI Materials Journal*, V. 110, No. 1, January-February 2013
- DeStefano, P. D., and Grivas, D. A. (1998). “Method for estimating transition probability in bridge deterioration models.” *J. Infrastruct. Syst.*, 4_2_, 56–62.
- Dilek, U. (2009). Condition Assessment of Concrete Structures. Failure, Distress and Repair of Concrete Structures, Chapter 4, 84-137.
- Djerbi, A., Bonnet, S., Khelidj, A., Baroghel-bouny, V. (2008). Influence of traversing crack on chloride diffusion into concrete. *Cement and Concrete Research*, 38, 877-883, ELSEVIER
- DuraCrete, General guidelines for durability design and redesign (2000). Tech. Rep. Report BE95-1347/R15, European Union, Luxembourg, part of the Brite-EuRam III Project BE95-1347 Probabilistic Performance based Durability Design of Concrete Structures, 109 pp.
- Eclipse 4500 (2011). Shrinkage reducing admixture, Grace Concrete Products, Patents Pending
- Edvardsen, C. (1999). Water permeability and autogenous healing of crack in concrete, *ACI Mater. J.* 96 (4) 448–454.

- Ehlen, M. A. (2003). BridgeLCC: Life-cycle costing software for the preliminary design of bridges. National Institute of Standards and Technology, Gaithersburg, Md.
- Ehlen, M. A., Thomas, M. D. A. and Bentz, E. C. (2009). Life-365 service life prediction model version 2.0 - widely used software helps assess uncertainties in concrete service life and life-cycle costs, *Concrete International - the Magazine of the American Concrete Institute*, 31 (5), 41.
- Enright, M. P., and Frangopol, D. M. (1999). Maintenance planning for deteriorating concrete bridges. *J. Struct. Eng.*, 125(12), 1407–1414.
- Estes, A. C., and Frangopol, D. M. (2001). Minimum expected cost oriented optimal maintenance planning for deteriorating structures: Application to concrete bridge decks. *Reliab. Eng. Syst. Saf.*, 73, 281–291.
- Fanous, F., Wu, H., Pape, J. (2000). Impact of Deck Cracking on Durability. IowaDOT project TR-405, CTRE Management project 97-5, Iowa State University, March 2000
- Fanous, F., and Wu, H., (2005). Performance of Coated Reinforcing Bars in Cracked Bridge Decks. *Journal of Bridge Engineering*, Vol. 10, No. 3, pp. 255–261.
- Federal Highway Administration (FHWA) (1995). Recording and Coding Guide for the Structure Inventory and Appraisal of the Nation's Bridges. Washington, D.C.
- Federal Highway Administration (FHWA) (2011). Bridge Preservation Guide. FHWA Publication No. FHWA-HIF-11042. Washington, D.C.
- Federal Highway Administration (FHWA) (2013). Draft - Long-Term Bridge Performance Program: Draft Data Collection and Inspection Protocols. Washington, D.C.
- fib Bulletin 34 (2006). Model code for service life design. Tech. Rep. fib Bulletin 34, International Federation for Structural Concrete (fib), Lausanne, Switzerland, 126 pp.
- Flood, I., Kartam, N. (1994). Neural Networks in Civil Engineering I: Principles and Understanding. *ASCE Journal of Computing in Civil Engineering*, 8(2), 131-148.
- Forde, M., McCann, D. (1997). Draft advisory note to highway agency on NDT of masonry arch bridges. Edinburgh, UK.

- Francois, R., Arliguie, G. (1999). Effect of microcracking and cracking on the development of corrosion in reinforced concrete members. *Magazine of Concrete Research*, 51(2) 143-150, 1999
- Francous, R., and Arliguie, G. (1994). Durability of loaded reinforced concrete in chloride environment. *Third CANMET/ACI International Conference on Durability of Concrete*, Nice, SP145- 30, 573±595.
- Frederiksen, J., and Poulsen, E., Hetek (1997). Chloride penetration into concrete - manual, Tech. Rep. Report No. 123, Road Directorate, Danish Ministry of Transport.
- French, C., Eppers, L., Le, Q., Hajjar, J. (1999). Transverse Cracking in Concrete Bridge Decks. *Transportation Research Record* 1688, Paper No. 99-0888, 21-29.
- Frosch, R., Blackman, D.T., and Radabaugh, R.D. (2003). Investigation of Bridge Deck Cracking in Various Bridge Superstructure Systems. *Purdue University*. West Layfayette, IN.
- Fu, G., Feng, J., Dimaria, J., Zhuang, Y. (2007). Bridge Deck Corner Cracking on Skewed Structures. Final Report No. RC-1490. Michigan Department of Transportation.
- Gagné R., Francois, R., Masse, P. (2001). Chloride penetration testing of cracked mortar samples, in: N. Banthia, et al., (Eds.), *Proc. of 3rd International Conference on Concrete under Severe Conditions*, The University of British Columbia, Vancouver, Canada, pp. 198–205.
- Ganapuram, S., Adams, M., Patnaik, A. (2012). Quantification of Cracks in Concrete Bridge Decks in Ohio District 3. Final Report No. FHWA/OH-2012/3. Ohio Department of Transportation.
- Geiker, M.; Bentz, D. P.; and Jensen, O. M. (2004). Mitigating Autogenous Shrinkage by Internal Curing,” *High-Performance Structural Lightweight Concrete*, SP-218, J. P. Ries and T. A. Holm, eds., American Concrete Institute, Farmington Hills, MI, pp. 143-154.
- Goodspeed, C., Vanikar, S., and Cook, R. (1996). High-performance concrete defined for highway structures. *Concrete International*, 18(2), 62-67
- Graybeal, B., Phares, B., Rolander, D., Moore, M., Washer, G. (2002). Visual Inspection of Highway Bridges. *Journal of Nondestructive Evaluation*, 21(3), 67-83.
- Grzybowski, M., and Shah, S. (1989). Model to predict cracking in fibre reinforced concrete due to restrained shrinkage. *Magazine of Concrete Research*, 41 (148), 125-135.

- Gucunski, N., Kruschwitz, S., Feldmann, R., Rascoe, C. (2009). Meeting LTBP Program Objectives through Periodical Bridge Condition Monitoring by Nondestructive Evaluation. ASCE Structures 2009.
- Gucunski, N., Imani, A., Romero, F., Nazarian, S., Yuan, D., Wiggenhauser, H., Shokouhi, P., Taffe, A., Kutrubes, D. (2013). Nondestructive Testing to Identify Bridge Deck Deterioration. Report S2-R06A-RR-1. The Second Strategic Highway Research Program (SHRP 2). Transportation Research Board. Washington, D.C.
- Gucunski, N., Moon, F. (2011). ANDERS: future of concrete bridge deck evaluation and rehabilitation. SPIE, 7983(21), 1-9.
- Guo, Y., He, X., Peeta, S., Zheng, H., Barrett, T., Miller, A., and Weiss, J. (2014). Internal Curing as a New Tool for Infrastructure Renewal: Reducing Repair Congestion, Increasing Service Life, and Improving Sustainability. NEXTRANS Project No. 082PY04. USDOT Region V Regional Transportation Center Final Report.
- Guthrie, W. S., Linford, E. T., & Eixenberger, D. (2007). Development of an Index for Concrete Bridge Deck Management in Utah. Transportation Research Record: Journal of the Transportation Research Board, 1991(1), 35-42.
- Guthrie, W. S., and Yaede, J. M. (2013). Internal curing of concrete bridge decks in Utah: preliminary evaluation. Transportation Research Board 38 92nd Annual Meeting 39 January 13-17, 2013 40 Washington, D.C.
- Hadidi, R., and Saadeghvaziri, M.A. (2005). Transverse Cracking of Concrete Bridge Decks: State of the Art. Journal of Bridge Engineering, 10(5) 503-510.
- Hasegawa, Y., Miyazato, S., and Oyamoto, T. (2004). Proposal for corrosion rate analytical model of reinforced concrete. 29th Conference on Our World in Concrete & Structures, pp. 281–288, Singapore
- Hawk, H. (2002). BLCCA. Life-cycle cost analysis for bridges, N.C.H.R. Program, Transportation Research Board, Washington, D.C.
- Hearn N. (1998). Self healing, autogenous healing and continued hydration: what is the difference? Mat. Struct./Matér. Constr. 31, 563–567.
- Hearn, G., Shim, H. (1998). Integration of Bridge Management Systems and Nondestructive Evaluations. ASCE Journal of Infrastructure Systems, 4(2), 49-55.

- Hong, T. and Hastak, M. MEMRRES: model for evaluating maintenance, repair and rehabilitation strategies in concrete bridge decks. *Civil Engineering and Environmental Systems* 22.4 (2005): 233-248.
- Hoseini, M., Bindiganavile, V., and Banthia, N. (2009). The Effect of Mechanical Stress on Permeability of Concrete: A Review. *Cement and Concrete Composites*, V. 31, pp. 213-220.
- Huang, Y. H., Adams, T. M., & Pincheira, J. A. (2004). Analysis of life-cycle maintenance strategies for concrete bridge decks. *Journal of Bridge Engineering*, 9(3), 250-258.
- Huang, Y. (2010). Artificial Neural Network Model of Bridge Deterioration. *ASCE Journal of Performance of Constructed Facilities*, 24, 597-602.
- Hwan Oh, B., Hyun Kim, K., and Seok Jang, B. (2009). Critical corrosion amount to cause cracking of reinforced concrete structures, *ACI Materials Journal*, 106 (4), 333–339.
- Hydromax Internal Curing Admixture (2012), ProCure, LCC, Patent Pending
- Ibrahim, Mohammed, Al-Gahtani, A., Maslehuddin, M., and Dakhil, F. (1999). Use of surface treatment materials to improve concrete durability. *Journal of materials in civil engineering* 11.1: 36-40.
- Iowa Department of Transportation (1986). A Study of Transverse Cracks in the Keokuk Bridge Deck. Final Report, Ames, IA.
- Isgor, O. B., and Razaqpur, A. G. (2006) Modelling steel corrosion in concrete structures. *Materials and Structures*, 39 (287), 259–270.
- Issa, M. (1999). Investigation of Cracking in Concrete Bridge Decks at Early Ages. *Journal of Bridge Engineering*, 4(2) 116-124.
- Jacobsen S., Marchand, J., Boisvert, L. (1996). Effect of cracking and healing on chloride transport in OPC concrete. *Cem Concr Res* 26(6):869–881
- Jacobsen, S., Marchand, J., Gérard, B. (1998). Concrete crack I: durability and self-healing, E&FN Spon, *Concrete under severe conditions*, vol. 2, Tromso, pp. 217–231.
- Jensen, O., and Hansen, P. (1996). Autogenous Deformation and Change of the Relative Humidity in Silica Fume-Modified Cement Paste. *ACI Materials Journal*. 93(6) 539-543.

- Jensen, O., and Hansen, P. (2001). Water-Entrained Cement-based Materials I. Principles and Theoretical Background. *Cement and Concrete Research*, 31, 647-654.
- Jensen, O. M., and Hansen, P. F. (2002). Water-Entrained Cement-Based Materials: II. Experimental Observations,” *Cement and Concrete Research*, V. 32, No. 6, pp. 973-978.
- Ji, J. Darwin, D. and Browning, J. (2005). Corrosion Resistance of Duplex Stainless Steels and MMFX Microcomposite Steel for Reinforced Concrete Bridge Decks. SM Report No. 80, University of Kansas Center for Research, Inc., Lawrence, Kans., Dec. 2005, 423 pp
- Jones, W., House, M., and Weiss, J. (2014). Internal Curing of High Performance Concrete using Lightweight Aggregates and Other Techniques. Report No. CDOT-2014-3. Colorado Department of Transportation. Denver, CO.
- Keane, B., Ball, J., Dimmick, F., Emmons, P., Gillespie, T., Golter, H., Joyce, B., Lozen, K., Lund, J., Montani, R., Paul, J., Taylor, G., Watson, P., Whitmore, D. (2003) Structural Crack Repair by Epoxy Injection. *ACI RAP Bulletin* 1, p. 4
- Kendall, A., Keoleian, G.A., and Helfand, G.E. (2008). Integrated Life-Cycle Assessment and Life-Cycle Cost Analysis Model for Concrete Bridge Deck Applications. *Journal of Infrastructure Systems*, Vol. 14, No. 3, September 1, 2008. ©ASCE, ISSN 1076-0342/2008/3-214-222
- Kerkhoff, B. (2007). Effects of Substances on Concrete and Guide to Protective Treatments. Portland Cement Association, Skokie, IL.
- Kevern, J. T., and Farney C. (2012). Reducing curing requirements for pervious concrete with a superabsorbent polymer for internal curing. *TRB: Journal of Transportation Research Board*, No. 2290, Transportation Research Board of the National Academies, Washington, D.C., 2012, pp. 115-121, DOI: 10.3141/2290-15
- Kim, B., and Weiss, J. (2003). Using Acoustic Emission to Quantify Damage in Restrained Fiber-Reinforced Cement Mortars. *Cement and Concrete Research*, 33, 207-214.
- Kochanaski, T., Parry, J., Pruess, D., Schuchardt, L., and Ziehr, J. (1990). Premature Cracking of Concrete Bridge Decks Study. Final Report, Wisconsin Department of Transportation, Madison, WI
- Kosmatka, S.H., Wilson, M.L. (2011). *Design and Control of Concrete Mixtures*. 15th Ed., Portland Cement Association, Skokie, Illinois

- Krauss, P., and Rogalla, E. (1996). Transverse Cracking in Newly Constructed Bridge Decks. NCHRP Report No. 380, Transportation Research Board. Washington, D.C.
- La, H., Lim, R., Basily, B., Gucunski, N., Yi, J., Maher, A., Romero, F., Parvardeh, H. (2013). Mechatronic Systems Design for an Autonomous Robotic System for High-Efficiency Bridge Deck Inspection and Evaluation. 2013 IEEE International Conference on Automation Science and Engineering.
- Lawler, J. S.; Zampini, D.; and Shah, S. P. (2002). Permeability of Cracked Hybrid Fiber-Reinforced Mortar under Load. *ACI Materials Journal*, V. 99, No. 4, July-Aug. 2002, pp. 379-385.
- Lee, K., Lee, H., S.H., L., and Kim, G. (2006). Autogenous Shrinkage of Concrete Containing Granulated Blast-Furnace Slag. *Cement and Concrete Research*, 36, 1279-1285.
- Lee, B., Shin, D., Seo, J., Jung, J., Lee, J. (2011). Intelligent Bridge Inspection Using Remote Controlled Robot and Imaging Processing Technique. Proceedings of the 28th ISARC, 1426-1431. Seoul, Korea.
- Lenett, M., Griessmann, A., Helmicki, A., Aktan, A. (1999). Subjective and Objective Evaluations of Bridge Damage. Paper No. 99-0411. Transportation Research Board.
- Lepech, M. D., Geiker, M., & Stang, H. (2013). Probabilistic design and management of environmentally sustainable repair and rehabilitation of reinforced concrete structures. *Cement and Concrete Composites*.
- Li, C.Q. (2001). Initiation of chloride-induced reinforcement corrosion in concrete structural members. *ACI Structural Journal* 98(4):502–510.
- Li, V.C. and Stang, H. (2004). Elevating FRC Material Ductility to Infrastructure Durability. Proc. 6th RILEM Symposium on FRC, Varenna, Italy, September 20-22, 2004.
- Li, V.C., and Yang, E.-H. (2007) Self healing in concrete materials. S. van der Zwan (ed.), *Self Healing Materials- An alternative approach to 20 centuries of Materials Science*, 161-193, Springer
- Li, C.-Q., Yang, Y., and Melchers, R. E. (2008). Prediction of reinforcement corrosion in concrete and its effects on concrete cracking and strength reduction. *ACI Materials Journal*, 105 (1), 3–10.

- Life-365 Consortium II (2010). Life-365 Service life prediction model and computer program for predicting the service life and life-cycle cost of reinforced concrete exposed to chlorides, version 2.0.1 ed., 2010
- Lim, R., La, H. (2011). A Robotic Crack Inspection and Mapping System for Bridge Deck Maintenance. *IEEE*.
- Lindquist, W. D., Darwin, D., Browning, J., and Miller, G., (2006). Effect of Cracking on Chloride Content in Concrete Bridge Decks. *ACI Materials Journal*, Vol. 103, No. 6, pp. 467–473.
- Lindquist, W., Darwin, D., Browning, J. (2005). Cracking and Chloride Contents in Reinforced Concrete Bridge Decks. Report No. K-TRAN: KU -01-9. Kansas Department of Transportation.
- Liu, Y., and Weyers, R. (1998). Modeling the time-to-corrosion cracking in chloride contaminated reinforced concrete. *ACI Materials Journal*, 95 (6), 675–681.
- Lura, P., Pease, B., Mazzotta, G., Rajabipour, F., and Weiss, J. (2007). Influence of Shrinkage Reducing Admixtures on the Development of Plastic Shrinkage Cracks. *ACI Materials Journal*. 104(2) 187-194
- Lura, P., Van Breugel, K., and Maruyama, I. (2001). Effect of Curing Temperature and Type of Cement on Early-age Shrinkage of High-performance Concrete. *Cement and Concrete Research*, 31, 1867-1872.
- Madanat, S., Karlaftis, M., McCarthy, P. (1997). Probabilistic Infrastructure Deterioration Models with Panel Data. *ASCE Journal of Infrastructure Systems*, 3(1), 4-9.
- Madanat, S., Lin, D. (2000). Bridge Inspection Decision Making Based on Sequential Hypothesis Testing Methods. *Transportation Research Board*, Paper No. 00-0269, 14-18.
- Maser, K., Martino, N., Doughty, J., Birken, R. (2012). Understanding and Detecting Bridge Deck Deterioration with Ground-Penetrating Radar. *Journal of the Transportation Research Board*, No. 2313, 116-123.
- Malasheskie G., Maurer D., Mellott D., and Arellano J. (1988). Bridge Deck Protective Systems: Final Report. PennDOT research project #85-17, Report No. FHWA-PA-88-001+85-17
- Mauch, M., Madanat, S. (2001). Semiparametric Hazard Rate Models of Reinforced Concrete Bridge Deck Deterioration. *ASCE Journal of Infrastructure System*, 7(2), 49-57.

- McCann, D., Forde, M. (2001). Review of NDT methods in the assessment of concrete and masonry structures. *NDT&E International*, 34, 71-84.
- McLeod, H.A.K., Darwin, D., and Browning, J. (2009). Development and Construction of Low-Cracking High Performance Concrete (LC-HPC) Bridge Decks: Construction Methods, Specifications, and Resistance to Chloride Ion Penetration. SM Report No. 94. University of Kansas Center for Research. Lawrence. KS.
- McLeod, H. (2010). Development and Construction of Low-Cracking High-Performance Concrete Bridge Decks: Construction Methods, Specifications and Resistance to Chloride Ion Penetration. Report No. FHWA-KS-09-10. Kansas Department of Transportation.
- Mehta, P.K. (1997). Durability—Critical Issues for the Future. *Conc. Inter.*, 19(6), pp. 27-33.
- Mindess, S., Young, J. F., and Darwin, D., (2003). *Concrete*, 2nd ed., Pearson Education, Inc., Upper Saddle River, NJ, 644 pp.
- Minnesota Department of Transportation (2011). Bridge Deck Cracking. Transportation Research Synthesis.
- Mohammed, T. U., Otsuki, N., Hamada, H., and Yamaji, T. (2002). Chloride-induced corrosion of steel bars in concrete with presence of gap at steel-concrete interface. *ACI Materials Journal*, 99 (2), 149–156.
- Mokarem, D., Weyers, R., and Lane, D. (2005). Development of a shrinkage performance specifications and prediction model analysis for supplemental cementitious material concrete mixtures. *Cement and Concrete Research* 35, 918-925.
- Moore, M., Phares, B., Graybeal, B., Rolander, D., Washer, G. (2001). Reliability of Visual Inspection for Highway Bridges, Volume 1: Final Report. Report No. FHWA-RD-01-020. Federal Highway Administration (FHWA). Washington, D.C.
- Morcous, G., Rivard, H., and Hanna, A. M. (2002) “Modeling Bridge Deterioration Using Case-Based Reasoning”, *Journal of Infrastructure Systems*, ASCE, 8 (3), 86-95
- Morcous, G. (2006). Performance Prediction of Bridge Deck Systems Using Markov Chains. *ASCE Journal of Performance of Constructed Facilities*. Vol. 20, pp. 146-155.
- Morcous, G. (2011). Developing Deterioration Models for Nebraska Bridges. Project SPR-P1(11) M302. Nebraska Department of Roads.

- Morcous, G., Rivard, H., Hanna, A. (2002). Modeling Bridge Deterioration Using Case-based Reasoning. *ASCE Journal of Infrastructure Systems*, 8, 86-95.
- Moyer, W. (1988). Cracks in New Concrete Decks. Pennsylvania Department of Transportation. Memo sent to District Engineers.
- Mu, S., Schutter, G.D., Ma, B. (2013). Non-steady chloride diffusion in concrete with different crack densities”, *Materials and Structures, RILEM*, 46:123-133.
- National Bridge Inspection Standards (NBIS) (2004). 69 FR 74436.
- National Cooperative Highway Research Program (NCHRP) (2009). Protection for Life Extension of Existing Reinforced Concrete Bridge Elements. NCHRP Synthesis 398 Report, Transportation Research Board, Washington, D.C., 2009.
- Neville, A.M. (2002). Autogenous healing – a concrete miracle? *Concrete International* 24(11): 76–82.
- New York State Department of Transportation (1995). The State of the Art Bridge Deck. Final Report. The Bridge Deck Task Force. Albany, NY
- Nielson, R., Schmeckpeper, E., Shiner, C., and Blandford, M. (2011). The Effect of Bridge Design Methodology on Crack Control. Transportation Research Board (TRB) Annual Meeting. Washington, D.C.
- Nilsson, L.-O., Poulsen, E., Sandberg, P., Sorensen, H. E., and Klinghoffer, O. (1996). Hetek, chloride penetration into concrete state-of-the-art - transport processes, corrosion initiation, test methods and prediction models, Tech. Rep. Report No. 53, The Danish Road Directorate.
- Nilsson, L.-O., Sandberg, P., Poulsen, E., Tang, L., Anderson, A., and Frederiksen, J. M. (1997). Hetek: A system for estimation of chloride ingress into concrete – theoretical background, Tech. Rep. Report No. 83, Road Directorate, Danish Ministry of Transport.
- Nygaard, P. V. (2003). Effect of steel-concrete interface defects on the chloride threshold for reinforcement corrosion. Master’s thesis, Technical University of Denmark, Kgs. Lyngby, Denmark, 2003.
- Nygaard, P.V., Geiker, M. (2005). A method for measuring the chloride threshold level required to initiate reinforcement corrosion in concrete. *Materials and Structures*, 38 (278), 489– 494.

- Office of Management and Budget (2005). Discount rates for cost effectiveness, lease, purchase and related analyses. Appendix C to guidelines and discount rates for benefit-cost analysis of federal programs. Office of Management and Budget, Washington, D.C.
- Oh, J., Lee, A., Oh, S., Choi, Y., Yi, B., Yang, H. (2007). Design and Control of Bridge Deck Inspection Robot System. 2007 IEEE International Conference on Mechatronics and Automation.
- Ontario Ministry of Transportation (2000). Ontario Structure Inspection Manual. St. Catharines, Ontario, Canada.
- Otieno, M. B., Alexander, M. G., and Beushausen, H. D. (2010a). Corrosion in cracked and uncracked concrete - influence of crack width, concrete quality and crack re-opening. *Magazine of Concrete Research*, doi: 10.1680/macrc.2008.62.00.1
- Otieno M., Beushausen, H., Alexander, M. (2010b). Prediction of Corrosion Rate in RC Structures – A Critical Review. Modelling of Corroding Concrete Structures, Proceedings of the Joint fib-RILEM Workshop held in Madrid, Spain, 22–23 November 2010
- Ozbay, K., Jawad, D., Parker, N. A., and Hussain, S. (2003). Life cycle cost analysis: State-of-the-practice vs state-of-the-art. Proc., 83rd Annual Meeting of the Transportation Research Board, Transportation Research Board, Washington, D.C.
- Palle, S. Hopwood, T. (2006). Coatings, Sealants and Fillers to Address Bridge concrete Deterioration and Aesthetics-Phase 1. Kentucky Transportation Center Report No. KTCO6-36/SPR291-04-1F.
- PCA Cement Manufacturing Fact Sheet (2012), accessed 2012, http://www.cement.org/briefingkit/pdf_files/ManufacturingFactSheet.pdf
- Pease (2010). Influence of concrete cracking on ingress and reinforcement corrosion. PhD Thesis, Department of Civil Engineering, Technical University of Denmark (DTU), Civil Engineering Report R-233 (UK), December 2010
- Pendergrass, B., Darwin, D., Browning, J. (2011). Crack Surveys of Low-cracking High-performance Concrete Bridge Decks in Kansas. SL Report 11-3. Project No. TPF-5(174). Construction of Crack-free Bridge Decks Transportation Pooled-Fund Study.
- Pennsylvania Department of Transportation (PennDOT) (2009). Bridge Management System 2 (BMS2) Coding Manual. Pub 100A.

- Pennsylvania Department of Transportation. Reinforced Concrete Repair Drawing BC-783M. 2010.
- Pennsylvania Department of Transportation (PennDOT) (2011). Bridge Inspection Terminology and Sufficiency Ratings. PennDOT (2011) Specifications Publication 408
- Pettersson, K., and Jorgensen, O. (1996). The effect of cracks on reinforcement corrosion in high-performance concrete in a marine environment. Proceedings of the 3rd ACI/CANMET International Conference on the Performance of Concrete in the Marine Environment St Andrews-by-the-Sea, Canada, 163, 185–200.
- Phares, B.M., Graybeal, B. A., Rolander, D.D., Moore, M.E., and Washer, G.A. (2001). Reliability and Accuracy of Routine Inspection of Highway Bridges. *Transportation Research Record: Journal of the Transportation Research Board*, No. 1749, TRB, National Research Council, Washington, D.C., 82-92.
- Phares, B., Washer, G., Rolander, D., Graybeal, B., Moore, M. (2004). Routine Highway Bridge Inspection Condition Documentation Accuracy and Reliability. *ASCE Journal of Bridge Engineering*, 20, 403-413.
- Poppe, J.B. (1981). Factors Affecting the Durability of Concrete Bridge Decks. Report No. FHWA/CA/SD-81/2. Division of Transportation Facilities, California Department of Transportation, Sacramento, CA.
- Portland Cement Association (1970). Durability of Concrete Bridge Decks - A Cooperative Study. Final Report, Skokie, IL.
- Portland Cement Association (2011). Corrosion of Embedded Metals. [cited 2011 June]; Available from: http://www.cement.org/tech/cct_dur_corrosion.asp.
- Poyet, S., Charles, S., Honoré, N., L'hostis, V. (2011). Assessment of the unsaturated water transport properties of an old concrete: Determination of the pore-interaction factor. *Cement and Concrete Research*, Volume 41, Issue 10, October 2011, Pages 1015–1023
- Qi, C., Weiss, J., & Olek, J. (2003a). Characterization of Plastic Shrinkage Cracking in Fiber Reinforced Concrete Using Image Analysis and a Modified Weibull Function. *Materials and Structures*, 36, 386-395, July 2003.
- Qi, C. (2003b). Quantitative Assessment of Plastic Shrinkage Cracking and Its Impact on the Corrosion of Steel Reinforcement. Ph.D. Dissertation, Purdue University, West Lafayette, IN, May

- Radcliffe D.E., Simunek, J. (2010). *Soil physics with HYDRUS: modeling and applications*, Boca Raton, FL: CRC Press/Taylor & Francis. xiii, 373 p.
- Radlinska , A., Pease, B., and Weiss, J. (2007). A Preliminary Numerical Investigation on the Influence of Material Variability in the Early-age Cracking Behavior of Restrained Concrete. *Materials and Structures*. 40(4) 375-386
- Radlinska, A., Rajabipour, F., Bucher, B., Henkensiefken, R., Sant, G., and Weiss, J. (2008). Shrinkage Mitigation Strategies in Cementitious Systems: A Closer Look at Differences in Sealed and Unsealed Behavior. *Transportation Research Record*. 2070. 59-67.
- Radlińska, A., Bucher, B., and Weiss, J. (2008). Comments on the Interpretation of Results from the Restrained Ring Test. *Journal of ASTM International*, Vol.5(10).
- Radlinska, A., and Weiss, J. (2012). Toward the Development of a Performance-Related Specification for Concrete Shrinkage. *Journal of Materials in Civil Engineering*. 24(1) 64-71
- Radlinska, A., Yost, J., McCarthy, L., Matzke, J., & Nagel, F. (2012). *Coatings and Treatments for Beam Ends* (No. FHWA-PA-2012-002-100402).
- Radocea, A. (1994). A Model of Plastic Shrinkage. *Magazine of Concrete Research*. 46(167) 125-132
- Rahim, A., Jansen, D., and Abo-Shadi, N., (2006). *Concrete Bridge Deck Crack Sealing: An Overview of Research*. California Department of Transportation, Final report, Contract Number 59A0459
- Rajabipour, F., Sant, G., Weiss, J. (2008). Interactions between Shrinkage Reducing Admixtures and Cement Paste's Pore Solution. *Cement and Concrete Research*, 38 (5) 606-615
- Rajabipour, F., Wright, J., Laman, J., Radlińska, A., Morian, D., Jahangirnejad, S., Cartwright, C. (2012) *Longitudinal Cracking in Concrete at Bridge Deck Dams on Structural Rehabilitation Projects*. The Pennsylvania Department of Transportation Project Report, FHWA-PA-2012-006-100303, p.220
- Ramey, G., Wright, R. (1994). *Assessing and Enhancing the Durability/Longevity Performances of Highway Bridges*. HRC Research Project No. 2-13506. Highway Research Center.
- Ramey, G.E., Wolff, A.R., and Wright, R.L. (1997). Structural Design Actions to Mitigate Bridge Deck Cracking. *Practice Periodical on Structural Design and Construction*, 2(3) 118-124.

- Rapoport, J.; Aldea, C. M.; Shah, S. P.; Asce, M.; Ankenman, B.; and Karr, A. (2002). "Permeability of Cracked Steel Fiber-Reinforced Concrete," *Journal of Materials in Civil Engineering*, ASCE, V. 14, July-Aug. 2002, pp. 355-358.
- Reinhardt, H. W., and Jooss, M. (2003). "Permeability and Self-Healing of Cracked Concrete as a Function of Temperature and Crack Width," *Cement and Concrete Research*, V. 33, No. 7, pp. 981-985
- Rens, K., Nogueira, C., Transue, D. (2005). *Bridge Management and Nondestructive Evaluation*. ASCE Journal of Performance of Constructed Facilities, 19(1), 3-16.
- Richardson, M.G. (2002). *Fundamentals of durable reinforced concrete*. Modern concrete technology. London ; New York: Spon Press. xii, 260 p.
- Riding, K.A., Poole, J.L., Schindler, A.K., Juenger, M.C.G., and Folliard, K.J. (2006). "Evaluation of Temperature Prediction Methods for Mass Concrete Members." *ACI Materials Journal*, 103(5) 357-365
- Riding, K.A., Poole, J.L., Schindler, A.K., Juenger, M.C., and Folliard, K. (2008). "Quantification of Effects of Fly Ash Type on Concrete Early-Age Cracking." *ACI Materials Journal*, 105(2), 149-155.
- Riding, K., Poole, J., Schindler, A., Juenger, M., and Folliard, K. (2009). "Effects of Construction Time and Coarse Aggregate on Bridge Deck Cracking." *ACI Materials Journal*, 106(5), 448-454.
- Robelin, C. A., and Madanat, S. M. (2007). "History-dependent bridge deck maintenance and replacement optimization with Markov decision processes." *Journal of Infrastructure Systems*, 13(3), 195-201.
- Romero, F., Parvardeh, H. (2013). "Mechatronic Systems Design for an Autonomous Robotic System for High-Efficiency Bridge Deck Inspection and Evaluation." 2013 IEEE International Conference on Automation Science and Engineering.
- Ryan, T., Mann, E., Chill, Z., Ott, B. (2012). *Bridge Inspector's Reference Manual*. Federal Highway Administration (FHWA). Washington, D.C.
- Russell, H. (2004). *Concrete Bridge Deck Performance*. Synthesis 333. National Cooperative Highway Research Program. Transportation Research Board. Washington, D.C.

- Russell, H. (2013). High Performance Concrete Specifications and Practices for Bridges. Synthesis 441. National Cooperative Highway Research Program. Transportation Research Board. Washington, D.C.
- Saadeghvaziri, M., and Hadidi, R. (2002). Cause and Control of Transverse Cracking in Concrete Bridge Decks. Final Report No. FHWA-NJ-2002-19. Federal Highway Administration (FHWA), Washington, D. C.
- Saadeghvaziri, M.A., and Hadidi, R. (2005). Transverse Cracking of Concrete Bridge Decks: Effects of Design Factors. *Journal of Bridge Engineering*, 10(5) 511-519
- Sagüés, A.A., Kranc, S.C., Presuel-Moreno, F., Rey, D., Torres-Acosta, A., and Yao, L. (2001). Corrosion Forecasting for 75-Year Durability Design of Reinforced Concrete. Final Report No. BA502 submitted to Florida Department of Transportation by University of South Florida, December 31, 2001.
- Samson, E., and Marchand, J. (1999) Numerical Solution of the Extended Nernst-Planck Model. *Journal of Colloid and Interface Science*, 215, 1-8.
- Sang, Z. (2010). "A Numerical Analysis of the Shear Key Cracking Problem in Adjacent Box Beam Bridges." The Pennsylvania State University Graduate School.
- Sansone, J. M., and Bron M.C. (2007). The effect of cracking on reinforcement corrosion in concrete bridge decks. NACE International Corrosion Conference.
- Schiessel, P. (1995). Admissible Crack Width in Reinforced Concrete Structures. Contribution no. II, Inter- Association Colloquium on the Behavior of Interservice Concrete Structures, Preliminary Report V.II, Liegep. 3.
- Schiessl, P., and Raupach, M. (1997). Laboratory Studies and Calculations on the Influence of Crack Width on Chloride-Induced Corrosion of Steel in Concrete. *ACI Materials Journal*, Vol. 94(1), January- February, 1997, p. 56.
- Schmeckpeper, E., and Lecoultre, S. (2008). Synthesis into the Causes of Concrete Bridge Deck Cracking and Observations on the Initial Use of High Performance Concrete in the US 95 Bridge Over the South Fork of the Palouse River. Final Report KLK491 Report N08-05. Idaho Transportation Department.
- Shiltstone, J.M. (1990). Concrete Mixture Optimization. *Concrete International* 12 (6) 33-39.

- Shindler, A., Hughes, M., Barnes, R., Byard, B. (2010). Evaluation of Cracking of the US 331 Bridge Deck. Project 930-645. Alabama Department of Transportation.
- Schlitter, J., R. Henkensiefken, J. Castro, K. Raoufi, J. Weiss, and T. Nantung. (2010). Development of Internally Cured Concrete for Increased Service Life. Publication FHWA/IN/JTRP-2010/10. Joint Transportation Research Program, Indiana Department of Transportation and Purdue University, West Lafayette, Indiana, doi: 10.5703/1288284314262.
- Schmitt, T.R., and Darwin, D. (1995). Cracking in Concrete Bridge Decks. Report No. KTRAN: KU-94-1, Kansas Department of Transportation. Topeka. KS
- Schmitt, T.R., and Darwin, D. (1999). Effect of Material Properties on Cracking in Bridge Decks. *Journal of Bridge Engineering*, 4(1) 8-13.
- Scott, A., and Alexander, M.G. (2007). The influence of binder type, cracking and cover on corrosion rates of steel in chloride-contaminated concrete. *Magazine of Concrete Research*, 2007, 59, No.7, September, 495-505, doi: 10.1680/macr.2007.59.7.495
- Scott, M., Rezaizadeh, A., Delahaza, A., Santos, C., Moore, M., Graybeal, B., Washer, G. (2003). A comparison of nondestructive evaluation methods for bridge deck inspection. *NDT&E International*, 36, 245-255.
- Shahrooz, B., Gillum, A., Cole, J., and Turer, A. (2000). Bond Characteristics of Overlays Placed over Bridge decks sealed with High-Molecular-Weight Methacrylate. *Transportation research Record 1697*, TRB, National Research Council, Washington, D.C., pp. 24-30.
- Shiltstone, J.M. (1990). Concrete Mixture Optimization. *Concrete International* 12 (6) 33-39.
- SIMCO Technologies Inc. (2009). Description of the STADIUM model, 203 - 1400 boul. du Parc-Technologique, Quebec, Canada, available at www.simcotechnologies.com
- Snyder, K.A., and Clifton, J.R. (1995). 4SIGHT Manual: A computer program for modeling degradation of underground low level waste concrete vaults. NISTIR 5612, National Institute of Standards and Technology, Gaithersburg, MD.
- Sobanjo, J., O. State transition probabilities in bridge deterioration based on Weibull sojourn times. *Structure and Infrastructure Engineering: Maintenance, Management, Life-Cycle Design and Performance*, 7:10, 747-764

- Sohanghpurwala, A. (2006). Manual on Service Life of Corrosion Damaged Reinforced Concrete Bridge Superstructure Elements. NCHRP Report 558, Transportation Research Board, Washington, D.C.
- Sprinkel, M.M., and DeMars, M. (1995). Gravity-fill Polymer Crack Sealers. Transportation Research Record 1490, TRB, National Research Council, Washington, D.C., pp 43-53.
- Suzuki, K., Ohno, Y., Praparntanatorn, S., and Tamura, H. (1990) Mechanism of steel corrosion in cracked concrete. In Corrosion of Reinforcement in Concrete (Page C, Treadaway K and Bramforth P (eds)). Society of Chemical Industry, London, pp. 19–28.
- Synder, K. A. (2001). Validation and modification of the 4sight computer program, National Institute of Standards and Technology (NIST), Gaithersburg, Maryland.
- Tabatabai, H. Ghorbanpoor, A. and Turnquist-Nass, A. (2005). Rehabilitation Techniques for Concrete Bridges. Wisconsin Highway Research Program, Report Number WHRP 05-01
- Tabatabai, H., Ghorbanpoor, A., and Pritzl, M.D. (2009). Evaluation of Select Methods of Corrosion Prevention, Corrosion Control, and Repair in Reinforced Concrete Bridges. Rep. no. No. 00920606. Wisconsin Highway Research Program
- Tawfiq, K., Armaghani, J., and Vysyaraju, J.-R. (1996). Permeability of Concrete Subjected to Cyclic Loading,” Transportation Research Record, V. 1532, No. 1, pp. 51-59.
- Tex-470-A (2006), Optimized Aggregate Gradation for Hydraulic Cement Concrete Mix Designs, TxDOT
- Thompson, N., Yunovich, M., and Dunmire, D. J., (2005). Corrosion Costs and Maintenance Strategies - A Civil/Industrial and Government Partnership. Materials Performance, Vol. 44, No. 9, pp. 16–20.
- Thompson, P. D., Small, E. P., Johnson, M., and Marshall, A. R. (1998). The Pontis Bridge management system. *Struct. Engrg. Int.*, Zurich, 8(4), 303-308.
- Tokdemir, O., Ayvalik, C., Mohammadi, J. (2000). Prediction of Highway Bridge Performance by Artificial Neural Networks and Genetic Algorithms.
- Tol, R. S. J. (1999). The marginal costs of greenhouse gas emissions. *Energy*, 20(1), 61–81.

- Tol, R. S. J., Heintz, R. J., and Lammers, P. E. A. (2003). Methane emission reduction: An application of FUND. *Clim. Change*, 57(1–2), 71–98.
- Transpo Industries. *Sealate (T-70 & T-70 MX-30) High Molecular Weight Methacrylate*. Product Brochure. Transpo Industries, New Rochelle, NY.
- Transportation Research Board (TRB) (2004). Concrete Bridge Deck Performance. Synthesis 333. TRB National Cooperative Highway Research Program. Washington, D.C.
- Transportation Research Board (TRB) (2006) Control of cracking, state of the art. TRANSPORTATION RESEARCH CIRCULAR E-C107, October 2006
- Transportation Research Board (TRB) (2013). High Performance Concrete Specifications and Practices for Bridges. Synthesis 441. TRB National Cooperative Highway Research Program. Washington, D.C.
- Tsukamoto, M. (1990). Tightness of Fiber Concrete. *Darmstadt Concrete*, 5, 215-225.
- Tuutti K. (1982). Corrosion of Steel in Concrete. Swedish foundation for concrete research, Stockholm.
- Van der Wielen, A., Courard, L., Nguyen, F. (2010). Nondestructive Detection of Delaminations in Concrete Bridge Decks. 13th International Conference on Ground Penetrating Radar.
- van Noortwijk, J. M., and Frangopol, D. M. (2004). Two probabilistic life-cycle maintenance models for deteriorating civil infrastructures. *Probab. Eng. Mech.*, 19, 345–359.
- Virginia Department of Transportation (1997). Specifications for Highway and Bridge Construction. Richmond, VA.
- Virginia Department of Transportation (2009). Guide Manual for Causes and Repair of Cracks in Bridge Decks. Virginia Department of Transportation Guide Manual.
- Virmani, Y. P., and Clemeña, G. G. (1998). Corrosion Protection—Concrete Bridges. *Report No. FHWA-RD-98-088*, Federal Highway Administration, McLean, Va., 80 pp.
- Vu, K., Stewart, M., and Mullard, J. (2005). Corrosion-induced cracking: Experimental data and predictive models, *ACI Structural Journal*, 102 (5), 719–726.
- Wang, K., Jansen, D. C., Shah, S. P., and Karr, A. F. (1997). Permeability Study of Cracked Concrete. *Cement and Concrete Research*, V. 27, No. 3, pp. 381-393.

- Weiss, J., Lura, P., Rajabipour, F., Sant, G. (2008). Performance of Shrinkage Reducing Admixtures at Different Humidities at Early Ages. *ACI Materials Journal*, 105 (5) 478-486
- Wenzlick, J.D. (2007). *Bridge Deck Concrete Sealers*. Missouri Department of Transportation Report No. OR07-009.
- Wittke, W. (1990). *Rock mechanics—Theory and applications with casehistories*. Springer, Berlin.
- Wittmann, F.H. (1976). On the Action of Capillary Pressure on Fresh Concrete. *Cement and Concrete Research*, 6(1) 49-56
- Yang, Z., Weiss, W. J., and Olek, J. (2004). Interaction Between Micro-Cracking, Cracking, and Reduced Durability of Concrete: Developing Methods for Considering Cumulative Damage in Life-Cycle Modeling. Publication FHWA/IN/JTRP-2004/10. Joint Transportation Research Program, Indiana Department of Transportation and Purdue University, West Lafayette, Indiana. doi: 10.5703/ 1288284313255.
- Yano, M., Iida, T., Kawabata, K., and Miyazato, S. (2002). Steel corrosion induced by chloride and carbonation in concrete with defects, in *The Ninth East Asia-Pacific Conference on Structural Engineering and Construction*, pp. 62–68.
- Yehia, S., Abudayyeh, O., Abdel-Qader, I., Zalt, A. (2008). Ground-Penetrating Radar, Chain Drag, and Ground Truth: Correlation of Bridge Deck Assessment Data. *Journal of the Transportation Research Board*, No. 2044, 39-50.
- Yehia, S., Abudayyeh, O., Fazal, I., Randolph, D. (2008) A decision support system for concrete bridge deck maintenance. *Advances in Engineering Software*, 39 (3): 2002-210
- Yunovich, M., Thompson, N. G., and Virmani, Y. P. (2005). Corrosion Protection System for Construction and Rehabilitation of Reinforced Concrete Bridges. *International Journal of Materials and Product Technology*, Vol. 23, No. 3/4, pp. 269– 285.

Appendix A: 40 Inspected Bridges

Table 33. Detailed information for 40 inspected bridges

Bridge Number	Protective System	Concrete Type	Wearing Surface	Year Built	Age (years)	Bridge Material	District	Traffic Route	ADT (current)	Beam Type- Bridge Type	No. of Spans	Structure Length (ft)
20613	None	AA	LMC	1978	36	Steel	4	SR	6604	Steel cont.- Stringer/Girder	2	251
20507	None	AA	LMC	1993	21	Steel	4	I	10216	Steel cont.- Stringer/Girder	3	473
20506	None	AA	LMC	1977	37	Steel	4	I	9589	Steel cont.- Stringer/Girder	3	485
30700	None	AA	Bituminous	1964	50	Steel	5	PA	3716	Stringer/Girder	1	100
30752	None	AA	Bituminous	1924	90	Concrete	5	SR	341	Concrete tee beam	1	34
4908	Epoxy-coated rebar	AA	Original	1962	52	Concrete	5	SR	5185	P/S con.- Multiple Beam Box	1	39
30643	Epoxy-coated rebar	AA	Original	1979	35	Concrete	5	US	4188	P/S con.- Single/Spread Box	1	60
5081	Epoxy-coated rebar	AA	Original	1978	36	Concrete	5	SR	8791	P/S con.- Multiple Beam Box	1	187
12893	Epoxy-coated rebar	AA	Original	1980	34	Steel	1	US	7134	Steel-Truss-Thru	2	300
36077	Epoxy-coated rebar	AA	Original	1977	37	Concrete	12	SR	7317	P/S con.- Single/Spread Box	3	149
36082	Epoxy-coated rebar	AA	Original	1977	37	Concrete	12	SR	6721	P/S con.- Stringer/Girder	3	206

Bridge Number	Protective System	Concrete Type	Wearing Surface	Year Built	Age (years)	Bridge Material	District	Traffic Route	ADT (current)	Beam Type- Bridge Type	No. of Spans	Structure Length (ft)
36084	Epoxy-coated rebar	AA	Original	1977	37	Concrete	12	SR	7317	P/S con.- Stringer/Girder	3	221
6457	Epoxy-coated rebar	AAA	Original	2011	3	Concrete	3	SR	89	P/S con.- Multiple Beam Box	1	85
12524	Epoxy-coated rebar	AAA	Original	2006	8	Steel	3	SR	14936	Steel cont.- Stringer/Girder	3	108
19168	Epoxy-coated rebar	AAA	LMC	2008	6	Concrete	10	US	3447	P/S con.- Single/Spread Box	3	159
12905	Epoxy-coated rebar	AAA	Original	1987	27	Steel	1	US	8533	Steel-Truss- Thru	1	203
8410	Epoxy-coated rebar	AAA	Original	1994	20	Concrete	9	PA	22909	P/S con.- Single/Spread Box	1	43
8406	Epoxy-coated rebar	AAA	Original	1994	20	Concrete	9	PA	18577	P/S con.- Stringer/Girder	1	38
3574	Epoxy-coated rebar	AAA	Original	2010	4	Concrete	11	PA	4879	P/S con.- Single/Spread Box	2	97
8407	Epoxy-coated rebar	AAA	Original	1994	20	Concrete	9	PA	18577	P/S con.- Single/Spread Box	1	73
19551	Epoxy-coated rebar	AAA	Original	1983	31	Concrete	10	PA	9948	P/S con.- Single/Spread Box	1	120
34391	Epoxy-coated rebar	AAA	Original	1993	21	Concrete	12	US	4845	P/S con.- Stringer/Girder	1	159
19724	Epoxy-coated rebar	AAA	Epoxy Overlay	1984	30	Concrete	10	SR	439	P/S con.- Stringer/Girder	2	181

Bridge Number	Protective System	Concrete Type	Wearing Surface	Year Built	Age (years)	Bridge Material	District	Traffic Route	ADT (current)	Beam Type- Bridge Type	No. of Spans	Structure Length (ft)
19784	Epoxy-coated rebar	AAA	Original	2009	5	Concrete	10	SR	138	P/S con.- Multiple Beam Box	2	168
47335	Epoxy-coated rebar	AAAP	Original	2012	2	Concrete	12	I	33967	P/S cont.- Single/Spread Box	2	173
11525	Epoxy-coated rebar	AAAP	Original	2012	2	Steel	2	PA	717	Steel cont.- Stringer/Girder	2	147
12517	Epoxy-coated rebar	AAAP	Original	2014	0	Concrete	3	I	15097	P/S con.- Multiple Beam Box	3	127
12518	Epoxy-coated rebar	AAAP	Original	2014	0	Concrete	3	I	15097	P/S con.- Single/Spread Box	3	115
26993	Galvanized Rebar	AA	Original	1976	38	Concrete	5	SR	707	P/S con.- Stringer/Girder	1	53
21651	Galvanized Rebar	AA	Original	1976	38	Concrete	8	SR	12775	P/S con.- Single/Spread Box	1	85
251	Galvanized Rebar	AA	Original	1977	37	Concrete	8	SR	294	Concrete/Fram e	1	18
252	Galvanized Rebar	AA	Original	1977	37	Concrete	8	SR	294	Concrete/Fram e	1	28
20588	Galvanized Rebar	AAA	LMC	2009	5	Concrete	4	I	14116	P/S con.- Single/Spread Box	3	162
20589	Galvanized Rebar	AAA	LMC	2009	5	Concrete	4	I	14441	P/S con.- Single/Spread Box	3	149
19170	Other-Coated Rebar	AAA	Original	2010	4	Steel	10	US	3447	Steel cont.- Stringer/Girder	3	196

Bridge Number	Protective System	Concrete Type	Wearing Surface	Year Built	Age (years)	Bridge Material	District	Traffic Route	ADT (current)	Beam Type- Bridge Type	No. of Spans	Structure Length (ft)
637	Polymer Impregnated	AAA	LMC	2008	6	Steel	11	PA	11827	Steel-Stringer/Girder	1	187
639	Polymer Impregnated	AAA	LMC	2008	6	Steel	11	PA	14243	Steel-Stringer/Girder	1	196
652	Polymer Impregnated	AAA	LMC	2005	9	Concrete	11	PA	12953	P/S cont.-Stringer/Girder	3	153
924	Polymer Impregnated	AAA	Bituminous	2009	5	Steel	11	I	19642	Steel-Stringer/Girder	1	238
645	Polymer Impregnated	AAA	LMC	2008	6	Steel	11	PA	18029	Steel cont.-Stringer/Girder	2	326
644	Polymer Impregnated	AAA	LMC	2008	6	Steel	11	PA	15442	Steel cont.-Stringer/Girder	2	326

Appendix B: Bridge Deck Inspection Protocols

Equipment

The following equipment is necessary for each inspection:

- 300' measuring tape
- Hand-held measuring tape
- Hammer and nails
- Crack comparator card
- Digital camera (tripod optional)
- Coring drill
- Wrapping material
- Patching material
- Sounding tool (rebar or chain drag)

Traffic Control

Immediately after arriving to the bridge site, traffic control will be established according to PennDOT Publication 213 – “Temporary Traffic Control Guidelines”

Crack Inspection

The inspections will begin with the right-hand lane and the right-hand shoulder and traffic control will be set up accordingly. An origin (reference point) will be established on the deck at the intersection of the expansion joint and the longitudinal axis of the right-hand side of the deck (i.e., parapet or curb). The x-axis will be along the right-hand side of the deck and the y-axis will extend transversely along the width of the deck. A measuring tape will start from the origin and continue along the length of the deck in the direction of the second pier.

The surface of the bridge deck will be observed for any visible cracks. Note: The inspector should only mark cracks which are visible when bending at the waist. Once a crack is detected the inspector will number the cracks using suitable markers/crayons. After detecting the crack the inspector can examine the surface with more detail and mark the start and end point of each crack with “X” marks. Afterwards, the inspectors will record the crack number, orientation (i.e., transverse, longitudinal or diagonal), average width, and location of start and end points of all cracks on the area of the deck (area enclosed by the curbs/parapets) using the “Bridge Deck Cracking Inspection Form” (Table 35). The x-coordinates of each point can be determined using the measuring tape that is placed along the x-axis. The y-coordinates will be determined by measuring the perpendicular distance from the point’s location to the edge of the bridge deck (i.e., length along y-axis). Approximate average crack widths will be measured using a comparator card.

Once the right-hand lane and shoulder are completed, traffic control will be adjusted to close off and inspect the left-hand lane (or any additional lanes) and shoulder (if applicable). The traffic

control set up will be adjusted accordingly until all lanes of the bridge deck have been inspected. Throughout the inspections for each bridge deck, the origin (0,0 reference point) will be kept constant and all coordinates will be recorded according to this point. For example, the origin can be set at the intersection of the skew line and the right-hand edge of the deck. When inspecting the left-hand lane, the x-axis measuring tape can be placed at a corresponding point ($x=0$) on the left-hand edge of the deck. This point can be identified using the skew angle (α) and distance from the right-hand edge to the left-hand edge (Y_{width}). Also the (Y) coordinates can be obtained using the distance of the point to the left-hand edge (\bar{Y}), and the distance from the right-hand edge to the left-hand edge (Y_{width}). For ease of notation, the \bar{Y} coordinates can be recorded and the Y-coordinates can be calculated using the Y_{width} afterwards.

Pictures should be taken of each crack using a digital camera (tripod optional). Preferably the picture should be taken at the intersection of the crack and the measuring tape, and the crack number should be visible in the picture. The inspector should note the general condition of the parapets and approach slabs. The inspector should also take pictures of any forms of distress on the deck including, but not limited to, patching, spalling, crack sealing, etc. Any relevant observations about these distresses should be recorded in the “notes” section of the inspection form.

Figure 95 and Table 34 show an example of crack inspection data for different types of cracks on a 1-direction 2-lane bridge deck.

Coring

Concrete coring will be performed using water-cooled/lubricated diamond impregnated core sampling bits mounted on a portable, trailer-mounted, or truck-mounted coring rig, according to the ASTM C 42 (2013) standard procedure.

Step 1. Core location: The location and position of test points will be identified using the FHWA global or local rectangular coordinate system (Protocol PRE001). The location of the cores will be determined on-site. 2 cores (3 inches in diameter) will be taken from each deck: one from on-crack and one off-crack location.

Step 2. Reinforcement detection: The surface will be cleaned of debris. Concrete pachometer (cover meter) will be used to locate reinforcement, indicating transverse (or skewed) reinforcement in the vicinity of the core location. Depth of detected reinforcement will be noted and recorded. Pictures will be taken of locations before test, after bar location and after coring is completed to show results.. Any details concerning the particular procedure in the “comment” field will be reported. It will be attempted to extract cores at locations of transverse rebar and, if possible, at locations where transverse and longitudinal rebar intersect. If the element incorporates prestressed/post-tensioned strand, extra care will be taken to detect and avoid these elements. If a feature that was to be avoided is encountered and impacted by the sampling method, the owner agency of the structure will be notified immediately. The owner shall be consulted regarding appropriate remedial actions to be taken.

Step 3. Coring precautions: Before coring, intended core depth will be marked onto coring bit with permanent marker. The desired depth of each core will be a minimum of 5 inches.

Step 4. Coring the Concrete: Once reinforcement is located, the core bit will be mounted onto the coring machine and adequate water will be placed in the reservoir for cooling. Care will be taken so that the core bit is perpendicular to the deck surface. Cooling water will be supplied to the bit and coring will begin. Care will be taken so that the bit doesn't advance too quickly by the application of too much pressure. While coring, it will be ensured that cooling water flows steadily from the core hole and the depth of penetration of the bit will be monitored. The coring laitance around the hole will be observed for evidence of steel shavings. During steel penetration, the coring rate may need to be slowed to enable the bit to cut through the stronger steel material.

Step 5. Sample Extraction: If coring at a location of delamination, the top portion of concrete will come loose in the core barrel once delamination depth is reached. Coring will be immediately stopped and the loose top section will be removed and retained, after which, further work will proceed. Coring will stop once the desired depth has been reached. Using a hammer and flat-head screwdriver, chisel, or other suitable lever instrument, the lever will be inserted into the annular space of the core and gently tapped with the hammer. This procedure may be repeated along different sectors of the core until the bond at the bottom of the core is broken. The core extraction tool will be used to grab the core and pull it out of the core hole. In some cases where reinforcement is taken within the core, particularly where epoxy-coating inhibits the bond of concrete to reinforcement, the core may break at the plane of reinforcement rather than at the bottom of the core. Coring will immediately stop and the loose top section will be removed and retained, then coring will proceed to the desired depth.

Step 6. Sample Storage: Prior to wrapping the specimen, the general dimensions of the core will be measured and recorded. The core diameter and the core length will be measured and recorded in accordance with ASTM C174 (2013). To preserve the "as-is" condition of the concrete, the cores will be allowed to air dry only long enough for visible water (from coring) on the core perimeter to evaporate. The core and all pieces will be clearly marked with permanent marker to indicate the structure and sample number as well as the orientation of the core in the structural element from which it was taken. Promptly (within 1 hour of extracting the core) the specimen will be wrapped in two layers (4-mil polyethylene sheet or similar, and duct tape) to preserve in-place moisture state of the concrete, and then the external wrapping will be clearly labeled with a unique sample number. The sample number will consist of the structure number, element from which the sample was taken ("Deck") and a sequential integer beginning with 1.

Step 7. Repair of Sample Locations: Each location where physical sampling results in a hole in the concrete element it should be repaired before leaving the site. The method of repair will be coordinated with and approved by the bridge owner/ agency. The use of rapid set cementitious repair materials is generally recommended, though gel-type polymer mortars may be used. Repairs to overlays or membranes should be compatible with the base material and approved by the owner. Allow deck repair materials time to reach adequate strength prior to opening to traffic.

Step 8. Sample Documentation: A log of samples obtained will be kept; the location and position of samples from the deck will be recorded according to the established coordinate system (FHWA

(2013) PRE001. The size, length (ASTM C 174 (2013)) and orientation of the sample and the structure identification will be recorded. If present, the orientation and depth of steel reinforcement as well as its visible condition will be documented. Also, the hole from which the core was removed will be observed for evidence of cracks, delaminations, and other features, such as reinforcement or other embedded items at the base or side of the core hole.

The specimens will be taken to the lab for chloride profile testing and visual observations of rebar condition. Whether or not rebar corrosion has initiated and the location of rust products relative to the rebar orientation (e.g., above or below rebar) will be noted. Also the crack geometry, depth will be observed for on-crack cores.

Required equipment: concrete pachometer (cover meter), permanent marker, temporary chalk marker water-cooled core-drilling machine (portable or vehicle-based, as appropriate), water (for cooling), wet-dry vacuum (with filter for cleaning core holes before patching), clean rags, diamond-impregnated coring bit(s) of appropriate diameter, wrapping materials, approved patching materials and hand tools, e.g., hammer, chisel or flat-head screwdriver, core extraction tool.

Sounding

Suitable rods or chains as specified in ASTM D4580 will be used for sounding of the bridge deck. The entire surface of the deck will be surveyed. On non-delaminated concrete, a clear ringing sound will be heard. A dull or hollow sound is emitted when delaminated concrete is encountered. Mark the areas of delamination on the deck surface with the spray paint or lumber crayon. Construct a scaled map of the deck surface. By referencing to the established grid system on the deck, plot the areas of delamination on the map. Determine the total area contained in the individual delaminated areas. Divide the total delaminated area by the total bridge deck area and multiply by 100 to yield the percent of deck area delaminated. The 2-ft wide chain set up shown in [Figure 94](#) shows a bridge deck being sounded by chain dragging.



Figure 94. Inspectors conducting chain drag on deck. (FHWA 2013)

Please note only a rough outline of the delaminated areas on the bridge deck map is required. The approximate location of delamination is sufficient and the use of a hammer will not be required. A template grid to be filled out is shown in [Figure 96](#). This grid has fields of 2ft by 2ft. The areas of delamination can be marked by highlighting the fields corresponding to the delaminated areas.

Post Inspection Analysis

Using the data recorded in the “Bridge Deck Cracking Inspection Form”(Table 35), additional analysis should be performed as follows:

- Calculate the crack density (yd/yd²) of the deck.

$$\text{crack density} = \frac{\sum \text{crack lengths}}{\text{deck area}}$$

Note: the crack density should also be calculated for each span, the positive and negative moment regions of each span, and transverse/longitudinal/diagonal cracks.

- Calculate the average crack width (in.).
- If necessary, create a crack map of the bridge deck showing lengths, widths, orientations, and locations of all cracks.
- Calculate the percentage of delaminated deck area.

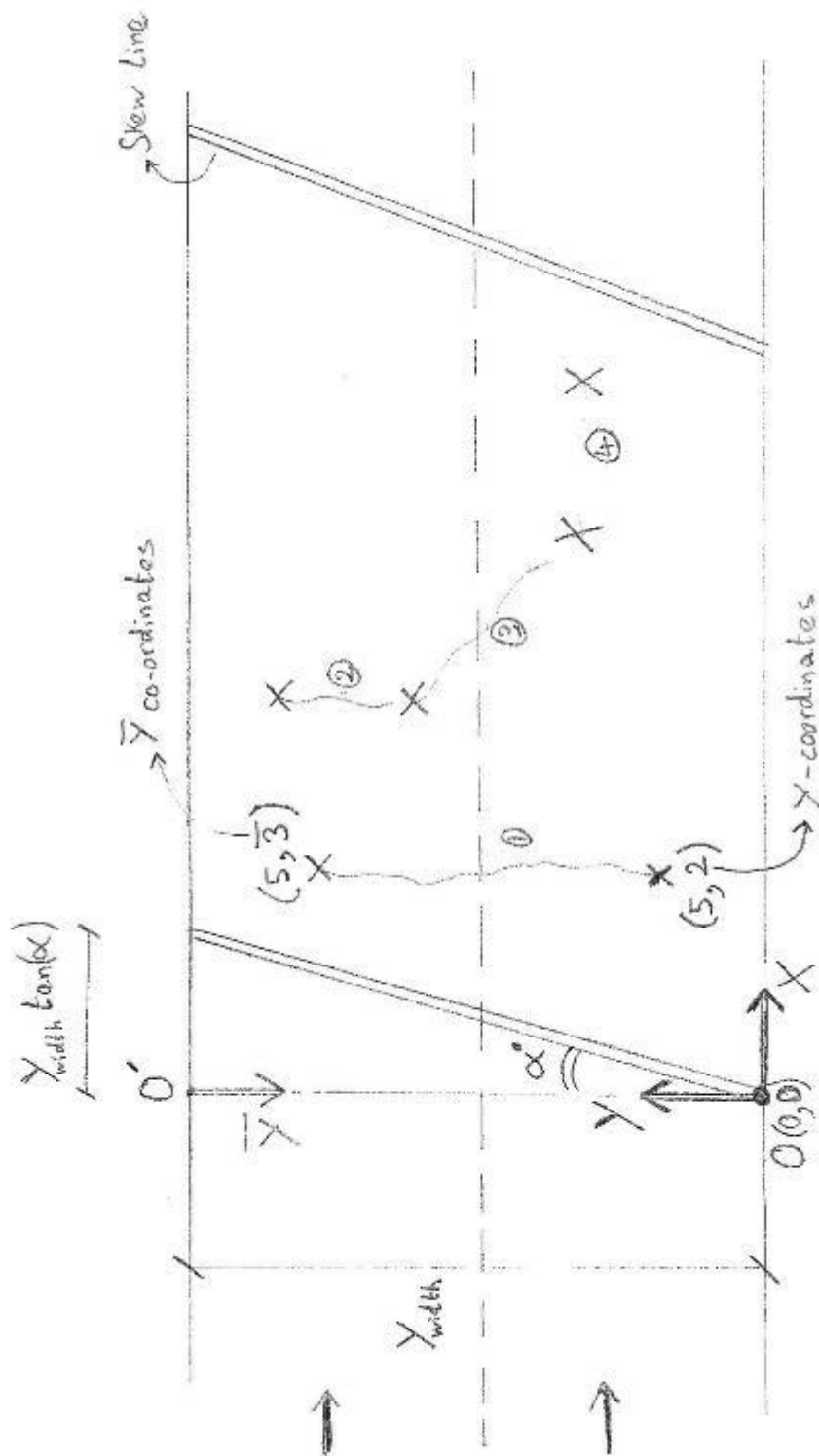


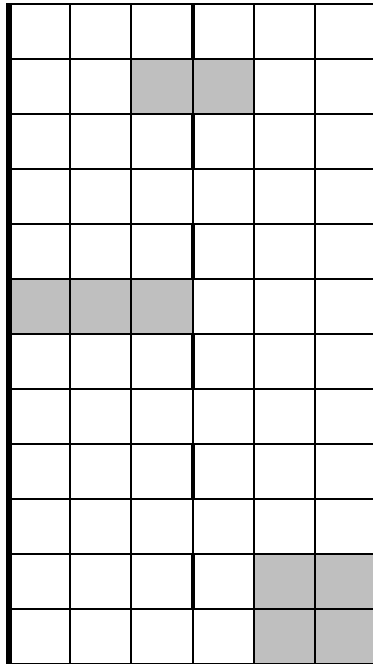
Figure 95. Example of crack inspection data for 1-direction 2-lane bridge deck

Table 34. Example of crack inspection form for Figure 44

Bridge Deck Cracking Inspection						
Bridge Information				Date		
	ECMS			Inspector		
	SR/Section					
	Structure Number					
	BMS Number					
	Crack #	Orientation (T/L/D)*	Start point (X, Y)	End Point (X, Y)	Width (in.)	Notes
Span 1	1	T	5,2	5,*3	-	sealed
	2	T	7,*2	7,*4	0.012	
	3	D	7,*4	9,3	0.012	
	4	L	9,3	11,3	0.005	

Please note:

- In the example above, all coordinates are schematic and approximate representations of the crack conditions shown in the figure above.
- In the table above, the * sign represents a reading made on the \bar{Y} axis.



Highlighted area= delamination

Figure 96. Example grid to be used for chain drag testing (sounding)

Table 35. Bridge Deck Cracking Inspection Form

Bridge Deck Cracking Inspection						
Bridge Information				Date		
	ECMS			Inspector		
	SR/Section					
	Structure Number					
	BMS Number					
	Crack #	Orientation (T/L/D)*	Start point (X, Y)	End Point (X, Y)	Width (in.)	Notes
Span 1						
Span 2						
Span 3						
* T = transverse, L = longitudinal, D = diagonal						
<u>Parapet Condition:</u>						
<u>Approach Slab Condition:</u>						
<u>Notes:</u>						

Appendix C: Core Sample Testing Procedure

Chloride Content Testing

The procedure for the sample preparation, chloride content testing, and calculations were as follows:

- 1) Extract at least 10g of powdered concrete at the rebar level for each core,
 - a. For cores with LMC overlays: Extract an additional 10 g sample from the LMC layer close to the concrete-overlay interface,
- 2) Disperse 10 g of powdered sample with 75 ml of deionized water,
- 3) Slowly add nitric acid drop-wise, while stirring with a glass rod in order to break up any lumps. Continue adding nitric acid so that the acidity of the solution reaches below a pH of 3 (i.e., until methyl orange indicator turns pink/red in the solution). The amount required for the pH to decrease to this level was about 10 ml of 40% Nitric Acid for each sample,
- 4) Add 3 ml of Hydrogen Peroxide and allow to stand for about 1-2 min,
- 5) Heat the solution in a covered beaker rapidly to boiling and remove from hot plate. The solution should not be allowed to boil for more than 10 seconds,
- 6) Conduct chromatography analysis (explained in detail in following paragraphs) on 10 ml of prepared solution. The chromatography test results will provide the chloride concentration of the solution (mg/L),
- 7) The chloride concentration (c_v) obtained from the chromatography result and the total volume of the solution containing the powdered concrete sample are used to calculate the total chloride weight (W_c) of the 10 g sample as shown in Equation (3).

$$W_c = c_v \times V \times 1000 \quad (3)$$

where W_c = total weight of acid-soluble chloride in 10 g powdered concrete sample (g)

c_v = chloride concentration of solution containing powdered sample obtained from chromatography testing (mg/L)

V = total volume of solution containing powdered sample (L)

- 8) Using the weight of the powdered concrete sample and total chloride weight, the chloride content (% weight of concrete) can be calculated according to Equation (4) below.

$$C = \frac{W_c}{W_{sample}} \quad (4)$$

where W_{sample} = weight of the powdered concrete sample (~10 g)

C = chloride content (% weight of concrete)

4110 DETERMINATION OF ANIONS BY ION CHROMATOGRAPHY*

4110 A. Introduction

Determination of the common anions such as bromide, chloride, fluoride, nitrate, nitrite, phosphate, and sulfate often is desirable to characterize a water and/or to assess the need for specific treatment. More recently, the need to measure the concentration of the disinfection by-products chlorite, chlorate, and bromate has arisen. Although conventional colorimetric, electrochrometric, or titrimetric methods are available for determining individual anions, ion chromatography provides a single instru-

mental technique that may be used for their rapid, sequential measurement. Ion chromatography eliminates the need to use hazardous reagents and it effectively distinguishes among the halides (Br^- , Cl^- , and F^-) and the oxyhalides (ClO_2^- , ClO_3^- , and BrO_3^-), and the oxy-ions (PO_4^{3-} , SO_4^{2-} , NO_2^- , and NO_3^-).

Methods 4110B and 4110C are applicable, after filtration to remove particles larger than $0.45 \mu\text{m}$, to surface, ground, and wastewaters as well as drinking water. Some industrial process waters, such as boiler water and cooling water, also may be analyzed by this method. Method 4110D is applicable to untreated and finished drinking water as well as drinking water at various stages of treatment.

* Approved by Standard Methods Committee, 2000. Editorial revisions, 2011. Joint Task Group: 21st Edition—Richard Mosher (chair), Bruce A. Hale, Daniel P. Hartman, Peter E. Jackson, S. V. Karmakar, James Krol, James W. O'Dell, Roy-Keith Smith.

4110 B. Ion Chromatography with Chemical Suppression of Eluent Conductivity

1. General Discussion

a. Principle: A water sample is injected into a stream of eluent and passed through a series of ion exchangers. The anions of interest are separated on the basis of their relative affinities for a low-capacity, strongly basic anion exchanger (guard and analytical columns). The separated anions are directed through a suppressor device that provides continuous suppression of eluent conductivity and enhances analyte response. In the suppressor the separated anions are converted to their highly conductive acid forms while the conductivity of the eluent is greatly decreased. The separated anions in their acid forms are measured by conductivity. They are identified on the basis of retention time as compared to standards. Quantitation is by measurement of peak area or peak height.

b. Interferences: Any substance that has a retention time coinciding with that of any anion to be determined and produces a detector response will interfere. Low-molecular-weight organic acids, bromate, and chlorite may interfere with the determination of chloride and fluoride. A high concentration of any one ion also interferes with the resolution, and sometimes retention, of others. Sample dilution or gradient elution overcomes many interferences. To resolve uncertainties of identification or quantitation use the method of known additions. Spurious peaks may result from contaminants in reagent water, glassware, or sample processing apparatus. Modifications such as preconcentration of samples, gradient elution, or reinjection of portions of the eluted sample may alleviate some interferences but require individual validation for precision and bias and are beyond the scope of this method.

c. Method detection level: The detection level of an anion is a function of sample size. Table 4110:1 presents detection levels obtained for reagent water with a $25\text{-}\mu\text{L}$ sample loop. Detection levels in natural waters may be substantially higher because of the presence of high levels of some of the anions.

TABLE 4110:1. DETECTION LEVEL FOR ANIONS IN REAGENT WATER.*

Anion	MDL $\mu\text{g/L}$
Fluoride	2.0
Chloride	4.0
Nitrite-N	3.7
Bromide	14
Nitrate-N	2.7
Orthophosphate-P	14
Sulfate	18

* See Figure 4110:1 for experimental conditions.

d. Limitations: Exercise caution if this method is used to determine F^- in unknown matrices. Two problems are commonly encountered: first, with some column/eluent combinations the fluoride peak elutes very close to the baseline depression caused by the elution of water, the so-called "water dip". This may cause difficulty in quantitating samples with low fluoride concentrations; second, the simple organic acids (formic, acetate) elute close to fluoride and may interfere. Determine precision and bias before analyzing samples. If fluoride is to be determined, preferably select a column/eluent combination that resolves water, fluoride, and simple organic acids.

Because of the utilization of nitrate, nitrite, and phosphate as nutrients by some species of bacteria, store samples at 4°C and analyze within 48 h. Disinfected samples to be analyzed for nitrate may be held for up to 14 d because all nitrite will already be converted to nitrate. Store samples to be analyzed for sulfate at 4°C and analyze within 28 d. The other analytes do not require cold storage. Complete analysis within 28 d.

4-8

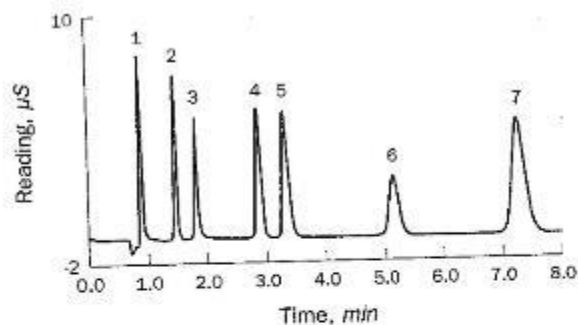


Figure 4110-1. Typical inorganic anion separation. Eluent: 1.7 mM NaHCO_3 , 1.8 mM Na_2CO_3 ; sample loop: 25 μL ; flow rate: 2.0 mL/min; column: Dionex AG4A-SC plus AS4A-SC.

Anion	Conc mg/L
1. Fluoride	2.0
2. Chloride	3.0
3. Nitrite	5.0
4. Bromide	10.0
5. Nitrate	10.0
6. Orthophosphate	15.0
7. Sulfate	15.0

2. Apparatus

a. Ion chromatograph, including an injection valve, a sample loop, guard column, analytical column, suppressor device, a temperature-compensated small-volume conductivity cell and detector (6 μL or less), and an electronic peak integrator or chromatography data acquisition system. Use an ion chromatograph capable of delivering 2 to 5 mL eluent/min at a pressure of 5600 to 28 000 kPa (800 to 4000 psi).

b. Analytical column: Any commercially available anion-exchange column capable of resolving fluoride, bromide, chloride, nitrate, nitrite, phosphate, and sulfate is acceptable.*

c. Guard column, identical to separator column† to protect analytical column from fouling by particulates or organics.

d. Suppressor device:‡ Place this ion-exchange-based device between column and detector to reduce background conductivity of the eluent and enhance conductivity of the target analytes. Several such devices with different operational principles are available commercially; any that provides the required sensitivity and baseline stability may be used.

3. Reagents

a. Reagent water free from interferences at the method detection level of each constituent with 18 megohm resistivity and containing no particles larger than 0.2 μm . See Section 1080.

* Dionex P/N 37041, Lachat P/N 28084, Waters P/N 26765, or equivalent.

† Dionex P/N 37042, Lachat P/N 28085, or equivalent.

‡ Dionex P/N 46081, Lachat P/N 28097, Alltech P/N 535101, or equivalent.

TABLE 4110-II. STOCK STANDARD PREPARATIONS

Anion	Salt	Amount g/100 mL
Fluoride	NaF	0.2210
Chloride	NaCl	0.1649
Bromide	NaBr	0.1288
Nitrate-N*	NaNO_3	0.6068
Nitrite-N*	NaNO_2	0.4925
Phosphate-P	KH_2PO_4	0.4394
Sulfate	K_2SO_4	0.1814

* Do not oven-dry. Dry to constant weight in a desiccator.

b. Eluent solution, appropriate to column used to resolve target anions. The eluent used to produce the chromatogram in Figure 4110-1 was sodium bicarbonate-sodium carbonate, 1.7 mM NaHCO_3 , 1.8 mM Na_2CO_3 . Dissolve 0.5712 g NaHCO_3 and 0.7632 g Na_2CO_3 in water and dilute to 4 L. Degas eluent before use either by vacuum filtration to simultaneously remove particles greater than 0.45 μm or by purging with helium for 10 min.

c. Regenerant solution: Required with some types of suppressors. See manufacturer's recommendations.

d. Standard anion solutions, 1000 mg/L: Purchase stock standard solutions as certified solutions or prepare from ACS reagent-grade salts. Prepare standard anion solutions by weighing the indicated amount of salt (Table 4110-II), dried to a constant weight at 105°C, and diluting to 100 mL with distilled/deionized water. Store in plastic bottles at 4°C. These solutions are stable for at least 6 months except for the nitrite and phosphate standards, which should be discarded after 1 month. Prepare most dilute working standards monthly, nitrite and phosphate, daily.

4. Procedure

a. System equilibration: Turn on ion chromatograph and adjust eluent flow rate to manufacturer's recommendations for the column/eluent combination being used. A representative chromatogram is presented in Figure 4110-1. Adjust detector to desired setting (usually 10 to 30 μS) and let system come to equilibrium (15 to 20 min). A stable base line indicates equilibrium conditions. Adjust detector offset to zero out eluent conductivity. If regenerant is used with the suppressor, adjust flow rate to manufacturer's specifications.

b. Calibration: Inject standards containing a single anion or a mixture and determine approximate retention times. Observed times vary with conditions. If the analytical column and eluent mentioned in 4110B.2b and 3b, respectively, are used, retention always is in the order F^- , Cl^- , NO_2^- , Br^- , NO_3^- , HPO_4^{2-} , and SO_4^{2-} . Inject at least three different concentrations for each anion to be measured. Use concentrations that will bracket the expected analyte concentrations in samples. Construct a calibration curve by plotting peak height or area versus concentration using appropriate software. Verify calibration curves with a mid-range check standard from a source independent of that of the calibration standards. Check validity of existing calibration curves daily with a mid-range calibration standard. Results should be within 10% of original curve at mid-range. Recalibrate whenever the detector setting, eluent, or regenerant is changed.

TABLE 4110-III. SINGLE-LABORATORY PRECISION (ONE STANDARD DEVIATION) AND BIAS DATA FOR 30 SETS OF SAMPLES OVER A 2-MONTH PERIOD

Element	LFB Concentration mg/L	LFB Recovery and Precision %	Known Addition Concentration mg/l.	Known Addition Recovery and Precision %
Chloride	25	104 ± 4.5	25	107 ± 10
Nitrite as N	1	97 ± 4	1	103 ± 7
Bromide	0.02	101 ± 8	0.1 to 0.5	106 ± 10
Bromide	0.3	102 ± 3	—	—
Nitrate as N	2.5	106 ± 2.6	2.5	113 ± 5
Orthophosphate-P	10	101 ± 4	10	102 ± 4
Sulfate	50	105 ± 4	50	111 ± 6

To minimize the effect of the "water dip"¹ on F⁻ analysis, analyze standards that bracket the expected result or eliminate the water dip by diluting the sample with eluent or by adding concentrated eluent to the sample to give the same concentration as in the eluent. If sample adjustments are made, adjust standards and blanks identically.

If linearity is established ($r \geq 0.99$) over the calibration range, the average response factor is acceptable. Record peak height or area for calculation of the response factor. RF. HPO_4^{2-} is nonlinear below 1.0 mg/L.

c. *Sample analysis:* If sample is collected with an autosampler that does not automatically filter samples, remove particulates by filtering through a prewashed 0.45- μm (or smaller) pore membrane. With either manual or automated injection, flush loop with several volumes of sample. Take care to prevent carryover of analytes from samples of high concentration. After last peak has appeared and detector signal has returned to base line, another sample can be injected.

d. *Solid matrices:* Soluble forms of the target anions may be determined in solid matrices (soils, sludges) after extraction and filtration of the extract. A slurry of the solid to be extracted is prepared with either reagent water or eluent and is either shaken or sonicated. (A representative standardized method for such extractions is available.¹) Document the precision of the extraction process and the analyte recovery achieved by analyzing duplicate laboratory-fortified matrices for each distinct matrix.

5. Calculations

Determine the concentration of each anion, in milligrams per liter, by referring to the appropriate calibration curve. Alternatively, when the response is shown to be linear, use the following equation:

$$C = H \times RF \times D$$

where:

C = mg anion/L.

H = peak height or area.

RF = response factor = concentration of standard/height (or area) of standard, and

D = dilution factor.

¹ Water dip occurs because water conductivity in sample is less than eluent conductivity (eluent is diluted by water).

6. Quality Control

The QC practices considered to be an integral part of each method are summarized in Table 4020.1. Preferably check recovery daily at reporting level using a reporting-level standard. Recovery should be between 75 and 125%. Alternate analysis of mid-range and high-range check standards after each 10 samples. Recovery should be between 90 and 110%. If the results are to be used for environmental compliance monitoring, document precision and accuracy of the method by the analysis of four replicates of a mid-range calibration standard and calculation of the average percent recovery, and the standard deviation of the recoveries, for each analyte. Additional QC may be required for regulatory purposes.

7. Precision and Bias

Multilaboratory data from a joint validation study with EPA and ASTM using older columns and hardware can be found in the 20th Edition of *Standard Methods*. Table 4110: III shows single-laboratory recoveries for laboratory-fortified blanks (LFB) and known additions to a variety of raw waters and finished drinking waters obtained with columns and equipment described herein.

8. Reference

1. AMERICAN SOCIETY FOR TESTING AND MATERIALS. 1992. Method D3987. Annual Book of ASTM Standards, Vol. 11.01 Water. American Soc. Testing & Materials, Philadelphia, Pa.

9. Bibliography

- SMALL, H., T. STEVENS & W. BALDAN. 1975. Novel ion exchange chromatographic method using conductimetric detection. *Anal. Chem.* 47:1801.
- JENKE, D. 1981. Anion peak migration in ion chromatography. *Anal. Chem.* 53:1536.
- BYNUM, M.L., S. TYREE & W. WEISS. 1981. Effect of major ions on the determination of trace ions by ion chromatography. *Anal. Chem.* 53:1935.
- WEISS, J. 1986. Handbook of Ion Chromatography. E.L. Johnson, ed. Dionex Corp., Sunnyvale, Calif.
- PRAYF, J.D., C.A. BROCKMUPP & J.W. O'DELL. 1994. The Determination of Inorganic Anions in Water by Ion Chromatography. Method 300.0A, U.S. Environmental Protection Agency, Environmental Monitoring Systems Lab., Cincinnati, Ohio.
- PRAYF, J.D., D.F. HAUFMAN & D.J. MUNCIE. 1997. Determination of Inorganic Anions in Drinking Water by Ion Chromatography. Method 300.1, U.S. Environmental Protection Agency, National Exposure Research Lab., Off. Research & Development, Cincinnati, Ohio.

Corrosion Testing Procedure

The rebar corrosion testing procedure was as follows:

- 1) With a wire brush, lightly brush loose concrete and rust off rebar,
- 2) Determine the length and diameter of the piece of rebar,
- 3) Mix a proportion of the following solution in a beaker:
 - a. 1,000 mL Hydrochloric Acid (sp gr 1.19)
 - b. 20 g Antimony Trioxide
 - c. 50 g Stannous Chloride
- 4) Place rebar in solution for intervals of 5 minutes,
- 5) Remove the rebar out of the solution every 5 minutes and lightly brush off any loose concrete and corrosion, in order to obtain the mass,
- 6) Repeat step 4 and 5 for a total of 5 times/25 minutes,
- 7) Finally brush off any remaining corrosion and concrete from rebar and obtain a final mass,
- 8) Based off the dimensions of the rebar, calculate the original mass of the piece of rebar before it was placed in the bridge,
- 9) Obtain the percent effectiveness of the rebar by subtracting the final mass of the specimen from the original mass, before it was placed in the bridge, then dividing that number by the original mass of the rebar.

Appendix D: Crack Density Results for 40 Inspected Bridge Decks

Bridge 251:

- Crack density (yd/yd²): 0.1423
- Current condition rating: 7
- Beam type-bridge type: concrete – frame
- Protective system: Galvanized rebar
- Concrete type: AA
- Age (years): 37

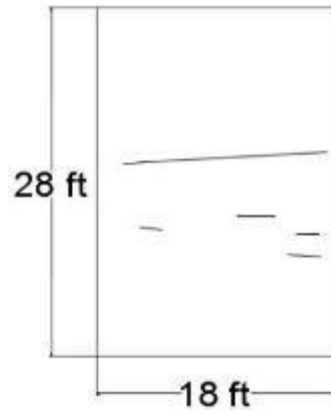


Figure 97. Bridge 251 crack map

Bridge 252:

- Crack density (yd/yd²): 0.1591
- Current condition rating: 6
- Beam type-bridge type: concrete - frame
- Protective system: Galvanized rebar
- Concrete type: AA
- Age (years): 37

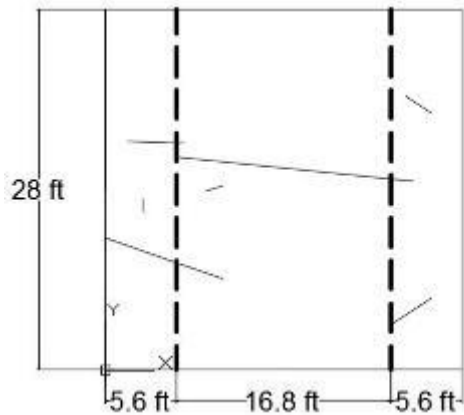


Figure 98. Bridge 252 crack map

Bridge 644:

- Crack density (yd/yd²): N/A (LMC)
- Current condition rating: 7
- Beam type-bridge type: steel continuous – stringer/girder
- Protective system: Latex modified concrete placed in 1980
- Concrete type: AAA
- Age (years): 39

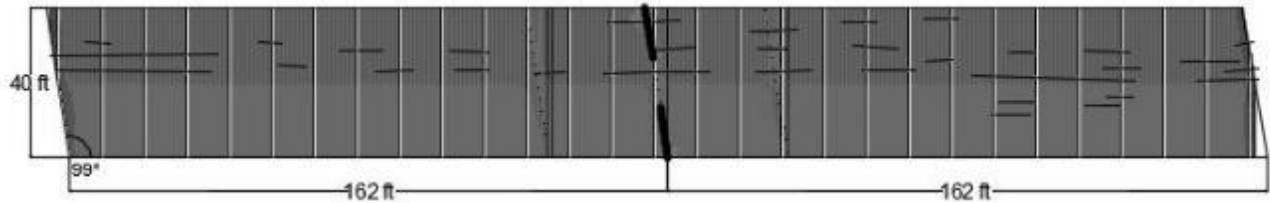


Figure 99. Bridge 644 crack map

Bridge 645:

- Crack density (yd/yd²): N/A (LMC)
- Current condition rating: 6
- Beam type-bridge type: steel continuous – stringer girder
- Protective system: Latex modified concrete placed in 1980
- Concrete type: AAA
- Age (years): 39

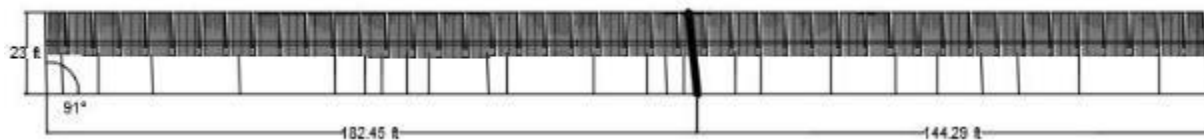


Figure 100. Bridge 645 crack map

Bridge 4908:

- Crack density (yd/yd²): 0.4300
- Current condition rating: 7
- Beam type-bridge type: prestressed concrete – multiple beam box
- Protective system: Epoxy-coated rebar
- Concrete type: AA
- Age (years): 52
- A part of #85-17 Study

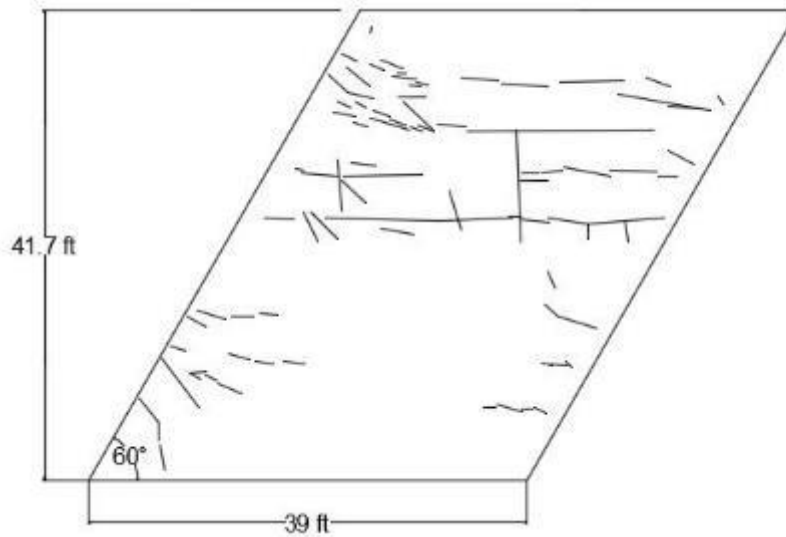


Figure 101. Bridge 4908 crack map

Bridge 5081:

- Crack density (yd/yd²): 0.3800
- Current condition rating: 7
- Beam type-bridge type: prestressed concrete – adjacent beam box
- Protective system: Epoxy-coated rebar
- Concrete type: AA
- Age (years): 36

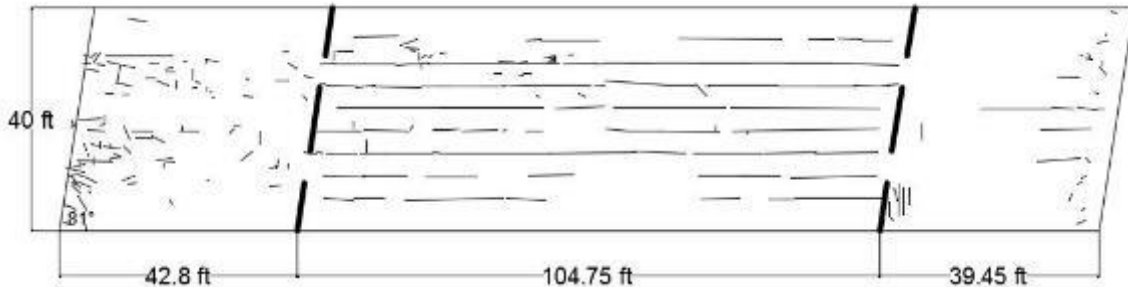


Figure 102. Bridge 5081 crack map

Bridge 6457:

- Crack density (yd/yd²): 0.0293
- Current condition rating: 8
- Beam type-bridge type: prestressed concrete – adjacent beam box
- Protective system: Epoxy-coated rebar
- Concrete type: AAA
- Age (years): 3

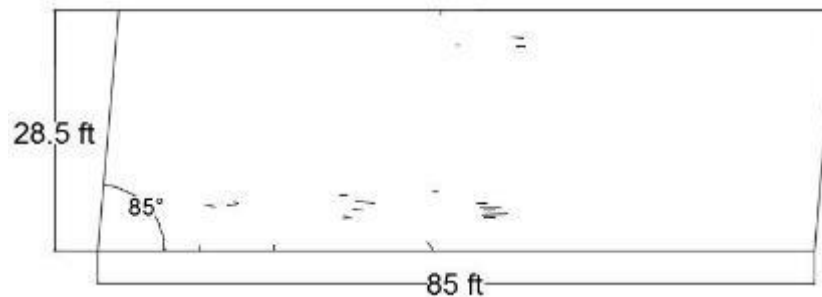


Figure 103. Bridge 6457 crack map

Bridge 11525:

- Crack density (yd/yd²): 0.0609
- Current condition rating: 9
- Beam type-bridge type: steel continuous – stringer/girder
- Protective system: Epoxy-coated rebar
- Concrete type: AAAP
- Age (years): 2

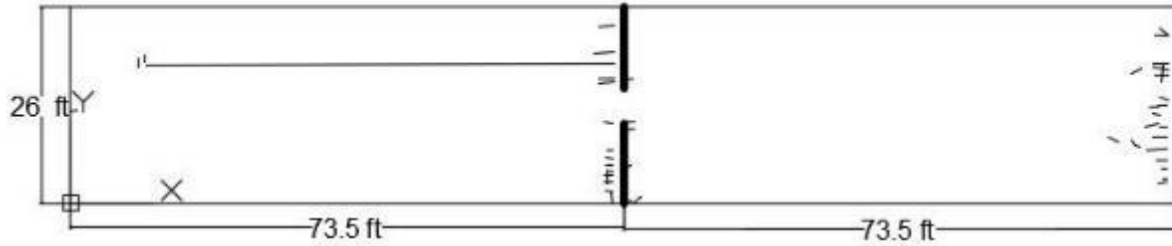


Figure 104. Bridge 11525 crack map

Bridge 12517:

- Crack density (yd/yd²): 0.1259
- Current condition rating: 8
- Beam type-bridge type: prestressed concrete – adjacent box beam
- Protective system: Epoxy-coated rebar
- Concrete type: AAAP
- Age (years): 0

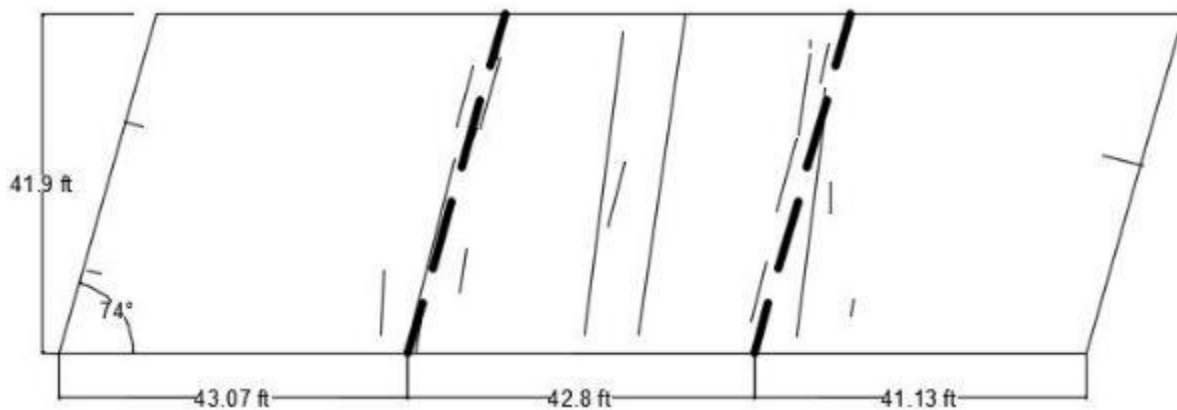


Figure 105. Bridge 12517 crack map

Bridge 12518:

- Crack density (yd/yd²): 0.1815
- Current condition rating: 8
- Beam type-bridge type: prestressed concrete – single/spread box
- Protective system: Epoxy-coated rebar
- Concrete type: AAAP
- Age (years): 0

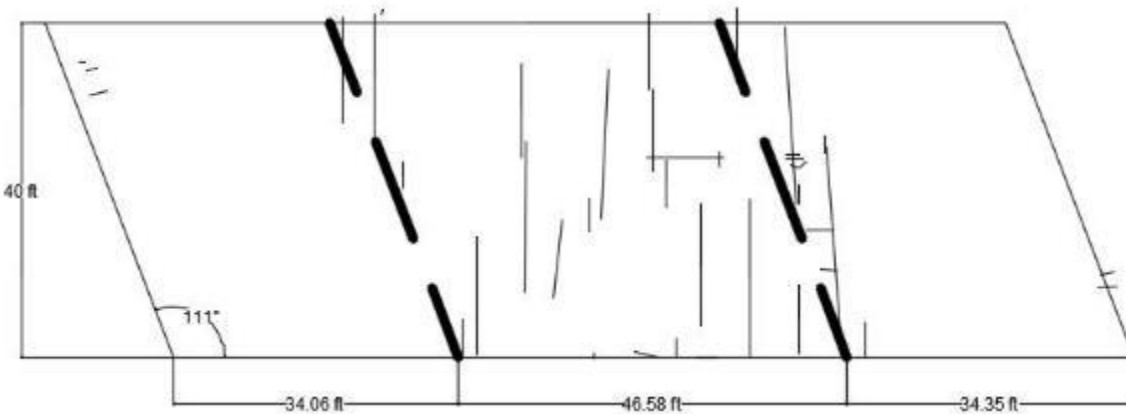


Figure 106. Bridge 12518 crack map

Bridge 12524:

- Crack density (yd/yd²): 0.7673
- Current condition rating: 6
- Beam type-bridge type: steel continuous – stringer/girder
- Protective system: Epoxy-coated rebar
- Concrete type: AAA
- Age (years): 8

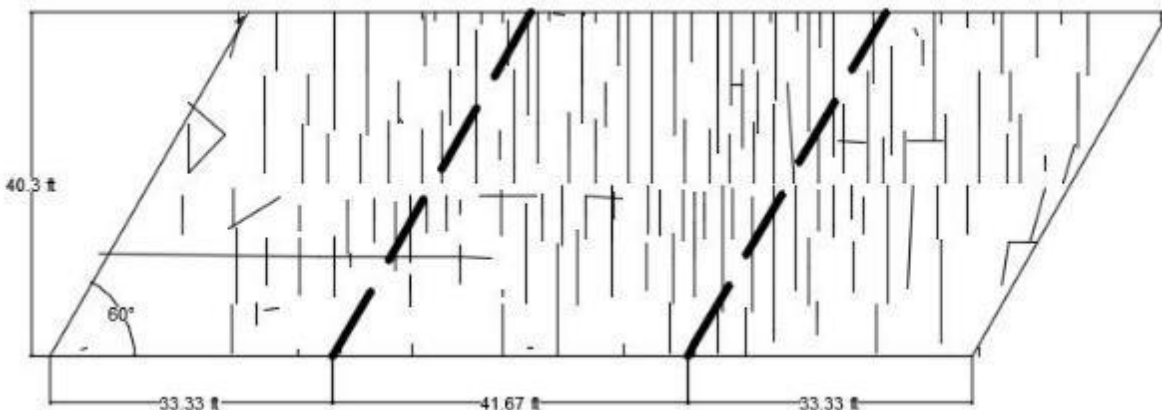


Figure 107. Bridge 12524 crack map

Bridge 19168:

- Crack density (yd/yd²): N/A (LMC)
- Current condition rating: 8
- Beam type-bridge type: prestressed concrete – single/spread box
- Protective system: Epoxy-coated rebar
- Concrete type: AAA
- Age (years): 6

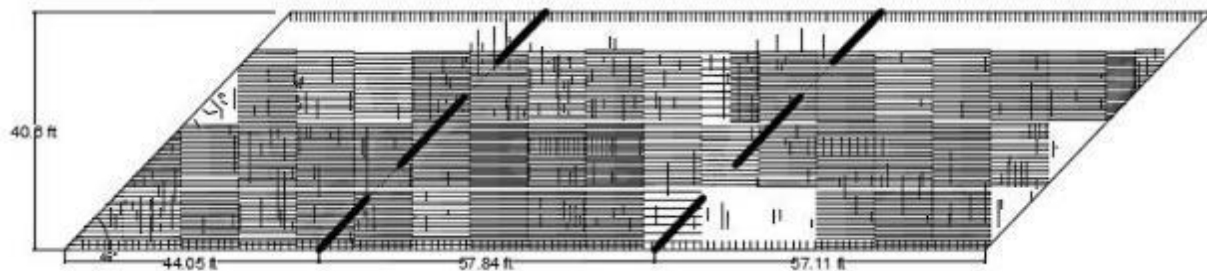


Figure 108. Bridge 19168 crack map

Bridge 19170:

- Crack density (yd/yd²): 0.0629
- Current condition rating: 8
- Beam type-bridge type: steel continuous – stringer/girder
- Protective system: Epoxy-coated rebar
- Concrete type: AAA
- Age (years): 4

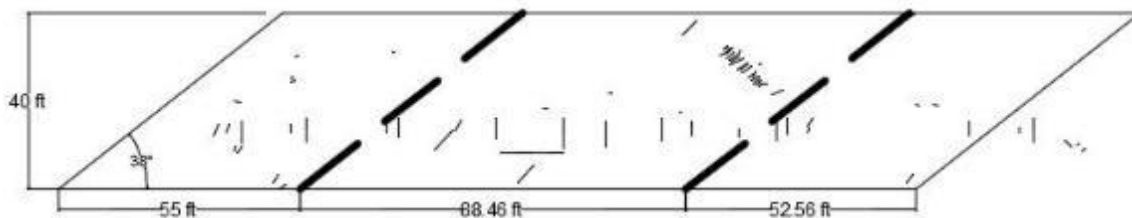


Figure 109. Bridge 19170 crack map

Bridge 20506:

- Crack density (yd/yd²): N/A (LMC)
- Current condition rating: 5
- Beam type-bridge type: steel continuous – stringer/girder
- Protective system: LMC placed with original deck.
- Concrete type: AA
- Age (years): 37
- A part of #85-17 Study

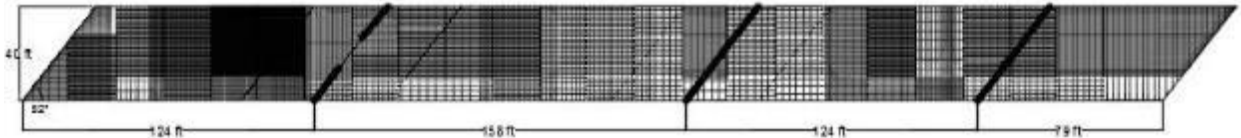


Figure 110. Bridge 20506 crack map

Bridge 20507:

- Crack density (yd/yd²): N/A (LMC)
- Current condition rating: 6
- Beam type-bridge type: steel continuous – stringer/girder
- Protective system: LMC placed with original deck.
- Concrete type: AA
- Age (years): 37
- A part of #85-17 Study



Figure 111. Bridge 20507 crack map

Bridge 20588:

- Crack density (yd/yd²): N/A (LMC)
- Current condition rating: 7 (rating in 2007 prior to LMC: 6)
- Beam type-bridge type: prestressed concrete – single/spread box
- Protective system: Galvanized rebar; LMC placed in 2009,
- Concrete type: AAA
- Age (years): 40
- A part of #85-17 Study

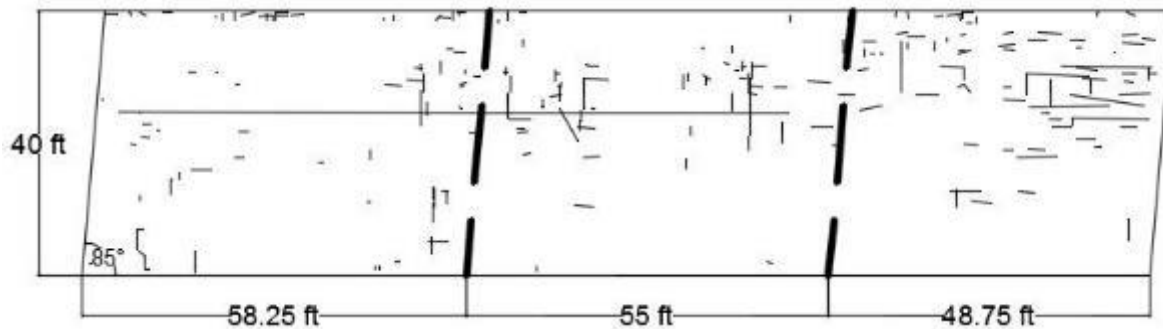


Figure 112. Bridge 20588 crack map

Bridge 20589:

- Crack density (yd/yd²): N/A (LMC)
- Current condition rating: 7 (rating in 2007 prior to LMC: 6)
- Beam type-bridge type: prestressed concrete – single/spread box
- Protective system: Galvanized rebar, LMC placed in 2009
- Concrete type: AAA
- Age (years): 40
- A part of #85-17 Study

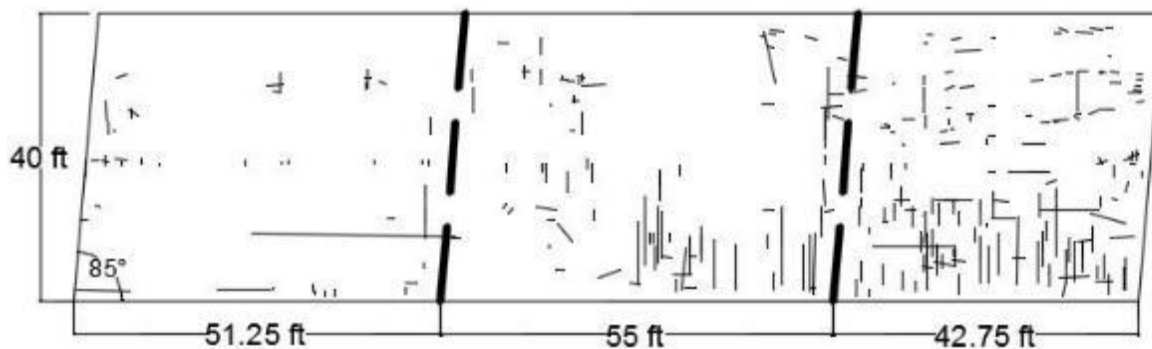


Figure 113. Bridge 20589 crack map

Bridge 20613:

- Crack density (yd/yd²): N/A (LMC)
- Current condition rating: 5
- Beam type-bridge type: steel continuous – stringer/girder
- Protective system: None
- Concrete type: AA
- Age (years): 36
- A part of #85-17 Study

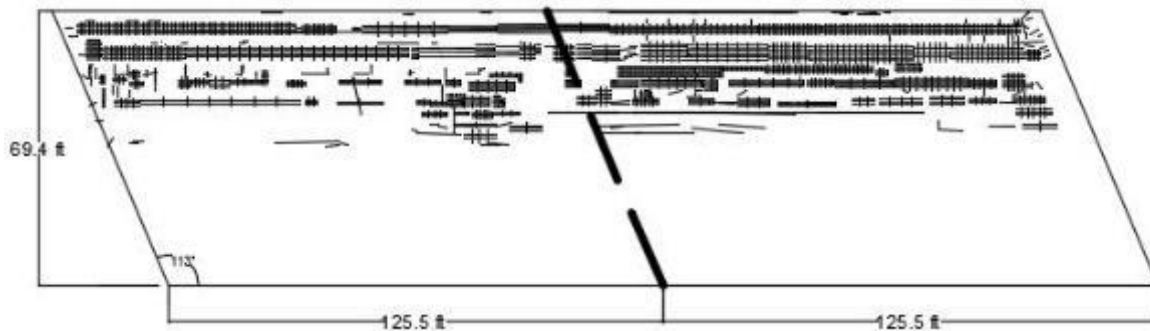


Figure 114. Bridge 20613 crack map

Bridge 21651:

- Crack density (yd/yd²): 0.2097
- Current condition rating: 7
- Beam type-bridge type: prestressed concrete – single/spread box
- Protective system: Galvanized rebar
- Concrete type: AA
- Age (years): 38
- A part of #85-17 Study

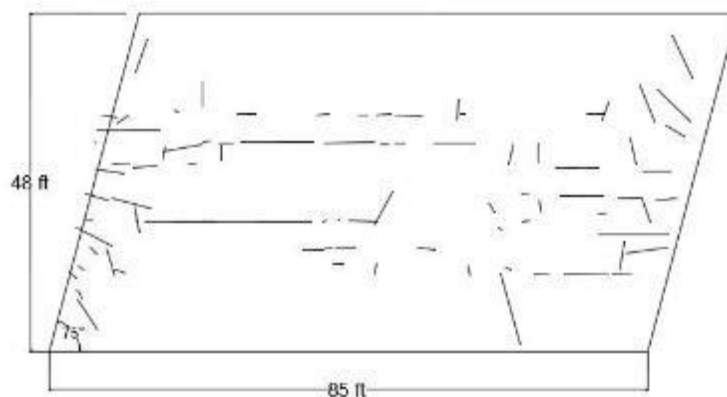


Figure 115. Bridge 21651 crack map

Bridge 26993:

- Crack density (yd/yd²): N/A (overlaid)
- Current condition rating: 5
- Beam type-bridge type: prestressed concrete – stringer/girder
- Protective system: Galvanized rebar
- Concrete type: AA
- Age (years): 38
- A part of #85-17 Study

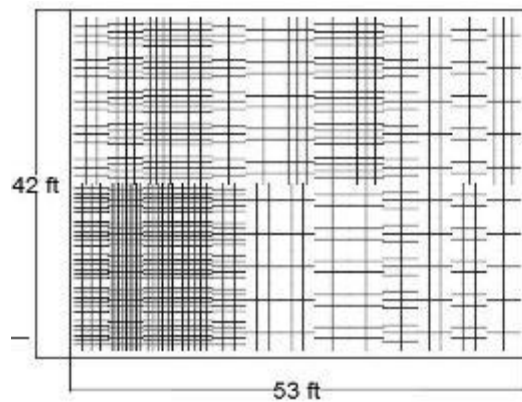


Figure 116. Bridge 26993 crack map

Bridge 30643:

- Crack density (yd/yd²): 0.3075
- Current condition rating: 6
- Beam type-bridge type: prestressed concrete – single/spread box
- Protective system: Epoxy-coated rebar
- Concrete type: AA
- Age (years): 35
- A part of #85-17 Study

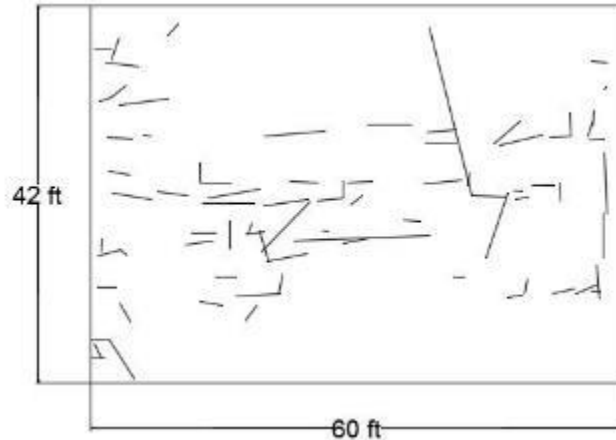


Figure 117. Bridge 30643 crack map

Bridge 30700:

- Crack density (yd/yd²): N/A (Bituminous)
- Current condition rating: 6
- Beam type-bridge type: steel – stringer/girder
- Protective system: None
- Concrete type: AA
- Age (years): 50

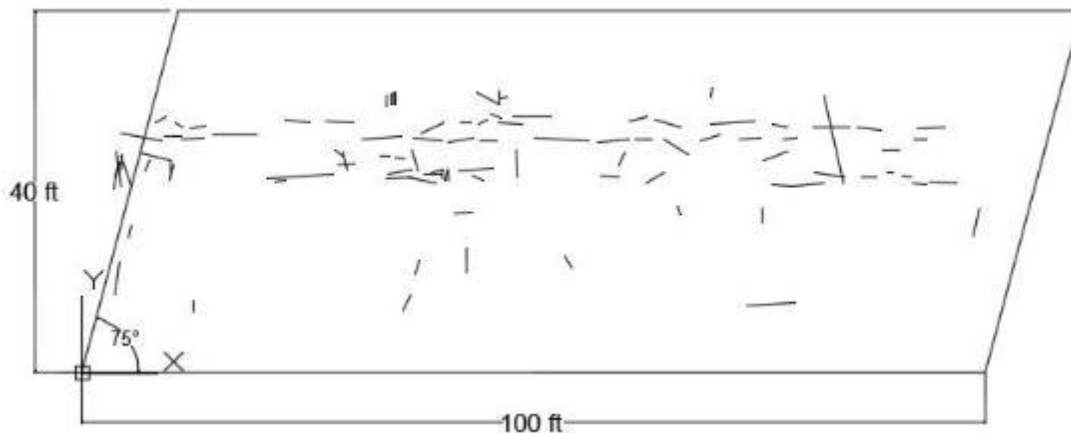


Figure 118. Bridge 30700 crack map

Bridge 30752:

- Crack density (yd/yd²): N/A (Bituminous)
- Current condition rating: 6
- Beam type-bridge type: concrete – tee beam
- Protective system: None
- Concrete type: AA
- Age (years): 90
- A part of #85-17 Study

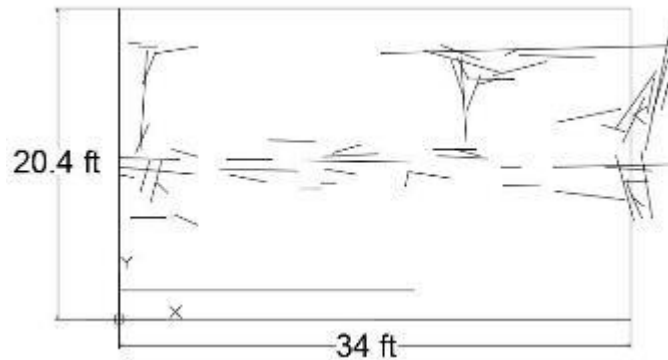


Figure 119. Bridge 30752 crack map

Bridge 34391:

- Crack density (yd/yd²): 0.2127
- Current condition rating: 6
- Beam type-bridge type: prestressed concrete – stringer/girder
- Protective system: Epoxy-coated rebar
- Concrete type: AAA
- Age (years): 21

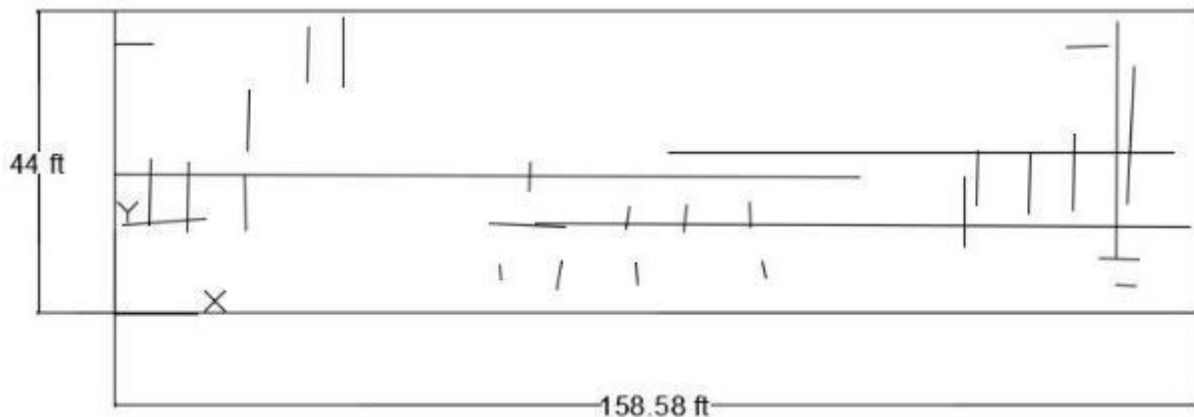


Figure 120. Bridge 34391 crack map

Table 36. Crack density, delamination and patching/spalling results for 40 inspected bridge decks with original deck wearing surface (used in analysis)

Bridge Number	Protective System	Concrete Type	Wearing Surface	Age (years)	Crack Density (yd/yd ²)					Delamination (% Area)	Patching/Spalling (% Area)
					Transverse	Longitudinal	Positive Moment	Negative Moment	Total		
4908	Epoxy-coated rebar	AA	Original	52	0.0723	0.3577	0.4300	N/A	0.4300	0.00	-
30643	Epoxy-coated rebar	AA	Original	35	0.1106	0.1968	0.3075	N/A	0.3075	0.00	-
5081	Epoxy-coated rebar	AA	Original	36	0.0346	0.3453	0.3800	N/A	0.3800	0.00	-
12893	Epoxy-coated rebar	AA	Original	34	0.2194	0.0068	0.2262	N/A	0.2262	0.55	0.00
36077	Epoxy-coated rebar	AA	Original	37	0.0000	0.0244	0.0244	N/A	0.0244	0.00	0.00
36082	Epoxy-coated rebar	AA	Original	37	0.0045	0.0165	0.0210	N/A	0.0210	0.00	0.05
36084	Epoxy-coated rebar	AA	Original	37	0.0188	0.0295	0.0483	N/A	0.0483	0.00	1.43
6457	Epoxy-coated rebar	AAA	Original	3	0.0041	0.0252	0.0293	N/A	0.0293	0.00	-
12524	Epoxy-coated rebar	AAA	Original	8	0.7077	0.1767	0.0691	1.3131	0.7673	0.00	-
12905	Epoxy-coated rebar	AAA	Original	27	0.1630	0.0040	0.1670	N/A	0.1670	0.23	0.00
8410	Epoxy-coated rebar	AAA	Original	20	0.5640	0.0120	0.5760	N/A	0.5760	-	-

Bridge Number	Protective System	Concrete Type	Wearing Surface	Age (years)	Crack Density (yd/yd ²)					Delamination (% Area)	Patching/ Spalling (% Area)
					Transverse	Longitudinal	Positive Moment	Negative Moment	Total		
8406	Epoxy-coated rebar	AAA	Original	20	0.7930	0.0160	0.4700	0.3390	0.8100	-	-
3574	Epoxy-coated rebar	AAA	Original	4	0.0098	0.0433	0.0531	N/A	0.0531	0.00	0.00
8407	Epoxy-coated rebar	AAA	Original	20	0.2726	0.1837	0.4563	N/A	0.4563	-	-
19551	Epoxy-coated rebar	AAA	Original	31	0.0337	0.1019	0.1356	N/A	0.1356	13.50	2.91
34391	Epoxy-coated rebar	AAA	Original	21	0.0740	0.1387	0.2127	N/A	0.2127	0.00	0.00
19784	Epoxy-coated rebar	AAA	Original	5	0.4045	0.2740	0.6785	N/A	0.6785	0.00	0.00
47335	Epoxy-coated rebar	AAAP	Original	2	0.1508	0.0289	0.1797	N/A	0.1797	0.00	0.00
11525	Epoxy-coated rebar	AAAP	Original	2	0.0035	0.0573	0.0609	N/A	0.0609	0.00	15.00
12517	Epoxy-coated rebar	AAAP	Original	0	0.1208	0.0051	0.1259	N/A	0.1259	0.00	0.00
12518	Epoxy-coated rebar	AAAP	Original	0	0.1596	0.0219	0.1815	N/A	0.1815	0.00	0.00
21651	Galvanized Rebar	AA	Original	38	0.0629	0.1468	0.2097	N/A	0.2097	0.00	0.00

Bridge Number	Protective System	Concrete Type	Wearing Surface	Age (years)	Crack Density (yd/yd ²)					Delamination (% Area)	Patching/ Spalling (% Area)
					Transverse	Longitudinal	Positive Moment	Negative Moment	Total		
251	Galvanized Rebar	AA	Original	37	0.0000	0.1423	0.1479	0.1338	0.1423	0.00	-
252	Galvanized Rebar	AA	Original	37	0.0038	0.1553	0.7597	0.4218	0.1591	0.00	-
19170	Other-Coated Rebar	AAA	Original	4	0.0397	0.0232	0.0629	N/A	0.0629	0.00	-

Table 37. Crack density, delamination and patching/spalling results for 40 inspected bridge decks with overlays (not used in analysis)

Bridge Number	Protective System	Concrete Type	Wearing Surface	Age (years)	Crack Density (yd/yd ²)					Delamination (% Area)	Patching/Spalling (% Area)
					Transverse	Longitudinal	Positive Moment	Negative Moment	Total		
20613	None	AA	LMC	36	0.5804	1.7792	2.2547	2.6745	2.3596	7.52	5.98
20507	None	AA	LMC	21	0.2651	0.1539	0.4420	0.3552	0.4190	2.00	2.40
20506	None	AA	LMC	37	2.6032	7.0184	10.4105	7.3545	9.6216	0.70	7.93
30700	None	AA	Bituminous	50	0.0508	0.1227	0.1736	N/A	0.1736	0.00	-
30752	None	AA	Bituminous	90	0.3120	0.6700	0.9820	N/A	0.9820	0.00	20.00
19168	Epoxy-coated rebar	AAA	LMC	6	0.5671	4.4243	4.9914	N/A	4.9914	0.00	-
19724	Epoxy-coated rebar	AAA	Epoxy Overlay	30	-	-	-	-	-	0.00	0.00
26993	Galvanized Rebar	AA	Unknown	38	1.7251	2.1563	3.8814	N/A	3.8814	3.65	5.11
20588	Galvanized Rebar	AAA	LMC	5	0.0704	0.1673	0.2377	N/A	0.2377	0.00	-
20589	Galvanized Rebar	AAA	LMC	5	0.2115	0.1187	0.3302	N/A	0.3302	0.00	-
637	Polymer Impregnated	AAA	LMC	6	0	0	0	N/A	0	-	-

Bridge Number	Protective System	Concrete Type	Wearing Surface	Age (years)	Crack Density (yd/yd ²)					Delamination (% Area)	Patching/ Spalling (% Area)
					Transverse	Longitudinal	Positive Moment	Negative Moment	Total		
639	Polymer Impregnated	AAA	LMC	6	0	0	0	N/A	0	-	-
652	Polymer Impregnated	AAA	LMC	9	5.709	3.7843	9.4932	N/A	9.4932	4.20	0.67
924	Polymer Impregnated	AAA	Bituminous	5	-	-	-	-	-	-	-
645	Polymer Impregnated	AAA	LMC	6	3.715	0.391	4.098	4.137	4.106	0.00	0.00
644	Polymer Impregnated	AAA	LMC	6	6.877	0.122	6.092	6.094	7.000	0.60	0.00

Table 38. Chloride content results for original concrete decks

BrKey	Concrete Type	Age	Core ID	C/NC*	Crack depth (in)	% Effectiveness of Rebar	Rebar Type	Delaminated/ separated at rebar level?	Depth of analysis (in)	Chloride content (%wt)	Diffusion coefficient (x 10 ⁽⁻⁴⁾ in ² /day)
251	AA	37	C2_251	C	1.67	No corrosion	Galvanized		4.33	0.032%	1.83
			C1_251	NC	0.00	No corrosion	Galvanized		3.86	0.008%	0.89
252	AA	37	C1_252	C	1.30	93.19	Galvanized, 2 levels		2.36	0.100%	1.03
			C2_252	NC	0.00	No corrosion	Galvanized		2.68	0.007%	0.42
644	AAA	6	C1_644	NC	0.00	No corrosion	Black rebar		3.39	0.005%	3.76
			C2_644	NC	0.00	N/A	No rebar		3.39	0.004%	3.56
652	AAA	9	C1_652	NC	0.00	~98.00	Black rebar		4.17	0.005%	3.80
			C2_652	C	0.98	N/A	No rebar		2.76	0.149%	8.11
4908	AA	52	C1_4908	C	3.35	No corrosion	Epoxy coated (green)	Yes	3.15	0.160%	1.96
			C2_4908	NC	0.00	No corrosion	Epoxy coated (green)		3.35	0.011%	0.52
8406	AAA	20	C1_8406	C	2.52	No corrosion	Epoxy coated (green)	Yes	2.52	0.114%	2.41
			C2_8406	NC	0.00	No corrosion	Epoxy coated (green)		2.95	0.069%	2.31
8407	AAA	20	C1_8407	C	2.95	No corrosion	Epoxy coated (green)	Yes	2.95	0.352%	16.26

BrKey	Concrete Type	Age	Core ID	C/NC*	Crack depth (in)	% Effectiveness of Rebar	Rebar Type	Delaminated/separated at rebar level?	Depth of analysis (in)	Chloride content (%wt)	Diffusion coefficient (x 10 ⁻⁴) in ² /day
			C2_8407	NC	0.00	No corrosion	Epoxy coated (green)		3.11	0.040%	1.92
12893	AA	34	C3_12893	C	Full depth	No corrosion	Epoxy coated (brown), 2 levels		3.58	0.199%	4.99
			C1_12893	NC	0.00	N/A	No rebar		3.54	0.057%	1.76
12893	AA	34	C2_12893	NC	0.00	97.85	Epoxy coated (Brown)	Yes	2.52	0.288%	4.40
12905	AAA	27	C1_12905	C	3.50	~95.00	Epoxy coated	Yes	3.50	0.224%	7.05
			C2_12905	NC	0.00	No corrosion	Epoxy coated (green)	Yes	2.95	0.083%	1.93
19551	AAA	31	C1_19551	C	2.95	No corrosion	Epoxy coated (Brown)		2.95	0.263%	5.64
			C2_19551	NC	0.00	No corrosion	Epoxy coated (Brown)		3.23	0.250%	6.19
19784	AAA	5	C1_19784	NC	0.00	No corrosion	Epoxy coated, 2 levels		2.60	0.094%	8.78
			C2_19784	NC	0.00	No corrosion	Epoxy coated		3.03	0.012%	4.61
20506	AA	37	C1_20506	C	3.35	74.01	Black rebar	Yes	2.17	0.484%	16.67
			C2_20506	NC	0.00	95.38 92.82	Black rebar, 2 layers		2.64	0.099%	1.27

BrKey	Concrete Type	Age	Core ID	C/NC*	Crack depth (in)	% Effectiveness of Rebar	Rebar Type	Delaminated/separated at rebar level?	Depth of analysis (in)	Chloride content (%wt)	Diffusion coefficient (x 10 ^{^-4}) in ² /day)
20507	AA	21	C1_20507	NC	0.00	93.72 92.63	Black rebar		2.13	0.025%	0.70
20588	AAA	5	C1_20588	C	2.68	99.14	Galvanized	Yes	2.68	0.256%	27.45
			C2_20588	C	2.56	99.62	Galvanized	Yes	2.56	0.326%	40.33
21651	AA	38	C1_21651	NC	0.00	Little rust on surface, somewhat deteriorated	Galvanized		2.05	0.006%	0.23
30700	AA	50	C1_30700	NC	0.00	95.00	Black rebar		3.74	0.384%	13.48
36082	AA	37	C2_36082	C	0.98	No corrosion	Brown epoxy coated		2.72	0.028%	0.68
			C1_36082	NC	0.00	No corrosion	Epoxy coated (Brown)	Yes	3.35	0.008%	0.68
36084	AA	37	C2_36084	C	0.30	98.46	Brown epoxy coated		2.36	0.306%	4.04
			C1_36084	NC	0.00	No corrosion	Epoxy coated (Brown)		3.07	0.060%	1.25

*C/NC: Cracked / Not Cracked

Table 39. Chloride content results for LMC overlay layers

BrKey Number	Concrete Type	Age	C/NC	Crack depth (in)	Overlay Type	Overlay Depth (in)	Depth of analysis (in)	Overlay chloride content (%wt)	Diffusion coefficient (x10 ^{^(-4)} in ² /day)
644	AAA	6	NC	0.00	LMC	1.57	1.18	0.078%	0.84
			NC	0.00	LMC	1.57	1.18	0.034%	1.32
652	AAA	9	NC	0.00	LMC	2.17	1.89	0.006%	0.81
			C	0.98	-	-	-	-	-
20506	AA	37	C	3.35	LMC	1.18	0.98	0.864%	-
			NC	0.00	LMC	1.22	0.98	0.510%	4.83
20507	AA	21	NC	0.00	LMC	1.50	1.38	0.163%	0.9418
20588	AAA	5	C	0.98	LMC	1.46	1.26	0.285%	7.22
			C	2.56	LMC	1.38	1.18	0.318%	7.99
30700	AA	50	NC	0.00	Asphalt	2.76	-	-	-

Appendix E: Bridge Decks Included in the #85-17 Study and the Current Study

Table 40. Bridge decks included in both the #85-17 Study and the Current Study

Bridge Number	1988 Protective System (Current)	Original Concrete Type (Current)	Current Wearing Surface	Year Built	Year Rebuilt	Age (years)	Deterioration Factor (#85-17)	Current Condition Rating
20613	Latex-Modified Concrete (None)	AA (AA)	LMC	1978	-	36	37.7	5
20507	Latex-Modified Concrete (None)	AA (AA)	LMC	1977	1993	21	28.0	6
20506	Latex-Modified Concrete (None)	AA (AA)	LMC	1977	-	37	28.0	5
30752	Galvanized Rebar (None)	AA (AA)	Bituminous	1924	-	90	25.8	6
4908	Low Slump Concrete (Epoxy-coated Rebar)	AA (AA)	Original	1962	2011	52	25.9	4*
30643	Epoxy-coated Rebar (Epoxy-coated Rebar)	AA (AA)	Original	1937	1979	35	28.0	6
19551	Epoxy-coated Rebar (Epoxy-coated Rebar)	AAA (AAA)	Original	1983	-	31	32.2	5
19724	Epoxy-coated Rebar (Epoxy-coated Rebar)	AAA (AAA)	Epoxy Overlay	1984	-	30	23.4	-
20588	Galvanized Rebar (Galvanized Rebar)	AA (AAA)	LMC	1975	2009	5	31.6	7
20589	Galvanized Rebar (Galvanized Rebar)	AA (AAA)	LMC	1975	2009	5	31.6	7
26993	Galvanized Rebar (Galvanized Rebar)	AA (AA)	Original	1976	-	38	30.3	5
21651	Galvanized Rebar (Galvanized Rebar)	AA (AA)	Original	1976	-	38	28.4	7

* The condition rating for bridge 4908 reflects the rating in 2011 prior to rebuilding. The total crack density in 2011 was recorded as 0.4300 yd/sy.

Appendix F: Data used for cracking data-condition rating correlation

Table 41. Crack density and ratings data for 40 inspected bridge decks (all overlaid decks eliminated)

Rating	Date of Rating	Bridge Number	Year Built	Total Density (yd/sy)
5	6/3/2013	12893	1980	0.2262
	3/21/2014	19551	1983	0.1356
6	9/20/2013	8410	1994	0.5760
	9/19/2013	8407	1994	0.4563
	1/17/2013	30643	1979	0.3075
	11/5/2013	34391	1993	0.2127
	10/11/2013	12905	1987	0.1670
	12/14/2012	252	1977	0.1591
	5/1/2013	36084	1977	0.0483
	5/3/2013	36077	1977	0.0244
	5/13/2013	36082	1977	0.0210
7	10/17/2013	8406	1994	0.8100
	7/3/2013	19784	2009	0.6785
	11/20/2013	4908	1962	0.4300
	5/21/2012	21651	1976	0.2097
	5/23/2012	5081	1978	0.1532
8	5/6/2013	47335	2012	0.1797
	12/19/2012	19170	2010	0.0629
	8/21/2012	6457	2011	0.0293
9	7/23/2012	3574	2010	0.0531
	6/11/2013	11525	2012	0.0609

Table 42. Crack density and ratings data for 163 new bridge decks

BMS#	Total Initial Density (yd/sy)	Rating
55-2037-0050-1797	0.0000	9
49-1025-0090-1781	0.0000	9
48-1017-0100-0891	0.0526	9
48-1002-0080-0000	0.0301	9
48-0191-0030-0875	0.6033	9
45-0191-0240-0097	0.0000	9
43-0718-0250-0000	0.0000	9
43-0173-0220-0280	0.0008	9
41-2039-0050-0000	0.0000	9

39-1014-0022-0789	0.0000	9
26-0166-0440-0399	0.0000	9
38-2014-0020-1262	0.0000	9
53-0645-0050-1369	0.0000	9
37-0551-0340-0001	0.0000	9
37-0065-0110-0415	0.0000	9
36-0741-0040-0449	0.0000	9
35-3005-0050-0000	0.0000	9
32-3035-0080-1440	0.0332	9
32-2011-0060-1818	0.0000	9
29-0030-0210-0169	0.0694	9
26-1054-0150-0000	0.0000	9
26-1037-0080-0682	0.0000	9
39-0145-0120-0000	0.0244	9
62-4037-0110-0195	0.0000	9
39-7301-0000-0039	0.0520	9
39-7301-0000-0013	0.0000	9
31-3053-0020-0000	0.0000	9
02-7430-0000-1002	0.0000	9
66-2019-0070-0530	0.0000	9
65-3001-0180-0000	0.0000	9
64-4034-0080-3022	0.0000	9
64-3037-0160-0000	0.0092	9
64-2003-0010-0000	0.0000	9
53-0061-0170-0031	0.0000	9
63-4043-0030-0763	0.0000	9
53-0081-1365-0000	0.0000	9
57-1011-0040-2180	0.0000	9
57-0547-0170-2887	0.0000	9
55-4021-0130-0375	0.0000	9
55-4017-0070-0000	0.0000	9
55-3001-0130-2674	0.0000	9
55-0403-0010-1553	0.0000	9
55-0281-0650-3865	0.0000	9
54-0522-0610-0387	0.0001	9
53-3015-0020-2220	0.0000	9
37-0551-0020-0370	0.0000	9
64-0286-0130-1246	0.0000	9
03-7202-0535-0017	0.0000	9
08-0187-0880-0000	0.0000	9
07-7215-0431-3080	0.0000	9
10-3025-0060-0001	0.0000	9
10-4006-0010-2906	0.0000	9

07-0164-0380-1418	0.0000	9
07-7213-0343-3052	0.0000	9
06-0061-0150-2336	0.0000	9
05-0056-0240-2987	0.0000	9
07-7205-0405-3027	0.0000	9
04-4033-0020-2658	0.0000	9
05-3009-0010-0020	0.0231	9
06-0176-0110-0000	0.0000	9
10-7217-0325-0096	0.0000	9
06-2077-0010-1861	0.0000	9
07-1001-0270-2597	0.0040	9
21-0641-0170-2444	0.0000	9
20-2028-0010-0533	0.0248	9
06-4012-0012-0000	0.0000	9
02-3121-0010-0096	0.0000	9
07-4015-0100-0000	0.0000	9
20-0285-0280-0000	0.0000	9
20-0006-0340-0000	0.0000	9
22-0022-0290-1786	0.0000	9
02-1013-0160-1928	0.0000	9
06-1026-0040-1288	0.0000	9
06-1022-0290-1889	0.0000	9
20-2018-0010-1162	0.0000	9
57-0106-0232-0000	0.0000	8
55-7210-0628-3032	0.0000	8
06-0345-0130-0560	0.0000	8
02-3031-0030-0551	0.1327	8
65-4002-0170-0525	0.0000	8
65-0307-0150-1712	0.0000	8
65-0006-0180-0000	0.0000	8
02-7301-0000-3100	0.0000	8
62-2018-0010-0089	0.2033	8
04-0288-0120-0001	0.0000	8
06-0345-0130-1488	0.0000	8
63-0084-0174-1424	0.1058	8
63-0084-0164-2421	0.2615	8
62-4047-0080-2082	0.0000	8
51-0006-0450-0000	0.0000	8
62-4030-0010-0000	0.0453	8
58-4024-0110-0000	0.0000	8
03-4010-0010-0036	0.0000	8
17-2024-0310-0000	0.0000	8
21-4029-0010-0000	0.0000	8

29-0030-0230-0000	0.0000	8
31-0026-0500-2073	0.0000	8
49-0405-0030-0000	0.0000	8
33-0119-0450-2140	0.0000	8
02-2040-0080-0640	0.1086	8
33-3003-0140-0005	0.0000	8
19-0044-0250-0163	0.0000	8
36-2001-0010-0000	0.0757	8
18-2004-0042-0000	0.0000	8
02-0910-0090-0360	0.0387	8
18-0880-0040-0000	0.0100	8
07-7202-0500-3075	0.0000	8
38-2014-0010-0151	0.0000	8
54-0522-0090-1932	0.0000	8
38-4011-0090-0000	0.0000	8
33-3014-0010-0046	0.0000	8
08-4013-0260-0915	0.0000	8
45-2030-0020-0000	0.1345	8
48-0191-0030-0000	0.2317	8
07-7207-0322-3011	0.0000	8
49-0061-0220-1723	0.0011	8
49-0405-0020-0512	0.0000	8
51-0084-0189-0000	0.0000	8
02-2122-0010-0025	0.0000	8
53-0081-1341-1225	0.0000	8
02-2080-0030-0321	0.0000	8
38-2014-0010-0111	0.0000	8
18-0144-0310-0000	0.0000	8
64-0056-0330-1980	0.0513	7
58-0049-0080-2742	0.0000	7
07-3013-0070-0833	0.0000	7
16-0208-0300-0005	0.0000	7
33-0949-0090-0500	0.0000	7
33-0310-0050-0420	0.3356	7
33-0119-0130-1960	0.0180	7
53-0895-0390-0500	0.0000	7

Appendix G: Deterioration Modeling Results

Table 43 AFT Weibull parameter estimations for CR4 to CR9 (only significant variables are shown)

	Estimated Parameters						
	CR3	CR4	CR5	CR6	CR7	CR8	CR9
Constant term	1.80 5	0.455	1.718	1.837	2.265	1.977	0.767
p-parameter	1.31 0	1.576	1.425	1.473	1.474	1.500	1.784
LENGTH in ft (Continuous)						-3.40E-04	-1.31E-03
DISTRICT (base=district 8)							
1					0.107		1.322
2			0.227				0.468
4				0.108			
5						-0.124	0.468
6					0.167	-0.350	
9					0.127	0.236	
10					0.301		0.468
12			0.260				
REBARTYPE (base=with protective coating)							
1 (Bare rebar)						-0.166	
INTERACT (base=all others)							
1 (Simple Span)			0.250	0.134			
MAINPHYSICAL (base=all others)							
1 (Reinforced)				0.205			
2 (Prestressed)		0.663		0.133			
6 (Rolled sections)				0.145	0.111		
SURFTYPE (base=1 (no overlay))							
2 (Concrete Overlay)					0.115		
5 (Epoxy Overlay)					0.219		
6 (Bituminous)					0.081		
SPANNUM (base= 1 (single-span))							
2 (multi-span)					0.119		0.514
NHS (base= 0 (non-interstate))							

1 (interstate)	-	0.189	-0.113	0.181
SOJTYPE (base= 1 (Type I))				

2 (Type II)	-	0.152	0.257	-0.165
-------------	---	-------	-------	--------

Note: All parameters were statistically significant at the 0.05 level, except SPANNUM and NHS parameter estimations for CR9 which were significant at the 0.10 level

Table 44. Ratio of average expected sojourn time to baseline average. All empty cells represent a value of 1.00

	CR5	CR6	CR7	CR8	CR9
DISTRICT (base=district 8)					
1			0.898		3.750
2	1.255				1.597
4		1.114			
5				0.883	1.597
6			0.846	0.705	
9			0.881	1.267	
10			0.740		1.597
12	1.297				
REBARTYPE (base=with protective coating)					
1 (Bare rebar)				0.847	
INTERACT (base=all others)					
1 (Simple Span)	1.284	1.143			
MAINPHYSICAL (base=all others)					
1 (Reinforced)		1.228			
2 (Prestressed)		1.142			
6 (Rolled sections)		1.156	1.118		
SURFTYPE (base=1 (concrete))					
2 (Concrete Overlay)			0.892		
5 (Epoxy Overlay)			0.803		
6 (Bituminous)			0.922		
SPANNUM (base= 1 (single-span))					
2 (multi-span)			0.888		1.672
NHS (base= 0 (non-interstate))					
1 (interstate)	0.828			0.893	1.199
SOJTYPE (base= 1 (Type I))					
2 (Type II)		0.859	0.773	0.848	

Acknowledgements

The Penn State Team would like to acknowledge QES' efforts in conducting 19 of the 40 inspections for Task 3.

The Penn State Team would also like to thank the following individuals in assisting with the following tasks:

- David Cantoran for assisting with analysis of bridge deck cracking data, chloride content testing, and percent loss of rebar testing.
- Chelci Mannarino and Ryan McDonald for assisting with the bridge deck selection process.
- Drs. Guler and Shokouhi for providing advice and conducting data analysis of cracking data and rating histories.
- Trevor Szabo for assisting with bridge inspections and data analysis.
- Ali Kazemian, Sara Ghahramani, Maryam Hojjati, Jared Wright, Stephen Salwocki, Leo B. Pereira, Ling Yao for assisting with bridge deck inspections.
- Betsy Jeschke for assisting with inspection organization and preparation.
- Tim Flynn (Technology Support at PennState) for assisting with the development of the Deck Performance Database.